Potentials of Ayurvedic Formulations as Anti-Cancer Agents

A thesis submitted in partial fulfilment of the requirement for the degree of

Doctor of Philosophy

by

Mohammed Rafi Uz Zama Khan

176106106

Dept. of Biosciences and Bioengineering,

Indian Institute of Technology-Guwahati,

Guwahati, Assam, 781039

India

Indian Institute of Technology Guwahati

Department of Biosciences and Bioengineering

Declaration

I hereby declare that the content encapsulated within this thesis, bearing the title "**Potentials of Ayurvedic formulations as anti-cancer agents**" constitutes an exhaustive assembly of research endeavors undertaken within the distinguished Department of Biosciences and Bioengineering at the renowned Indian Institute of Technology, Guwahati, India, in collaboration with Gifu University, Gifu, Japan. This scholarly pursuit has been meticulously conducted under the guidance and mentorship of **Prof. Vishal Trivedi** and **Dr. Emiko Yanase.** I hereby affirm that the research conducted for this thesis is entirely original and devoid of any form of plagiarism, to the best of my understanding. It is imperative to emphasize that all external sources utilized in this study have been meticulously credited and acknowledged within the thesis. Additionally, I have diligently adhered to scholarly norms by properly citing and attributing all textual materials, illustrations, tables, figures, and other elements obtained from external origins. This declaration underscores my unwavering commitment to academic integrity and ethical research practices.

06/10/2023

October 2023 ----------

(Mohammed Rafi Uz Zama Khan)

176106106

Indian Institute of Technology Guwahati

Department of Biosciences and Bioengineering

Certificate

This certificate hereby affirms the authenticity and scholarly integrity of the research encapsulated within the thesis titled "**Potentials of Ayurvedic formulations as anti-cancer agents**," done by **Mr. Mohammed Rafi Uz Zama Khan** (Roll number: **176106106**). This comprehensive body of work was diligently undertaken and subsequently submitted to Indian Institute of Technology-Guwahati, India, in pursuit of the dual degree of Doctor of Philosophy under "International Joint Ph.D. Program" with Gifu University. We hereby affirm that work done in this thesis has not been submitted, in part or in its entirety, to any other academic institution for the purpose of attaining a degree or diploma. Moreover, we wish to underline that any and all research materials sourced from external origins have been scrupulously acknowledged within the thesis. Furthermore, we have conscientiously cited and attributed any textual content, illustrations, tables, figures, and other elements derived from external sources to the best of our knowledge and in adherence to scholarly conventions.

Vishal 06/10/2023

Emiko Yanase.

Prof. Vishal Trivedi

(Co-ordinating supervisor)

Dr. Emiko Yanase

(Supervisor)

Acknowledgements

Foremost and above all, I humbly extend my profound gratitude to the Almighty God, the omnipotent creator and unwavering guardian, to whom I am indebted for the very essence of my existence.

I wish to convey my heartfelt and unwavering appreciation and gratitude to Professor Vishal Trivedi, my esteemed supervisor, for his enduring guidance, extraordinary patience, continuous encouragement, and profound wisdom throughout the course of my doctoral research endeavors.

I am equally eager to extend my profound gratitude to Dr. Emiko Yanase, my mentor at Gifu University in Japan, for her unwavering support and invaluable assistance throughout the entirety of my sojourn in Japan. Her dedicated guidance not only facilitated my smooth integration into the academic landscape at Gifu University but also significantly eased the attainment of my goals, which would have otherwise posed a formidable challenge.

I wish to extend my heartfelt appreciation to the esteemed members of the committee: Professor Rakhi Chaturvedi, Professor Kannan Pakshirajan, Professor Nitin Chaudhary, and Dr. Kosei Yamauchi, for their invaluable counsel and unwavering encouragement throughout my thesis research.

I would also like to thank my parents, my wife and my brothers for their constant motivation during my thesis work.

I am deeply compelled to convey my profound gratitude to both current and former members of my academic journey: Dr. Sooram Banesh, Dr. Anil Kumar, Mr. Alok Kumar Pandey, Mr. Siddharth Neog, Mr. Rajendra Prasad, Mr. Rakesh, Late Ms. Shikha, Mr. Umesh, Mr. Sai, Mr. Shyam Ji, Ms. Neha, Mr. Sandeep, Mr. Divyanshu, Ms. Eena Dodwani, Mr. Shirish, and Ms. Arunima. Their unflagging dedication and invaluable contributions have been a steadfast beacon of support throughout the entirety of my thesis work.

I would also like to thank Dr. Sartaj, Dr. Himanshu, Mr, Sukumar, Mr. Ryuya, Mr. Yuto, Mr. Ayumi, Ms. Kataoka, Ms. Tsuboi, and Ms. Maya for their help and support during my stay at Gifu University, Japan.

I would also like to extend my thanks to Mr. Ajit, Mr. Armaan, Mr. Nikhil, Ms. Sonia, Mr. John, Mr. Noor, Ms. Sosmitha, Ms. Sweta, Ms. Shabnam, Ms. Anjali, Mr. Rohan, Mr. Smit, Ms. Sujisha, Mr. Sayan, Mr. Jean, Dr. Sudheer, Mr. Atif, Mr. Ismail, Mr. Adnan and Mr. Mostakim for their continuous support, encouragement and help in one way or another during my entire course of Ph.D. work.

I would also like to extend my thanks to Department of Biosciences and Bioengineering and Central Instruments facility (CIF) for providing analytical instruments that were extremely helpful during my research work.

I would also like to thank Indian Institute of Technology for providing the financial assistance.

06/10/2023

Mohammed Rafi Uz Zama khan

Table of contents

List of Figures

List of Tables

Abbreviations

ACTN4	Actin-binding protein alpha-actinin 4	**MD**	Molecular dynamics
ADMET	Absorption, distribution, metabolism, excretion and toxicity	**MEK**	Mitogen-activated protein kinase kinase
AIA	Adjuvant induced arthritis	**MeOH**	Methanol
ALD	Alcoholic liver disease	**MF**	Molecular function
AMC	Amalaki Churna	**MIP-1-α**	Macrophage inflammatory protein-1 alpha
AMCAE	Amalaki Churna aqueous extract	**MLKL**	Mixed lineage kinase domain like pseudokinase
AMPK	Adenosine-monophosphate activated-protein kinase	**MMPBSA**	Molecular Mechanics Poisson–Boltzmann Surface Area
AO	Acridine orange	**mTOR**	mammalian target of rapamycin
AR	Androgen receptor	**MTT**	3-(4,5-dimethylthiazol-2-yl)-2,5-diphenyl tetrazolium bromide
Atg	Autophagy related	**NF-KB**	Nuclear factor kappa B
AXIN	Axis inhibition	**NMR**	Nuclear magnetic resonance
BCy	Betweenness centrality	**NPT**	Isothermal–isobaric (NPT) ensemble
CAM	Complementary and alternative medicine	**NVT**	Canonical ensemble
CC	Cellular components	**PARP**	Poly (ADP-ribose) polymerases
CCNB	Cyclin B1	**PBMCS**	Peripheral blood mononuclear cells
CM	Complete mixture/Complete media	**PBS**	Phosphate buffered saline
c-Myc	Cellular Myc	**PDB**	Protein data bank
COX1/COX2	Cyclooxygenase1/2	**PI**	Propidium Iodide
CRC	Colorectal cancer	**PI3K/Akt**	phosphoinositide-3-kinase–protein kinase B/Akt
c-Src	Cellular sarcoma kinase	**PPI**	Protein-protein interaction
CCy	Closeness centrality	**rhTRAIL**	Recombinant human tumour necrosis

DAVID	Database for Annotations, Visualization, and Integrated Discovery
DCy	Degree centrality
DPPH	2,2-Diphenyl-1-picrylhydrazyl
EA	Ellagic acid
EBM	Evidence based medicine
EDTA	Ethylenediamine tetraacetic acid
EGFR	Epidermal growth factor receptor
EMT	Epithelial to mesenchymal transition
ERK	Extracellular signal-regulated kinase
FeSSIF	Fed state simulated intestinal fluid
FTIR	Fourier transform infrared
Fz	Frizzled
FACS	Fluorescence activated cell sorter
FasL	Fas ligand
FaSSIF	Fasted state simulated intestinal fluid
FBS	Fetal bovine serum
GA	Gallic acid
GAPDH	Glyceraldehyde-3-Phosphate Dehydrogenase
GO	Gene ontology
GSK3β	Glycogen synthase kinase 3-beta
	factor–related apoptosis-inducing ligand
RIP	Receptor interacting protein
RIPA	Radio immunoprecipitation assay buffer
RMSD	Root mean square deviation
RMSF	Root mean square fluctuation
RP-HPLC	Reverse phase-High pressure liquid chromatography
STRING	Search Tool for the Retrieval of Interacting Genes/Proteins
SDS	Sodium dodecyl sulphate
SGF	Simulated gastric fluid
SIF	Simulated intestinal fluid
SD	Standard deviation
TTC	Total terpenoid content
UPLC	Ultra-high-pressure liquid chromatography
TAC	Total alkaloid content
TC	Trikatu Churna
TCF	T-cell factor/lymphoid enhancer factor
TCM	Traditional Chinese medicine
TFC	Total flavonoid content
TGF-β	Transforming growth factor-β
TLC	Thin layer chromatography
TM	Traditional medicine

HBA	Hydrogen bond acceptors
HBD	Hydrogen bond donors
HC	Haritaki Churna
HCAE	Haritaki Churna aqueous extract
HPLC	High performance liquid chromatography
HPTLC	High performance thin layer chromatography
HRP	Horse radish peroxidase
HSP90AA1	Heat shock protein 90 alpha family class A member 1
IC50	half-maximal inhibitory concentration
LEF-1	Lymphoid enhancer-binding factor 1
LPS	Lipopolysaccharide
LRP4/6	Low-Density Lipoprotein Receptor-Related Protein 4
LC-MS	Liquid chromatography-mass spectrometry
TMS	Tetra methyl silane
TNFR1	Tumour necrosis factor receptor-1
TNFR2	Tumour necrosis factor receptor-1
TNFα	Tumour necrosis factor-alpha
TPC	Total phenolic content
TPrC	Total protein content
TRAIL	Tumour necrosis factor–related apoptosis-inducing ligand
TRB	Total rotatable bonds
TPC	Total phenolic content
UPLC BEH	Ultra-high-pressure liquid chromatography-Ethylene Bridged Hybrid
UPLC-MS	Ultra-high-pressure liquid chromatography- mass spectrometry
VEGFR2	Vascular endothelial growth factor receptor 2

Units

℃	Degree Celsius
ml	Millilitre
L	Litre
mg	Milligram
µg	Microgram
kDa	Kilodaltons
hr	Hour
min	Minutes
nm	Nanometer

Chapter I

Introduction

1.1 Homeostasis: Homeostasis is a fundamental biological concept that underpins the survival and proper functioning of all living organisms. Derived from the Greek words "homeo" (meaning "similar") and "stasis" (meaning "standing still"), homeostasis refers to the body's ability to maintain a stable internal environment despite ever-changing external conditions. This intricate balance is crucial for the well-being and survival of organisms, as it ensures that essential physiological parameters remain within a narrow range. The internal environment comprises a range of physical and chemical factors, including body temperature, blood pressure, pH levels, fluid balance, blood oxygen content, glucose levels in blood, and the concentration of various ions and molecules [1]. These factors must be tightly regulated to ensure the proper functioning of cells, tissues, and organs. Homeostasis serves as the machine's operator, continuously monitoring various parameters and making adjustments as needed to keep them within an acceptable range [2]. The receptor-effector control mechanism plays a central role in maintaining homeostasis, which is the body's inherent ability to balance its internal environment (**Figure 1.1**). Receptors, often found as specialized cells or sensory devices, constantly monitor essential physiological factors like temperature, blood pressure, and glucose levels. When these factors deviate from their established norms, receptors trigger signaling pathways that communicate with effectors through a control center, which, in the case of the human body, is the brain. This system ensures that the body can regulate and restore equilibrium in response to changing conditions.

Homeostasis, a fundamental biological concept, governs the precise regulation of various physiological processes in the human body. For example, these processes encompass temperature homeostasis, characterized by negative feedback mechanisms that invoke strategies like perspiration, shivering, and modulation of cutaneous blood flow to maintain temperature stability. Equally critical is the tight control over blood glucose levels, with postprandial glucose elevation prompting insulin secretion for cellular glucose uptake and declining levels triggering glucagon release to mobilize hepatic glucose reserves [3]. The maintenance of pH balance relies on blood buffer systems, which selectively sequester or release H+ ions to counteract acidity or alkalinity, facilitating essential biochemical reactions [4]. Concurrently, blood pressure regulation relies on vigilant baroreceptors in vessel walls, promptly signaling cardiac adjustments to ensure adequate perfusion [5]. Finally, electrolyte balance, governing ions like sodium, potassium, and calcium, safeguards nerve and muscle function, preventing detrimental imbalances [6]. These intricate homeostatic mechanisms

collectively underscore the body's remarkable ability to uphold internal equilibrium with precision.

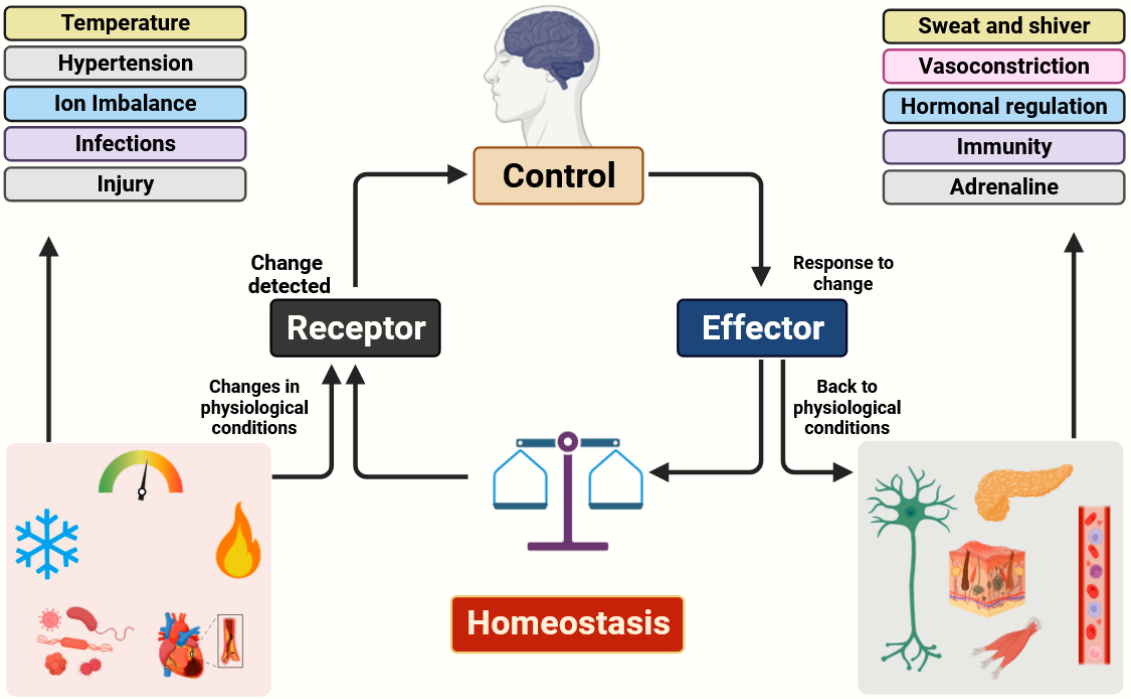

Figure 1.1: Homeostasis orchestrates the symphony of balance within Human body.

(Source: The figure is adapted and modified from khanacademy.org)

Homeostasis relies on a variety of mechanisms and feedback loops that work together to maintain equilibrium. The two primary mechanisms involved in homeostasis are negative feedback and positive feedback [7]. Negative feedback is the most common mechanism in homeostasis and serves to maintain stability by opposing changes in the internal environment. It operates to counteract any deviation from the set point or ideal condition, effectively dampening any change [8]. When a physiological parameter (e.g., body temperature, blood glucose levels, blood pressure) deviates from its set point, negative feedback mechanisms act to bring it back to the set point. An example of negative feedback is the regulation of body temperature. When the body temperature rises above the set point (typically around 98.6°F or 37°C), thermoreceptors in the skin and brain detect the increase. The hypothalamus, acting as the control center, sends signals to sweat glands (effectors) to produce sweat, and blood vessels in the skin to dilate, allowing heat to be dissipated (**Figure 1.2**). As the body cools down and returns to the set point, the hypothalamus ceases these responses [9]. While negative feedback maintains stability, positive feedback amplifies changes in the internal environment, often to reach a specific goal. This mechanism is less common in homeostasis but plays a vital role in

certain physiological processes. A classic example of positive feedback is blood clotting. When a blood vessel is injured, platelets begin to adhere to the site and release chemical signals that attract more platelets. This cascade continues until a stable blood clot forms to stop bleeding [10]. Positive feedback in this case ensures that the clotting process is swift and effective. Positive feedback can also be seen in childbirth, where contractions of the uterus intensify and increase in frequency until the baby is born [11]. The birth of the baby ends the positive feedback loop.

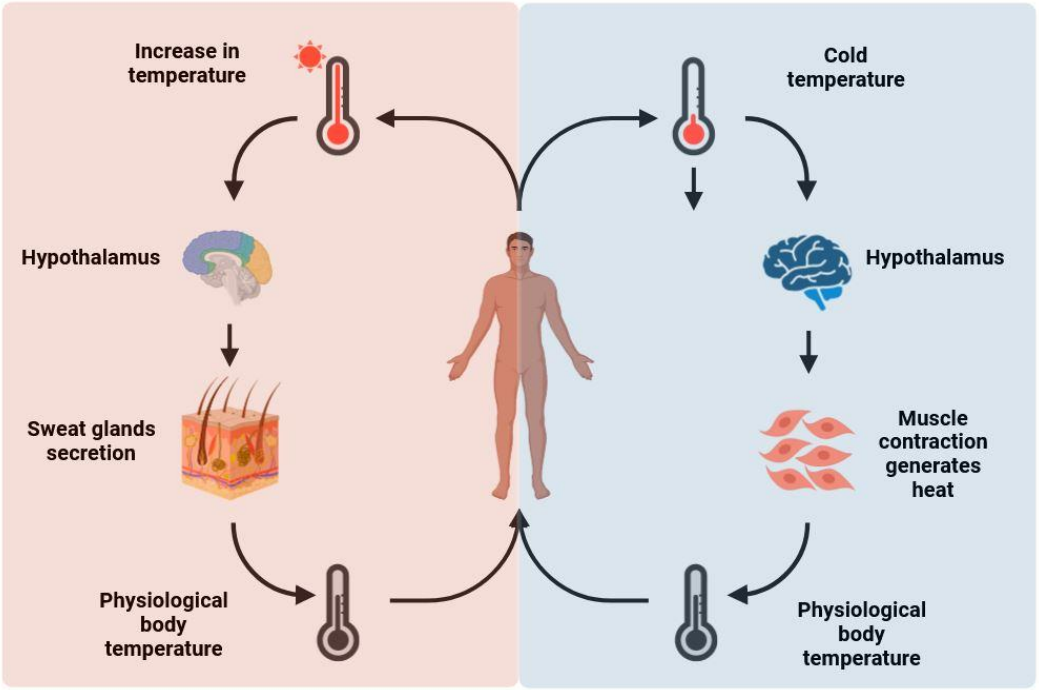

Figure 1.2: Negative feedback mechanism to restore homeostasis. (Source: The figure is adapted and modified from https://wou.edu/).

1.2 Homeostasis in the Diseased State: A Delicate Balance: Homeostasis is a fundamental biological concept that encompasses the body's intrinsic capacity to uphold stability and equilibrium within its internal environment, irrespective of external perturbations [12]. In a state of physiological well-being, homeostasis rigorously regulates critical parameters such as temperature, pH, blood glucose levels, and fluid equilibrium, maintaining them within a narrow, optimal range through intricate feedback loops and control systems [13]. This delicate balance is paramount for the seamless operation of various physiological processes. Nevertheless, when pathological conditions disrupt the normal functioning of the body either by falling ill through infection, injury or a chronic ailment, the integrity of homeostasis becomes challenged, necessitating adaptive responses for survival and recuperation. A

quintessential exemplification of regaining homeostasis in the diseased state manifests in the scenarios wherein individuals experience hypoglycemia, often stemming from conditions such as diabetes, the body mobilizes counter-regulatory mechanisms to restore glucose levels to their customary range. This entails the release of glucagon by the pancreas, prompting the liver to instigate glycogen conversion into glucose, which is then released into the bloodstream [14]. This response assumes a pivotal role in averting grave complications like unconsciousness or seizures. Herein, the body once more underscores its ability to maintain homeostasis, albeit through transient alterations in glucose levels. When the body is unable to autonomously regulate blood glucose levels, necessitating external intervention, the administration of exogenous insulin becomes imperative to sustain appropriate blood glucose homeostasis. Chronic conditions like hypertension result in prolonged disturbances in the delicate balance of the human body's homeostasis [15]. In this complex state, the body's inherent mechanisms for regulating blood pressure experience impairment, often due to various factors, including genetics, dietary choices, and lifestyle habits. As a result, the body attempts to counteract this disturbance through a series of physiological adjustments, including the narrowing or widening of blood vessels, modulation of heart rate, and careful regulation of sodium retention or excretion [16]. Although these adaptive responses temporarily maintain blood pressure within a survivable range, they place a significant burden on the cardiovascular system, increasing the susceptibility to further complications if not managed vigilantly [17]. Nevertheless, while the body's remarkable capacity to maintain homeostasis amidst pathological challenges is indeed commendable, its efficacy is not without limitations, occasionally leading to the exacerbation of underlying ailments. In such instances, the body's concerted efforts to restore equilibrium can inadvertently amplify the existing disease pathology. When intrinsic mechanisms fall short in reinstating physiological homeostasis, it frequently necessitates external intervention in the form of medical remedies.

1.3 Different approaches to restore homeostasis of the body: Over the course of history, humanity has consistently turned to various forms of medicinal interventions to achieve the noble goal of restoring homeostasis, thus attesting to the enduring reliance on therapeutic solutions to navigate these intricate health challenges. Modern medicine frequently integrates scientific principles and pharmaceuticals to target specific health conditions, with the dual objectives of symptom relief and treatment of underlying causes. Conversely, traditional systems such as Siddha, Unani, and Ayurvedic medicine offer unique methodologies for reestablishing the body's homeostasis.

1.3.1 Modern medicine: Modern medicine, often simply referred to as "medicine" or "Allopathic medicine," is the standard medical practice that uses drugs, surgery, and other interventions to treat diseases and alleviate symptoms. Allopathy also has an alias known as Evidence based medicine (EBM). Evidence-based medicine primarily refers to a method, practice, or end result that is employed for the benefit of the general public after thoroughly assessing the core tenets associated with it [18]. EBM through time has developed and further incorporated the science of placing the practice of medicine purely on a scientific basis, the development of hierarchies of evidence and methodology development for trustworthy recommendations [19]. Evidence-based medicine has contributed to a reduction in the importance of intuition, pathophysiological reasoning, and unsystematic clinical experience in clinical decision making. The practice of evidence based medicine deals with integrating individual clinical expertise with best evidence from systematic research [20].

1.3.2 Siddha: The practitioners of siddha medicine are known as siddhars, but they are more often known as vaithiyars in Tamil Nadu (a state in southern India). The siddha system of medicine recognizes predominance of vatham, pitham and kabam in child hood, adulthood and old age respectively, where as in Ayurveda it is quite opposite [21]. In Siddha, kabam is dominant in childhood, pitham in adults and vatham in old age people. In siddha medicine, lifestyle and diet play an important role in both curing a disease and maintaining health. The basic do's and dont's are known as pathya and apathy respectively. The national institute of siddha, located in Tamil Nadu, is one of the primary institutes that assists in the training of students in the field of siddha medicine. Apart from the aforementioned institute, there are others that are overseen by the Central Council of Ayurveda and Siddha (CCRAS comes under the ministry of AYUSH), the same independent authority that also regulates and monitors ayurveda medical research.

1.3.3 Homeopathy: Homeopathy is derived from the Greek words "homeos" meaning similar and "pathos" means suffering. Homeopathy is founded on the fundamental premise of "like cures like" and may be defined as a treatment practise that employs various preparations whose effects match to the signs of the condition in healthy individual patients. "Like can be cure with like" and "less is more" are the two main axioms of homeopathy [22]. The principle of having same symptoms when herbs are given in either high or low doses was first observed by Hippocrates. It was originated by Samuel Hahnemann, a German physician in 1796 who used highly diluted substance to promote healing. The presence of contradicting evidences is very common in scientific literature. In the case of homeopathy, there is a consensus that

homeopathy still remains most controversial subject in the field of therapeutics [23]. The strength of available evidence seems to be incomplete/insufficient to conclude that homeopathy is clinically effective. For example, two publications published in the Lancet journal with the identical title "Are the clinical effects of homoeopathy placebo effects?" concluded with one indicating that the homoeopathic benefits are purely placebo and the other suggesting that they are not entirely due to placebo [24, 25]. Regardless, for homoeopathy to be considered clinically beneficial, there must be scientifically organized and thorough study.

1.3.4 Ayurvedic medicine: Ayurvedic medicine, a holistic system of healing that originated in India over 5,000 years ago, offers a comprehensive approach to health and well-being. Rooted in the ancient Sanskrit words "Ayur" (life) and "Veda" (knowledge), Ayurveda embodies a profound understanding of the interconnectedness of mind, body, and spirit. At its core, Ayurvedic medicine seeks to achieve balance within the body and with the external environment, aiming to prevent illness and promote optimal health through natural remedies and lifestyle practices. Central to Ayurveda is the belief that each individual possesses a unique constitution or "Prakriti," which defines their physical and mental characteristics. By identifying one's Prakriti and any current imbalances or "Vikriti," Ayurvedic practitioners tailor treatments to restore equilibrium [26]. Ayurveda categorizes the human body into three fundamental doshas: Vata, Pitta, and Kapha which play essential roles in governing various physiological and psychological aspects of an individual's constitution and health [27]. Vata, associated with the elements of air and ether, primarily oversees bodily movements such as circulation, respiration, and nerve impulses. Pitta, aligned with the elements of fire and water, is responsible for regulating metabolism, digestion, and body temperature. Kapha, grounded in the elements of earth and water, maintains structural integrity and stability within the body, influencing aspects such as muscle development, joint lubrication, and immune function. The harmonious equilibrium of these doshas is paramount, and Ayurveda deploys an array of therapies and natural herbal interventions to reinstate this equilibrium. Diverse formulations, each tailored to precise delivery mechanisms and disease profiles, encompass a spectrum of compositions (**Figure 1.3**). These range from arishta/asava (essences derived through distillation), churna (finely powdered blends), bhasma (calcinated powders), and bati (compact tablets) to ghrita (formulations steeped in clarified butter) and guggulu, derived from botanical, zoological, and mineral origins [28]. Geographically rooted predominantly in the Indian subcontinent, Ayurveda's historical roots trace back to the Vedic era. Its canonical texts expound a plethora of formulations, such as arka, asava, Arishta, avaleha, paka, churna,

gutika/vati, Rasayan, lauha, rasayoga, taila, bati, guggulu, etc. as given in ayurvedic "central guidelines for drug development in ayurvedic formulations" published by CCRAS, ministry of AYUSH. Authoritative resources like the Ayurvedic Formulary and Ayurvedic Pharmacopoeia of India delve into the creation and standardization of these formulations [29, 30].

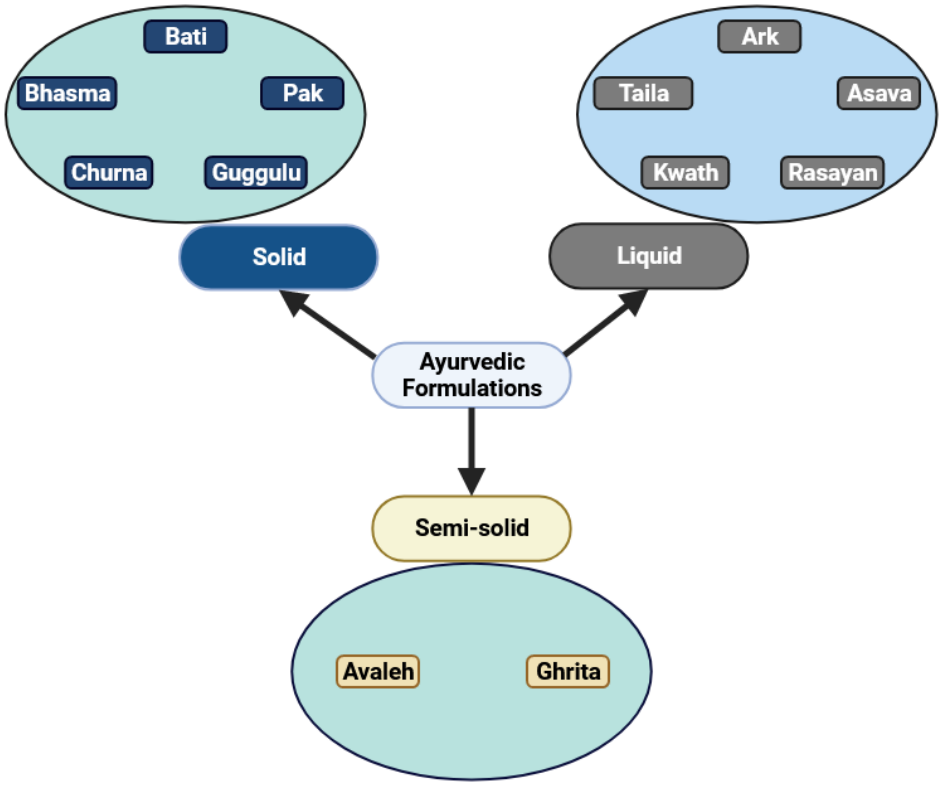

Figure 1.3: Ayurvedic medicine uses different formulations tailored to specific disorder.

Categorized fundamentally into solid, liquid, and semi-solid forms, the crafting of these formulations follows meticulously detailed procedures, a testament to Ayurveda's intricate and time-honoured approach. Ayurvedic treatments encompass a diverse range of modalities, including dietary recommendations, herbal remedies, yoga, meditation, and detoxification practices. Dietary choices are particularly emphasized, as food is seen as a primary source of healing or imbalance [31]. Ayurvedic herbs and formulations, derived from plants, minerals, and even animal products, are carefully prescribed to address specific health concerns and promote overall vitality. In recent years, Ayurvedic medicine has gained global recognition and acceptance as an alternative and complementary approach to conventional healthcare [32]. Its emphasis on personalized care, natural remedies, and preventive measures resonates with individuals seeking holistic and integrative solutions. However, it's essential to seek guidance

from qualified Ayurvedic practitioners who can provide accurate assessments and tailor treatments to an individual's unique constitution and health concerns.

1.4 Ayurvedic formulations are repleted with potent phytochemicals: One of the key focuses in drug discovery is the identification of bioactive molecules within a given sample. While certain plant sources, such as Haritaki (*Terminalia chebula*), have been extensively studied for their bioactive chemicals, there has been less research on identifying bioactive components from entire Ayurvedic formulations [33]. The primary reason for investigating bioactive components within a formulation rather than extracting them from individual plants is that the process of creating an Ayurvedic formulation may generate intermediate molecules that are bioactive. Additionally, the combination of various plant metabolites from different sources in a formulation can result in a fortuitous synergy, leading to superior and synergistic activities compared to individual plant extracts. With this perspective in mind, several research groups have examined extracted Ayurvedic formulations using different methods to characterize their bioactive compounds (**Table 1.1**). For instance, one study utilized an HPLC method to identify polyphenols such as Caffeic acid, chlorogenic acid, catechin, ferulic acid, gallic acid, protocatechuic acid, quercetin, rutin, syringic acid, and vanilic acid in a methanol extract of Chyavanprash [34]. Similarly, another study investigated two different formulations, namely L52 and L38, consisting of eight and nine individual plants/herbs, respectively. Polyphenols such as quercetin, ellagic acid, rutin, cinnamic acid, ferulic acid, and other known compounds were discovered in the aqueous and ethanolic extracts of these formulations using different HPLC, TLC, FTIR, and HPTLC investigations [35, 36]. Furthermore, gallic acid was found in abundance in three batches of Pathyashadnagam Kwath, a polyherbal formulation comprising seven distinct plants, as determined by HPLC analysis [37, 38]. The phytochemical, organoleptic, physical, and chromatographic properties of this formulation, known for treating upper respiratory infections, earache and night blindness, migraine and headache, were thoroughly assessed [38]. In addition to describing the chemicals present in complete formulations, some studies have quantified the amount of a specific bioactive ingredient found in a single plant used to create various formulations. For example, one research focused on the presence of hinokinin, a lignin found in *P. cubeba*, the plant used in these formulations [39]. Certain Ayurvedic formulations are prepared in the form of decoctions using alcohol fermentation. Asava and Arishta formulations are developed to enhance the longevity of the formulations and extract chemicals that are soluble in both aqueous and organic solvents. Pancharistha is one such formulation prepared by decoction of 21 different plant materials.

Analysis of aqueous extracts of the Pancharishta formulation (ZP A-H) using HPTLC, GC-MS, UPLC-MS, and HPLC revealed the presence of polyphenols such as quercetin, kaempferol, ellagic acid, gallic acid, and tannic acid [40].

Table 1.1: Phytochemicals and bioactive compounds from various Ayurvedic formulations.

S. No.	Ayurvedic formulation	No of plants	Extract	Class of molecules identified	Reference
1	Chyavanprash	40	Methanol	Caffeic acid, chlorogenic acid, catechin, ferulic acid, gallic acid, protocatechuic acid, quercetin, rutin, syringic acid and vanilic acid	[34]
2	L52, L38	8	Aqueous & Ethanolic	Quercetin, ellagic acid, rutin, cinnamic acid, ferulic	[36]
3	Pathyashadangam kwath	7	Methanolic	Gallic acid	[37]
4	Khadiradi gutika, Ganaprabha tablet, Manasamitra gutika and Dhanwantari Gutika	----------	Methanolic	Hinokinin (Lignan)	[39]
5	Pancharishta	21	Aqueous	quercetin, kaempferol, ellagic acid, gallic acid and tannic acid and Metabolites	[40]
6	Vidangadi churna	4	Methanol	Embelin, Rottlerin, Ellagic acid	[43]
7	Peedantak vati	23	70% ethanolic	rutin, caffeic acid, withaferin A, colchicine, curcumin	[44]
8	Draksharishta	10	Ethyl acetate	Gallic acid, catechin, resveratrol	[41]
9	jatiphaladi churna, sitopaladi churna, caturjata churna, lavangadi vati	15, 3, 4, and 5 respectively	Methanolic	Eugenol	[45]
10	Dashamoola arishta	10	70% Ethanolic	Polyphenols	[42]
11	Dhatrinisha churna	2	------	Curcumin & Ellagic acid	[46]
12	Trikatu	3	70% methanolic	6-Gingerol & piperine	[47]
13	Ridayarishta	25	Chloroform	Arjunetin, arjunolic acid, berberine, piperine	[48]

Eugenol was identified using the RP-HPLC technique in Jatiphaladi Churna, Sitopaladi Churna, Caturjata Churna, and Lavangadi Vati [45]. Additionally, curcumin and ellagic acid

were measured in Dhatrinisha Churna, which has historically been used to treat hyperlipidemia [46].

Similarly, the HPLC validation of gallic acid, catechin, and resveratrol was carried out in both commercially available and in-house prepared Draksharishta formulations [41]. The differential extraction of Draksharishta and Dashamoola in aqueous and organic extracts revealed the possibility of isolating bioactive molecules using different extraction procedures [42]. Likewise, RP-HPLC technique along with FTIR, Mass, and ^{1}H NMR spectroscopy allowed for the easy separation and identification of embelin, rottlerin, and ellagic acid in Vidangadi Churna and Peedantak Vati, with relative contents of 0.647%, 4.419%, and 0.459% (w/w), respectively [43, 44]. Polyphenols such as rutin, caffeic acid, withaferin A, colchicine, and curcumin were also found in Peedantak Vati extract, and their composition was determined using similar chromatographic and spectroscopic techniques [44].

1.5 Ayurvedic formulations have anti-cancer activity: Ayurvedic texts define "arbuda" as a term indicating swelling or deep tissue lumps, often associated with non-healing ulcers referred to as "asadhyavrana." Ayurvedic medicine incorporates numerous individual plants and herbs known for their anti-cancer, anti-inflammatory, and antioxidant properties. For example, Arkeshwara ras (AR), a herbo-metallic preparation, exhibited significant growth inhibition in human pancreatic cancer cells (MaPaCa) while not affecting epithelial carcinoma cells (KB) [49]. Additionally, Panchakola, a polyherbal formulation, demonstrated cytotoxic activity against breast cancer cells (MCF-7) comparable to curcumin [50]. Rasagenthi Leyham, a complex Ayurvedic remedy containing 38 botanical species, displayed promising anti-cancer effects against prostate cancer cells (PC-3) [51]. Ashwagandha (Withania somnifera) showed anticancer efficacy against human malignant melanoma cells (A375) [52]. Bhasma formulations like Manikya bhasma exhibited immunomodulation and anticancer effects, while Shataputi abhrak bhasma demonstrated anticancer activity against various cell lines [53]. Triphala, an herbal concoction deeply rooted in the annals of Ayurvedic medicine, has garnered substantial scientific attention due to its potential as an anti-cancer agent. This triad of botanical wonders – Amla (*Emblica officinalis*), Haritaki (*Terminalia chebula*), and Bibhitaki (*Terminalia bellerica*) – endows Triphala with a reservoir of bioactive compounds and antioxidants, including polyphenols, tannins, and flavonoids. In a harmonious symphony, these constituents synergize to wage war against oxidative stress and chronic inflammation, two hallmark contributors to carcinogenesis [54, 55]. Triphala's anti-cancer prowess extends beyond mere defensive measures. Experimental studies have unveiled its impressive

cytotoxicity against malignant cells, orchestrating the orchestration of apoptosis, impeding angiogenesis, and suppressing the unbridled proliferation of tumors [56-58]. While these preliminary findings offer a glimmer of hope, the journey toward harnessing Triphala's full potential as a bona fide anti-cancer therapeutic necessitates rigorous and comprehensive clinical investigations to decipher the intricate mechanisms at play.

Ayurvedic formulations have garnered attention due to their potential anti-cancer properties; however, the scientific literature lacks comprehensive elucidation of the specific phytochemical constituents responsible for these effects and the intricate interplay of synergistic phytochemicals underlying their anti-cancer activity. Furthermore, there is a conspicuous gap in understanding the mechanistic pathways that underlie the observed anti-cancer properties of these Ayurvedic formulations. Despite promising therapeutic potential, the current research lacks meticulous molecular insights necessary to fully comprehend their mode of action. Consequently, while these ancient remedies have historically shown efficacy, the precise bioactive compounds and the intricate mechanisms governing their anti-cancer activities within Ayurvedic formulations remain elusive. In pursuit of addressing this knowledge gap and unlocking valuable insights for the advancement of innovative cancer therapeutics grounded in traditional medicinal practices, our study is designed to comprehensively elucidate the potential efficacy of Ayurvedic formulations as anti-cancer agents, while concurrently unraveling the intricate mechanisms by which these Ayurvedic formulations may exert their anti-cancer effects.

1.6 Aims and objectives of the study

1.6.1 Screening of ayurvedic formulations with anti-cancer activity: Ayurvedic formulations, recognized for their medicinal properties, were meticulously studied for their anti-cancer potential against colorectal cancer cells.

1.6.2. Isolation, identification and structural characterization of bioactive agents present in Ayurvedic formulation: Ayurvedic formulations demonstrating potent cytotoxicity against colorectal cancer cells will be selected for phytochemical characterization and subsequent isolation of bioactive compounds.

1.6.3 Exploring the role of protein cross-talk in anti-cancer action of phytochemicals present in Ayurvedic formulations: The phytochemicals extracted and isolated from Ayurvedic formulations have the potential to interact with either a singular protein or a diverse array of proteins within cells. To comprehend the nuanced interplay of individual effects and

synergistic interactions of these bioactive agents with their respective protein targets, we conducted the study to intricately elucidate the intricate protein cross-talk occurring among different protein targets.

1.6.4 Molecular mechanism of anti-cancer action of Ayurvedic formulation in colorectal cancer cells: The Ayurvedic formulations, abundant in phytochemicals, exhibit potential in eradicating cancer cells. Despite their efficacy, the intricate mechanisms underlying their anti-cancer properties remain unexplored. This study aims to investigate and elucidate the precise mechanism of action of the selected Ayurvedic formulations on colorectal cancer cells.

1.7 References

1. Baptista, V., *Starting physiology: understanding homeostasis.* Advances in Physiology Education, 2006. **30**(4): p. 263-264.
2. Modell, H., et al., *A physiologist's view of homeostasis.* Advances in physiology education, 2015.
3. Gerich, J.E., *Physiology of glucose homeostasis.* Diabetes, Obesity and Metabolism, 2000. **2**(6): p. 345-350.
4. Caon, M. and M. Caon, *Homeostasis.* Examination Questions and Answers in Basic Anatomy and Physiology: 2900 Multiple Choice Questions and 64 Essay Topics, 2020: p. 173-183.
5. Kohan, D.E., et al., *Regulation of blood pressure and salt homeostasis by endothelin.* Physiological reviews, 2011. **91**(1): p. 1-77.
6. Pollock, J.S., et al., *Water and electrolyte homeostasis brings balance to physiology.* American Journal of Physiology-Regulatory, Integrative and Comparative Physiology, 2014. **307**(5): p. R481-R483.
7. Kiesewetter, A. and P. Schmiemann, *Understanding Homeostatic Regulation: The Role of Relationships and Conditions in Feedback Loop Reasoning.* CBE—Life Sciences Education, 2022. **21**(3): p. ar56.
8. Turrigiano, G., *Homeostatic signaling: the positive side of negative feedback.* Current opinion in neurobiology, 2007. **17**(3): p. 318-324.
9. Tan, C.L. and Z.A. Knight, *Regulation of body temperature by the nervous system.* Neuron, 2018. **98**(1): p. 31-48.
10. Abdel-Sater, K.A., *Physiological positive feedback mechanisms.* Am J Biomed Sci, 2011. **3**(2): p. 145-55.

11. Prabhu, S., *Homeostasis*, in *Textbook of General Pathology for Dental Students*. 2023, Springer. p. 5-10.
12. Seiwert, C., *Homeostasis and the Human Body.* Human Biology, 2019.
13. Billman, G.E., *Homeostasis: the underappreciated and far too often ignored central organizing principle of physiology.* Frontiers in physiology, 2020: p. 200.
14. Tups, A., et al., *Central regulation of glucose homeostasis.* Comprehensive Physiology, 2011. **7**(2): p. 741-764.
15. Aung, K., et al., *Sodium Homeostasis and Hypertension.* Current Cardiology Reports, 2023: p. 1-7.
16. Gordan, R., J.K. Gwathmey, and L.-H. Xie, *Autonomic and endocrine control of cardiovascular function.* World journal of cardiology, 2015. **7**(4): p. 204.
17. Carey, R.M., et al., *Prevention and control of hypertension: JACC health promotion series.* Journal of the American College of Cardiology, 2018. **72**(11): p. 1278-1293.
18. Signore, A. and G. Campagna, *Evidence-based medicine: reviews and meta-analysis.* Clinical and Translational Imaging, 2023. **11**(2): p. 109-112.
19. Djulbegovic, B. and G.H. Guyatt, *Progress in evidence-based medicine: a quarter century on.* The lancet, 2017. **390**(10092): p. 415-423.
20. Masic, I., M. Miokovic, and B. Muhamedagic, *Evidence based medicine–new approaches and challenges.* Acta Informatica Medica, 2008. **16**(4): p. 219.
21. Shukla, S. and S. Saraf, *Fundamental aspect and basic concept of siddha medicines.* Systematic Reviews in pharmacy, 2011. **2**(1): p. 48.
22. Ernst, E., *The truth about homeopathy.* British Journal of Clinical Pharmacology, 2008. **65**(2): p. 163.
23. Ernst, E., *A systematic review of systematic reviews of homeopathy.* British journal of clinical pharmacology, 2002. **54**(6): p. 577-582.
24. Linde, K., et al., *Are the clinical effects of homoeopathy placebo effects? A meta-analysis of placebo-controlled trials.* The Lancet, 1997. **350**(9081): p. 834-843.
25. Shang, A., et al., *Are the clinical effects of homoeopathy placebo effects? Comparative study of placebo-controlled trials of homoeopathy and allopathy.* The Lancet, 2005. **366**(9487): p. 726-732.
26. Kalavade, V.A. and D.U.G. Prakash Mane, *A CLINICAL OBSERVATIONAL STUDY ON PRAKRITI ANALYSIS AND ITS APPLICATION IN AYURVEDA.* Journal of Pharmaceutical Negative Results, 2023: p. 2215-2222.

27. Shilpa, S. and C.V. Murthy, *Understanding personality from Ayurvedic perspective for psychological assessment: A case.* Ayu, 2011. **32**(1): p. 12.
28. Kumar, S., G.J. Dobos, and T. Rampp, *The significance of ayurvedic medicinal plants.* Journal of evidence-based complementary & alternative medicine, 2017. **22**(3): p. 494-501.
29. Committee, I.A.P., I.D.o.I.S.o. Medicine, and Homoeopathy, *The Ayurvedic Formulary of India*. 2003: Controller of Publications.
30. PCIH, P.C.f.I.m.a.h. *The Ayurvedic pharmacopoeia of India*. 2016 [cited IX; Available from: https://cdn.ayush.gov.in/wp-content/uploads/2021/03/Ayurvedic-Pharmacopoeia-of-India-part-1-volume-IX.pdf.
31. Payyappallimana, U. and P. Venkatasubramanian, *Exploring ayurvedic knowledge on food and health for providing innovative solutions to contemporary healthcare.* Frontiers in public health, 2016. **4**: p. 57.
32. Chaudhary, A. and N. Singh, *Contribution of world health organization in the global acceptance of Ayurveda.* Journal of Ayurveda and integrative medicine, 2011. **2**(4): p. 179.
33. Riaz, M., et al., *Chemical constituents of Terminalia chebula.* Nat Prod Ind J, 2017. **13**(2): p. 112.
34. Govindarajan, R., D. Singh, and A. Rawat, *High-performance liquid chromatographic method for the quantification of phenolics in 'Chyavanprash'a potent Ayurvedic drug.* Journal of Pharmaceutical and Biomedical Analysis, 2007. **43**(2): p. 527-532.
35. Dinakaran, S.K., S. Chelle, and H. Avasarala, *Profiling and determination of phenolic compounds in poly herbal formulations and their comparative evaluation.* Journal of traditional and complementary medicine, 2019. **9**(4): p. 319-327.
36. Dinakaran, S.K., B. Sujiya, and H. Avasarala, *Profiling and determination of phenolic compounds in Indian marketed hepatoprotective polyherbal formulations and their comparative evaluation.* Journal of Ayurveda and integrative medicine, 2018. **9**(1): p. 3-12.
37. Abraham, A., L. Mathew, and S. Samuel, *HPLC analysis of Pathyashadangam kwath, a classical Ayurvedic polyherbal formulation.* Materials Today: Proceedings, 2020. **25**: p. 115-121.
38. Abraham, A., S. Samuel, and L. Mathew, *Phytochemical analysis of Pathyashadangam kwath and its standardization by HPLC and HPTLC.* Journal of Ayurveda and integrative medicine, 2020. **11**(2): p. 153-158.

39. Haribabu, K., M. Ajitha, and U.V. Mallavadhani, *Quantitative estimation of (-)-hinokinin, a trypanosomicidal marker in Piper cubeba, and some of its commercial formulations using HPLC-PDA.* Journal of pharmaceutical analysis, 2015. **5**(2): p. 130-136.
40. Khan, W., et al., *Chromatographic profiling of Pancharishta at different stages of its development using HPTLC, HPLC, GC–MS and UPLC–MS.* Phytochemistry letters, 2017. **20**: p. 391-400.
41. Pillai, D. and N. Pandita, *Validated high performance thin layer chromatography method for the quantification of bioactive marker compounds in Draksharishta, an ayurvedic polyherbal formulation.* Revista Brasileira de Farmacognosia, 2016. **26**(5): p. 558-563.
42. Abraham, B., et al., *Phytochemical rich extract from the spent material generated from Industrial Dashamoola preparation (a medicinal Ayurvedic decoction) with antioxidant, antidiabetic and anti-inflammatory potential.* Industrial crops and products, 2020. **151**: p. 112451.
43. Patel, R.K., V.R. Patel, and M.G. Patel, *Development and validation of a RP-HPLC method for the simultaneous determination of Embelin, Rottlerin and Ellagic acid in Vidangadi churna.* Journal of pharmaceutical analysis, 2012. **2**(5): p. 366-371.
44. Balkrishna, A., et al., *Evaluation of polyherbal ayurvedic formulation 'Peedantak Vati' for anti-inflammatory and analgesic properties.* Journal of ethnopharmacology, 2019. **235**: p. 361-374.
45. Saran, S., et al., *Validated RP-HPLC method to estimate eugenol from commercial formulations like Caturjata Churna, Lavangadi Vati, Jatiphaladi Churna, Sitopaladi Churna and clove oil.* Journal of Pharmacy Research, 2013. **6**(1): p. 53-60.
46. Patel, V.R. and R.K. Patel, *HPTLC method Development & Validation for quantification of Markers of Dhatrinisha churna.* Pharmacognosy Journal, 2012. **4**(29): p. 26-29.
47. Harwansh, R.K., et al., *Cytochrome P450 inhibitory potential and RP-HPLC standardization of trikatu—A Rasayana from Indian Ayurveda.* Journal of ethnopharmacology, 2014. **153**(3): p. 674-681.
48. Pandit, S., et al., *Evaluation of herb-drug interaction of a polyherbal Ayurvedic formulation through high throughput cytochrome P450 enzyme inhibition assay.* Journal of ethnopharmacology, 2017. **197**: p. 165-172.

49. Nafiujjaman, M., et al., *Anticancer activity of Arkeshwara Rasa-A herbo-metallic preparation.* Ayu, 2015. **36**(3): p. 346.
50. Shamsi, T.N., R. Parveen, and S. Fatima, *Panchakola reduces oxidative stress in MCF-7 breast cancer and HEK293 cells.* Journal of dietary supplements, 2018. **15**(5): p. 704-714.
51. Ranga, R.S., et al., *Rasagenthi lehyam (RL) a novel complementary and alternative medicine for prostate cancer.* Cancer chemotherapy and pharmacology, 2004. **54**(1): p. 7-15.
52. Halder, B., S. Singh, and S.S. Thakur, *Withania somnifera root extract has potent cytotoxic effect against human malignant melanoma cells.* PLoS One, 2015. **10**(9): p. e0137498.
53. Jha, S. and V. Trivedi, *Manikya Bhasma is a nanomedicine to affect cancer cell viability through induction of apoptosis.* Journal of Ayurveda and integrative medicine, 2021. **12**(2): p. 302-311.
54. Naik, G., et al., *In vitro antioxidant studies and free radical reactions of triphala, an ayurvedic formulation and its constituents.* Phytotherapy Research: An International Journal Devoted to Pharmacological and Toxicological Evaluation of Natural Product Derivatives, 2005. **19**(7): p. 582-586.
55. Sandhya, T., et al., *Potential of traditional ayurvedic formulation, Triphala, as a novel anticancer drug.* Cancer letters, 2006. **231**(2): p. 206-214.
56. Sandhya, T. and K. Mishra, *Cytotoxic response of breast cancer cell lines, MCF 7 and T 47 D to triphala and its modification by antioxidants.* Cancer letters, 2006. **238**(2): p. 304-313.
57. Tsering, J. and X. Hu, *Triphala suppresses growth and migration of human gastric carcinoma cells in vitro and in a zebrafish xenograft model.* BioMed Research International, 2018. **2018**.
58. Wang, M., Y. Li, and X. Hu, *Chebulinic acid derived from triphala is a promising antitumour agent in human colorectal carcinoma cell lines.* BMC complementary and alternative medicine, 2018. **18**(1): p. 1-9.

Chapter II

The therapeutic potentials of Ayurvedic formulations for cancer treatment

2.1 Introduction: Throughout the course of human history, diseases have held a central role in shaping our understanding of health and medicine. Diseases encompass a wide spectrum, ranging from mild and self-resolving ailments to severe and life-threatening afflictions. These are defined as abnormal conditions or disorders that disrupt the normal functioning of an organism, often leading to physical or mental impairment, discomfort, pain, or other adverse symptoms [1, 2]. The origins of diseases can be complex, arising from a variety of sources, including pathogens such as bacteria, viruses, fungi, and parasites, genetic mutations, environmental factors, lifestyle choices, or a combination of these factors [3, 4]. Diseases are typically categorized using various frameworks, which help in organizing and understanding the multitude of health challenges humanity faces. These categorizations can be based on causative agents, the specific organ systems affected, the severity of symptoms, or the duration of the ailment. Consequently, diseases can be broadly classified into categories such as infectious or non-infectious, acute or chronic, genetic or acquired, autoimmune or allergic, depending on the chosen classification system [5]. Infectious diseases, for instance, are caused by pathogens and can be transmitted from one individual to another [6, 7]. Non-infectious diseases, on the other hand, stem from factors other than pathogens and include conditions like heart disease, diabetes, and cancer [8]. The duration and intensity of diseases are also vital factors in classification. Acute diseases typically have a sudden onset and short duration, while chronic diseases persist over a longer period, often with less severe but enduring symptoms. Genetic diseases result from inherited genetic mutations, whereas acquired diseases are developed over time due to external factors like smoking, poor diet, or exposure to environmental toxins [9, 10]. Autoimmune diseases involve the body's immune system mistakenly attacking its own tissues, leading to conditions such as rheumatoid arthritis and multiple sclerosis [11] whereas allergic diseases are characterized by hypersensitivity reactions to allergens, causing conditions like hay fever and food allergies [12]. These classifications serve as essential tools for healthcare professionals and researchers, enabling a structured approach to understanding, diagnosing, and treating a vast array of health conditions.

2.2 Cancer: Cancer, a group of diseases characterized by uncontrolled cell growth and proliferation, poses a significant global health challenge. It is a multifactorial condition, influenced by genetic, environmental, and lifestyle factors. Understanding the underlying mechanisms of cancer is crucial for its prevention, early detection, and effective treatment. At its core, cancer originates from genetic mutations that disrupt the normal regulatory processes of cell division and death [13]. In a healthy organism, cells follow a strict cycle of growth,

replication, and programmed cell death (apoptosis). This cycle is tightly controlled by a complex network of genes and signaling pathways. However, when mutations occur in these genes, cells can evade these controls, leading to uncontrolled proliferation and the formation of tumours [14]. Genetic mutations can be inherited or acquired during a person's lifetime. Inherited mutations, often associated with hereditary cancer syndromes, increase an individual's susceptibility to specific types of cancer [15]. Acquired mutations, on the other hand, result from exposure to carcinogens, such as tobacco smoke, radiation, or certain chemicals, and are responsible for the majority of cancer cases [16].

Tumours can be benign or malignant. Benign tumours grow slowly and are confined to a specific location, while malignant tumours grow rapidly, invade nearby tissues, and can metastasize (spread) to distant organs. The process of metastasis is a complex and poorly understood aspect of cancer biology. It involves tumour cells breaking away from the primary tumour, entering the bloodstream or lymphatic system, and establishing secondary tumours in other parts of the body [17]. Metastasis is a critical factor that often determines the severity and prognosis of cancer, as the spread of malignant cells to vital organs can significantly compromise a patient's health and make treatment more challenging. Understanding and developing strategies to target metastasis remains a crucial area of ongoing research in the fight against cancer, with the ultimate goal of improving patient outcomes and finding more effective treatments for this devastating disease.

2.3 Cancer prevalence and mortality: Cancer, a prevailing malady in the 21st century, ensues from unbridled cellular proliferation, stemming from intrinsic causes such as genetic aberrations and extrinsic factors including carcinogenic agents acquired through diverse routes. As per Globocan 2020, the global incidence of new cancer cases exceeded 19 million, with a mortality quotient approximating 50% (9.9 million). Leading this panorama, breast cancer accounted for 11.6% of new cases, while lung cancer remained leading cause of cancer related deaths exhibiting the highest mortality at 18% closely followed by colorectal, stomach and liver cancers (**Figure 2.1A & B**). Further, it was observed with few regional disparities that lung cancer dominated in developed countries, while liver and stomach cancers were more prevalent in parts of Asia and Africa. India witnessed an estimated 1.39 million new cancer cases in 2020, making it one of the top countries in terms of cancer incidence. Alarmingly, it also reported approximately 7,84,821 cancer-related deaths. Among Indian men, oral cancer was particularly prevalent, largely attributed to tobacco and betel nut consumption, while breast cancer was the most common cancer among Indian women (**Figure 2.1C & D**). Interestingly,

there was a noticeable shift towards younger age groups being affected, partly due to lifestyle factors such as smoking and unhealthy diets. Globally, projections for 2040 presage an elevation in the incidence rate, potentially cresting at nearly 30 million cases (**Figure 2.1E**). These trends emphasize the impending challenge that cancer poses at a global scale. [18]. Approximately 75% of global cancer cases are concentrated in Asia and Europe, with Asia bearing the highest burden of cases. The highest number of cancer incidences was reported in various regions around the world, with Asia being particularly prominent (**Figure 2.1F**).

Figure 2.1: Cancer, a relentless adversary claims millions of lives. (A) Incidence rate of cancer globally. **(B)** Mortality of cancer globally. **(C)** Incidence rate of cancer in India. **(D)** Mortality of cancer in India. **(E)** Estimation of cancer incidence rate globally. **(F)** Sun-burst plot of cancer cases distribution. (**Data source:** GLOBOCAN 2020 (http://gco.iarc.fr))

2.4 Cancer progression: The progression of cancer is a highly complex and intricate series of events that is defined by abnormal cell proliferation. This eventually leads to the formation of tumours and the ominous possibility of metastasis, posing significant challenges in the field of clinical medicine. This multifaceted process begins with the conversion of previously healthy cells into cancerous entities. This transformation can be primarily attributed to a range of genetic mutations and epigenetic modifications occurring within the DNA of these cells [19]. These alterations are frequently instigated by a multitude of factors, encompassing exposure to carcinogenic agents, an inherent genetic predisposition to cancer, or even random errors that occur during the process of DNA replication [20]. In the initial stages, these genetic perturbations initiate the development of a restricted cluster of abnormal cells, commonly termed as a tumour [21]. This tumour typically exhibits a localized and clinically quiescent behavior (**Figure 2.2**). Nevertheless, over time, further genetic mutations accrue, bestowing upon the tumour an enhanced propensity for invasiveness and aggressiveness [17, 22]. It is at this critical juncture that the cancer gains the capacity to infiltrate neighboring tissues and establish intricate connections with both the vascular and lymphatic networks, marking a significant turning point in its progression.

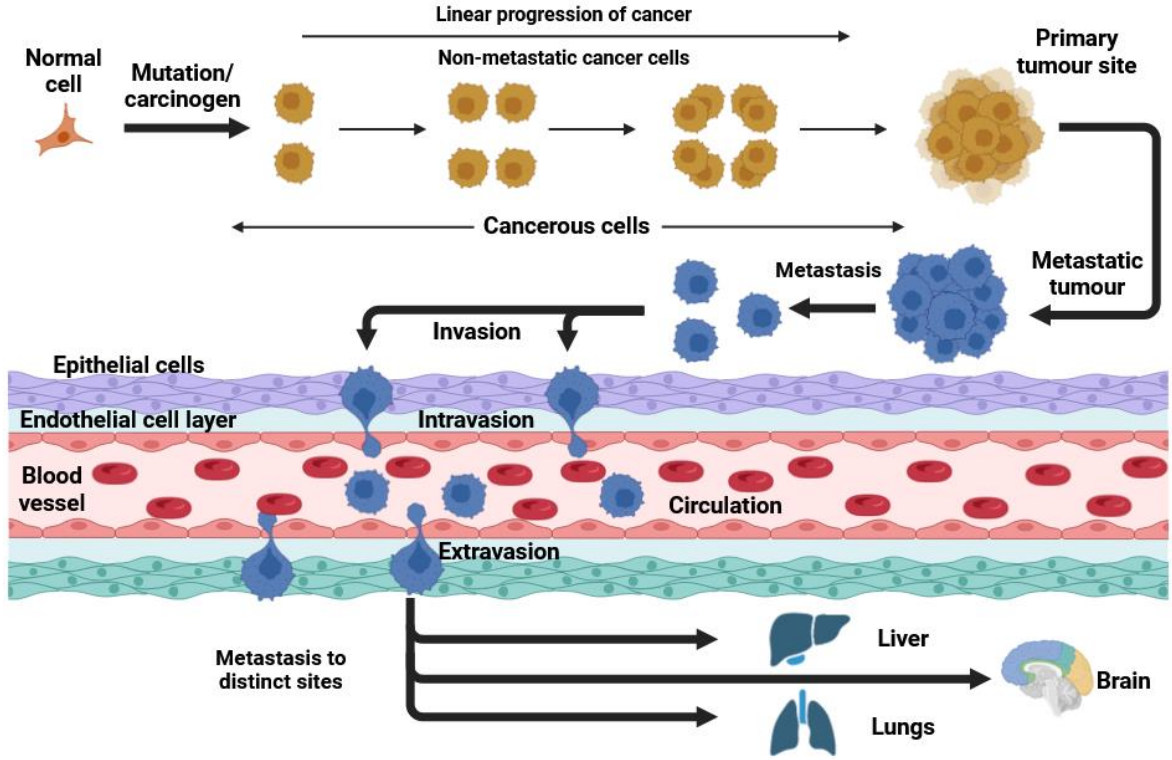

Figure 2.2: The complex processes leading to cancer: From genetic mutations to metastasis.

This transformative process bestows cancer cells with the capability to emancipate themselves from their original site, allowing them to access the bloodstream or lymphatic system, a phenomenon acknowledged as metastasis [23]. Metastasis emerges as the leading cause of cancer-related mortality, as it empowers cancer to initiate secondary tumour growth in distant anatomical locations, thereby substantially complicating therapeutic interventions and posing a formidable challenge to the effectiveness of treatment strategies.

2.5 Hallmarks of cancer: The hallmarks of cancer, as proposed by researchers Douglas Hanahan and Robert Weinberg, are a set of key characteristics that define the fundamental properties of cancer cells [24, 25]. These hallmarks include sustained proliferation, evasion of growth suppressors, resistance to cell death, enabling replicative immortality, induction of angiogenesis, activation of invasion and metastasis, reprogramming of energy metabolism, and evasion of immune destruction [26]. Understanding these hallmarks is crucial for both cancer research and treatment, as they provide insights into the underlying mechanisms of cancer development and progression (**Figure 2.3**). Targeting these hallmarks has become a cornerstone of cancer therapy, with the goal of developing more effective treatments and improving patient outcomes [27].

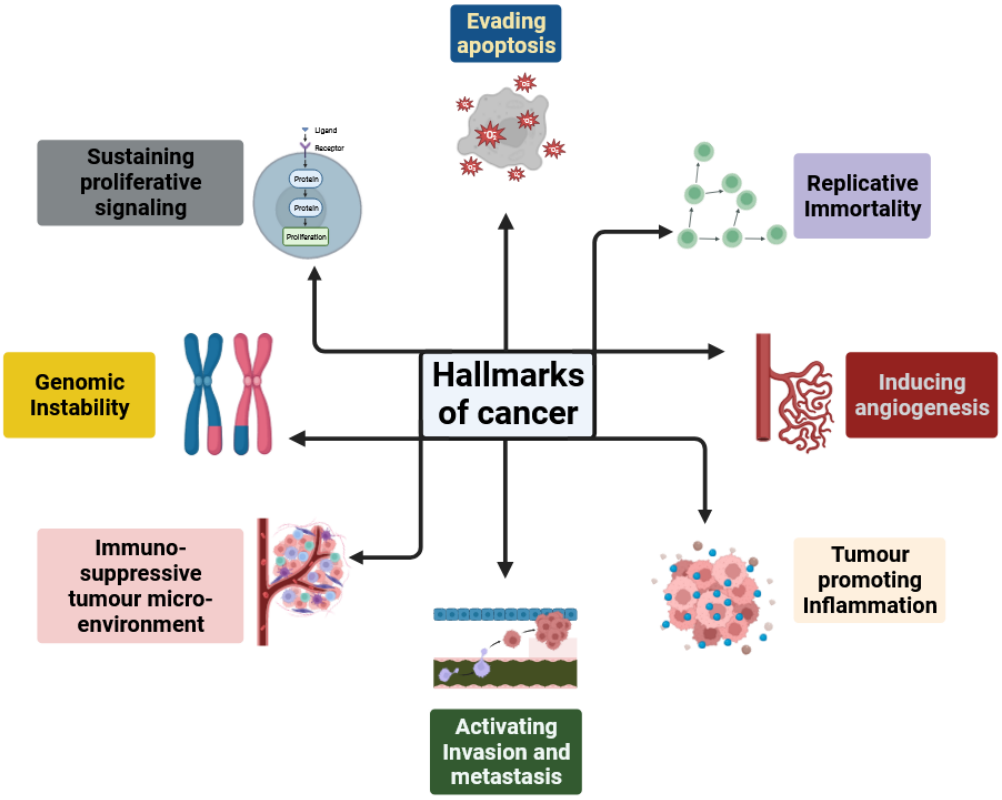

Figure 2.3: The Hallmarks of Uncontrolled Growth and Spread in cancer.

Over the years the understanding of hallmarks of cancer has increased exponentially due to extensive research in the field of cancer biology. Cancer is a complex process driven by alterations in cellular signaling pathways and regulatory mechanisms. It begins with modifications in cell cycle-related proteins, initiating persistent signaling activation that supports the survival and expansion of cancer stem cells. These signaling abnormalities affect various cellular processes, including metabolism, hormone production, angiogenesis, epithelial-mesenchymal transition, autophagy, and interactions with adjacent stromal cells, promoting tumour growth and metastasis [28, 29]. Simultaneously, cancer cells evade growth suppressors by subverting key regulatory pathways, effectively bypassing constraints on growth inhibition, arrest, and senescence [30]. Furthermore, cancer cells exhibit resistance to apoptosis through diverse mechanisms involving the modulation of pro- and anti-apoptotic gene expression, post-translational modifications of apoptotic proteins, and the involvement of key regulators [31]. Additionally, cancer cells acquire replicative immortality, facilitated by alterations in critical protein pathways [32] while the progression of cancer is overseen by angiogenesis, which is orchestrated by a network of proteins, ensuring a continuous supply of nutrients and oxygen to sustain neoplastic growth [33]. The invasive and metastatic potential of cancer cells is driven by the concerted action of various factors, enabling cancer cell migration, tissue infiltration, and the establishment of secondary tumour sites [34]. Cancer cells also employ mechanisms to evade immune destruction, including the modulation of immune checkpoint proteins, while the tumour microenvironment contributes to immunosuppression through interactions with various immune cells [35]. Alterations in cellular energetics, characterized by increased glycolysis, divert glucose away from oxidative phosphorylation, promoting rapid proliferation and survival [36]. Genomic instability and mutational events are foundational attributes underpinning the uncontrolled proliferation and development of cancer cells [37] . Tumour-promoting inflammation fosters a microenvironment conducive to tumourigenesis and metastasis by activating key biomolecules and chemokines that recruit immune cells [38]. These intricate processes collectively drive cancer progression, illustrating the complex interplay of factors underlying malignancy's relentless advance.

2.6 Types of cancer: Cancer represents a complex and diverse spectrum of diseases characterized by the uncontrolled proliferation and dissemination of abnormal cells within the organism (**Figure 2.4**). This pathology encompasses more than 100 distinct types, each distinguished by unique molecular, cellular, and clinical attributes, as well as varying etiological determinants. Some common cancers are listed below.

2.6.1 Carcinomas: Carcinomas are a class of malignant neoplasms characterized by their epithelial cell origin. They account for a significant majority of human cancers, with notable subtypes including adenocarcinomas and squamous cell carcinomas. These malignancies typically arise from the epithelial lining of various organs, such as the lung, breast, prostate, and skin. Carcinomas often exhibit histopathological heterogeneity and are influenced by diverse genetic mutations and environmental factors.

2.6.2 Sarcomas: Sarcomas constitute a heterogeneous group of rare malignancies originating from mesenchymal tissues, including muscles, bones, fat, and connective tissues. Distinguished by their mesodermal lineage, sarcomas encompass diverse subtypes, such as osteosarcoma, leiomyosarcoma, and liposarcoma. These tumours are characterized by aggressive behavior, propensity for metastasis, and distinct genetic alterations [39-42]. Diagnosis often involves histopathological examination and molecular profiling.

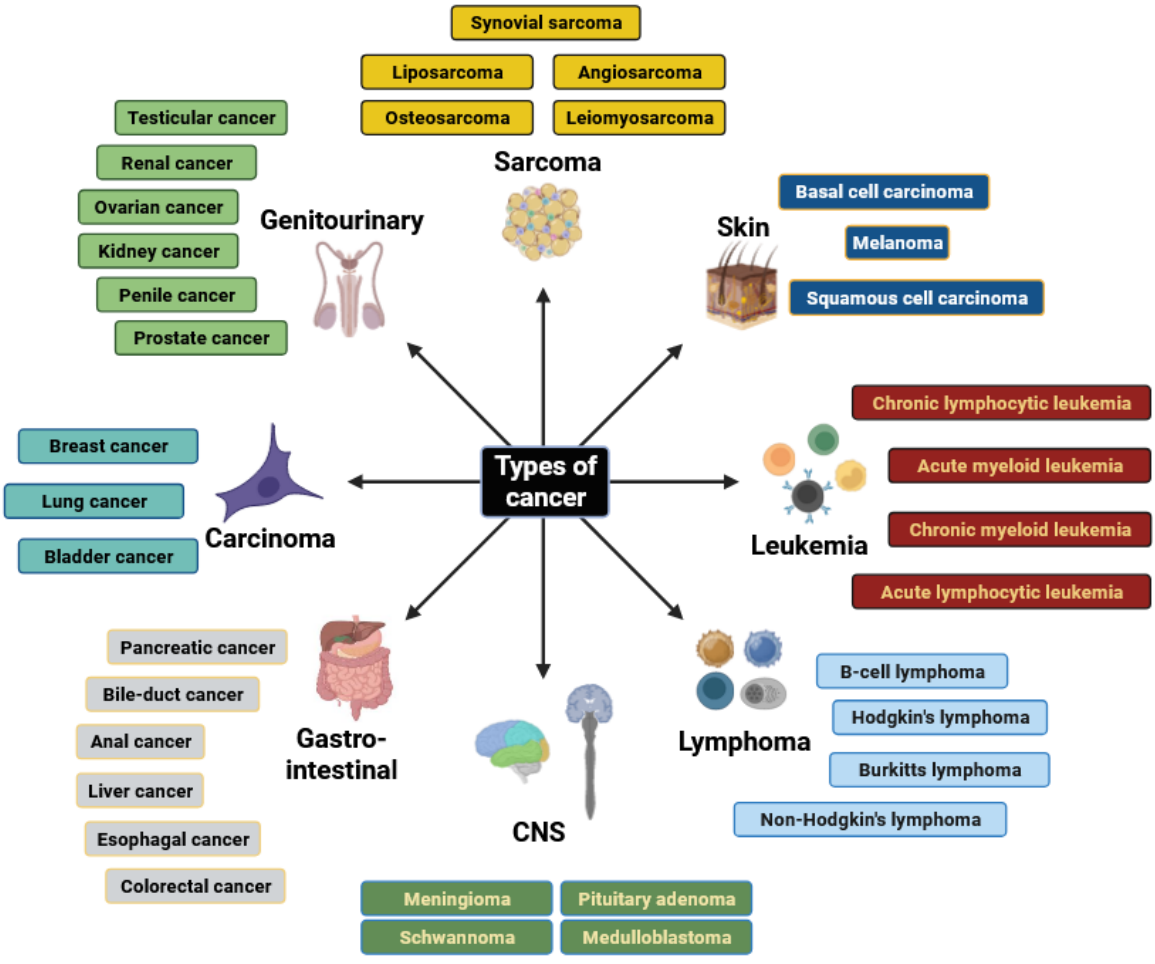

Figure 2.4: Types of cancer.

2.6.3 Genitourinary cancers: Genitourinary cancers encompass a group of malignancies originating from the genitourinary system, including the kidneys, bladder, prostate, testes, and adrenal glands [43]. These cancers exhibit considerable diversity in terms of histology, clinical behavior, and treatment modalities. Renal cell carcinoma, urothelial carcinoma, prostate cancer, and testicular germ cell tumours are notable examples [44]. Genitourinary cancers often present with non-specific symptoms, and diagnosis relies on imaging, histopathology, and molecular profiling.

2.6.4 Skin cancers: Skin cancers are neoplastic disorders arising from the uncontrolled proliferation of skin cells. The three primary types are basal cell carcinoma (BCC), squamous cell carcinoma (SCC), and melanoma. BCC and SCC, known as non-melanoma skin cancers, typically originate from keratinocytes, the predominant epidermal cells [45, 46]. They are often linked to chronic sun exposure and display varying degrees of invasiveness. Melanoma, originating in melanocytes, can be highly malignant, prone to metastasis, and associated with genetic and environmental factors [47].

2.6.5 Leukemia: Leukemia is a hematological malignancy characterized by the uncontrolled proliferation of abnormal white blood cells in the bone marrow and peripheral blood. This disease encompasses several subtypes, including acute lymphoblastic leukemia (ALL), acute myeloid leukemia (AML), chronic lymphocytic leukemia (CLL), and chronic myeloid leukemia (CML), each exhibiting distinct clinical and genetic features. Leukemia disrupts normal hematopoiesis, leading to anemia, bleeding tendencies, and increased susceptibility to infections [48-50].

2.6.6 Lymphomas: Lymphomas are malignancies originating from lymphoid tissue, primarily the lymph nodes, spleen, and bone marrow. They comprise two major categories: Hodgkin lymphoma (HL) and non-Hodgkin lymphoma (NHL). HL is distinguished by the presence of Reed-Sternberg cells and often exhibits predictable clinical behavior. NHL, conversely, comprises a diverse group of lymphoid malignancies with varied histological subtypes, clinical presentations, and genetic alterations. Lymphomas disrupt the body's immune system and may cause symptoms such as lymphadenopathy, fever, night sweats, and weight loss [50-53].

2.6.7 Gastrointestinal cancers: Gastrointestinal (GI) cancers encompass a range of malignancies affecting the digestive system, including the esophagus, stomach, liver, pancreas, colon, and rectum [54, 55]. These cancers often emerge from epithelial cells lining the GI tract and are influenced by genetic, environmental, and lifestyle factors [56]. The spectrum includes

esophageal, gastric, hepatic, pancreatic, and colorectal cancers, each exhibiting distinct clinical behaviors and therapeutic challenges. Treatment modalities encompass surgery, chemotherapy, radiation therapy, targeted therapies, and immunotherapies, with the choice of approach guided by cancer subtype, stage, and individual patient factors [57].

2.6.8 Cancers of CNS: Cancers of the central nervous system (CNS) are neoplastic conditions arising within the brain and spinal cord. These malignancies are classified into primary CNS tumours, which initiate within the CNS tissues, and secondary CNS tumours, which result from metastases from distant cancer sites. Primary CNS tumours include gliomas, meningiomas, and medulloblastomas, with glioblastoma being one of the most aggressive forms [58-60]. Symptoms vary based on tumour location but may involve neurological deficits.

2.7 Types of cancer treatment and their side effects: The realm of cancer treatment encompasses a spectrum of nuanced approaches tailored to the unique characteristics, stage, and type of the disease. Serving as an unyielding adversary to human well-being, cancer has propelled the evolution of a diverse array of treatments, each distinguished by its distinctive mechanisms while accompanied by a diverse range of associated side effects (**Figure 2.5**). Among these modalities, chemotherapy, a fundamental pillar of cancer therapy, deploys cytotoxic agents to hinder the unchecked proliferation of malignant cells [61].

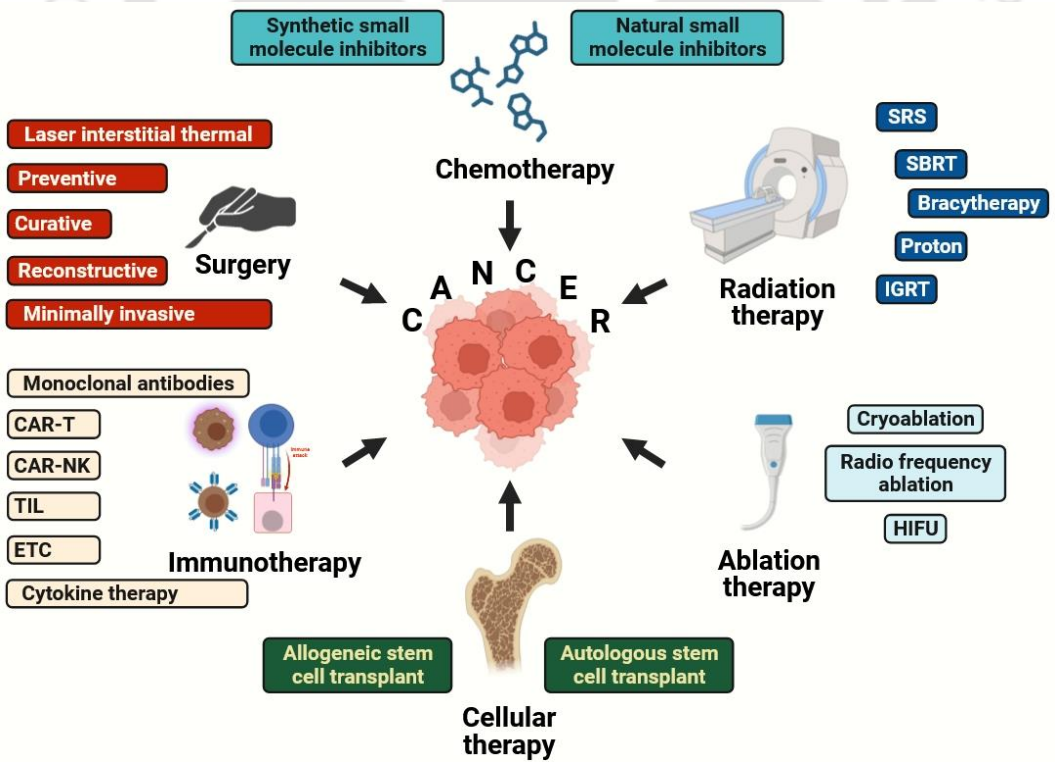

Figure 2.5: Different types of cancer treatments.

Though effective, its action lacks discrimination, impacting not only malignant cells but also healthy tissues with heightened turnover rates, yielding consequences like nausea, alopecia, fatigue, and heightened susceptibility to infections [62]. Notably vulnerable are the gastrointestinal tract, bone marrow, and hair follicles, inherent in their rapid cellular renewal [63]. In parallel, radiation therapy employs potent high-energy rays to disrupt cancer cell DNA, impeding their reproductive capability [64]. While contemporary techniques endeavour to minimize healthy tissue exposure, the spectre of side effects remains present, encompassing immediate responses such as skin irritation, fatigue, and localized discomfort that echo the aftermath of tissue disruption [65]. In the surgical sphere, interventions seek the physical excision of tumours, thereby eradicating a bulk of malignant tissue; however, contingent on the involved organ, enduring effects may encompass functional compromise, trigger metastases or the alteration of physical aesthetics [66]. Beyond this, immunotherapy harnesses the intricate arsenal of the body's immune system to discern and dismantle cancer cells [67]. Though lauded for its potential to yield enduring outcomes, immunotherapy can incite immune-related untoward effects. These encompass autoimmune responses, where the immune system erroneously targets healthy tissues, provoking inflammation within organs like the skin, gastrointestinal tract, and endocrine glands [68]. Furthermore, stem cell therapy for cancer complements chemo and radiation, targeting blood cell-forming stem cells. High doses of these treatments can harm these cells, necessitating transplants from patient or donor. Yet, risks include graft-versus-host disease, infection vulnerability, organ issues, and possible tumourigenesis [69]. Managing side effects like fatigue, nausea, and skin problems while closely monitoring is vital for patient care and treatment success. Due to the aforementioned side effects, numerous individuals battling cancer have frequently shifted their focus towards alternative medicine for treatment. This shift can be attributed to the significant adverse effects of conventional treatments, the exorbitant expenses associated with new pharmaceuticals, discontent with the outcomes of curative treatments, and the escalating resistance of microflora to existing medications.

2.8 Ayurveda and cancer: In Ayurvedic texts, ‘arbuda’ is the name for swelling or lumps situated in deep structures or as a chronic ulcer. The non-healing ulcers have been known as ‘asadhyavrana’. There are many individual plants and herbs which are used in the preparation of Ayurvedic medicine. These individual plants and herbs are well known for their anticancer activity contemporaneous with anti-inflammatory, anti-oxidant activities [70]. Many Ayurvedic medicines have been reported to have anticancer effect (**Figure 2.6)**. Arkeshwara

ras (AR) which is a herbo-metallic preparation of different plants (*Terminalia chebula, Terminalia bellerica, Phyllanthus Emblica, Plumbago zeylenica, Calotropic procera*) has been studied on two different cell line MaPaCa (Pancreatic cell line) and KB (Epithelial carcinoma). AR is an Ayurvedic formulation that has been usually used for treating ailments related to arthritis. Although originally anti-arthritic Ayurvedic medicine, it exhibited an IC_{50} of 333.33g/ml in MaCaPa cells but has no impact on KB cells. The study concluded that human pancreatic cancer cells are very sensitive to AR, as evaluated by growth inhibition and LDH release activity [71]. Panchakola which is a polyherbal formulation of five herbs & plants (*Piper longum, Piper longumLinn. (Pippalimula), Piper chaba hunter (Chavya), Plumbagozeylenicalinn. (Chitraka), ZingiberOfficinale roscoe (Sunthi)*) has been studied on MCF-7 (Breast cancer cell line) and HEK-293 (human embryonic kidney) cell lines. The cytotoxic activity of Panchakola is reported as 16.466µg/ml on MCF-7 cell line was comparable to that of curcumin (10.265 µg/ml). The Panchakola is also shown to possess anti-oxidant property and demonstrate that it is a potential source of scavenging free radicals and killing cancer cells in vitro [72]. It is intriguing that panchakola, an Ayurvedic remedy traditionally employed for alleviating nausea and aiding digestion, has gained attention for its potential anti-cancer properties. Ayurvedic formulation can be as simple as Triphala which is just a combination of three plants and can be as complex as Rasagenthi Leyham which is a formulation comprising of 38 different botanical species [73].

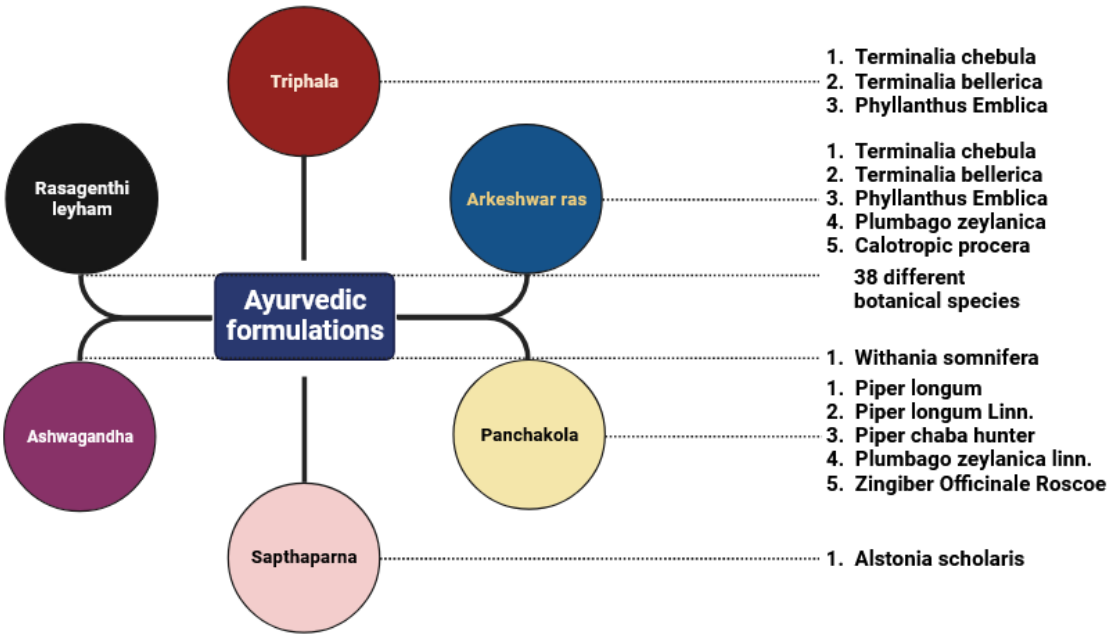

Figure 2.6: Different Ayurvedic formulations reported with anti-cancer activity.

Apart from the various Ayurvedic formulations mentioned, one of the most promising Ayurvedic formulations that has been mentioned in recent reports is Ashwagandha (*Withania somnifera*), which has been known in classical Ayurvedic texts to cure a variety of ailments such as memory impairments, musculoskeletal issues, pregnancy problems, and in general related to restoring the physical balance of the system. A research on A375 cells, a human malignant melanoma cell line, was done to see if it had anticancer efficacy. Further biochemical experiments demonstrated that the crude extract promoted apoptosis in the treated cells and produced DNA fragmentation, indicating that ashwagandha is a good candidate for anticancer activities [74].

2.8.1 Manikya Bhasma: Bhasma is a type of Ayurvedic formulation which contains metallic/non-metallic preparations. Manikya bhasma (MB), derived from ruby, arsenic sulfide, and orpiment, was studied for nano-medicinal qualities, revealing potential immunomodulation and enzymatic effects [75, 76]. Our laboratory conducted a comprehensive investigation into the potential of Manikya Bhasma as a nanomedicine with anticancer properties. Biophysical and chemical analysis unveiled crystalline, 70 nm particles within Manikya Bhasma, which exhibited significant spherical particle aggregation, as confirmed by FESEM, FETEM, and DLS assessments (**Figure 2.7**).

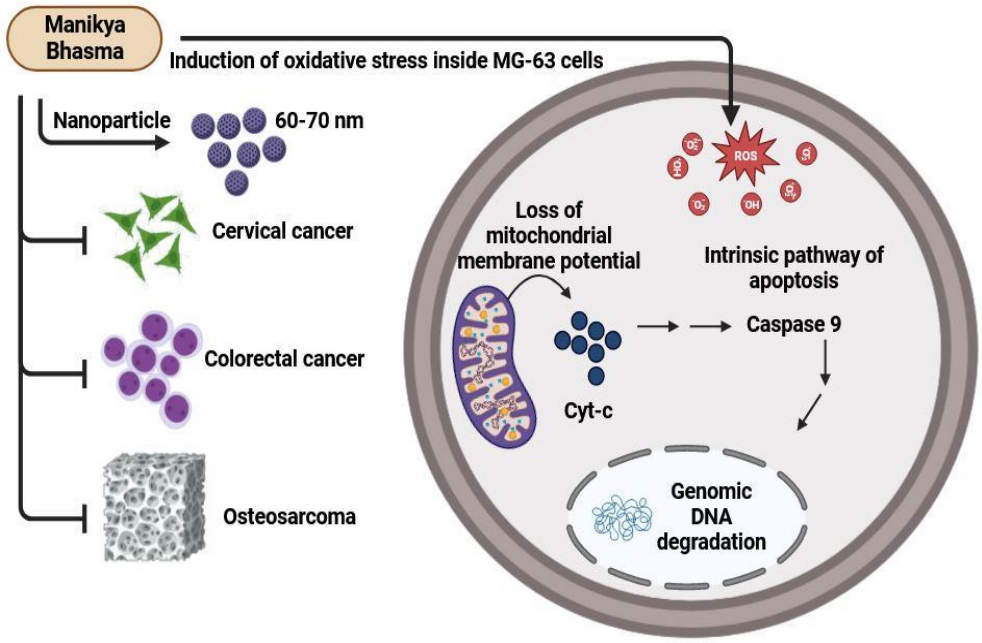

Figure 2.7: Manikya Bhasma is a nanomedicine which causes apoptosis in cancer cells.

Notably, Manikya Bhasma displayed a dose-dependent reduction in the cellular viability of various cancer cell lines, with an irreversible cytotoxic impact, suggesting its potential utility

in combating cancer relapses. Mechanistically, our study revealed that Manikya Bhasma-induced cell death followed the apoptotic pathway, with aqueous extract exhibiting substantial anticancer activity (IC_{50}: 105-155 µg/ml). This effect was likely mediated through G1 phase arrest induced by antioxidants, accompanied by apoptosis characterized by caspase activation, cytochrome-c release, and DNA degradation. [77]. The aqueous extracts of shataputi abhrak bhasma was also shown to have anticancer activity against lung cancer (HOP62), leukemia (U937) and prostate cancer (DU145) cell lines in vitro [78].

2.8.2 Rasagenthi Leyham: Rasagenthi Leyham is an Ayurvedic herbal preparation primarily employed for gastrointestinal health. It offers potential benefits in the management of digestive disorders such as dyspepsia, indigestion, and constipation, owing to its digestive and laxative properties. Additionally, it may alleviate symptoms of flatulence, mild abdominal pain, and serve as an appetite stimulant. Some traditional usage extends to providing relief from respiratory conditions like asthma and bronchitis, although its primary function remains rooted in digestive health. In addition to its digestive benefits, Rasagenthi Leyham (RL) is renowned for its potent anti-cancer activity, attributed to its composition of various plants and minerals, which endows it with a high phytochemical content. Rasagenthi Leyham (RL), a herbal preparation, exhibited significant anti-cancer potential against lung cancer cell lines (A-549 and H-460) [79].

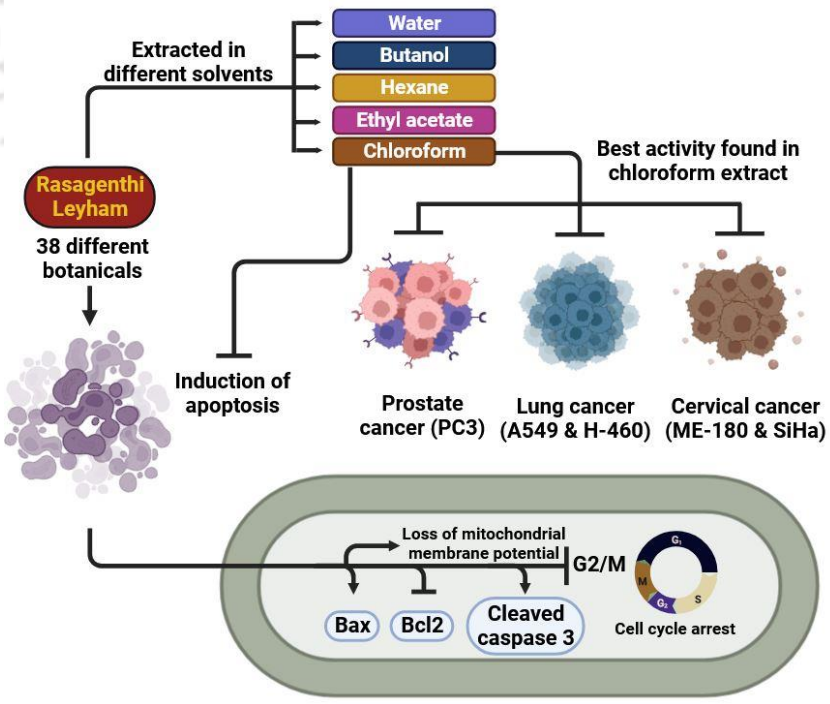

Figure 2.8: Rasagenthi Leyham chloroform extract is active against several cancers.

The chloroform fraction of RL (cRL) demonstrated remarkable inhibition of cell proliferation and induced apoptosis in these lung cancer cells while sparing normal bronchial epithelial cells (BEAS-2B). cRL achieved this by up-regulating pro-apoptotic genes (p53 and Bax), activating caspase-3, and down-regulating the pro-survival gene Bcl-2, leading to G2/M cell cycle arrest and increased sensitivity to radiation in lung cancer cells (**Figure 2.8**). Further, RL was evaluated for its potential as a complementary and alternative medicine (CAM) for prostate cancer. Extracts of RL effectively killed PC-3 prostate cancer cells and induced apoptosis, with the chloroform extract showing significant radiation-sensitizing properties [73]. This suggests that RL, either in its original formulation or as an extract, could serve as an alternative therapy for prostate cancer, especially in conjunction with radiation treatment. Furthermore, Rasagenthi Mezhugu (RGM), another traditional Siddha medicine, demonstrated efficacy against HPV-positive cervical cancer cells (ME-180 and SiHa) without the presence of toxic heavy metals [80]. The chloroform fraction of RGM (cRGM) induced DNA damage and mitochondria-mediated apoptosis, particularly in ME-180 cells, supporting its potential use as a complementary and alternative medicine for HPV-positive cervical cancer. These studies collectively emphasize the rich potential of Ayurvedic formulations such as Rasagenthi leyham in the development of novel cancer therapies and highlight the importance of evidence-based research.

2.8.3 Triphala: Triphala, a blend of three plants, has been extensively studied for its potential in treating various types of cancer. Its heterogeneous composition contains phytoconstituents that are crucial in combating cancer of different origins. Researchers have used different solvents to extract phytoconstituents from Triphala and maximize its benefits. The aqueous extract of Triphala has been found to disrupt microtubule assembly and effectively inhibit the proliferation of cells from various origins [81]. The extract has shown differential effects on normal and malignant cells, with breast cancer and thymic lymphoma cells experiencing varying levels of reactive oxygen species (ROS) generation. In mice implanted with thymic lymphoma, the aqueous extract significantly reduced tumour growth [82]. In the case of breast and prostate cancer, the cytotoxic effects of Triphala and its individual components were assessed using acetone extracts. *Terminalia chebula*, one of the components of Triphala, exhibited higher activity compared to the other components and Triphala itself when evaluated separately at different doses. This activity was attributed to the presence of gallic acid, a polyphenol in Triphala [83]. Even ethanolic extracts of Triphala showed activity against prostate cancer and normal epithelial cells, thanks to the abundant polyphenols present. Gallic

acid, detected using HPLC and FC methods, demonstrated three times greater cytotoxicity than Triphala extracts [84]. Triphala's anti-cancer activity was also found to be influenced by the p53 status of cells. It was effective against MCF-7 (p53 positive) and T47D (p53 negative) cell lines, but the magnitude of apoptosis induction differed, with MCF-7 showing slightly higher levels. The generation of ROS in cells was suggested as a potential cause for apoptosis [85]. Hydro alcoholic extracts of Triphala were used to treat mouse melanoma cells (B16F10) and Swiss albino mice. The 50% methanolic extract of Triphala was able to prevent skin cancer induced by the melanoma cell line in rats [86].

Triphala, a traditional herbal formulation, has shown promise in inhibiting multiple pathways involved in cancer development and progression. Triphala exerts its influence on key cellular pathways involved in cancer, including the P13/Akt/mTOR and ERK signaling cascades. These pathways play critical roles in tumour development and progression (**Figure 2.9**). Triphala has demonstrated its ability to modulate these pathways, thereby affecting processes such as cell growth and proliferation [87-89].

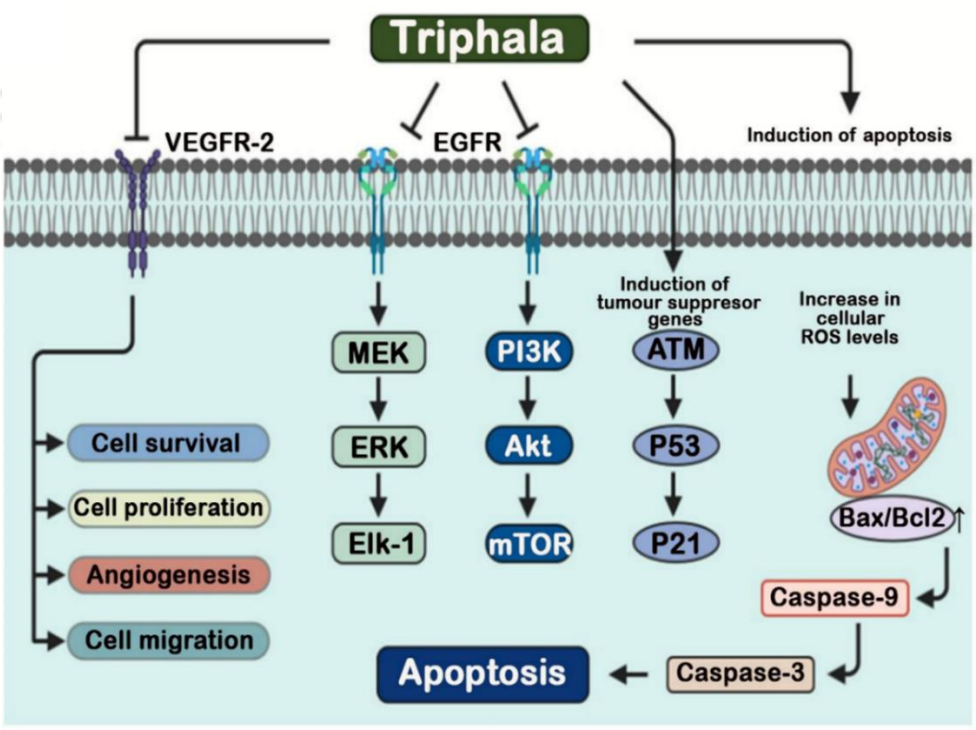

Figure 2.9: Triphala blocks multiple cellular pathway in cancer cells.

However, it is important to note that there is an exception to this inhibitory effect. In certain pancreatic cancer cells (Capan2/BXPC3 cells), Triphala actually induces the ERK pathway. This induction of ERK phosphorylation (p-ERK) has been confirmed through western blot analysis, which also showed the activation of downstream substrate Elk-1 and upstream

regulator Mek-1. This activation of p-ERK has been linked to apoptosis, as evidenced by the presence of apoptosis-related proteins such as caspase-3, caspase-9, and PARP [90] (**Table 2.1**). Interestingly, the induction of apoptosis and activation of p53 and ERK by Triphala were observed in pancreatic cancer cells (Capan-2 cells), but not in normal human pancreatic ductal epithelial cells (HPDE-6). This suggests that Triphala specifically targets cancer cells while sparing normal cells [90].

Table 2.1: Changes in protein expression in cancer cells upon Triphala treatment.

S. No.	Cell line	Cancer type	Changes in protein expression	Ref.
1	MGC-803	Human gastric tumour	p-EGFR ↓, p-Akt ↓, p-ERK1/2 ↓	[87]
2	HR8348, LoVo, LS174T	Colorectal carcinoma	p-Akt ↓, p-ERK1/2 ↓, caspase-3↑	[88]
3	SK-OV-3, HeLa & HEC-1-B	Human ovarian carcinoma, cervical carcinoma & endometrial carcinoma	p-Akt ↓, p-p44/42 ↓, p-NF-kBp56↓	[89]
4	Capan-2 & BxPC-3	Human pancreatic cancer	p-p53 ↑, p-ERK (Thr202/Tyr204) ↑, p-H2A.X ↑, p-MEK(Ser217/221) ↑, p-Elk ↑, p-ATM ↑, p21 ↑, caspase-3 ↑, caspase-9 ↑, cleaved-PARP ↑	[90]
5	HCCSC & HCT-116	Human colon cancer stem cells & human colon cancer cells.	Bax ↑, Bcl-2 ↓, PARP ↑, c-Myc ↓, Cyclin D1 ↓	[91]
6	HUVEC	Human umbilical vein endothelial cells	p-VEGFR2 ↓	[92]
7	HUVEC	Human umbilical vein endothelial cells	PTGS2 ↓, MMP9 ↓, IL6 ↓	[93]

In addition to its effects on the P13/Akt/mTOR and ERK pathways, Triphala has been shown to suppress the phosphorylation of Akt, P44/42 (also known as ERK1/2), and NF-KB in various cell lines [98]. Moreover, Triphala extracts have demonstrated significant inhibitory effects on the growth of ovarian cancer cells (SK-OV-3), cervical cancer cells (HeLa), and endometrial cancer cells (HEC1-B) [89]. Triphala has also been found to exhibit sensitivity towards the p53 status of cells. For example, it showed a difference in clonogenic growth between breast cancer cells with functional p53 (MCF-7) and those without functional p53 (T47D) [85]. The induction of p53 expression by Triphala has been confirmed in pancreatic cancer cells (Capan2 and BxPC3 cells) through the presence of upstream and downstream proteins such as p-ATM and p21, respectively, as detected by western blot analysis [90].

Interestingly, Triphala can reduce cell proliferation regardless of the p53 status. Studies have demonstrated its p53-independent effects on reducing the proliferation of colon cancer cells (HCT-116) and hepatocellular carcinoma stem cells (HCCSCs). Additionally, Triphala has been shown to decrease the levels of c-myc and cyclin-D1, while increasing the Bax/Bcl2 ratio, which are all involved in regulating cell growth and proliferation [91]. Triphala has also been found to suppress the activation of cell surface proteins such as EGFR (in MGC-803 cells) and VEGFR-2 (in HUVEC cells). EGFR is known to play a role in cell growth and proliferation, and its downstream signaling pathways are affected by Triphala. However, further research is needed to fully understand the downstream signaling changes resulting from the inhibition of VEGFR-2. VEGFR-2 is involved in various cellular processes, including cell proliferation, migration, angiogenesis, gene expression, and cell survival. Triphala and its active constituent chebulinic acid have been shown to reduce VEGFR-2 phosphorylation in HUVEC cells [87, 92, 94]. Although the scientific data on the effects of Triphala in these aspects is limited, there is a strong possibility that Triphala can inhibit cell migration, invasion, angiogenesis, and other associated processes that are critical in combating cancer at various stages of development. Understanding the detailed mechanisms of Triphala's action will require further investigation, but the existing literature provides valuable insights into its potential therapeutic effects in cancer treatment.

2.9 References

1. Amzat, J., et al., *Health, disease, and illness as conceptual tools.* Medical sociology in Africa, 2014: p. 21-37.
2. Raffaeli, W. and E. Arnaudo, *Pain as a disease: an overview.* Journal of pain research, 2017: p. 2003-2008.
3. Alberts, B., et al., *Introduction to pathogens*, in *Molecular Biology of the Cell. 4th edition*. 2002, Garland Science.
4. Church, D.L., *Major factors affecting the emergence and re-emergence of infectious diseases.* Clinics in laboratory medicine, 2004. **24**(3): p. 559-586.
5. Jakob, R., *Disease classification.* Epidemiology and Demography in Public Health, 2017: p. 37.
6. Baker, R.E., et al., *Infectious disease in an era of global change.* Nature Reviews Microbiology, 2022. **20**(4): p. 193-205.
7. Watkins, K., *Emerging infectious diseases: a review.* Current Emergency and Hospital Medicine Reports, 2018. **6**: p. 86-93.

8. Karolewski, B., T.W. Mayer, and G. Ruble, *Non-infectious diseases*, in *The Laboratory Rabbit, Guinea Pig, Hamster, and Other Rodents*. 2012, Elsevier. p. 867-873.
9. Jackson, M., et al., *The genetic basis of disease.* Essays in biochemistry, 2018. **62**(5): p. 643-723.
10. Rappaport, S.M., *Discovering environmental causes of disease.* J Epidemiol Community Health, 2012. **66**(2): p. 99-102.
11. Wang, L., F.S. Wang, and M.E. Gershwin, *Human autoimmune diseases: a comprehensive update.* Journal of internal medicine, 2015. **278**(4): p. 369-395.
12. Wang, J., et al., *Pathogenesis of allergic diseases and implications for therapeutic interventions.* Signal Transduction and Targeted Therapy, 2023. **8**(1): p. 138.
13. Hassanpour, S.H. and M. Dehghani, *Review of cancer from perspective of molecular.* Journal of cancer research and practice, 2017. **4**(4): p. 127-129.
14. Waarts, M.R., et al., *Targeting mutations in cancer.* The Journal of clinical investigation, 2022. **132**(8).
15. Hodgson, S., *Mechanisms of inherited cancer susceptibility.* Journal of Zhejiang University Science B, 2008. **9**: p. 1-4.
16. Rosendahl Huber, A., A. Van Hoeck, and R. Van Boxtel, *The mutagenic impact of environmental exposures in human cells and cancer: imprints through time.* Frontiers in Genetics, 2021: p. 2065.
17. Fares, J., et al., *Molecular principles of metastasis: a hallmark of cancer revisited.* Signal transduction and targeted therapy, 2020. **5**(1): p. 28.
18. Sung, H., et al., *Global cancer statistics 2020: GLOBOCAN estimates of incidence and mortality worldwide for 36 cancers in 185 countries.* CA: a cancer journal for clinicians, 2021. **71**(3): p. 209-249.
19. Kanwal, R. and S. Gupta, *Epigenetic modifications in cancer.* Clinical genetics, 2012. **81**(4): p. 303-311.
20. Dixon, K. and E. Kopras. *Genetic alterations and DNA repair in human carcinogenesis*. in *Seminars in cancer biology*. 2004. Elsevier.
21. Aguirre-Ghiso, J.A., *Models, mechanisms and clinical evidence for cancer dormancy.* Nature Reviews Cancer, 2007. **7**(11): p. 834-846.
22. Rivlin, N., et al., *Mutations in the p53 tumour suppressor gene: important milestones at the various steps of tumourigenesis.* Genes & cancer, 2011. **2**(4): p. 466-474.
23. Klein, C.A., *Cancer progression and the invisible phase of metastatic colonization.* Nature Reviews Cancer, 2020. **20**(11): p. 681-694.

24. Hanahan, D. and R.A. Weinberg, *The hallmarks of cancer.* cell, 2000. **100**(1): p. 57-70.
25. Hanahan, D. and R.A. Weinberg, *Hallmarks of cancer: the next generation.* cell, 2011. **144**(5): p. 646-674.
26. Fouad, Y.A. and C. Aanei, *Revisiting the hallmarks of cancer.* American journal of cancer research, 2017. **7**(5): p. 1016.
27. Luengo, A., D.Y. Gui, and M.G. Vander Heiden, *Targeting metabolism for cancer therapy.* Cell chemical biology, 2017. **24**(9): p. 1161-1180.
28. Feitelson, M.A., et al. *Sustained proliferation in cancer: Mechanisms and novel therapeutic targets*. in *Seminars in cancer biology*. 2015. Elsevier.
29. Schiliro, C. and B.L. Firestein, *Mechanisms of metabolic reprogramming in cancer cells supporting enhanced growth and proliferation.* Cells, 2021. **10**(5): p. 1056.
30. Scheel, C.H. and R. Schäfer, *Hallmark of cancer: Evasion of growth suppressors.* Frontiers in Oncology, 2023. **13**: p. 1170115.
31. Sharma, A., L.H. Boise, and M. Shanmugam, *Cancer metabolism and the evasion of apoptotic cell death.* Cancers, 2019. **11**(8): p. 1144.
32. Bailey, S.M., *Hallmark of cancer: replicative immortality.* Frontiers in Oncology, 2023. **13**: p. 1204094.
33. Saman, H., et al., *Inducing angiogenesis, a key step in cancer vascularization, and treatment approaches.* Cancers, 2020. **12**(5): p. 1172.
34. Meirson, T., H. Gil-Henn, and A.O. Samson, *Invasion and metastasis: the elusive hallmark of cancer.* Oncogene, 2020. **39**(9): p. 2024-2026.
35. Messerschmidt, J.L., G.C. Prendergast, and G.L. Messerschmidt, *How cancers escape immune destruction and mechanisms of action for the new significantly active immune therapies: helping nonimmunologists decipher recent advances.* The oncologist, 2016. **21**(2): p. 233-243.
36. Zhao, Y., E.B. Butler, and M. Tan, *Targeting cellular metabolism to improve cancer therapeutics.* Cell death & disease, 2013. **4**(3): p. e532-e532.
37. Yao, Y. and W. Dai, *Genomic instability and cancer.* Journal of carcinogenesis & mutagenesis, 2014. **5**.
38. Roncati, L. and C.R. Figueiredo, *Hallmark of cancer: tumour promoting inflammation.* Frontiers in Oncology, 2023. **13**.
39. Cormier, J.N. and R.E. Pollock, *Soft tissue sarcomas.* CA: a cancer journal for clinicians, 2004. **54**(2): p. 94-109.

40. Potter, J.W., K.B. Jones, and J.J. Barrott, *Sarcoma–The standard-bearer in cancer discovery.* Critical reviews in oncology/hematology, 2018. **126**: p. 1-5.
41. Gamboa, A.C., A. Gronchi, and K. Cardona, *Soft-tissue sarcoma in adults: an update on the current state of histiotype-specific management in an era of personalized medicine.* CA: a cancer journal for clinicians, 2020. **70**(3): p. 200-229.
42. Damerell, V., M.S. Pepper, and S. Prince, *Molecular mechanisms underpinning sarcomas and implications for current and future therapy.* Signal transduction and targeted therapy, 2021. **6**(1): p. 246.
43. Tan, W. and R. Kanesvaran, *Current standards and practice changing studies in genitourinary (GU) cancers—a review of studies in localized/early GU cancers.* ESMO open, 2022. **7**(2): p. 100432.
44. Daneshmand, S. and K.G. Chan, *Genitourinary Cancers*. 2018: Springer.
45. Craythorne, E. and F. Al-Niami, *Skin cancer.* Medicine, 2017. **45**(7): p. 431-434.
46. Urban, K., et al., *The global burden of skin cancer: A longitudinal analysis from the Global Burden of Disease Study, 1990–2017.* JAAD international, 2021. **2**: p. 98-108.
47. Saladi, R.N. and A.N. Persaud, *The causes of skin cancer: a comprehensive review.* Drugs of today (Barcelona, Spain: 1998), 2005. **41**(1): p. 37-53.
48. Bozzone, D.M., *The biology of cancer: Leukemia.* Infobase, New York, 2009.
49. Polychronakis, I., et al., *Work-related leukemia: a systematic review.* Journal of Occupational Medicine and Toxicology, 2013. **8**(1): p. 1-16.
50. Mughal, T.I., et al., *Understanding leukemias, lymphomas and myelomas*. 2013: CRC Press.
51. Evans, L.S. and B.W. Hancock, *Non-hodgkin lymphoma.* The Lancet, 2003. **362**(9378): p. 139-146.
52. Küppers, R., *The biology of Hodgkin's lymphoma.* Nature Reviews Cancer, 2009. **9**(1): p. 15-27.
53. Singh, R., et al., *Non-Hodgkin's lymphoma: a review.* Journal of family medicine and primary care, 2020. **9**(4): p. 1834.
54. Bordry, N., et al., *Recent advances in gastrointestinal cancers.* World Journal of Gastroenterology, 2021. **27**(28): p. 4493.
55. Manu, K.A., F. Bronte, and E.F. Giunta, *Reviews in gastrointestinal cancers.* Frontiers in Oncology, 2023. **13**.

56. Jardim, S.R., L.M.P. de Souza, and H.S.P. de Souza, *The Rise of Gastrointestinal Cancers as a Global Phenomenon: Unhealthy Behavior or Progress?* International Journal of Environmental Research and Public Health, 2023. **20**(4): p. 3640.
57. Sexton, R.E., et al., *Gastric cancer: a comprehensive review of current and future treatment strategies.* Cancer and Metastasis Reviews, 2020. **39**: p. 1179-1203.
58. Brem, S.S., et al., *Central nervous system cancers.* Journal of the National Comprehensive Cancer Network, 2011. **9**(4): p. 352-400.
59. Nabors, L.B., et al., *Central nervous system cancers.* Journal of the National Comprehensive Cancer Network, 2013. **11**(9): p. 1114-1151.
60. Salari, N., et al., *The global prevalence of primary central nervous system tumours: a systematic review and meta-analysis.* European journal of medical research, 2023. **28**(1): p. 1-16.
61. Anand, U., et al., *Cancer chemotherapy and beyond: Current status, drug candidates, associated risks and progress in targeted therapeutics.* Genes & Diseases, 2022.
62. Schirrmacher, V., *From chemotherapy to biological therapy: A review of novel concepts to reduce the side effects of systemic cancer treatment.* International journal of oncology, 2019. **54**(2): p. 407-419.
63. Amjad, M.T., A. Chidharla, and A. Kasi, *Cancer chemotherapy*. 2020.
64. Baskar, R., et al., *Cancer and radiation therapy: current advances and future directions.* International journal of medical sciences, 2012. **9**(3): p. 193.
65. Majeed, H. and V. Gupta, *Adverse effects of radiation therapy*. 2020.
66. Tohme, S., R.L. Simmons, and A. Tsung, *Surgery for cancer: a trigger for metastases.* Cancer research, 2017. **77**(7): p. 1548-1552.
67. McCune, J.S., *Rapid advances in immunotherapy to treat cancer*, 2018, Wiley Online Library. p. 540-544.
68. Kichloo, A., et al., *Systemic adverse effects and toxicities associated with immunotherapy: A review.* World Journal of Clinical Oncology, 2021. **12**(3): p. 150.
69. Chu, D.-T., et al., *Recent progress of stem cell therapy in cancer treatment: molecular mechanisms and potential applications.* Cells, 2020. **9**(3): p. 563.
70. Kumar, S., T. Jawaid, and S.D. Dubey, *Therapeutic plants of Ayurveda; a review on anticancer*. Pharmacognosy Journal, 2011. **3**(23): p. 1-11.
71. Nafiujjaman, M., et al., *Anticancer activity of Arkeshwara Rasa-A herbo-metallic preparation.* Ayu, 2015. **36**(3): p. 346.

72. Shamsi, T.N., R. Parveen, and S. Fatima, *Panchakola reduces oxidative stress in MCF-7 breast cancer and HEK293 cells.* Journal of dietary supplements, 2018. **15**(5): p. 704-714.
73. Ranga, R.S., et al., *Rasagenthi lehyam (RL) a novel complementary and alternative medicine for prostate cancer.* Cancer chemotherapy and pharmacology, 2004. **54**(1): p. 7-15.
74. Halder, B., S. Singh, and S.S. Thakur, *Withania somnifera root extract has potent cytotoxic effect against human malignant melanoma cells.* PLoS One, 2015. **10**(9): p. e0137498.
75. Dash, B., *Alchemy and metallic medicines in Ayurveda*. 1986: Concept Publishing Company.
76. Suneetha, M., *Pharmaceutico analytical study of Manikya bhasma*, 2010, Rajiv Gandhi University of Health Sciences (India).
77. Jha, S. and V. Trivedi, *Manikya Bhasma is a nanomedicine to affect cancer cell viability through induction of apoptosis.* Journal of Ayurveda and integrative medicine, 2021. **12**(2): p. 302-311.
78. Tamhankar, Y.L. and A.P. Gharote, *Effect of Puta on in vitro anticancer activity of Shataputi Abhrak Bhasma on lung, leukemia and prostate cancer cell lines.* Journal of Ayurveda and integrative medicine, 2020. **11**(2): p. 118-123.
79. Ranga, R.S., et al., *A herbal medicine for the treatment of lung cancer.* Molecular and cellular biochemistry, 2005. **280**: p. 125-133.
80. Riyasdeen, A., et al., *Chloroform extract of Rasagenthi Mezhugu, a Siddha formulation, as an evidence-based complementary and alternative medicine for HPV-positive Cervical Cancers.* Evidence-Based Complementary and alternative medicine, 2012. **2012**.
81. Cheriyamundath, S., et al., *Aqueous extract of Triphala inhibits cancer cell proliferation through perturbation of microtubule assembly dynamics.* Biomedicine & Pharmacotherapy, 2018. **98**: p. 76-81.
82. Sandhya, T., et al., *Potential of traditional Ayurvedic formulation, Triphala, as a novel anticancer drug.* Cancer letters, 2006. **231**(2): p. 206-214.
83. Kaur, S., et al., *The in vitro cytotoxic and apoptotic activity of Triphala—an Indian herbal drug.* Journal of ethnopharmacology, 2005. **97**(1): p. 15-20.

84. RUSSELL, L.H., et al., *Differential cytotoxicity of Triphala and its phenolic constituent gallic acid on human prostate cancer LNCap and normal cells.* Anticancer research, 2011. **31**(11): p. 3739-3745.
85. Sandhya, T. and K. Mishra, *Cytotoxic response of breast cancer cell lines, MCF 7 and T 47 D to Triphala and its modification by antioxidants.* Cancer letters, 2006. **238**(2): p. 304-313.
86. Birla, N. and P.K. Das, *Phytochemical and anticarcinogenic evaluation of Triphala powder extract, against melanoma cell line induced skin cancer in rats.* Pharm. Biol. Eval, 2016. **3**(3): p. 366-370.
87. Tsering, J. and X. Hu, *Triphala suppresses growth and migration of human gastric carcinoma cells in vitro and in a zebrafish xenograft model.* BioMed Research International, 2018. **2018**.
88. Wang, M., Y. Li, and X. Hu, *Chebulinic acid derived from Triphala is a promising antitumour agent in human colorectal carcinoma cell lines.* BMC complementary and alternative medicine, 2018. **18**(1): p. 1-9.
89. Zhao, Y., et al., *An integrated study on the antitumour effect and mechanism of Triphala against gynecological cancers based on network pharmacological prediction and in vitro experimental validation.* Integrative Cancer Therapies, 2018. **17**(3): p. 894-901.
90. Shi, Y., R.P. Sahu, and S.K. Srivastava, *Triphala inhibits both in vitro and in vivo xenograft growth of pancreatic tumour cells by inducing apoptosis.* BMC cancer, 2008. **8**(1): p. 1-16.
91. Vadde, R., et al., *Triphala extract suppresses proliferation and induces apoptosis in human colon cancer stem cells via suppressing c-Myc/Cyclin D1 and elevation of Bax/Bcl-2 ratio.* BioMed research international, 2015. **2015**.
92. Lu, K., et al., *Triphala and its active constituent chebulinic acid are natural inhibitors of vascular endothelial growth factor-a mediated angiogenesis.* 2012.
93. Wang, W., et al., *Study on the multi-targets mechanism of Triphala on cardio-cerebral vascular diseases based on network pharmacology.* Biomedicine & pharmacotherapy, 2019. **116**: p. 108994.
94. Wang, X., et al., *Molecular bases of VEGFR-2-mediated physiological function and pathological role.* Frontiers in Cell and Developmental Biology, 2020. **8**: p. 599281.

Chapter III

Experimental Procedures

3.1 Introduction: This chapter provides a comprehensive and detailed account of the experimental procedures undertaken throughout the course of this thesis, with the primary aim of facilitating reproducibility and comprehension of the research endeavors detailed herein (**Figure 3.1**). The following sections presents a broad overview of the experimental methodologies employed during the course of thesis work.

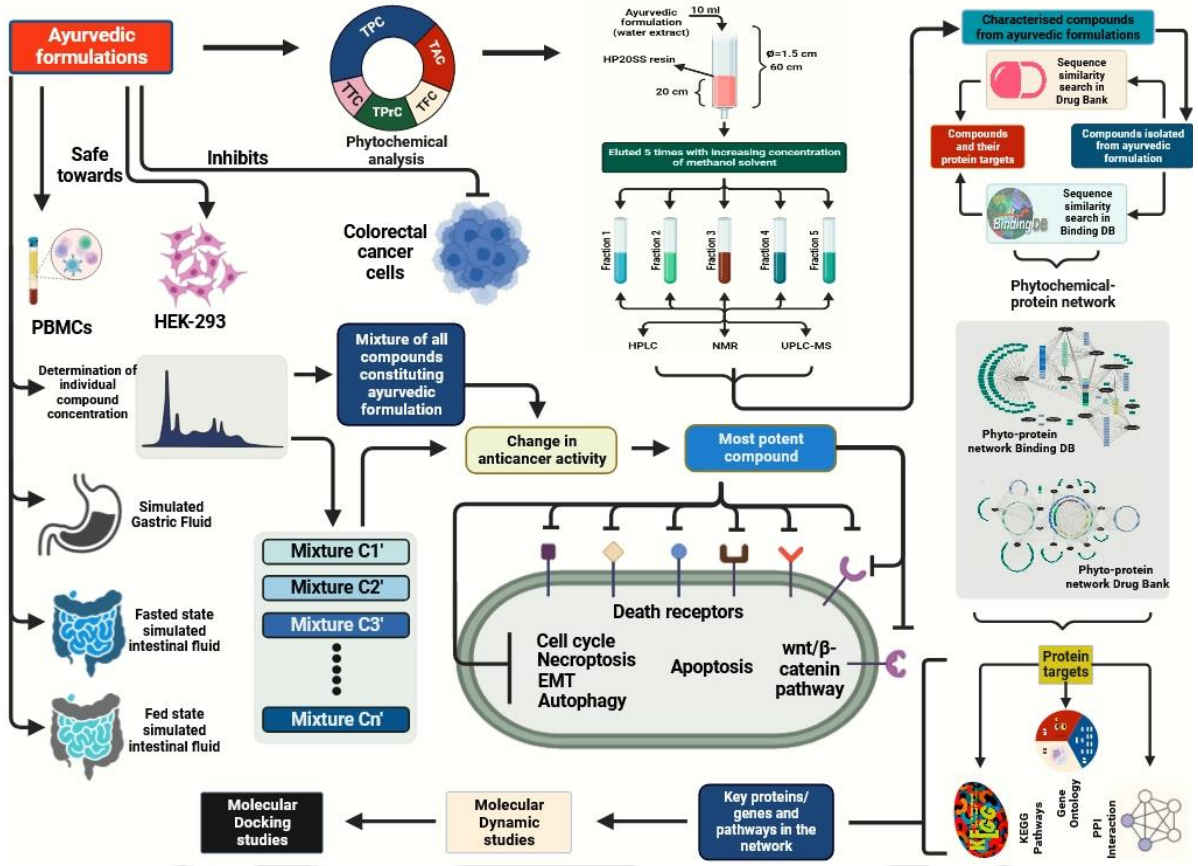

Figure 3.1: A schematic of the experimental procedures followed in current thesis work.

3.2 Materials: Ayurvedic formulations were purchased from a local Baidyanath store in Guwahati, Assam, India. Dulbecco's modified eagle's medium, 3-(4, 5-dimethylthiazol-2-yl)-2, 5-diphenyltetrazolium bromide (MTT) from Sigma Aldrich (St. Louis, MO, USA) and Percoll were purchased from Sigma (St. Louis, MO, USA). Acridine orange (AO), propidium iodide (PI), Ethidium bromide (Et-Br), DMSO (cell-culture grade), Proteinase K, RNase-A, ethylenediamine tetraacetic acid (EDTA), 100% ethanol, sodium chloride, Tris-base, NP-40 detergent and Triton-X 100 were purchased from Merck (Massachusetts, USA). DMEM: F12 media was purchased from GIBCO (USA). Foetal Bovine Serum (FBS), Penicillin-Streptomycin (100X) antibiotic solution, Phosphate Buffer Saline (PBS), Sodium Azide, tween-20, trypan blue, and trypsin were obtained from HiMedia (Mumbai, India). All the cell

culture plates and dishes were purchased from Corning, Lowell, MA, USA. MDAMB-231 (Breast cancer cell line), DLD-1 (Colorectal cancer), HCT-116 (Colorectal cancer), HT-29 (Colorectal cancer), MG-63 (Osteosarcoma), HeLa (Cervical cancer), and HEK-293 (Kidney epithelial) cell lines were procured from National Centre for Cell Sciences, Pune, India.Acetone-d_6 (Deuterated acetone), DMSO-d_6 (Deuterated DMSO), CD_3OD (Deuterated methanol), and D_2O (Deuterated water) were purchased from Kanto Chemical Co. Inc. Tokyo, Japan. Pancreatin, Sodium taurocholate, lecithin, and maleic acid were procured from HiMedia (Mumbai, India). Glyceryl monooleate and sodium oleate were procured from sigma Aldrich. Death receptor antibody sampler kit (cat. # 29603), autophagy antibody sampler kit (cat. # 4445), apoptosis/necroptosis antibody sampler kit (cat. # 92570), and antibodies to cyclin A2 (cat. # 67955), GAPDH (cat. # 5174) were purchased from cell signaling technology, Inc (USA). Antibodies detecting β-actin (cat. # BB-AB0024), Bcl2 (cat. # BB-AB0230), PARP-1 (cat. # BB-AB0280) were procured from Bio-Bharathi Life science private ltd. (India). Wnt pathway antibody sampler panel (cat. # ab242226), and EMT marker/Epithelial to mesenchymal transition marker panel (cat. # ab216833) were purchased from Abcam (UK). Anti-Cytochrome-C (338200) antibody was procured from Invitrogen. All other reagents and chemicals were of analytical grade purity.

3.3 Aqueous extract of Ayurvedic formulation: One gram of an Ayurvedic formulation was dissolved in 5 ml of distilled water. The mixture was then incubated at 37°C for 2 hours while being gently agitated at 150 RPM. This process aimed to simulate the physiological conditions under which Ayurvedic formulations are typically consumed, ensuring the extraction of only water-soluble components from the formulation. After incubation, the mixture was subjected to centrifugation at 6000 RPM for 10 minutes at room temperature. The supernatant was carefully collected, and the pellet was re-suspended in 5 ml of water. The mixture was thoroughly shaken and incubated once again at 37°C for 2 hours at 150 RPM to maximize the extraction of water-soluble components from the Ayurvedic formulation. Following the second incubation, the mixture underwent another round of centrifugation at 6000 RPM for 10 minutes at room temperature. Once again, the supernatant was collected and combined with the supernatant obtained from the first extraction. The resulting combined supernatant was then subjected to lyophilisation to remove the water content, resulting in a dry powder form of the water-soluble components from the Ayurvedic formulation. This powder was stored at 4ºC until it was ready for further use.

3.4 Cell Culture: Cancer cell lines of interest were procured from CDRI (Central Drug Research Institute)-Lucknow. MDAMB-231 cells (Breast cancer cell line), HeLa (Cervical cancer cell line), DLD1, HT29, HCT-116 (Colon cancer cell lines), MG-63 (Osteosarcoma cell line), and HEK-293 (Human embryonic kidney) cells were cultured in DMEM: F12 High glucose media, supplemented with 10% fetal bovine serum (FBS) and 1% penicillin-streptomycin antibiotic solution (100units/ml penicillin and 100µg/ml streptomycin sulphate). Cells were grown in humidified 5% CO_2 incubator at 37°C.

3.5 MTT cell viability assay: The MTT viability assay was employed to measure cellular viability, using the dye MTT (3-(4,5-Dimethylthiazol-2-yl)-2,5-Diphenyltetrazolium Bromide). To prepare the MTT solution, it was dissolved in sterile phosphate-buffered saline (PBS) at a concentration of 0.5 mg/ml. In each well of a 96-well plate, ten thousand cells were seeded in 0.2 ml of DMEM: F12 complete medium and left to incubate overnight. Following overnight incubation, the cells were washed twice with cell culture-grade PBS and then treated with varying concentrations (0-1000 µg/ml) of Ayurvedic formulation in 0.2 ml of serum-free medium (incomplete medium) for 48 hours. Cells treated only with incomplete medium were used as the reference for 100% viability. After the treatment period, the cells were washed twice with PBS and exposed to 100 µl of MTT solution (0.5 mg/ml) for 4 hours at 37°C with 5% CO2. Subsequently, the MTT solution was removed, and the formazan crystals formed were dissolved in 100 µl of cell culture-grade DMSO. The optical density was measured using a spectrophotometer (SpectraMax M2) at 570 nm and 660 nm (to account for scattering effects of crystals). The results were expressed as the percentage of survival compared to the control [1, 2]. Images of the untreated and treated cells were taken from random 10 fields using the Cytell cell imaging system (GE healthcare).

3.6 Phytochemical analysis of aqueous extract of Ayurvedic formulation: The presence of phenolics, flavonoids, terpenoids, alkaloids and proteins in the Ayurvedic formulation was qualitatively analyzed using standard detection methods [3-7].

3.7 Fractionation of aqueous extract of Ayurvedic formulation using Reverse-phase open column chromatography: Open column chromatography was performed for the separation of fractions from the supernatant obtained by dissolving the Ayurvedic formulation in water as discussed previously. The column is prepared with Diaion HP20SS (Mitsubishi chemical, Japan) resin. The column is filled with HP20SS resin to 20 cm in a 60 cm long column having an inner diameter of 1.5 cm. The column was then conditioned with water equivalent to four

volumes of resin length. The sample was poured onto the resin and allowed to settle for few minutes. The column was then eluted serially with increasing ratio of methanol to water as follows: Fraction 1: Methanol-water (0:100), Fraction 2: Methanol-water (20:80), Fraction 3: Methanol-water (50:50), Fraction 4: Methanol-water (80:20), Fraction 5: Methanol-water (100:0). The fractions were dried using rotary evaporator and kept at 4^0C for further use

3.8 Gradient HPLC analysis: The High-performance liquid chromatography analysis was used to determine the polyphenols present in the aqueous extract of Ayurvedic formulation. The column used was YMC-TRIART C_{18}- (4.6ID X 250mm) and the flow rate was maintained at 1mL/min. The oven temperature was kept constant at 35^0C throughout the HPLC runtime and absorbance was recorded at 254 nm. The mobile phases were A: acetonitrile (0.5% HCOOH) and B: water (0.5% HCOOH). The linear gradient of A in B from 0% to 100% over 30 minutes.

3.9 Isolation of individual compounds from reverse phased fractions: The open phase column chromatography yielded five distinct fractions, which were subsequently analyzed using High-Performance Liquid Chromatography (HPLC). In this analysis, the solvent phases were fine-tuned based on the results obtained from gradient HPLC experiments. Each of the five fractions (fraction **1**, fraction **2**, fraction **3**, fraction **4**, and fraction **5**) was separately subjected to HPLC using different solvent compositions. Fraction **1** was analyzed using a solvent consisting of 1% methanol, fraction **2** with 5% methanol, fraction **3** with 10% acetonitrile, fraction **4** with 30% methanol, and fraction **5** with 20% acetonitrile in water acidified with 0.5% formic acid. During the HPLC analysis, a reverse phased YMC-TRIART-C_{18} column with dimensions of 4.6mm internal diameter and 250 mm length was employed. The flow rate was set at 1mL/min to maintain a consistent separation rate. To ensure accuracy, the column temperature was tightly controlled and kept constant at 35°C throughout the analysis. The detection wavelength for measuring absorbance was set at 254nm.

3.10 NMR analysis: ^{1}H, ^{13}C NMR, and 2D NMR were recorded in JEOL ECA 500 spectrometer (500 MHz, JEOL Ltd, Tokyo Japan) and BRUKER Biospin AVANCEIII 600 (600 MHz, Bruker, Massachusetts, USA). The spectra were recorded in Acetone-d_6, DMSO-d_6, CD3OD, and D_2O at 298K. The expression of coupling constants is in hertz and chemical shifts are represented by δ in (parts per million) ppm scale. Tetramethylsilane (TMS) was added to the samples which served as an internal standard.

3.11 Mass spectra analysis: Analysis was performed on a UPLC system coupled to a QTOF-MS (Waters Xevo G2 QTof, Waters, Milford, MA, USA) instrument operated in electrospray ionization (ESI) mode at a mass resolution of 20,000 and controlled by Mass Lynx 4.1 software. An Acquity UPLC BEH C_{18} column (2.1 mm I.D. x 100 mm, 1.7 µm, Waters, USA) at 35 °C was used for chromatographic separation. The sample (1 µL) was injected using an autosampler. The mass spectrometer was calibrated with 0.5 mM sodium formate. Leucine enkephalin (2 µg/mL, m/z 554.2615 in negative mode) was used as lock spray at a flow rate of 10 µL/min. The collision energy equalled 6V. The source parameters were as follows: capillary voltage 2.5kV, sampling cone voltage 30V, extraction cone voltage 4V, source temperature 150^0C, desolvation temperature 500^0Cgas flow 1000L/h, cone gas flow 50L/h. The mass spectrum analysis was done using Waters Xevo G2 QTof. The column used is AQUITY UPLC BEH C_{18} 1mm ID x 100mm.

3.12 Preparation of peripheral blood mononuclear cells (PBMCs): Blood was taken from a healthy volunteer and PBMCs were isolated using HiSeP from HiMedia™ [8] as per manufacturer's protocol. The PBMC cells were re-suspended in DMEM: F12 high glucose medium supplemented with 1% Penicillin-Streptomycin antibiotic solution and 10% FBS. The cells were treated with varying concentrations of Haritaki Churna aqueous extract and the cell viability of the PMBCs was calculated using MTT cell viability assay.

3.13 Preparation of biological fluids present in digestive system

3.13.1 Simulated gastric fluid (SGF): Simulated gastric fluid was prepared as described [9]**.** To begin, 2 grams of sodium chloride was dissolved into 600-700 ml of deionized or distilled water. The pH of the solution was adjusted to 1.2 with HCl. Once the pH was adjusted, 3.2 grams of pepsin (with an activity range of 800-1200 units per milligram) was added and continuously stirred until fully dissolved. Later volume of the solution was made-up to 1 litre with deionized or distilled water. To reach a final volume of 1 litre, the mixture is supplemented with deionized or distilled water.

3.13.2 Fasted state Simulated Intestinal Fluid (FaSSIF): The development of FaSSIF aimed to improve the representation of fasting conditions in the stomach during drug dissolution testing. This biorelevant medium mimics the fasting environment found in the upper portion of the small intestine. It consists of a stable phosphate buffer, sodium taurocholate (to mimic bile salts), and lecithin (as a phospholipid source). This combination facilitates the formation of mixed micelles, leading to enhanced dissolution of drugs with low solubility and high

lipophilicity. FaSSIF was prepared as described [9]. FaSSIF was prepared with sodium taurocholate (3 mM), lecithin, (0.2 mM), maleic acid (19.12 mM), sodium chloride (68.62 mM), and sodium hydroxide (34.8 mM) in 1 litre of deionized water with a pH of 6.5.

3.13.3 Fed state Simulated Intestinal Fluid (FeSSIF): The conditions for drug dissolution in the proximal part of the small intestine are influenced by whether the drug is taken in a fed or fasted state. After a meal, changes occur in hydrodynamics, intralumenal volume, pH, buffer capacity, osmolality, and bile output, all of which can affect drug bioavailability. To simulate the fed state, a fed state simulating intestinal fluid (FeSSIF) was prepared as described [9]. FeSSIF was prepared with sodium taurocholate (10 mM), lecithin, (2 mM), glyceryl monooleate (5mM), sodium oleate (0.8 mM), maleic acid (55.02 mM), sodium chloride (125.5 mM), and sodium hydroxide (81.65 mM) in 1 litre of deionized water with a pH of 5.8.

3.14 Identification of the crucial agent for anti-cancer activity in Ayurvedic formulations: The concentrations of each compound identified from Ayurvedic formulation were evaluated by calculating area under the peak from gradient HPLC chromatogram. Based on the composition of Ayurvedic formulation obtained, different mixtures such as CM, C1′-Cn′ were made. CM (Complete mixture) contained all the identified compounds which was formulated as per the composition. Mixture C1′ was made using all identified compounds except compound C1. Mixture C2′ was made using all identified compounds except compound C2 and so forth. The IC_{50} values of all the resultant mixtures were evaluated using MTT assay to find out the variations in their ability to kill cancer cells in a dose dependent manner.

3.15 Cell cycle analysis: Propidium Iodide was used to measure the DNA content of cells through flow cytometry. Cells were initially seeded in a 6-well plate with $5*10^5$ cells in each well and allowed to grow overnight in DMEM: F12 complete medium. The following day, DLD1/HCT-116 cells treated using different concentrations of most potent compound from Ayurvedic formulation in DMEM: F12 serum-free medium for 24 hours. After the treatment, cells were washed twice with cell-culture grade PBS and then detached from the wells using a 0.6% EDTA solution in sterile PBS. The cells were then centrifuged, and the pellet was re-suspended in 500 µl of PBS. The cells were fixed by adding 70% ethanol while continuously stirring the cell suspension. After fixing, the cells were stored at -20°C for 2-3 hours. Subsequently, the cells were washed twice with ice-cold PBS by centrifuging at 5000 RPM at 4°C. The resulting cell pellet was re-suspended in ice-cold PBS, and RNase-A was added at a final concentration of 10 µg/ml. The mixture was then incubated at 37°C for 2 hours.

Subsequently, the staining was performed with a final concentration of 30 µg/ml of Propidium Iodide. The stained cells were immediately analyzed at room temperature using a BD FACS Caliber flow cytometer. Each sample consisted of 50,000 cells, and the excitation was carried out at 488 nm, with emission collected at 585/42 nm filter (FL-2). The distribution of cells in different cell cycle phases was analyzed using FCS-5 express software. For comparison, cells treated only with the medium, without any experimental treatment, were considered as the control group.

3.16 Live and apoptotic cell staining by Acridine orange/Propidium iodide method: The live and apoptotic cells were stained by acridine orange and propidium iodide as described previously [1, 2]. $1*10^5$ DLD1/HCT-116 cells were placed in each well of a 24-well plate overnight, using DMEM: F12 complete medium. The following day, these cells were treated with most potent compound from Ayurvedic formulation at various concentrations, prepared in serum-free medium, for 48 hours. After treatment, the cells were detached from the culture plates using PBS containing 0.6% EDTA. They were then centrifuged and re-suspended in 500 µl of PBS. To assess cell viability and apoptosis, the cells were stained using Acridine Orange (1 µg/ml) and Propidium Iodide (10 µg/ml) and incubated for 30 minutes at room temperature. Subsequently, the data was acquired for the stained cells immediately using BD FACS Caliber using Cell Quest pro software (BD Biosciences, USA). Both fluorophores were excited at 488 nm, and their emission signals were collected at different wavelengths: acridine orange at 530/30 nm filter (FL-1) and propidium iodide at 650 nm filter (FL-3). The acquired data was then analyzed using FCS-5 express software. To distinguish between healthy, early apoptotic, late apoptotic, and necrotic cells within the total cell population, quadrant analysis was employed. A control group, treated with serum-free medium alone, was used to set the initial quadrant for comparison.

3.17 DNA fragmentation assay: The DNA fragmentation assay is a method used to differentiate between healthy, apoptotic, and necrotic cells based on their patterns of DNA fragmentation. To conduct the assay, $5*10^5$ cells (DLD1, HCT-116 and HT-29) were initially seeded in each well of a 6-well plate and left overnight in a complete medium (DMEM: F12). The following day, the cells were treated with most potent compound from Ayurvedic formulation at appropriate IC_{50} concentrations in serum-free medium for 48 hours at 37°C. The control group consisted of cells treated with serum-free medium only. After the treatment period, the cells were washed twice with sterile ice-cold PBS and then lysed using a lysis buffer containing 100 mM Tris-HCl (pH 8.0), 2 mM EDTA, and 0.8% w/v SDS. To eliminate any

RNA present in the samples, DNase-free RNase A (50 mg/ml) was added to the lysate and incubated at 37°C for 30 minutes. Subsequently, Proteinase K (10 µl of 20 mg/ml) was added to the samples and incubated for 2 hours at 55°C to digest proteins. The lysate samples were then mixed with 6x DNA loading buffer from NEB (USA) and separated on a 1.8% agarose gel containing ethidium bromide (0.3 µg/ml) at 50 mA for 6 hours at 4°C. The DNA laddering was observed under UV light and images were taken in a BIO-RAD chemidoc™ imaging system [1, 2].

3.18 Western blotting: Colorectal cancer cells were seeded in a 6 well plate prior to the day of the experiment. Cells were washed twice with PBS and were treated with Ayurvedic formulations/most potent compound from Ayurvedic formulation for 24 and 48 hours. Cells were harvested and lysed with RIPA lysis buffer and the protein content was measured using standard protein assays. Proteins were separated on a 10% SDS-polyacrylamide gel and then transferred to nitrocellulose membrane (Bio-Rad cat. # 162-0112) on a Trans-Blot Turbo (Bio-Rad). The membrane was blocked with 5% BSA for 1-2 hours at room temperature. The blots were then incubated with primary antibodies (DR3 (1:2500), DR4 (1:2500), DR5 (1:2500), DR6 (1:2000), TNFR1 (1:2000), TNFR2 (1:2000), Fas (1:2000), RIP (1:2000), MLKL (1:2000) p-RIP (1:1000), p-MLKL (1:1000), Cleaved caspase 3 (1:2000), Cleaved caspase 8 (1:2000), Caspase 3 (1:2000), Caspase 8 (1:2000), Bcl2 (1:2000), Cytochrome-C (1:1000), CyclinA2 (1:4000), Axin-2 (1:5000), GSK-3β (1:5000), LEF-1 (1:5000), β-catenin (1:5000), Cyclin D1 (1:5000), E-cadherin (1:2500), N-cadherin (1:2500), vimentin (1:2500), snail+slug (1:2500), Atg3 (1:2000), Atg5 (1:2000), Atg7 (1:2000), Atg12 (1:2000), Atg16L1 (1:2000), Beclin-1 (1:2000), LC3I/II (1:2000), GAPDH (1:5000) and β-actin (1:5000)) overnight at 4ºC followed by incubation with appropriate HRP conjugated secondary antibodies for 1-2 hours at room temperature. Proteins bands were analyzed by using Bio-Rad Clarity™ Western ECL substrate kit and images were developed in Bio-Rad chemiDoc system

3.19 Statistical analysis: Sample values are expressed as mean ± standard deviation (SD), N=3. All the IC_{50} values were calculated using a non-linear curve fit model in ORIGIN 2019 software

3.20 References

1. Deka, S.J., et al., *Danazol has potential to cause PKC translocation, cell cycle dysregulation, and apoptosis in breast cancer cells.* Chemical biology & drug design, 2017. **89**(6): p. 953-963.

2. Deka, S.J., et al., *Alkyl cinnamates induce protein kinase C translocation and anticancer activity against breast cancer cells through induction of the mitochondrial pathway of apoptosis.* Journal of breast cancer, 2016. **19**(4): p. 358-371.
3. Singleton, V.L., R. Orthofer, and R.M. Lamuela-Raventós, *[14] Analysis of total phenols and other oxidation substrates and antioxidants by means of folin-ciocalteu reagent*, in *Methods in enzymology*. 1999, Elsevier. p. 152-178.
4. Zhishen, J., T. Mengcheng, and W. Jianming, *The determination of flavonoid contents in mulberry and their scavenging effects on superoxide radicals.* Food chemistry, 1999. **64**(4): p. 555-559.
5. Sreevidya, N. and S. Mehrotra, *Spectrophotometric method for estimation of alkaloids precipitable with Dragendorff's reagent in plant materials.* Journal of AOAC international, 2003. **86**(6): p. 1124-1127.
6. Ernst, O. and T. Zor, *Linearization of the Bradford protein assay.* JoVE (Journal of Visualized Experiments), 2010(38): p. e1918.
7. Das, B., et al., *Phytochemical screening and evaluation of analgesic activity of Oroxylum indicum.* Indian journal of pharmaceutical sciences, 2014. **76**(6): p. 571.
8. Böyum, A., *Isolation of mononuclear cells and granulocytes from human blood. Isolation of monuclear cells by one centrifugation, and of granulocytes by combining centrifugation and sedimentation at 1 g.* Scandinavian journal of clinical and laboratory investigation. Supplementum, 1968. **97**: p. 77-89.
9. Klein, S., *The use of biorelevant dissolution media to forecast the in vivo performance of a drug.* The AAPS journal, 2010. **12**(3): p. 397-406.

Chapter IV

Identification and characterization of anti-cancer agents from selected Ayurvedic formulations*

*The content of this chapter is partly published as **"Khan, M.R.U.Z.,** Yanase, E. and Trivedi, V., 2023**. Extraction, phytochemical characterization and anti-cancer mechanism of Haritaki Churna: An Ayurvedic formulation.** Plos one, 18(5), p.e0286274**."**

4.1 Introduction: Despite the rich reservoir of phytochemicals and bioactive agents present in Ayurvedic formulations, a significant number of them have not been thoroughly investigated for their phytochemical composition. In this comprehensive study, Ayurvedic formulations, well-known for their diverse range of activities including anti-cancer properties, are systematically evaluated with a primary focus on inhibiting and eradicating colorectal cancer cells (CRCs), as depicted in **Figure 4.1**. This chapter aims to address this gap by conducting a rigorous assessment of Ayurvedic formulations to determine their effectiveness against CRCs. Moreover, an exhaustive analysis of aqueous extracts derived from the selected Ayurvedic formulations is performed, focusing on the identification and quantification of phytochemicals present in these extracts

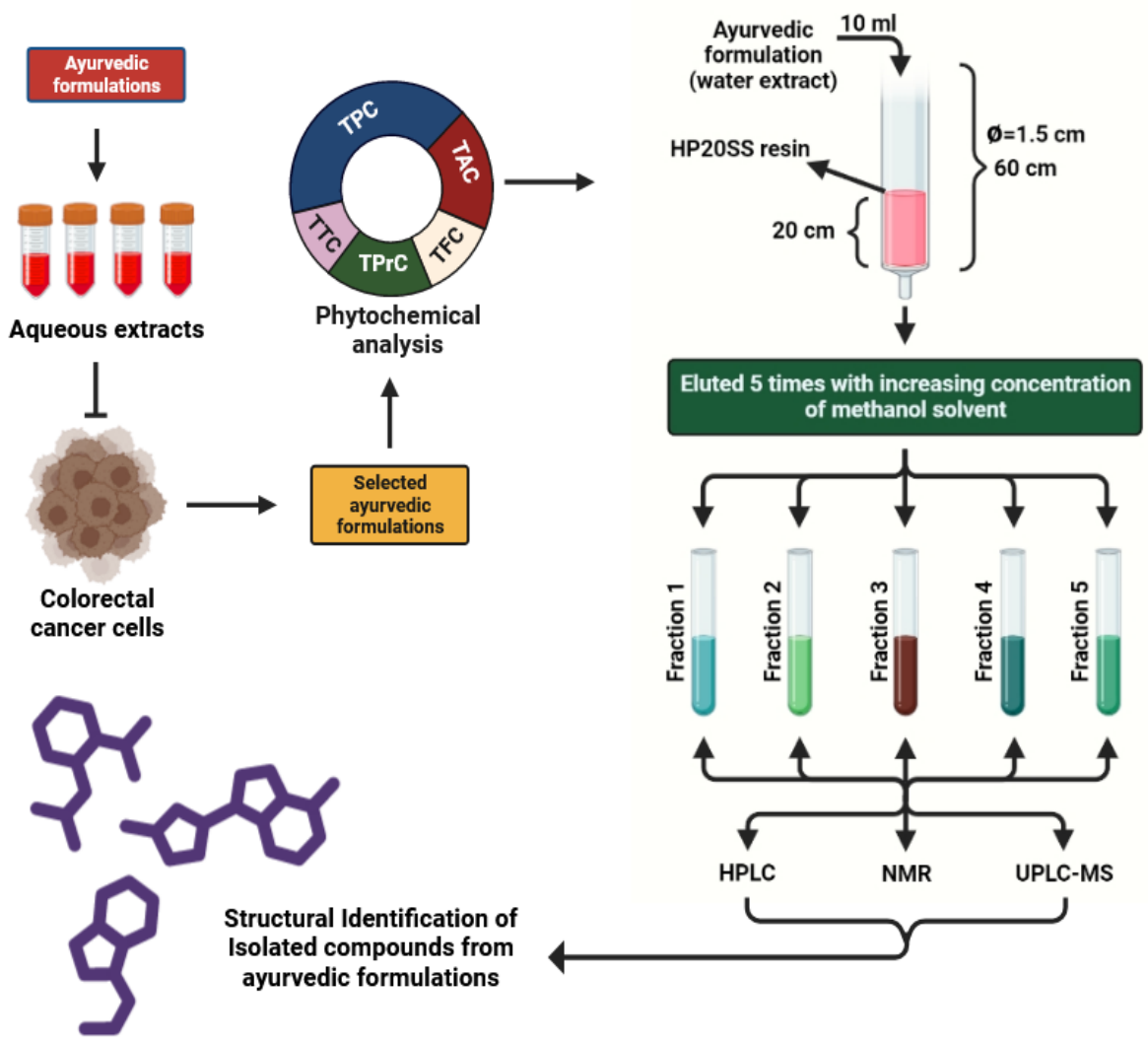

Figure 4.1: **Anti-cancer activity, phytochemical analysis, separation and identification of compounds in Ayurvedic formulations.**

4.2 Experimental procedures

4.2.1 Aqueous extract of Ayurvedic formulation: Aqueous extract of Ayurvedic formulation was prepared as described in section **3.3**.

4.2.2 Cell Culture: Colorectal cancer cell lines DLD1, HT29 and HCT-116 were cultured in DMEM: F12 High glucose media, supplemented with 10% fetal bovine serum (FBS) and 1% penicillin-streptomycin antibiotic solution as described in section **3.4**.

4.2.3 MTT cell viability assay: The colorectal cancer cells were treated with different Ayurvedic formulations at 100 µg/ml for a period of 48 hours and the loss in cellular viability of CRCs were measured using MTT cell viability assay as described in section **3.5**.

4.2.4 Phytochemical analysis of aqueous extract of Ayurvedic formulations: The presence of phenolics, flavonoids, terpenoids, alkaloids and proteins in the Ayurvedic formulations was qualitatively analyzed using standard detection methods as described in section **3.6**.

4.2.5 Fractionation of aqueous extract Ayurvedic formulations using Reverse-phase open column chromatography: Open column chromatography was performed to separate fractions from Ayurvedic formulations dissolved in water as described in section **3.7**.

4.2.6 Gradient HPLC analysis: High-performance liquid chromatography (HPLC) analysis of aqueous extract of Ayurvedic formulation was performed as described in section **3.8**.

4.2.7 Isolation of individual compounds from reverse phased fractions: Individual compounds were isolated from Ayurvedic formulations as described in section **3.9**.

4.2.8 NMR Analysis: ^{1}H, ^{13}C NMR, and 2D NMR of the isolated compounds were performed in different deuterated solvents as mentioned in section **3.10**.

4.2.9 Mass spectra analysis: The mass spectra analysis of the isolated compounds was performed using UPLC-MS as mentioned in section **3.11**.

4.3 Results

4.3.1 Ayurvedic formulations possess anti-cancer activity against colorectal cancer cells: The meticulous selection process involved the careful curation of twenty-eight distinct Ayurvedic formulations, renowned for their well-established efficacy in addressing various ailments. The primary objective was to identify formulations with the potential for repurposing, capable of manifesting beneficial effects beyond their original intended uses, thereby diverging

into novel therapeutic avenues. Consequently, these 28 Ayurvedic formulations underwent evaluation for their anti-cancer activity against diverse colorectal cancer cell lines (HCT-116, DLD1 and HT-29). The findings revealed that the majority of these formulations, at a concentration of 100 µg/ml, did not elicit cancer cell death. Remarkably, even after a 48-hour treatment duration, the viability of cancer cells remained within the range of 85%-100%, indicating their resilience to the treatment (**Table 4.1**).

Table 4.1: Anti-cancer activity of different Ayurvedic formulations

S. No.	Ayurvedic formulations	Type of formulation	State of formulation	Cell viability (%) ± S. D		
				DLD1	HCT-116	HT-29
1	Sanjivani bati	Bati/Tablet	Solid	97 ± 5.5	94 ± 5.6	99 ± 5.6
2	**Hridayarnav ras**	**Ras**	**Solid**	**55 ± 4.9**	**58 ± 2.8**	**49 ± 6.3**
3	Ichabedi ras	Ras	Solid	101 ± 5.1	95 ± 4.6	100 ± 4.2
4	Gaisantak bati	Bati/Tablet	Solid	100 ± 5.4	97 ± 5.3	98 ± 8.2
5	Bhubaneshwar ras	Ras	Solid	98 ± 6.9	97 ± 4.6	94 ± 4.6
6	Amoebica	Bati/Tablet	Solid	92 ± 6.1	90 ± 8.2	90 ± 7.6
7	Mahasudharshan Churna	Churna/powder	Solid	98 ± 7.3	98 ± 6.8	100 ± 6.2
8	Arogyavardhini gutika	Tablet	Solid	99 ± 3.9	85 ± 8.1	96 ± 4.9
9	Giloya satwa	Bati/Tablet	Solid	100 ± 4.9	98 ± 7.6	96 ± 4.8
10	**Haritaki Churna**	**Churna**	**Solid**	**34 ± 4.6**	**49 ± 7.1**	**88 ± 5.1**
11	Agnikumar Ras	Ras	Solid	99 ± 3.8	92 ± 4.2	98 ± 2.6
12	Brahmi rasayan	Rasayan	Liquid	92 ± 7.2	95 ± 3.6	100 ± 4.8
13	Ajwain ark	Ark/Distillation	Liquid	100 ± 6.7	96 ± 7.6	98 ± 9.6
14	Amalaki rasayan	Rasayan	Liquid	99 ± 5.8	92 ± 6.6	95 ± 4.6
15	Shwaskuthar ras	Tablet	Solid	98 ± 4.5	101 ± 5.6	100 ± 6.3
16	Leuconil	Bati/Tablet	Solid	98 ± 6.1	98 ± 7.8	85 ± 4.2
17	Sarpagandhagan bati	Bati/Tablet	Solid	105 ± 7.8	92 ± 2.9	91 ± 6.5
18	Mahashank bati	Bati/Tablet	Solid	95 ± 5.3	85 ± 5.9	95 ± 5.2
19	Dashamoola rishta	Arishta/asava	Liquid	98 ± 4.9	91 ± 4.3	102 ± 4.1
20	Mustakarishta	Arishta/asava	Liquid	91 ± 6.1	95 ± 4.6	99 ± 3.8
21	Ashokarishta	Arishta/asava	Liquid	90 ± 7.2	92 ± 5.6	91 ± 2.1
22	Kumariasava	Arishta/asava	Liquid	92 ± 5.3	90 ± 4.8	98 ± 6.1
23	Rohitikarishta	Arishta/asava	Liquid	90 ± 4.2	91 ± 5.1	100 ± 7.3
24	Ayucid	Bati/Tablet	Solid	90 ± 3.9	70 ± 5.9	72 ± 4.8
25	Khadiradi bati	Bati/Tablet	Solid	85 ± 5.8	101 ± 6.2	90 ± 5.6
26	**Amalaki Churna**	**Churna**	**Solid**	**45 ± 6.3**	**38 ± 4.2**	**90 ± 6.3**
27	Lavangadi bati	Bati/Tablet	Solid	95 ± 4.5	98 ± 7.8	92 ± 4.9
28	**Arjunchal Churna**	**Churna**	**Solid**	**39 ± 3.8**	**30 ± 6.8**	**75 ± 4.8**

Cancer cells were treated with 100µg/ml Aqueous extract of Ayurvedic formulations and cellular viability was measured by MTT assay. The Ayurvedic formulations highlighted in bold are the most active against colorectal cancer cells.

Haritaki Churna and Amalaki Churna, derived from *Terminalia chebula* and *Emblica Officinalis* fruits respectively, demonstrated significant efficacy in inducing cell death in colorectal cancer cell lines DLD1 and HCT-116. These findings established the need for further investigation, highlighting these formulations as promising candidates for in-depth studies. Concurrently, Hridayarnav ras and Arjunchall churna exhibited notable reductions in cellular viability of colorectal cancer cells. However, Hridayarnav ras and Arjunchall churna were not selected for further studies due to their failure to induce dose-dependent killing of cancer cells.

4.3.2 Aqueous extract of Haritaki Churna and Amalaki Churna have several bioactive agents: The aqueous extract of Haritaki Churna, obtained from one gram of powder, showed an average yield of 539.6 ± 14.5 mg, making up more than 50% of the original Haritaki Churna powder. This extract is primarily composed of hydrophilic components, which are the key elements responsible for its medicinal properties. A qualitative phytochemical analysis confirmed the presence of various bioactive compounds such as polyphenols, proteins, alkaloids, flavonoids, and terpenoids in the extract, with polyphenols being the most abundant group.The extract was found to have a total polyphenolic content (TPC) of 395.9 mg gallic acid equivalents per gram of dry weight, indicating a high concentration of polyphenols (**Figure 4.2A**). Additionally, gradient HPLC chromatography analysis revealed a complex chromatogram consisting of 13 major peaks and 11 minor peaks, representing different bioactive agents found in the extract.

On the other hand, the aqueous extract of Amalaki Churna makes up more than half (one gram of Amalaki Churna yielded 543.3 ± 48.6 mg of aqueous extract) of the raw Amalaki Churna powder, which implicates the majority of its constituents to be hydrophilic. Several biochemical tests were used to assess the qualitative phytochemical content of AMCAE. The presence of polyphenols, protein, alkaloids, flavonoids, and terpenoids was detected, with polyphenols accounting for the largest share of the aqueous extract **(Figure 4.2B).** The total phenolic content (TPC) of AMCAE was found to be 466 ± 31.5 mg gallic acid equivalents/gram dry weight of extract. Following phenolics, the total protein content (TPrC) was found to be 67.2 ± 11.5 mg BSA equivalents/gram dry weight of extract. column chromatography. In a similar manner, TAC (Total alkaloid content), TTC (Total terpenoid content) and TFC (Total flavonoid content) were found to be 33.3 ± 12.6 mg equivalents of berberine, 30.9 ± 9.6 mg equivalents of enoxolone and 21.9 ± 12.6 mg equivalents of quercetin per gram dry weight of extract respectively. Since, the largest share of AMCAE comprised of phenolics, the presence of different bioactive phenols was detected by injecting AMCAE into YMC-TRIART C18-

(4.6ID X 250mm) and elution was monitored at 254 nm in gradient HPLC which yielded 8 distinct major peaks.

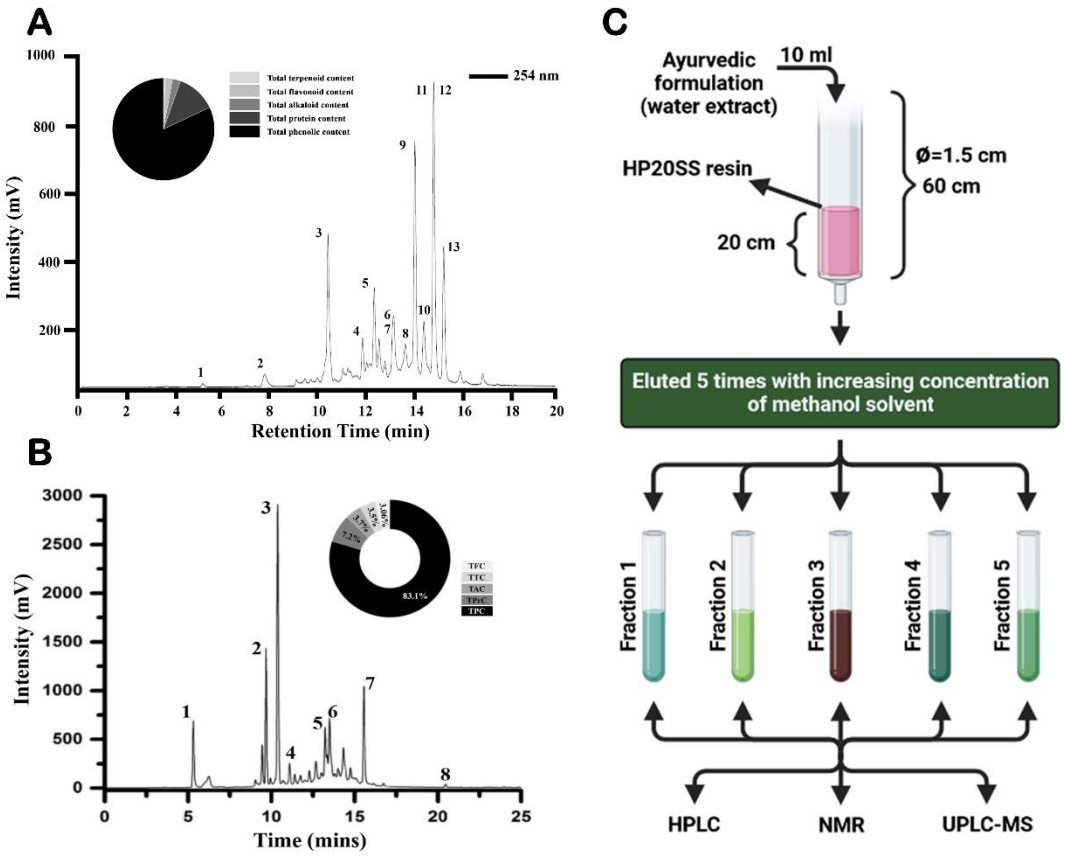

Figure 4.2: The aqueous extract of Ayurvedic formulations contains multiple bioactive agents. (A) The phytochemical analysis of Haritaki Churna aqueous extract (HCAE) was conducted using a variety of biochemical analysis methods, and the HPLC chromatogram of HCAE at 254 nm is displayed. **(B)** The phytochemical analysis of Amalaki Churna aqueous extract (AMCAE) was conducted using a variety of biochemical analysis methods. HPLC chromatogram of AMCAE at 254 nm. **(C)** Schematic representing the method followed for fractionation of aqueous extract of Ayurvedic formulations using open column chromatography.

4.3.3 Multiple phytochemicals were extracted and isolated from aqueous extracts of Haritaki Churna and Amalaki Churna: Further, the aqueous extract of both the formulations were serially eluted with solvents with varying polarity in an open column chromatography using HP20SS resin. The schematic of the procedure for separating the fractions using open column chromatography is illustrated in (**Figure 4.2C**)**.** By eluting the open column filled with reverse-phase resin using a progressively increasing methanol-to-water ratio, five distinct fractions were obtained (**Figure 4.3A**). In the case of separation of fractions from HCAE, the yields of fractions **1-5** have was calculated to be 140.4 ± 15.6 mg, 47.5 ± 3.09 mg, 157.6 ± 16.6 mg, 81.2 ± 7.02 mg, 10.2 ± 2.6 mg. The chromatograms of different fractions were developed

and the obtained fractions were subjected to isocratic HPLC analysis for setting up the condition for isolation of individual compounds from the fractions. The fraction **1** has the most hydrophilic compounds whereas fraction **5** contains the most hydrophobic ones providing us a gradient advantage in separating compounds. A copious number of compounds was present in fraction **3** which may be because of intermediary solubility in organic and aqueous solvents (**Figure 4.3B-F**). The fraction **1** and fraction **4** contained two compounds each (compound **1** & **2** in fraction **1** and compound **11**& **12** in fraction **4**) whereas fraction **2** & **5** composed of one compound each. In a similar manner, distinct fractions were obtained, each with unique mass compositions from AMCAE as well (**Figure 4.3G)**. Among the fractions, fractions **1** and **2** stood out for containing the highest concentration of hydrophilic compounds, making them the major components of the separation process. Fraction **1** weighed in at 232.8 ± 38.4 mg, while fraction **2** accounted for 114.4 ± 18.4 mg. Fraction **3**, eluted with a solvent blend of 50% methanol and 50% water, was the most intriguing observation. It exhibited the highest number of different compounds compared to the other fractions, with a total mass of 65.9 ± 14 mg. This suggested that the intermediate polarity of the elution solvent enabled the extraction of a diverse range of compounds from AMCAE. Fractions **4** and **5** were particularly hydrophobic compounds, with each fraction featuring a prominent main compound accounting for 22.9 ± 5.1 mg and 13.9 ± 6.7 mg, respectively. The fractions obtained were subsequently subjected to chromatographic analysis using gradient High-Performance Liquid Chromatography (HPLC) conditions. Among the fractions, fraction **3** exhibited the highest number of detected compounds, followed by fraction **1** and fraction **2** in descending order of compound abundance (**Figure 4.3H-L**). Interestingly, despite fraction **1** and fraction **2** having the highest weights, as determined by mass, they contained a relatively lower number of compounds compared to fraction **3**. Furthermore, upon analysis, it was observed that fraction **4** and fraction **5** each contained a single predominant compound as evidenced by their largest peak intensities. Notably, fraction **5** exhibited a singular compound with the highest level of purity among all the fractions examined.

4.3.4 Structural elucidation of chemical compounds isolated from HCAE and AMCAE:

Chemical compounds present in HC aqueous extract was purified to homogeneity and purity was confirmed by spiking the compound in HPLC. The structure of purified compound was determined by spectroscopic techniques ^{1}H NMR (600 MHz), ^{13}C NMR (600 MHz) and ESI-MS (**Appendix-I**). The composition, retention time, molecular formulae and the purity of the

compounds isolated from HC aqueous extract is shown in **Table 4.2.** The molecular weight of compound was determined by using mass spectra UPLC system coupled to a QTOF-MS.

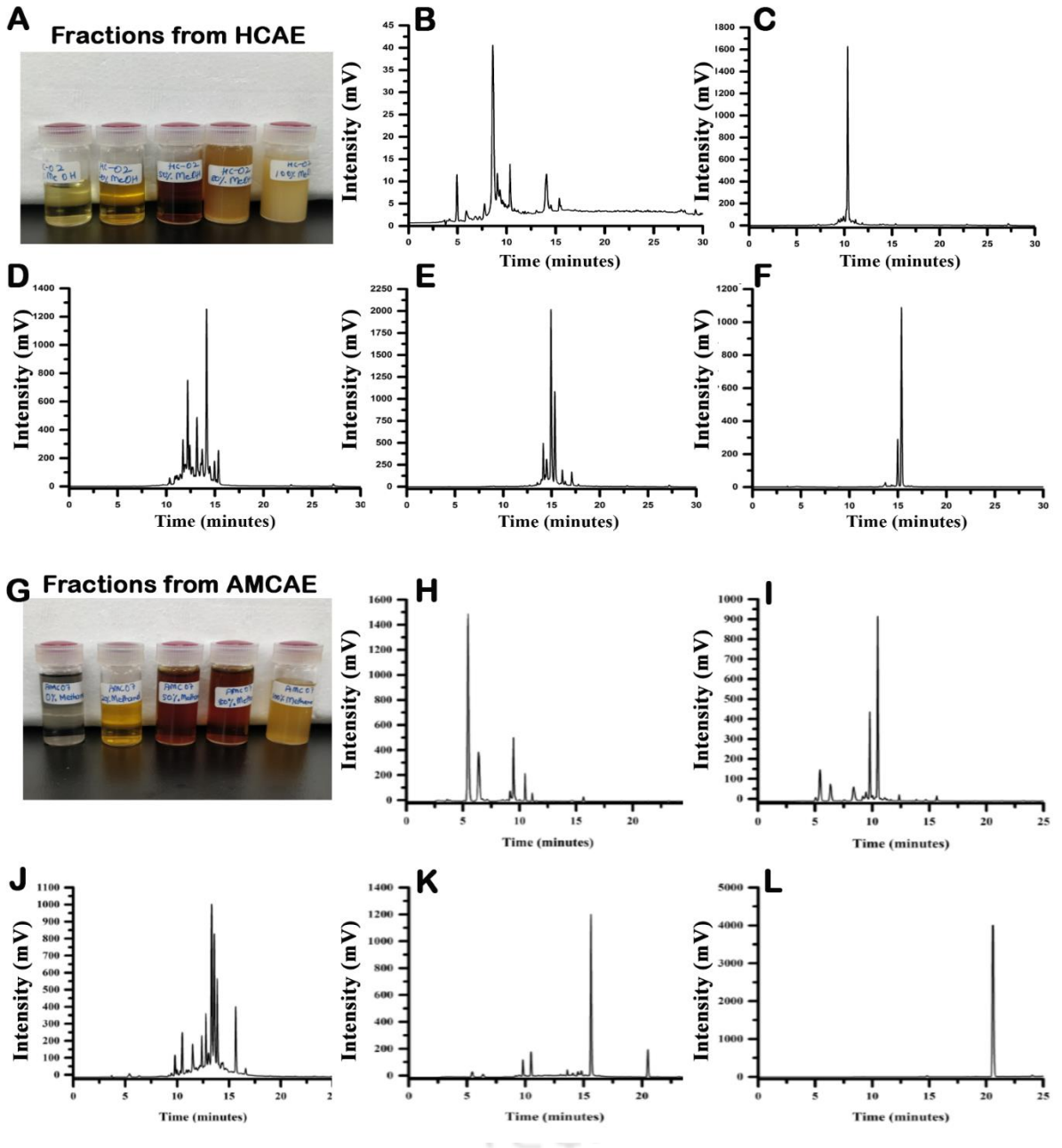

Figure 4.3: Open column chromatography yielded distinct fractions with divergent phytochemical compositions in each fraction. (A) Obtained fractions aftert fractionation of HCAE using open column chromatography. **(B-F)** Gradient HPLC chromatograms of Fraction **1** (0% MeOH fraction), Fraction **2** (20% MeOH fraction), Fraction **3** (50% MeOH fraction), Fraction **4** (80% MeOH fraction) and Fraction **5** (100% MeOH fraction) from HCAE respectively were developed at 254 nm. **(G)** Fractions from AMCAE obtained using open column chromatography. **(H-L)** Gradient HPLC chromatograms of Fraction **1** (0% MeOH fraction), Fraction **2** (20% MeOH fraction), Fraction **3** (50% MeOH fraction), Fraction **4** (80% MeOH fraction) and Fraction **5** (100% MeOH fraction) from HCAE respectively were developed at 254 nm.

Compound **1** showed a molecular ion peak at *m/z* 173.0025 $[M-H]^-$. The molecular formula $C_7H_{10}O_5$ was deduced using ^1H NMR, mass spectra analysis and was identified as shikimic acid by comparing it with already published literature [1]. Compound **2** showed two molecular ions at *m/z* 336.9633 $[M-H]^-$ and 354.9868 $[M-H]^-$. The peak at *m/z* 336.9633 $[M-H]^-$is due to the loss of water molecules from the parent molecule because of high ionization energy. The ^1H, mass spectra analyses were used in deducing $C_{14}H_{12}O_{11}$ and are identified as chebulic acid by comparing it with already published literature [2]. Compound **3** showed the highest peak at *m/z* 168.9744 $[M-H]^-$. $C_7H_6O_5$ was deduced as the molecular formula by analysing the ^1H NMR and was identified as gallic acid) by comparing it with already published literature [3]. Compound **4** showed molecular ion peaks at *m/z* 108.9870 $[M+H]^+$, 127.0182 $[M+H]^+$in positive mode. The peak at *m/z* 108.9870 $[M]^+$ could be because of the loss of water molecules from the parent molecule because of high ionization energy. Molecular formula $C_6H_6O_3$ was obtained by analysing ^1H NMR and was identified as 5-hydroxymethylfurfural by comparing it with already published literature [4].

Table 4.2: The compounds isolated from Haritaki Churna aqueous extract.

Peak No.	Compound name	Molecular formula	Composition (%)	Retention time (min)	Molecular weight (Da)	Peak purity (%)
1	Shikimic acid	$C_7H_{10}O_5$	0.351	5.1	174	83.2
2	Chebulic acid	$C_{14}H_{12}O_{11}$	2.168	7.99	336	91.2
3	Gallic acid	$C_7H_6O_5$	19.781	10.37	170	98.9
4	5-Hydroxymethylfurfural	$C_6H_6O_3$	0.921	11.01	126	96.2
5	Protocatechuic acid	$C_7H_6O_4$	2.839	11.89	154	98.5
6	4-*O*-galloyl shikimic acid	$C_{14}H_{14}O_9$	3.247	13.12	326	98.2
7	5-*O*-galloyl shikimic acid	$C_{14}H_{14}O_9$	3.247	13.12	326	97.1
8	Methyl gallate	$C_8H_8O_5$	5.202	13.8	184	94.5
9	Corilagin	$C_{27}H_{22}O_{18}$	15.919	14.08	634	92.2
10	1,2,6 Tri-O-galloyl-β-D-glucose	$C_{27}H_{24}O_{18}$	6.861	14.35	636	82.1
11	Chebulagic acid	$C_{41}H_{30}O_{27}$	11.838	15.05	954	97.5
12	Chebulinic acid	$C_{41}H_{32}O_{27}$	7.889	15.05	956	92.6
13	Ellagic acid	$C_{14}H_6O_8$	12.662	15.5	302	98.2
14	Rest of the compounds	NA	7.08	NA	NA	NA

Compound **5** showed the highest molecular ion peak at *m/z* 153.0059 $[M-H]^-$. The ^1H and mass spectra analysis helped us deduce the molecular formula as $C_7H_6O_4$ and were identified as protocatechuic acid) after comparing it with published literature [5]. Major ion peak of compound **6** under negative mode showed a peak at *m/z* 325.0143 $[M-H]^-$. This ion was also accompanied by cluster ion at *m/z* 651.0958 $[2M-H]^-$. The fragment ions *m/z* 169.0021 $[M-H]^-$

and *m/z* 173.0442 [M-H]$^-$ corresponded to the gallic acid moiety and shikimic acid moiety, respectively. ESI-MS data of **7** was similar to **6**, the molecular weight was the same. Therefore, **6** and **7** were assumed positioning isomer each other. Based on ^{1}H NMR analysis and comparing it to the previously published literature, the compound **6** and compound **7** were identified as 4-*O*-galloyl shikimic acid and 5-*O*-galloyl shikimic acid [6].

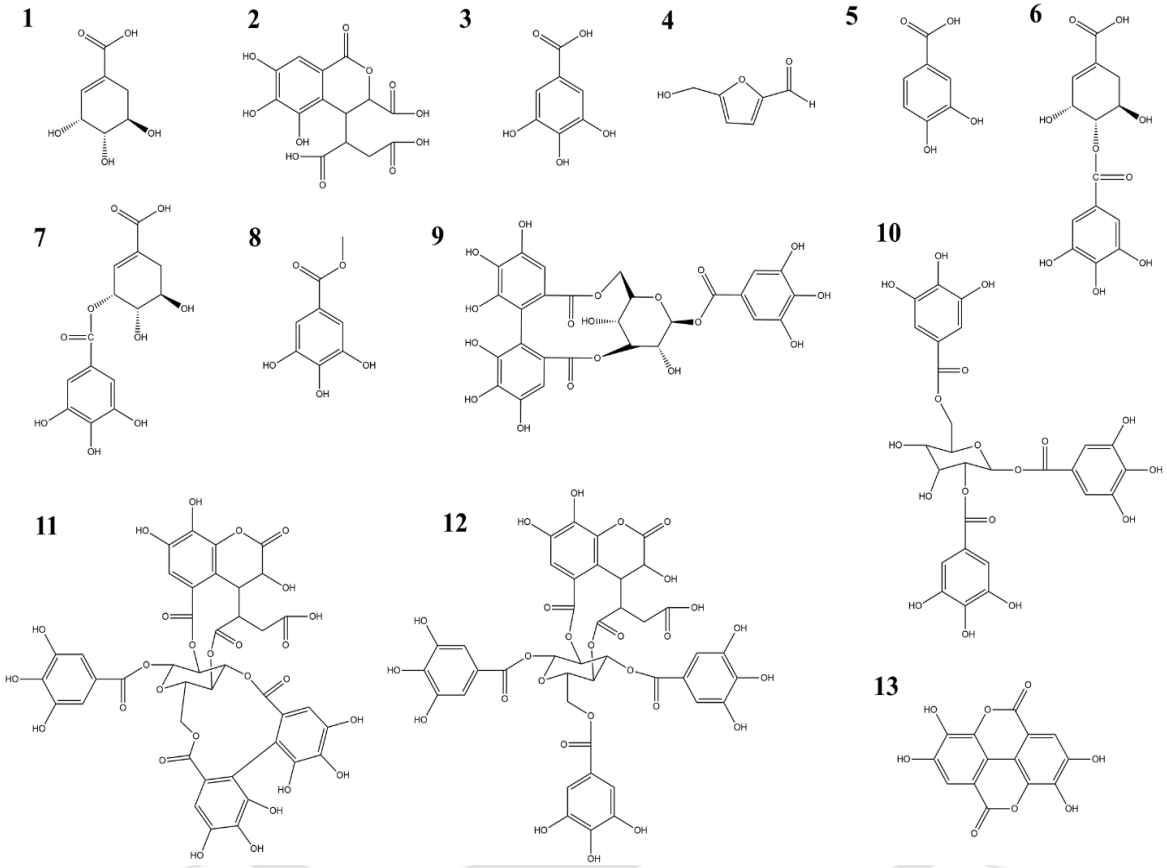

Figure 4.4: Chemical structures of isolated compounds from aqueous extracts of Haritaki Churna. (**1**: Shikimic acid, **2**: Chebulic acid, **3**: Gallic acid, **4**: 5 hydroxymethyfurfural, **5**: Protocatechuic acid, **6**: 4-O-galloyl shikimic acid, **7**: 5-O-galloyl shikimic acid, **8**: Methyl gallate, **9**: Corilagin, **10**: 1,2,6-Tri-*O*-galloyl-β-D glucose, **11**: Chebulagic acid, **12**: Chebulinic acid, **13**: Ellagic acid).

Compound **8** showed a molecular ion peak at *m/z* 183.2640 [M-H]$^-$. The molecular formula was deduced as $C_8H_8O_5$ with the help of ^{1}H NMR analysis and was identified as methyl gallate by comparing with published literature [7]. Compound **9** showed two molecular ion peaks at *m/z* 634.0134 [M-H]$^-$ and 1267.0637 [2M-H]$^-$. The ^{1}H NMR analysis helped us in deducing the formula as $C_{27}H_{22}O_{18}$ and was identified as corilagin by comparing it with published literature [8]. The chemical structures of the compounds **1-13** are displayed in **Figure 4.4.** Compound **10** showed two molecular ion peaks at *m/z* 634.9866 [M-H]$^-$and 1271.1479 [2M-H]$^-$. After ^{1}H NMR analysis, the molecular formula was deduced as $C_{27}H_{24}O_{18}$ and was identified as 1, 2, 6,

tri-*O*-galloyl β-D-glucose after comparing it with published literature [8]. Compound **11** showed two molecular ion peaks at *m/z* 953.5759 $[M-H]^-$ and 1907.0813 $[2M-H]^-$. The ^1H NMR analysis helped us in deducing the formula as $C_{41}H_{30}O_{27}$ and was identified as chebulagic acid by comparing it with published literature [7]. Compound **12** showed two molecular ion peaks at *m/z* 954.9651 $[M-H]^-$ and 1911.1218 $[2M-H]^-$. The ^1H NMR analysis helped us in deducing the formula as $C_{41}H_{32}O_{27}$ and was identified as chebulinic acid by comparing it with published literature [7]. Compound **13** showed a molecular ion peak at *m/z* 300.9498 $[M-H]^-$. The ^1H NMR, mass spectra analysis and comparison of Ellagic acid standard on isocratic HPLC helped us identify compound **13** as ellagic acid.

The bioactive substances present in Amalaki Churna were isolated and purified to a state of complete uniformity, and the level of purity was verified through (HPLC). Spectroscopic methods such as ^1H NMR (600 MHz) and 13C NMR (600 MHz), as well as 2D NMR techniques were used to identify the structure of isolated compounds. The NMR spectroscopic and ESI-MS spectra data are provided in **Appendix-II**. The details required to denote the retention time and purity are illustrated (**Table 4.3**). Compound **1** which was purified to 91.2% showed a molecular ion peak at m/z 361[M-H]-. The ^1H NMR chemical shifts and coupling patterns of the compound **1** confirmed the presence of galloyl group and an oxidized sugar moiety. The chemical formula $C_{13}H_{14}O_{12}$ was deduced and compound was identified to be mucic acid-2-*O*-gallate that also corroborates to previous study (Zhang et al., 2001).

Table 4.3: The compounds isolated from Amalaki Churna aqueous extract.

Peak No.	Compound name	Molecular formula	Retention time (min)	Molecular weight (Da)	Peak purity (%)
1	Mucic acid 2-*O*-gallate	$C_{13}H_{14}O_{12}$	5.4	362	91.2
2	β-Glucogallin	$C_{13}H_{16}O_{10}$	9.7	332	91.7
3	Gallic acid	$C_7H_6O_5$	10.4	170	96.6
4	5-hydroxymethylfurfural	$C_6H_6O_3$	10.6	126	88.1
5	Macabarterin	$C_{46}H_{38}O_{32}$	12.7	1102	95.7
6	Corilagin	$C_{27}H_{22}O_{18}$	13.3	634	94.1
7	Ellagic acid	$C_{14}H_6O_8$	15.6	302	95.5
8	Trans-cinnamic acid	$C_9H_8O_2$	20.5	148	98.2

A molecular ion peak was observed for Compound **2**, specifically at m/z 331 [M-] and m/z 355 [M+Na]+. Further, compound 2's ^1H NMR spectrum revealed the presence of a galloyl group with a sugar moiety attached to its hydroxyl group, as observed by the chemical shift pattern. Its purity was measured to be 91.7%. Compound **2**, with a chemical formula of $C_{13}H_{16}O_{10}$, was identified as 1-*O*-galloyl β-D-glucose (β-glucogallin), a compound previously documented in

E. Officinalis (Puppala et al., 2012). Compound 3, was extracted with a commendable purity of 93.6%. Since there was only one proton peak observed at δ7.05 (2H, s) in ^{1}H NMR spectrum and a maxima peak at m/z 169 [M-H]-in UPLC-MS analysis, the chemical formula $C_7H_6O_5$ was ascertained, unequivocally establishing its identity as gallic acid (Dao et al., 2019). The fractions **1** and **2** included the most hydrophilic compounds, with compounds **1**, **2**, and **3** varying in concentrations. The chemical structures of the identified compounds are represented (**Figure 4.5**). The fraction **1** contained higher quantity of compound 1 with trace amounts of compound **2** & **3** and vice-versa was noticed in fraction **2** Compound **4** exhibited molecular ion peaks at m/z 109 [M+H]+ and 127 [M+H]+. The appearance of the peak at m/z 109 [M]+ can be attributed to the possible expulsion of water molecules from the parent molecule, owing to its high ionization energy. The presence of an aldehyde and a furan ring was confirmed with proton peaks at δ9.4 (1H, s, aldehyde), δ7.5 (1H, d, aromatic), and δ6.6 (1H, d, aromatic). Upon comparison with a previous study, Compound 4, with a purity of 88.1%, was identified as 5-hydroxymethylfurfural ($C_6H_6O_3$) (Luo et al., 2009).

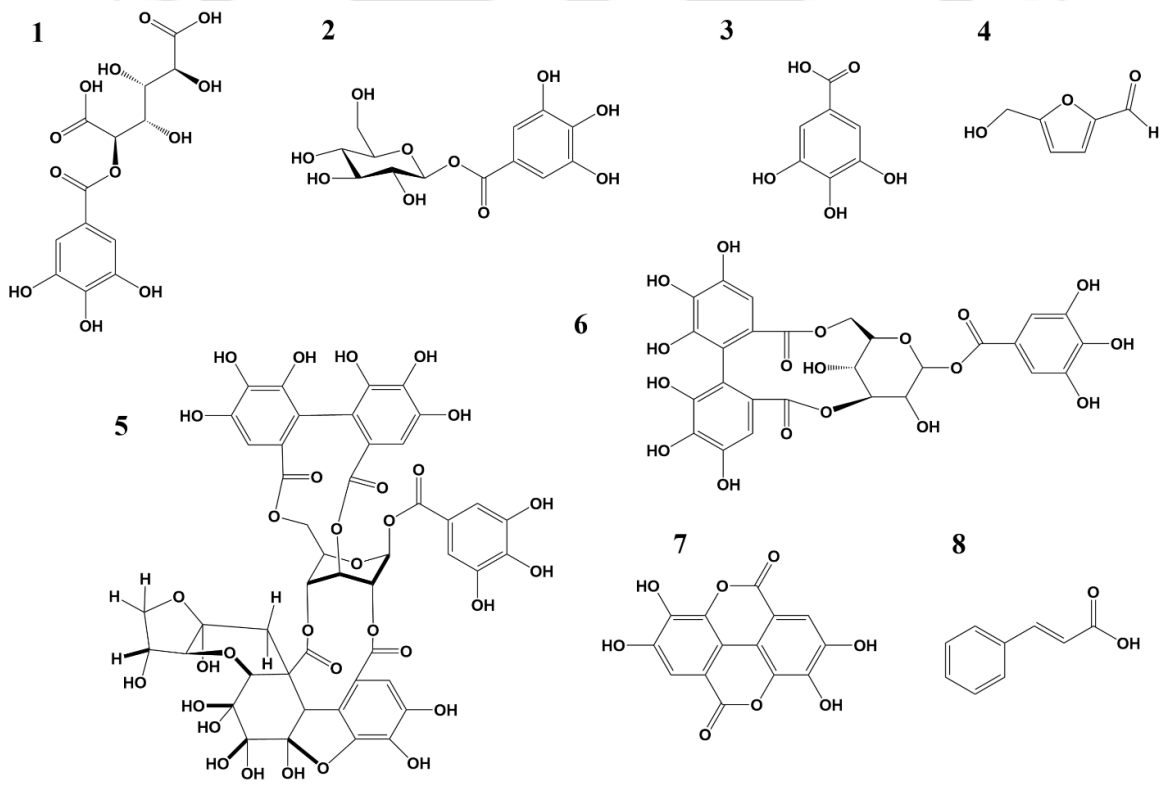

Figure 4.5: Chemical structures of compounds isolated from AMCAE. (1) Mucic acid 2-*O*-gallate, (2) β-glucogallin, (3) Gallic acid, (4) 5-hydroxymethylfurfural, (5) Macabarterin, (6) Corilagin, (7) Ellagic acid, and (8) Trans-cinnamic acid.

Compound **5** exhibited a distinctive molecular ion peak at m/z 1083 [M-] and m/z 1103 [M+H]+. The occurrence of the peak at m/z 1083 [M]- could plausibly be attributed to the

potential loss of water molecules from the parent molecule. The presence of four aromatic rings and acyl group were confirmed with the presence of multiple protons at δ7.324 (1H, s, acyl group), δ7.076 (2H, s, galloyl group), δ6.87 (1H, s, HHDP (3,5-hexahydroxydiphenic acid)), and δ6.63 (1H, s, HHDP). The central sugar ring was further confirmed by chemical shifts in the range of δ5.49 and δ4.1. The compound Macabarterin, an ellagitannin, was identified by analyzing and comparing data with published studies with a chemical formula of $C_{46}H_{38}O_{32}$. Significantly, this is the inaugural instance of isolating macabarterin, with a purity level of 95.7%, from amla (*E. Officinalis*), a plant from which it had solely been documented in association with *Macaranga barteri* (Ngoumfo et al., 2008). Compound **6** with a purity of 94.1% displayed a molecular ion peak at m/z 633 [M-H]-. Corilagin was identified through spectroscopic analysis, specifically ^{1}H NMR. The analysis confirmed the existence of three galloyl rings and a central sugar molecule, and the molecular formula was determined to be $C_{27}H_{22}O_{18}$. The spectroscopic data obtained for corilagin matched well with previously reported results (Yakubu et al., 2019). The ^{1}H NMR spectrum of the compound **7** revealed a single proton peak at δ6.89 (2H, s). Additionally, in the UPLC-MS analysis, a prominent peak at m/z 301 [M-H]- was observed. These findings conclusively determined the precise chemical formula of the compound to be $C_{14}H_6O_8$. Compound **7** (purity-95.5%) was identified as ellagic acid by comparing the retention time with the available standard compound and the NMR data also matches with that of previously reported data (Goriparti et al., 2013). Compound **8** showed molecular ion peak at m/z 131 [M+H]+. The peak at m/z 131 in positive mode could be due to loss of water ion from the parent molecule. We confirmed the compound to be trans-cinnamic acid by comparing its retention time with the standard available and also with published studies (Kim et al., 2012). The molecular formula for trans-cinnamic acid with a purity of 98.2% was deduced to be $C_9H_8O_2$.

4.4 References

1. Usuki, T., et al., *Extraction and isolation of shikimic acid from Ginkgo biloba leaves utilizing an ionic liquid that dissolves cellulose.* Chemical Communications, 2011. 47(38): p. 10560-10562.
2. Lee, H.-S., et al., *Isolation of chebulic acid from Terminalia chebula Retz. and its antioxidant effect in isolated rat hepatocytes.* Archives of Toxicology, 2007. 81(3): p. 211-218.

3. Dao, N.T., et al., *Chemical Constituents and Anti-influenza Viral Activity of the Leaves of Vietnamese Plant Elaeocarpus tonkinensis.* Records of Natural Products, 2019. 13(1).
4. Luo, W., et al., *Identification of bioactive compounds in Phyllenthus emblica L. fruit and their free radical scavenging activities.* Food Chemistry, 2009. 114(2): p. 499-504.
5. López-Martínez, L.M., et al., *A 1H NMR investigation of the interaction between phenolic acids found in Mango (Manguifera indica cv Ataulfo) and Papaya (Carica papaya cv Maradol) and 1, 1-diphenyl-2-picrylhydrazyl (DPPH) Free Radicals.* PloS one, 2015. 10(11): p. e0140242.
6. Ishimaru, K., G.-I. Nonaka, and I. Nishioka, *Gallic acid esters of proto-quercitol, quinic acid and (−)-shikimic acid from quercus mongolica and q. myrsin aefolia.* Phytochemistry, 1987. 26(5): p. 1501-1504.
7. Anil, M. and P. Nandini, *Simultaneous isolation and identification of phytoconstituents from Terminalia chebula by preparative chromatography.* Journal of Chemical and Pharmaceutical Research, 2010. 2(5): p. 97-103.
8. Yakubu, O.F., et al., *Cytotoxic effects of compounds isolated from Ricinodendron heudelotii.* Molecules, 2019. 24(1): p. 145.

4.5 Appendix-I: NMR and ESI-MS data for compounds from HCAE

Compound 1: -$C_7H_{10}O_5$: Negative ESI-MS *m/z* =173.0025 $[M-H]^-$, ^{1}H NMR (600MHz, D_2O): δ_H6.82 (1H, brt, *J*=2.4Hz), 4.45 (1H, brt, *J*=4.2Hz), 4.04 (1H, m), 3.78 (1H, q, *J*=8.4, 4.2Hz), 2.75 (1H, overlap), 2.23 (1H, dd, *J*=18, 6.6Hz)

Compound 2: -$C_{14}H_{12}O_{11}$: Negative ESI-MS *m/z* =336.9633 $[M-H]^-$, 337$[M-H_2O-H]^-$, ^{1}H NMR (600MHz, D_2O) : δ_H7.2 (1H,s), 5.4 (1H, d, *J*=1.2Hz), 4.01 (1H, dd,*J*=7.8, 1.2Hz), 3.3 (1H, ddd, *J*=14.4, 8.4, 6Hz), 2.9 (1H, dd, *J*=17.4, 8.4Hz), 2.6 (1H, dd, *J*=17.4, 6Hz).

Compound 3: -$C_7H_6O_5$: Negative ESI-MS *m/z* =168.9744 $[M-H]^-$, ^{1}H NMR (600MHz, D_2O): δ_H7.08 (2H, s, H-2, H-6).

Compound 4: -$C_6H_6O_3$: Negative ESI-MS *m/z*$[M+H]^+$ =108.9870, ^{1}H NMR (600MHz, D_2O): δ_H9.4 (1H, s), 7.5 (1H, brd, *J*=3.35Hz), 6.6 (1H, brd, *J*=3.4Hz), 4.8 (1H, s), 4.6 (1H, s).

Compound 5: -$C_7H_6O_4$: Negative ESI-MS *m/z* $[M-H]^-$ =153.0059, ^{1}H NMR (600MHz, DMSO-d_6): δ_H7.3 (1H, brd, *J*=1.8Hz), 7.2 (1H, dd, *J*=8.4, 1.8Hz), 6.7 (1H, d, *J*=8.4Hz).

Compound 6: -$C_{14}H_{14}O_9$: Negative ESI-MS *m/z* $[M-H]^-$ = 325.0143, ^1H NMR (600MHz, Acetone-d_6): δ_H7.08 (2H, s), 6.8 (1H, s), 5.35 (1H, dd, *J*=11.4, 4.2Hz), 4.49 (1H, s), 4.02 (1H, m), 2.8 (1H, overlap), 2.4 (1H, dd, *J*=18.6, 4.8Hz).

^1H NMR (600MHz, Acetone-d_6 + D_2O): δ_H7.1 (2H, s), δ6.8 (1H, s), 5.3 (1H, m), 4.5 (1H, brs), 4.04 (1H, overlap), 2.86 (1H, dd, *J*=17.4, 3.6Hz), 2.4 (1H, dd, *J*=19.2, 4.8Hz).

Compound 7: -$C_{14}H_{14}O_9$: Negative ESI-MS *m/z* $[M-H]^-$ = 325.0257, ^1H NMR (600MHz, Acetone-d_6): δ_H7.1 (2H, s), 6.8 (1H, brd, J=3Hz), 5.78 (1H, m), 4.19 (1H, dd, *J*=12.6, 4.8Hz), 4.03 (1H, dd, *J*=6.6, 4.2Hz), 2.8 (1H, overlap), 2.32 (1H, m).

Compound 8: -$C_8H_8O_5$**:** Negative ESI-MS *m/z* $[M-H]^-$ = 183.2640, ^1H NMR (600MHz, CD_3OD): δ_H7.055 (2H, s, H-2, H-6), 3.82 (3H, s).

Compound 9: -$C_{27}H_{22}O_{18}$**:** Negative ESI-MS *m/z* $[M-H]^-$ = 634.0134, $[2M-H]^-$ = 1267.0637, ^1H NMR (600MHz, CD_3OD) : δ_H7.055 (2H, s), 6.69 (1H, s), 6.66 (1H, s), 6.36 (1H, brs), 4.9 (1H, t, *J*=10.8Hz), 4.8 (1H, overlap), 4.5 (1H, t, *J*=9Hz), 4.4 (1H, brt, *J*=1.4Hz), 4.15 (1H, dd, *J*=10.8, 7.8Hz), 3.98 (1H, brd, *J*=1.2Hz).

Compound 10: -$C_{27}H_{24}O_{18}$**:** Negative ESI-MS *m/z* $[M-H]^-$ = 634.9866, $[2M-H]^-$ = 1271.1479, ^1H NMR (600MHz, CD_3OD) : δ_H7.16, 7.14, 7.1 (each 2H, s), 5.8 (1H, d, *J*=8.4Hz), 5.2 (1H, t, *J*=9Hz), 4.59 (1H, dd, *J*=11.4, 1.2Hz), 4.4 (1H, dd, *J*=12.6, 6Hz), 3.89 (1H, ddd, *J*=9.6, 4.8, 2.4Hz), 3.7-3.8 (2H, m).

Compound 11: -$C_{41}H_{30}O_{27}$**:** Negative ESI-MS *m/z* $[M-H]^-$ = 953.5759, $[2M-H]^-$= 1907.0813, ^1H NMR (600MHz, CD_3OD) : δ_H7.47 (1H, s), 7.07 (2H, s), 6.84 (1H, s), 6.63 (1H, s), 6.5 (1H, s), 5.8 (1H, brs), 5.39 (1H, s), 5.23 (1H, s), 5.04 (1H, dd, *J*=6.6, 1.2Hz), 4.3 (1H, dd, *J*=10.8, 7.8Hz), 3.8 (1H, ddd, *J*= 11.89, 4.9, 3.6, 1.5Hz), 3.72 (1H, brs), 2.2 (1H, dd, *J*=17.4, 3.6Hz), 2.1 (1H, dd, *J*=16.8, 11.4Hz).

Compound 12: -$C_{41}H_{32}O_{27}$**:** Negative ESI-MS *m/z* $[M-H]^-$ = 954.9651, $[2M-H]^-$= 1911.1218, ^1H NMR (600MHz, CD_3OD) : δ_H7.517 (1H, s), 7.18, 7.11, 6.96 (2H each, s, galloyl group), 6.5 (1H, d, *J*=1.8Hz), 6.24 (1H, brs), 5.4 (1H, t, *J*=5.4Hz), 5.11 (1H, dd, *J*=7.2Hz, 1.8Hz), 5.05 (1H, d, *J*=3.6Hz), 4.8 (1H, dd, *J*=5.4, 2.4Hz), 4.7 (1H, t, J=6.6Hz), 4.6 (1H, dd, *J*=11.4, 7.2Hz), 3.9 (1H, dd, *J*=10.2, 4.2Hz), 2.2 (2H, d, *J*=12Hz).

Compound 13: -$C_{14}H_6O_8$**:** Negative ESI-MS *m/z* $[M-H]^-$ = 300.9498, ^1H NMR (600 MHz, Acetone-d_6): δ_H7.59 (2H, s).

4.6 Appendix-II: NMR and ESI-MS data for compounds from AMCAE

Compound 1:-*$C_{13}H_{14}O_{12}$*: Negative ESI-MS m/z [M^-] =361, ^{1}H NMR (600 MHz, D2O): δ7.2 (2H, s), δ5.45 (1H, s), δ4.6 (1H, s), δ4.3 (1H, m), δ4.15 (1H, d, J=9.6 Hz).

Compound 2:-*$C_{13}H_{16}O_{10}$*: Negative ESI-MS m/z [M^-] =331, Positive ESI-MS m/z [M+Na] =355. ^{1}H NMR (500 MHz, CD3OD) : δ7.1 (2H, s), δ5.6 (1H, dd, *J*=5.5Hz, 2.5Hz), δ3.8 (1H, dd,*J*=12Hz, 1.5Hz), δ3.7 (1H, dd, *J*=12Hz, 4.5Hz), δ3.49 (3/2H, dd, *J*=6Hz, 2.5Hz), δ3.41 (1H, m),δ3.3 (3/2H, m).

Compound 3:-*$C_7H_6O_5$*: Negative ESI-MS m/z [M^-] =169. ^{1}H NMR (500 MHz, CD3OD): δ7.05 (2H, s).

Compound 4:-*$C_6H_6O_3$*: Negative ESI-MS m/z [M^-] =125, Positive ESI-MS m/z [M^+] =127. ^{1}H NMR (600 MHz, CD3OD): δ9.4 (1H, s), δ7.5 (1H, d, *J*=2.5Hz), δ6.6 (1H, d, *J*=3 Hz), δ4.6 (2H, s).

Compound 5:-*$C_{46}H_{38}O_{32}$*: Negative ESI-MS m/z [M^-] =1083, Positive ESI-MS m/z [M^+] =1103. ^{1}H NMR (600 MHz, CD3OD): δ7.324 (1H, s), δ7.076 (2H, s), δ6.87 (1H, s), δ6.63 (1H, s), δ6.51 (1H, s), δ5.55 (1H, m), δ5.49 (1H, brs), δ5.26 (1H, brd, *J*=3.6Hz), δ4.99 (1H, s), δ4.82 (1H, m), δ4.77 (1H, d, *J*=1.8Hz), δ4.37 (1H, dd, *J*=10.8, 7.8 Hz), δ4.23 (1H, dd, *J*=9.6, 5.4 Hz), δ4.17 (1H, brd, *J*=0.6Hz), δ4.1 (1H, m), δ3.9 (1H, dd, *J*=9.6, 3 Hz), δ2.7 (1H, m), δ1.5 (1H, d, *J*=13.8 Hz).

Compound 6:-*$C_{27}H_{24}O_{18}$*: Negative ESI-MS m/z [M^-]=633, ESI-MS [M+Na]=657, ^{1}H NMR (600 MHz, CD3OD) : δ7.059 (2H, s), δ6.7 (1H, s), δ6.6 (1H, s), δ6.3 (1H, s), δ4.9 (1H, t, *J*=10.8Hz), δ4.8 (1H, brs), δ4.5 (1H, t, *J*=9Hz), δ4.4 (1H, brt, *J*=2.4), δ4.1 (1H, dd, *J*=10.8Hz, 8.4Hz), δ4 (1H, brd, *J*=1.2Hz)

Compound 7:-*$C_{14}H_6O_8$*: Negative ESI-MS m/z [M^-] =301. ^{1}H NMR (600 MHz, DMSO): δ6.89 (2H, s).

Compound 8:-*$C_9H_8O_2$*:^{1}H NMR (600 MHz, CD3OD): δ7.6 (1H, d, *J*=16.2 Hz), δ7.5 (2H, m), δ7.4 (3H, m), δ6.4 (1H, d, *J*=15.6Hz).

Chapter V

Protein cross-talk is responsible for anti-cancer action of phytochemicals present in Ayurvedic formulations*

*The content of this chapter is published as **"Khan, M.R.U.Z.** and Trivedi, V., 2023**. Molecular modelling, docking and network analysis of phytochemicals from Haritaki Churna: role of protein cross-talks for their action.** Journal of Biomolecular Structure and Dynamics, pp.1-16**."**

*The content of this chapter is published as **"Khan MRUZ,** Trivedi V. **Phytochemical Cross-talk in Indian Gooseberry Preparation to Explain Therapeutic Potentials of Dietary Supplements.** Pharmacog Res. 2023;15(4)**"**

5.1 Introduction: The phytochemicals isolated in the previous chapter have the ability to target the colorectal cancer cells either individually or synergistically. On the other hand, a single phytochemical can target multiple proteins. Understanding the intricate interplay between proteins and both phytochemicals and other proteins is fundamental to unravel the mechanisms underlying the action of these Ayurvedic compounds. In this chapter, a systematic approach was employed to predict protein targets for the isolated phytochemicals, as outlined in **Figure 5.1**. Leveraging network-based pharmacology, a comprehensive phytochemical-protein network was meticulously constructed, shedding light on the complex relationships between the identified phytochemical compounds and their potential protein targets. Subsequent to the network assembly, a detailed analysis of the protein targets within the network was undertaken to pinpoint key hub proteins. These hub proteins underwent rigorous examination through molecular docking and molecular dynamics studies, where they were evaluated against their corresponding ligands. This systematic methodology not only facilitated the identification of potential therapeutic targets but also provided valuable insights into the molecular interactions driving the efficacy of these Ayurvedic formulations against colorectal cancer.

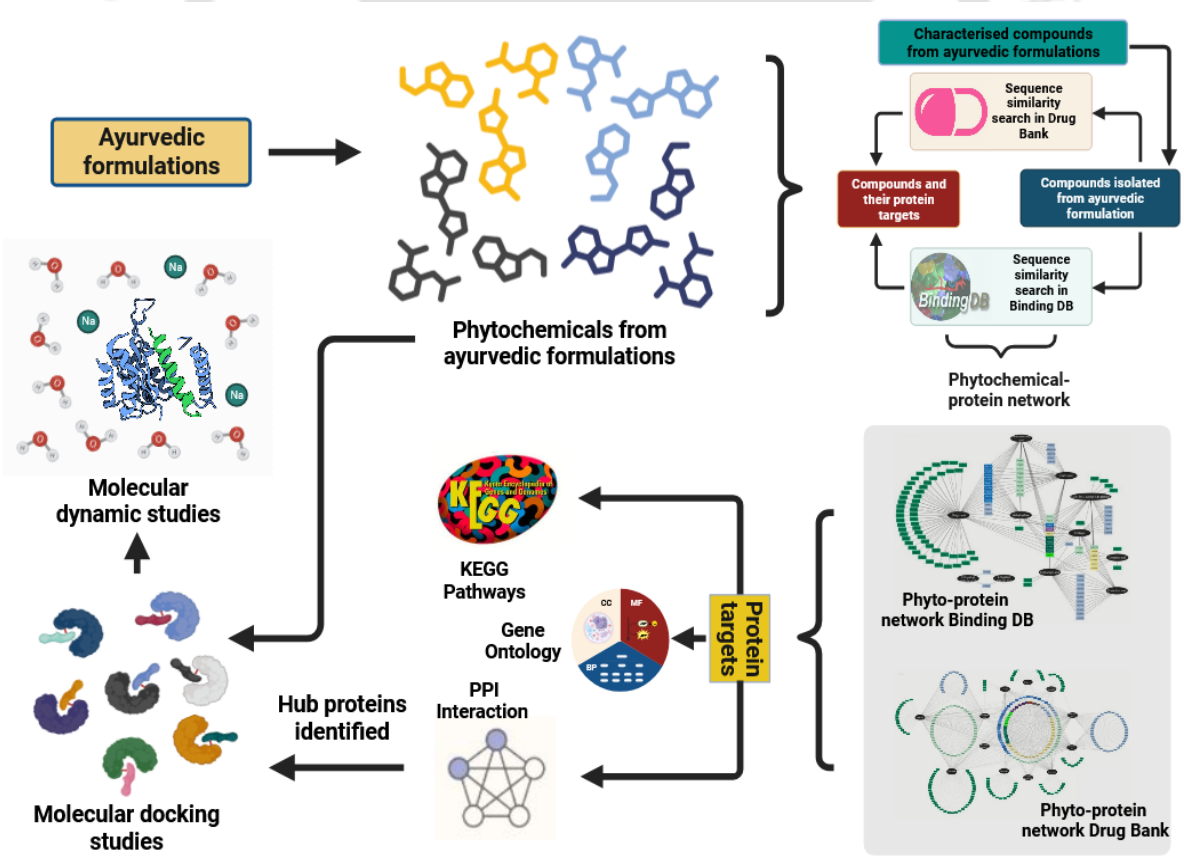

Figure 5.1: **Identification of protein targets for Ayurvedic formulations using network-based pharmacology.**

5.2 Experimental procedures

5.2.1 Collection of similar compounds from databases: A cheminformatics approach was used for shortlisting drugs and small molecules, from Binding DB (https://www.bindingdb.org/rwd/bind/index.jsp) and Drug bank (https://go.drugbank.com/), that had greater than or equal to 50% structural similarity with the phytochemicals isolated from Ayurvedic formulations [1, 2]. The chemical candidates and their respective protein targets were collected and used to create networks, which aids in understanding the crosstalk between the phytochemicals and their protein targets. The proteins identified were later converted to their corresponding ensemble gene IDs (https://david.ncifcrf.gov/conversion.jsp) [3].

5.2.2 Development of phytochemical-protein (target) network using Cytoscape: A pharmacology network correlating the phytochemical-protein interaction obtained from the similarity search results was developed using Cytoscape (Version-3.9.1). The phytochemicals and proteins were labelled as source nodes and target nodes respectively before generating the network.

5.2.3 GO functional enrichment and KEGG pathway analysis: The gene ontology (GO) studies comprising of molecular functions (MF), cellular components (CC), and biological processes (BP) of the targets obtained from similarity search against isolated compounds (from Ayurvedic formulations) were analyzed using Database for Annotation, Visualization and Integrated Discovery (DAVID-2022) (https://david.ncifcrf.gov/) software [3]. The top 10 GO terms for each process was selected based on Gene count, p-value (<0.05), and fold enrichment which would statistically be significant for representing the necessary functions that are being targeted. The functional pathways related to the targets obtained were analyzed using Kyoto Encyclopedia of Genes and Genomes (KEGG) pathway analysis.

5.2.4 Development of protein-protein interaction (PPI) network by STRING and Cytoscape: The proteins (in the form of UniProt IDs) obtained as targets from similarity search was further analyzed to develop the protein-protein interaction network. The PPI network was developed using "Search Tool for the Retrieval of Interacting Genes-STRING" software available online (https://string-db.org/) [4]. The PPI network was enriched by setting a confidence level of 0.999. The STRING software automatically detects the UniProt IDs and convert them to their corresponding canonical Gene names. Networks in biological systems are often represented by nodes and edges. The proteins are represented as nodes and the links

between them are the edges. The nodes having no neighbors were excluded and the resultant STRING network was analyzed using Cytoscape (Version-3.9.1). The parameters Degree centrality (DCy), Betweenness centrality (BCy) and Closeness Centrality (CCy) were employed to further enrich the PPI network which could help us reveal the minimal set of proteins that are required for the functioning of the network. The degree of a node is determined by the number of first neighbors it has and is sometimes referred to as degree centrality (DCy). The degree centrality is regarded as the most essential topological characteristic of a PPI network [5]. Betweenness centrality (BCy) measures the extent to which a particular node lies on the shortest distance on other nodes. BCy often represents how two distinct clusters in a network are linked and serves as a bridge spanning function in a network [5]. Closeness centrality (CCy) indicates how near a node is to all other nodes in a particular network. In other words, it represents how rapidly a certain node is accountable for the flow of information to all other nodes in a network [5]. Considering these topological parameters in the network, the leading protein with most connections were selected as the important targets for the network.

5.2.5 Molecular docking of isolated compounds (from Ayurvedic formulations) against protein targets obtained: The chemical compounds obtained from Ayurvedic formulations were downloaded from PubChem in SDF format which were later converted into Mol2 format after their energy minimization in Chem3D pro software. The suitable PDB files for the protein targets obtained were downloaded from RCSB PDB (https://www.rcsb.org/) [6]. All the protein PDB files were subjected to energy minimization in Swiss-PDB viewer. Molecular docking of ligands and proteins were performed using Autodock tools-1.5.6 [7] . The binding energy obtained was used to evaluate the binding affinity of ligands to their respective targets. The 2D structure of the ligand-protein complex structure was visualized in Discovery studio.

5.2.6 Molecular dynamic simulation studies: The molecular dynamics simulation of the target proteins in complex with the phytochemicals obtained were studied using GROMACS 2018.1 [8]. The topology files were generated using CHARMM-GUI server (https://charmm-gui.org/) and the force fields were generated using CHARMM36. The system was neutralized with sodium (Na^+) and chloride (Cl^-) wherever necessary and the energy minimization was done with Lincs algorithm. The phytochemical-compound complexes were solvated in a dodecahedron box with a 1nm distance from the edges of the resultant solvated box. The temperature and the pressure of the system were set to 300K and 1 atmospheric pressure to pretend physiological conditions. The Vander Waals short range distance cut off was set to 1.2nm. Hydrogen bonds, electrostatic interactions, and Vander Waals interactions were each

constrained using the LINCS algorithm, particle-mesh Ewald (PME), and Verlet algorithms, respectively. The 100ns MD simulation run was performed with integration step of 2fs under NVT thermal equilibration conditions followed by isothermal-isobaric (NPT equilibrations) equilibrations under same temperature conditions. The quality and stability of molecular dynamics (MD) simulations were assessed using commonly employed MD simulation parameters. Radius of gyration (Rg) indicated protein compactness, while root mean square deviation (RMSD) measured structural deviation from a reference structure (protein backbone). Root mean square fluctuation (RMSF) determined residue flexibility, and hydrogen bond count evaluated stability. Minimum paired distance identified close atom/group approaches. MM-PBSA estimated binding energy by combining molecular mechanics and Poisson-Boltzmann calculations. GROMACS software facilitated these analyses, providing insights into simulation dynamics and protein-ligand interactions. The results obtained were analyzed and the images were developed in QtGrace version 0.2.6

5.2.7 ADMET studies of phytochemicals: The phytochemicals obtained from Ayurvedic formulations were subjected to ADMET analysis using Swiss-ADME (http://www.swissadme.ch/) [9] to predict their physicochemical properties. Important parameters such as molecular weight (MW), octanol/water partition coefficient (logP), total polar surface area (TPSA), number of hydrogen bond donors/acceptors (HBD & HBA) and total number of rotatable bonds (TRB) were considered as stated by Lipinski's rule of five. These parameters are routinely used as standards to predict their molecular flexibility, oral bioavailability, absorptivity in gastro-intestinal tract, etc. which determines whether a particular phytochemical/chemical compound can be considered as a candidate drug.

5.2.8 Cell Culture: Colorectal cancer cell lines DLD1, HT29 and HCT-116 were cultured in DMEM: F12 High glucose media, supplemented with 10% fetal bovine serum (FBS) and 1% penicillin-streptomycin antibiotic solution as described in section **3.4**.

5.2.9 MTT cell viability assay: The colorectal cancer cells were treated with different Ayurvedic formulations at varying concentrations for a period of 48 hours and the loss in cellular viability of CRCs were measured using MTT cell viability assay as described in section **3.5**.

5.2.10 Western blotting: DLD1 and HCT-116 ($1*10^6$) cells were seeded in a 6 well plate prior to the day of the experiment. Cells were washed twice with PBS and were treated with various concentrations of HCAE and AMCAE. Cells were harvested and lysed with RIPA lysis buffer

and the protein content was measured using standard protein assays. Proteins were separated on a 10% SDS-polyacrylamide gel and then transferred to nitrocellulose membrane (Bio-Rad cat. # 162-0112) on a Trans-Blot Turbo (Bio-Rad). The membrane was blocked with 5% BSA for 1-2 hours at room temperature. The blots were then incubated with primary antibodies (Akt1 (1:2500), Src-kinase (1:2000), vimentin (1:2500), cyclin D1 (1:5000), and β-actin (1:5000)). overnight at 4^0C followed by incubation with appropriate HRP conjugated secondary antibodies for 1-2 hours at room temperature. Proteins bands were analyzed by using Bio-Rad Clarity™ Western ECL substrate kit and images were developed in Bio-Rad chemiDoc system.

5.3 Results

5.3.1 Phytochemicals cross-talk to each other by sharing similar drug targets: Polyphenols, the secondary metabolites derived from higher plants are present abundantly in plant based supplements [10]. Polyphenol rich food is shown to have oxidative, metabolic and anti-inflammatory effects [11]. Given its wide range of potential therapeutic applications, polyphenols tend to have a wide range of interacting proteome network [12]. A total of thirteen phytochemicals were identified in HCAE which are polyphenols. Polyphenols are known to bind with various intracellular protein targets and modulate their activities [12] The in-silico network based pharmacology approach is high throughput and was used to identify 382 protein targets from Drug Bank (**Figure 5.2A**). The 13 phytochemicals with their resultant protein targets was used to create a phytochemical-protein network comprising of 394 nodes and 1023 edges, which highlights the cross-talk between them (**Figure 5.2B**). Protein-drug interaction is a crucial parameter to determine the relevance of target protein in the action of the drug [13]. To explore such possibilities, Binding Data Bank (Binding DB) was explored to the potential targets and their interaction with small molecules to understand the inhibition and kinetics studies of the targets. A total of 132 protein targets were selected from Binding DB to create network comprising of 143 nodes and 275 edges (**Figure 5.2C**). The results obtained from the analysis of the protein networks showed that each phytochemical has specific protein targets, while a single protein is a target for multiple phytochemicals. Hence, the resulting network distinguishes between protein targets depending on the number of neighbors it has. The network from Drug Bank showed that protocatechuic acid (PA), gallic acid (GA) and methyl gallate (MG) exclusively target 1, 18 and 44 proteins respectively. Also, both GA and PA were found to share 22 protein targets and the altogether a total of 53 proteins. Similarly, Q9Y694 **(**Solute carrier family 22 member 7), P08183 (ATP-dependent translocase ABCB1), P03372

(Estrogen receptor-α) and P08684 (Cytochrome P450 3A4) having 8, 9, 10 and 11 phytochemical neighbors respectively were considered to be the most important targets from a sum of 469 (132 from Binding DB and 382 from Drug Bank (after removing 45 duplicates)) proteins. These results demonstrate that the phytochemicals from HCAE has the potential to target proteins in both synergistic and individualistic manner.

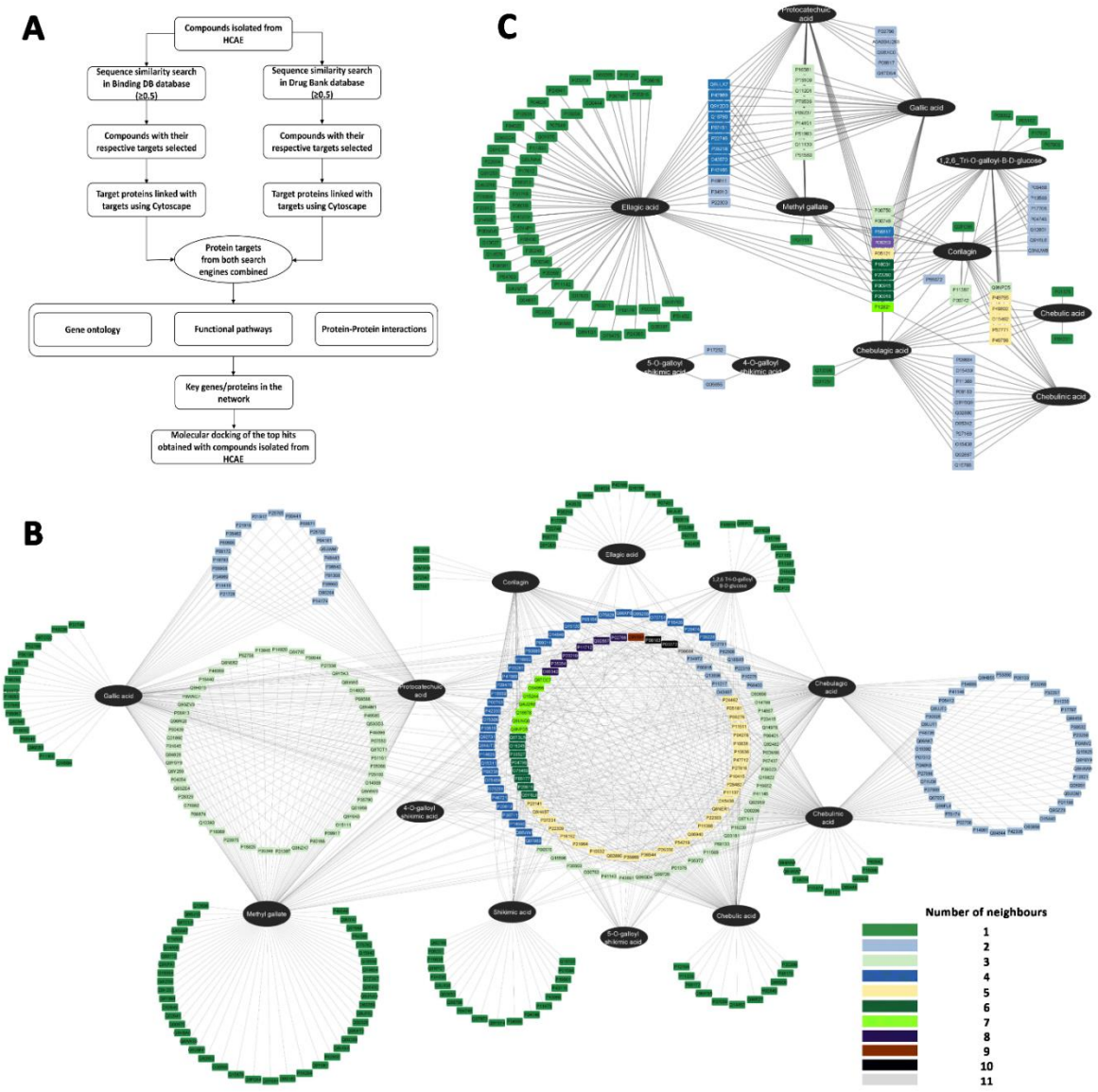

Figure 5.2: Phytochemicals from HCAE share multiple protein target for their action. **(A)** Overall scheme to select and screen protein targets for phytochemicals present in HCAE**.** **(B)** Protein target cross-talk is crucial for phytochemical action (Cytoscape network for phytochemical from Drug Bank). **(C)** Phytochemical-protein target interaction highlights role of crucial proteins (Cytoscape network for phytochemical from Binding DB)

In a similar manner, a phytochemical-protein network was constructed using the 8 polyphenols isolated from AMCAE by mapping with their protein targets. A total of 273 nodes and 417 edges with 3.02 average number of neighbors highlighted the cross-talk between

phytochemicals ant their protein targets obtained from Drug Bank (**Figure 5.3A**). Because protein and drug interactions are critical in finding relevant targets, we constructed a network of protein targets with a total number of 168 nodes and 262 edges with 3.1 average number of neighbors using Binding DB to aid in understanding the kinetics of the protein targets (**Figure 5.3B**). The protein network analysis revealed that each phytochemical has distinct protein targets, whereas a single protein is a target for numerous phytochemicals. The generated networks differentiate between protein targets based on the number of neighbors they have. For example, the network from Drug Bank showed that β-glucogallin, corilagin and macabarterin exclusively target 3, 10 and 31 proteins respectively. Also, both corilagin and macabarterin were found to share 26 protein targets amongst them. All the three polyphenols share a sum of 14 targets between them (Figure **5.3B**). The protein targets with most neighbors were selected from a sum of 387 proteins (159 from Binding DB and 271 from Drug Bank (after removing 43 duplicates)) which were having 6 neighbors.

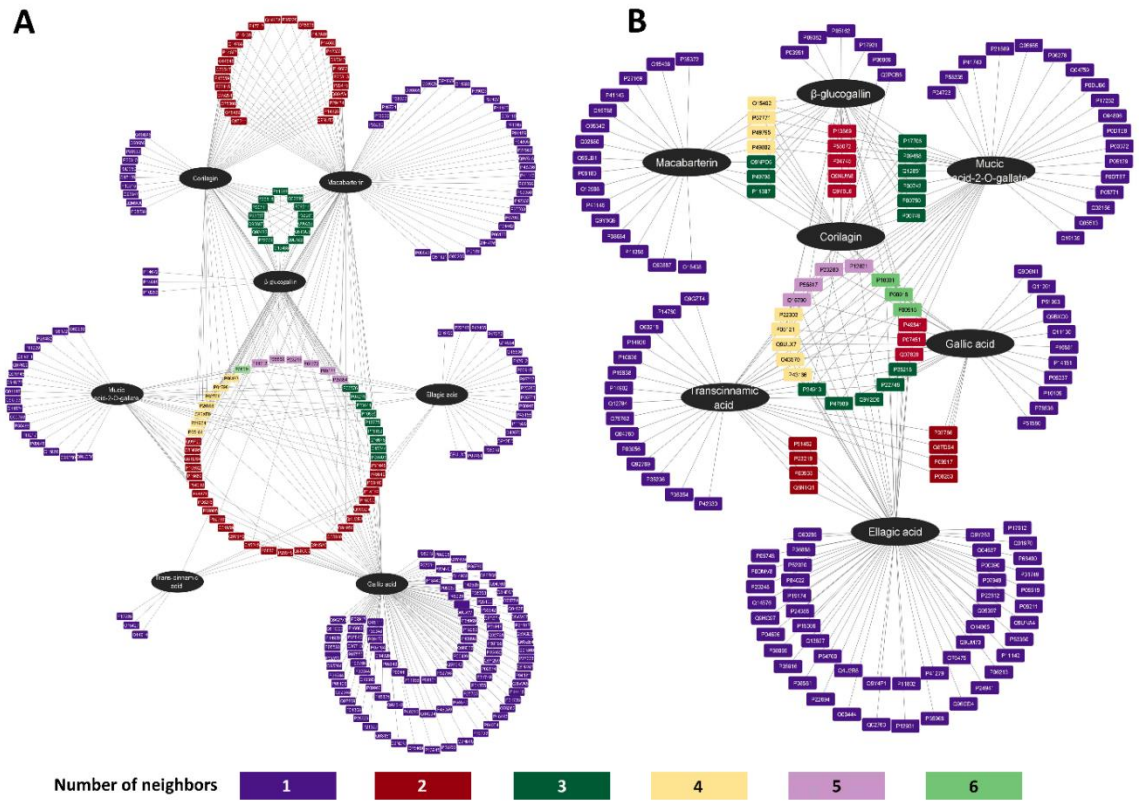

Figure 5.3: Phytochemical-protein network depicts sharing of protein targets amongst them. (A) Cross-talk across protein targets is critical for phytochemical activity. (Cytoscape network for phytochemical from Drug Bank) **(B)** Target-phytochemical interaction shows importance of key proteins. (Cytoscape network for phytochemical-target network from Binding DB)

The top most connected targets revealed from both phytochemical-protein networks were cytochrome P450-3A4 (P08684), tyrosine protein phosphatase (P18031), carbonic anhydrase 1 (P00918), and carbonic anhydrase 2 (P00915). The results illustrate the importance of synergistic and individualistic actions of phytochemicals from AMCAE.

5.3.2 Phytochemicals disturbs multiple crucial cellular pathways and identification of hub protein using PPI analysis: The phytochemical-protein networks revealed that these small molecules were interacting many proteins with significant role in cellular processes. The KEGG pathway analysis has revealed a total of 178 significant pathways (with a p-value < 0.05) associated with the protein targets targeted by phytochemicals from HCAE, indicating that these phytochemicals possess the potential to influence key biological pathways. The proteins targeted by the phytochemicals were found to be involved not only in metabolic pathways of the cell but also in chemical carcinogenesis-receptor activation and different cell survival pathways in cancer (**Figure 5.4A**). Basic signal transduction pathways such as the MAPK pathway, calcium signaling pathway and others were also among the top hits. Further analysis with GO enrichment of the query targets yielded 784, 136 & 268 GO terms for BP, CC & MF respectively. The top 8 hits of GO functional annotation results indicate that most of the proteins targeted by the phytochemical are localized in the plasma membrane and are receptors responsible for signal transduction, drug response, apoptotic regulation, protein phosphorylation etc. (**Figure 5.4B)**. Combining the GO and KEGG pathway analyses suggest that the majority of the target proteins are either connected to cellular metabolism, cancer related pathways, cell survival & proliferation. The complex nature of different diseases, and their interaction patterns are widely explained by the help of a biological protein network [14]. The list of protein targets collected from Drug Bank and Binding DB was utilized to examine the PPI interaction network and its most significant proteins that are responsible for network stability. The STRING network analysis, at a very high confidence level, yielded a protein-protein interaction (PPI) network having a p-value < 1.0e-16 (**Figure 5.4C**). The network consisted of 451 nodes with 169 edges having 3.605 as average number of neighbors per protein. There were 113 proteins in the network who shared at least one neighbour. The following parameters (DCy ≥ 0.8, BCy ≥ 0.07 & CCy ≥ 0.3) were set to screen the network to further funnel down the most important proteins in the network. The screening resulted in an enriched PPI network of eight proteins involving HSP90AA1 (Heat shock protein HSP90 alpha), Src kinase (Proto-oncogene tyrosine-protein kinase Src (c-Src)), NCOA1 (Nuclear receptor coactivator 1), PIK3R1 (Phosphatidylinositol 3-kinase regulatory subunit alpha),

AKT1 (RAC-alpha serine/threonine-protein kinase), ESR1 (estrogen receptor), EGFR (Epidermal growth factor receptor) & AR (androgen receptor) (**Figure 5.4D & E**). Similarly, when conducting STRING analysis for protein targets derived from phytochemicals sourced from AMCAE at a confidence level of 0.990, it resulted in a network with PPI enrichment values reaching as low as 1.0e-16. The hub proteins identified through protein-protein interaction (PPI) analysis for the protein targets influenced by phytochemicals in both formulations are the same.

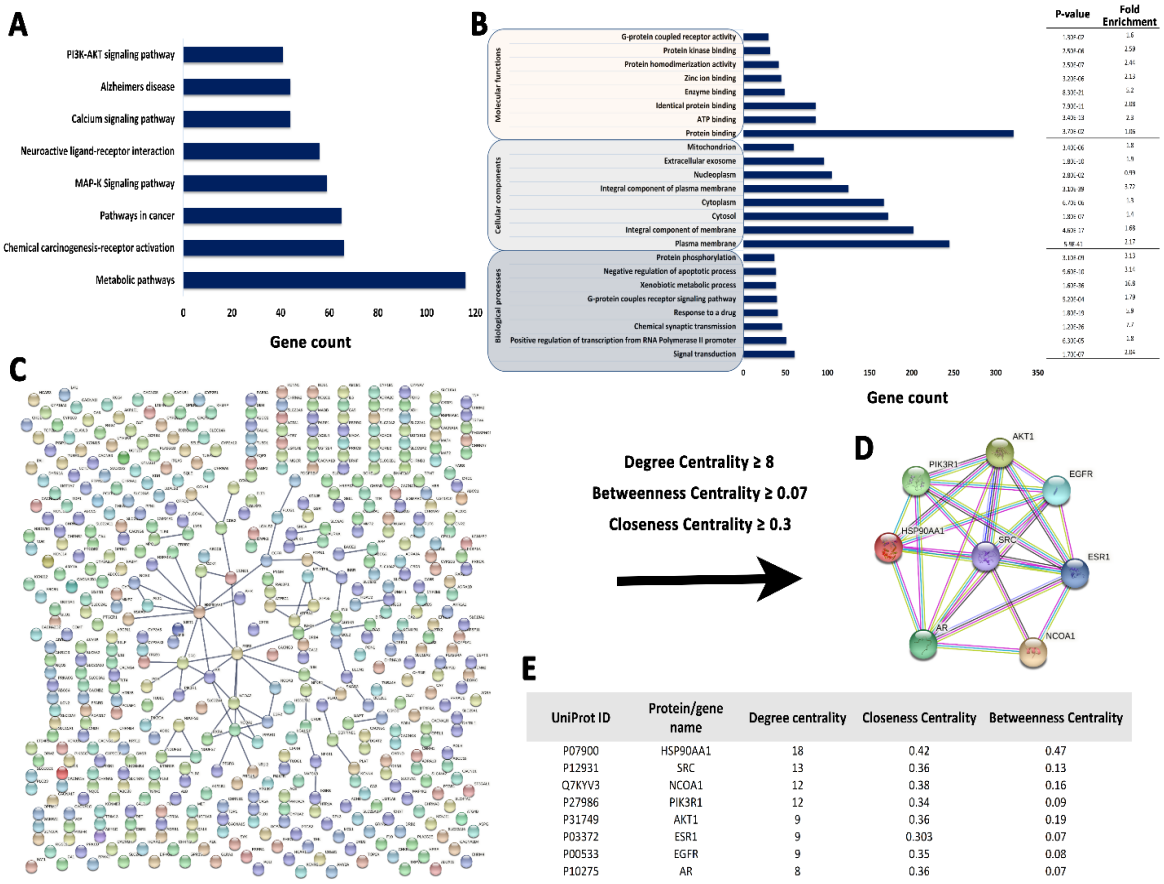

E

UniProt ID	Protein/gene name	Degree centrality	Closeness Centrality	Betweenness Centrality
P07900	HSP90AA1	18	0.42	0.47
P12931	SRC	13	0.36	0.13
Q7KYV3	NCOA1	12	0.38	0.16
P27986	PIK3R1	12	0.34	0.09
P31749	AKT1	9	0.36	0.19
P03372	ESR1	9	0.303	0.07
P00533	EGFR	9	0.35	0.08
P10275	AR	8	0.36	0.07

Figure 5.4: Phytochemicals from HCAE targets multiple cellular pathways. (A) KEGG Pathway analysis for candidate targets obtained from similarity search. **(B)** GO enrichment analysis of candidate targets by DAVID software. **(C)** Protein-protein interaction analysis of candidate targets at 0.999 level of confidence. **(D & E)** The top 8 targets of HCAE based on Cytoscape network analysis.

The PPI network comprised of 372 nodes and 135 edges with average number of neighbors as 3.6 (**Figure 5.5A**). A total of 96 proteins had at least one neighbor in the network even though the confidence level was set to 0.99. In order to find the most important proteins responsible for the integrity of the network, certain parameters (DC ≥ 7, BC ≥ 0.08 & CC > 0.3) were employed. This screening of proteins resulted a total of 8 proteins namely HSP90AA1 (Heat

shock protein HSP90 alpha), PI3KR1 (Phosphatidylinositol 3-kinase regulatory subunit alpha), ESR-α (estrogen receptor- alpha), c-Src (Proto-oncogene tyrosine-protein kinase Src (c-Src)), EGFR (Epidermal growth factor receptor), AR (androgen receptor), NCOA1 (Nuclear receptor coactivator 1), and Akt1 (RAC-alpha serine/threonine-protein kinase) (**Figure 5.5B**). Similarly, for protein targets obtained from AMCAE, the GO enrichment performed using DAVID software yielded 724, 129 and 251 GO terms for BP, CC and MF respectively. The top 10 hits of all three functional annotations sheds light on the localization, function and which cellular process they affect the most. The protein targeted by AMCAE are related mostly to interacting kinases that are localized in plasma membrane and cytoplasm which affect multiple signal transduction pathways (**Figure 5.5C**).

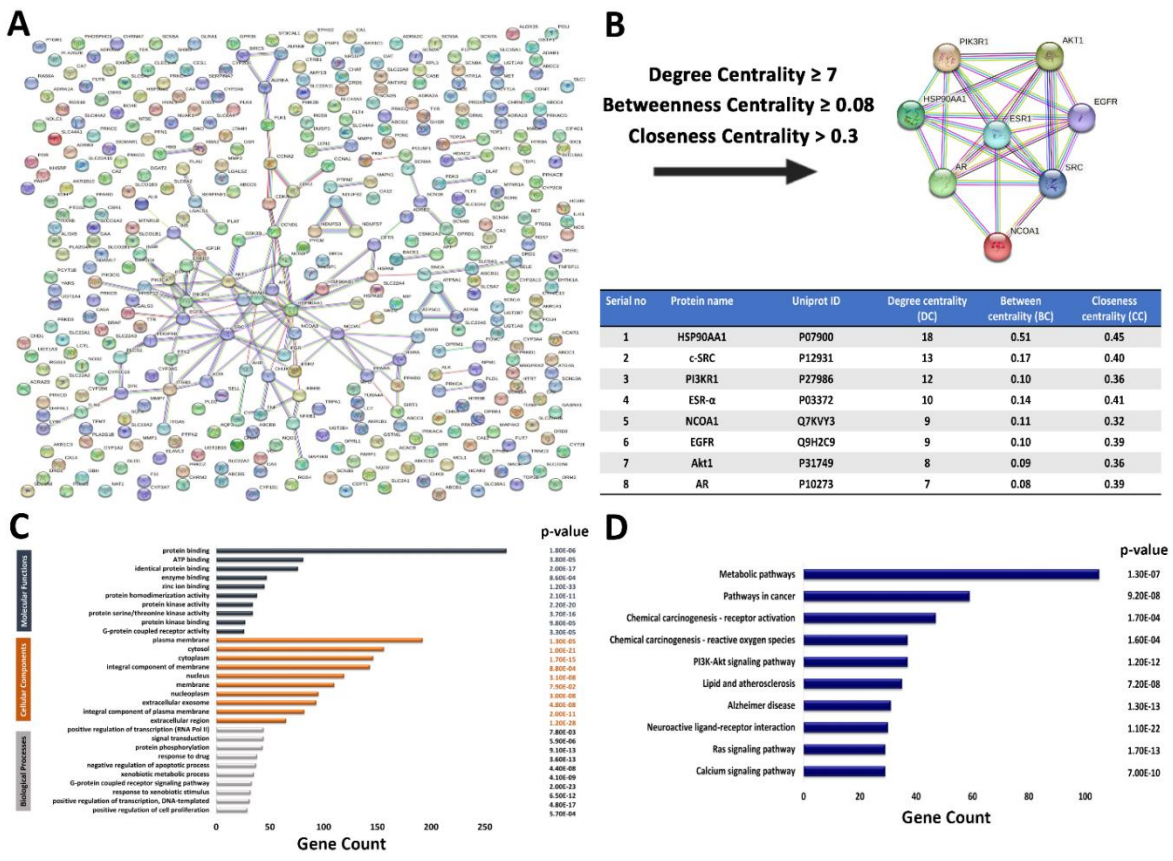

Figure 5.5: Phytochemicals from AMCAE targets multiple cellular pathways. (A) Protein-protein interaction analysis of protein targets at 0.990 level of confidence. **(B)** The top 8 targets of AMCAE based on Cytoscape network analysis. **(C)** GO enrichment analysis of protein targets obtained by DAVID software. **(D)** KEGG Pathway analysis for candidate targets obtained from similarity search.

The KEGG pathway analysis of molecular targets revealed that there are 178 significant pathways (p-value < 0.02) that can be restricted or suppressed by phytochemical from AMCAE

(**Figure 5.5D**). The effectuated pathways from KEGG analysis are mostly metabolic and cellular pathways that have a role in cancer related signaling.

5.3.3 Phytochemicals are binding to the selected protein targets from network: Ligand-protein interaction studies are a crucial step in determining the signal transduction events that is being modulated by a particular ligand. The comparison between the binding affinities of known inhibitors versus the ligand of interest might help us decide which is better. The phytochemicals being small molecules could bind to many sites in their protein targets. However, only the protein targets with known inhibitors and defined binding sites were taken, as it gives an attractive opportunity to determine if they could be better inhibitors than the molecules already reported. Thus, the phytochemicals were docked with their protein targets at the specific binding sites of their inhibitors (**Table 5.1**). The phytochemicals being small molecules could bind to many sites in their protein targets. However, only the protein targets with known inhibitors and defined binding sites were taken, as it gives an attractive opportunity to determine if they could be better inhibitors than the molecules already reported. Thus, the phytochemicals were docked with their protein targets at the specific binding sites of their inhibitors.

Table 5.1: Binding site and residues of the protein targets

S. No.	Protein	PDB ID	Binding site	Binding residues
1	c-Src	2H8H	Kinase domain	270-523
2	HSP90AA1	1YET	N-terminal domain	9-232
3	Akt1	3O96	Pleckstrin homology & Kinase domain	6-108 & 150-447
4	PI3KR1	5AUL	C-terminal SH2 domain	624-718
5	AR	2AX6	Ligand binding domain	665-919
6	EGFR	2ITY	Kinase domain	685-953
7	ESR-α	1X7R	Ligand binding domain	355-549

The molecular docking results demonstrated that the phytochemicals from HCAE and AMCAE have stronger binding affinity towards their targets when compared to their positive controls (known inhibitors) (**Table 5.2 & 5.3**). For instance, wortmannin which is a well-known inhibitor of PI3KR class of proteins binds to its SH2 domain. Chebulagic acid was found to have better affinity when docked in to the binding site of wortmannin, although both of them shared some key residues. Apart from the key amino acids such as R631, V667, N707 & L710, additional 4 residues (K668, C670, V671, & F681) were found to be interacting with chebulagic acid. This could account for the lower binding energy of the chebulagic acid in comparison with wortmannin. Additionally, many phytochemicals such as shikimic acid, gallic

acid, chebulic acid, 5 hydroxymethyfurfural, protocatechuic acid, 4-O-galloyl Shikimic acid, 5-O-galloyl Shikimic acid, methyl gallate and ellagic acid showed uniform binding to all protein targets (binding energy range) that demonstrates the lack of specificity but a broader range of action across the proteome.

Table 5.2: Binding energy values of HCAE isolated compounds against protein targets.

		Binding energy (kcal/mole)						
		c-Src	**HSP90AA1**	**Akt1**	**PI3KR1**	**AR**	**EGFR**	**ESR-α**
Positive Control	EA	-7.7						
	Rif		-11.2					
	Res			-7.5				
	Wor				-6.4			
	Ho					-8.6		
	EA						-7.6	
	PG							-6.4
C1		-4.5	-4.9	-5	-7.9	-5.2	-2.7	-4.8
C2		-5.4	-5.1	-6	-6.9	-6.3	-4.3	-5.6
C3		-4.7	-4.6	-5	-5.6	-4.7	-5.3	-5
C4		-4.7	-4	-5	-4.7	-4.7	-5.4	-5.1
C5		-4.7	-4.9	-5.3	-6.1	-5.1	-5.6	-5.3
C6		-6.9	-6.6	-7.5	-6.5	-7.9	-6	-7
C7		-7.4	-5.6	-8.8	-6	-8.3	-6.7	-7.2
C8		-5.4	-5	-5.9	-4.1	-5.2	-5.9	-5.7
C9		-0.7	-7.8	-7.8	-4.7	13.3	-7.2	-4.2
C10		-8.9	-6.7	-10.8	-5.3	-1.9	-6.2	-2.2
C11		-2	-16.1	26	-12	306	-12.7	163
C12		-8.9	-5.7	-9.6	-5.06	225	-6.1	102
C13		-7.7	-5.6	-7.1	-5.7	-7.8	-7.6	-7.7

EA- Ellagic acid, **Rif**- Rifabutin, **Res**- Resveratrol, **Wor**- Wortmannin, **Ho**- Homosalate, **PG**- Propyl gallate. (EA, Rif, Res, Wor, Ho and PG were considered as positive control for molecular docking studies). **C1**- Shikimic acid, **C2**- Chebulic acid, **C3**- Gallic acid, **C4**- 5Hydroxymethylfurfural, **C5**- Protocatechuic acid, **C6**- 4-*O*-galloyl Shikimic acid, **C7**- 5-*O*-galloyl Shikimic acid, **C8**- Methyl gallate, **C9**- Corilagin, **C10**- 1,2,6 Tri-*O*-galloyl-β-D-glucose, **C11**- Chebulagic acid, **C12**- Chebulinic acid, **C13**- Ellagic acid

On the other hand, chebulagic acid was found to have specific mode of action it targeted only three proteins namely HSP90AA1, PIK3R1 & EGFR with binding energies of -16.1, -12 & -12.7 kcal/mole respectively and showed no affinity towards the rest of the protein targets. The protein-ligand interactions for the protein targets against their best docked phytochemicals are demonstrated (**Figure 5.6)**. Further, chebulinic acid, 1, 2, 6, Tri-*O*-galloyl β-D-glucose, 5-*O*-galloyl Shikimic acid and ellagic acid were found to target Src kinase, Akt1, AR and ESR-α respectively.

Table 5.2: Binding energy values of AMCAE isolated compounds against protein targets

		Binding energy (kcal/mole)						
		AR	**Akt1**	**ESR-α**	**HSP90AA1**	**PI3KR1**	**EGFR**	**c-Src**
Positive Control	Ho	-8.6						
	Res		-7.5					
	PG			-6.4				
	Rif				-11.1			
	Wor					-6.4		
	EA						-7.6	
	EA							-7.7
C1		-5.4	-5.6	-4.9	-3.1	-5	-3.2	-5.1
C2		-6.3	-6.5	-7.5	-6.1	-4.2	-4.8	-6.7
C3		-4.9	-5.1	-4.9	-4.7	-5.6	-5.2	-4.7
C4		-4.6	-5	-5	-4	-4.7	-5.3	-4.6
C5		1856	102.7	759	-3.3	-2.7	-6.1	11
C6		11.9	-7.4	-4.2	-7.9	-7.9	-7	-6.8
C7		-7.8	-7.1	-7.7	-5.6	-5.7	-7.6	-7.7
C8		-6.1	-6.3	-5.1	-4.4	-6.6	-4.7	-5.1

EA- Ellagic acid, **Rif**- Rifabutin, **Res**- Resveratrol, **Wor**- Wortmannin, **Ho**- Homosalate, **PG**- Propyl gallate. (EA, Rif, Res, Wor, Ho and PG were considered as positive control for molecular docking studies). **C1**- Mucic acid 2-O-gallate, **C2**- β-glucogallin, **C3**- Gallic acid, **C4**- 5Hydroxymethylfurfural, **C5**- Macabarterin, **C6**- Corilagin, **C7**- Ellagic acid, **C8**- Transcinnami acid.

The findings of the molecular docking showed that the phytochemicals from AMCAE have a higher affinity for binding to their targets than their respective controls or known inhibitors (**Table 5.3**). Resveratrol is a well-known inhibitor of Akt1 that binds to its kinase domain.

Corilagin a polyphenol isolated from AMCAE was found to have identical binding energy as suggested by molecular docking studies. The identical affinities or binding energies of both resveratrol and corilagin towards with kinase domain of Akt1 is largely due to sharing of common amino acids (Trp80, Val270, Val271, and Asp292).

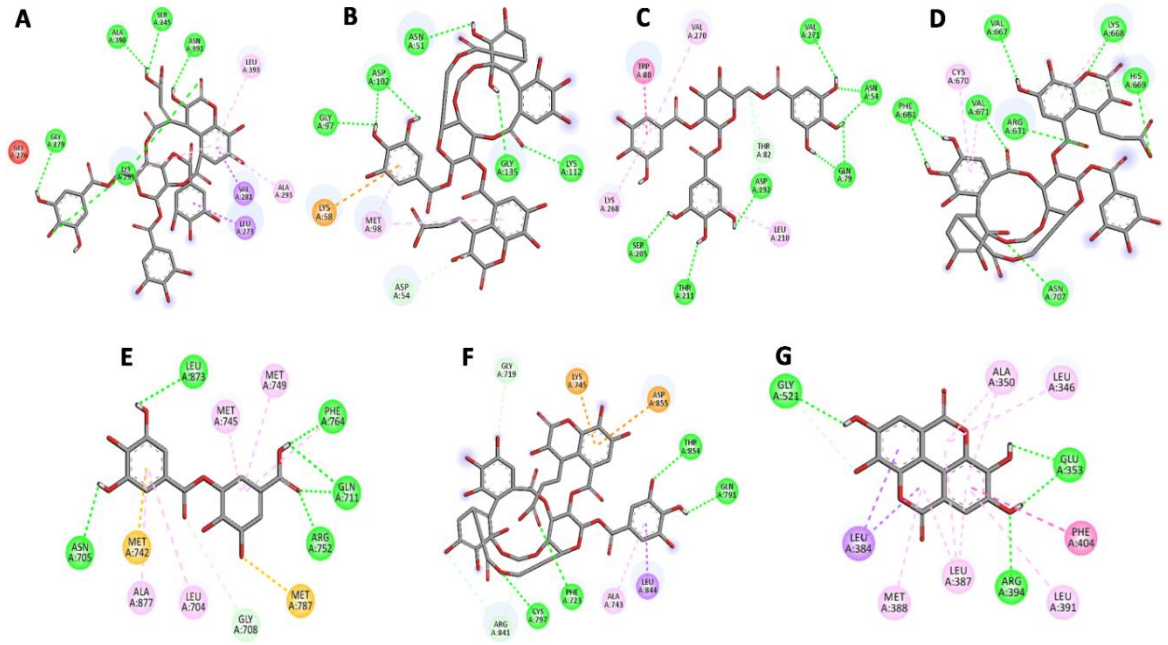

Figure 5.6: Phytochemicals from HCAE fit well into target protein with multiple interactions. Molecular modelling and docking of phytochemicals into selected protein target to generate phytochemical-protein target model. Analysis of molecular model indicate extensive interactions of phytochemical with protein target. **(A)** Src kinase-Chebulinic acid, **(B)** HSP90AA1-Chebulagic acid, **(C)** Akt1-1, 2, 6 Tri-*O*-galloyl β-D-glucose, **(D)** PIK3R1-Chebulagic acid, **(E)** AR-5-*O*-galloyl Shikimic acid, **(F)** EGFR-Chebulagic acid, **(G)** ESRα-Ellagic acid. (Color code: Green-Conventional hydrogen bond, Orange-Π-anion, Purple-Π sigma, Light pink- Π alkyl, Cream- Carbon-hydrogen bond, Yellow-Π-sulfur/Sulfur-X bond)

In addition, corilagin was shown to have the highest affinity for HSP90AA1 among the phytochemicals identified from AMCAE, despite the fact that its recognized inhibitor rifabutin had a higher affinity. Further, ellagic acid was found to be the most potent of all phytochemicals from AMCAE (**Figure 5.7).** Ellagic acid showed lowest binding energies (strongest affinity) towards EGFR, AR, ESR-α and c-Src kinase with binding energies of -7.6, -7.8, -7.7 and -7.7 kcal/mole respectively. Higher order polyphenol macabarterin was discovered to have negligible interactions with HSP90AA1, PI3KR1, and EGFR, but no affinity for AR, Akt1, ESR-, and c-Src. The interactive amino acids of the best docked protein-ligand complexes are demonstrated.

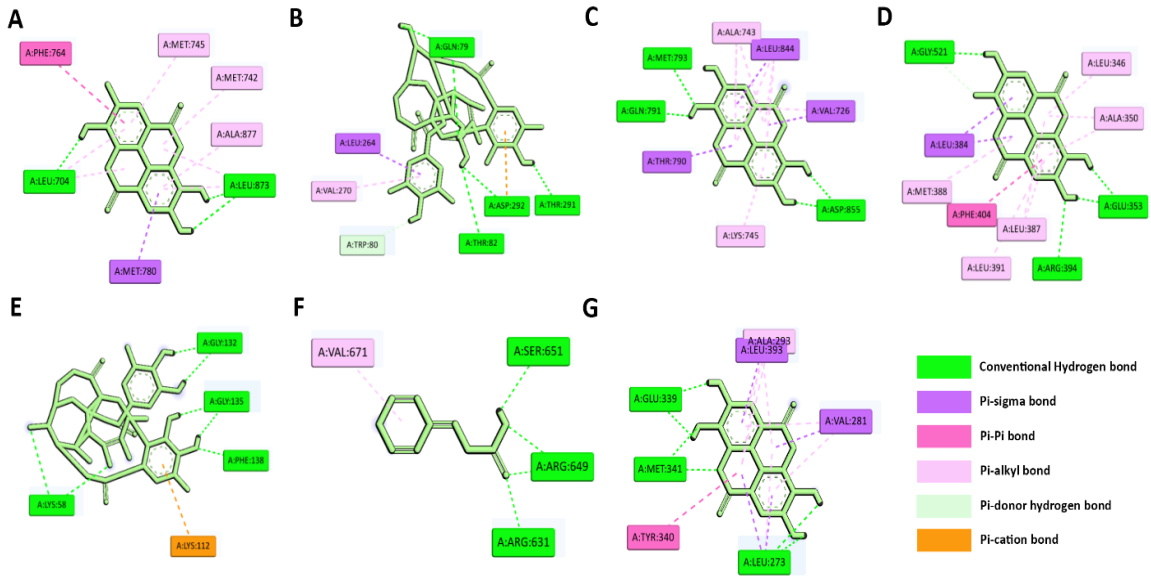

Figure 5.7: Phytochemicals from AMCAE bind well with their protein targets. Molecular modelling and docking of phytochemicals into specified protein targets to produce a phytochemical-protein target model. The molecular model analysis shows that phytochemicals have extensive interactions with protein targets**. (A)** Androgen receptor- Ellagic acid, **(B)** Akt1-Corilagin, **(C)** EGFR-Ellagic acid, **(D)** Estrogen receptor α-Ellagic acid, **(E)** HSP90AA1-Corilagin, **(F)** PI3KR1-Transcinnamic acid **(G)** c-Src-Ellagic acid.

5.3.4 ADMET studies highlight drug likeliness of phytochemicals present in Ayurvedic formulations: The key factors in drug discovery are the pharmacodynamics and pharmacokinetic properties of a compound or molecule that manifests its drug likeliness. The ADMET (Absorption, Distribution, Metabolism, Excretion and Toxicity) tool is a crucial for selecting the compounds based on its pharmacokinetic and pharmacodynamics properties. Lipinski's rule of 5 states that there should not be more than one violation in the parameters stated. As per Lipinski's rule of 5, there should not be more than one violation in the parameters such as molecular weight, number of rotatable bonds, number of hydrogen bond acceptor & donors, lipophilicity, and total polar surface area. Out of a total of 13 phytochemicals isolated from HCAE, 9 were found to obey Lipinski's rule with 6 phytochemicals having no violations (**Table 5.4**). Although the compounds having high molecular weights (such as 1, 2, 6 Tri-*O*-galloyl β-D-glucose, corilagin and chebulagic acid) were having more than one violation, further studies are required to study their drug likeliness (**Figure 5.8**). Four of the eight phytochemicals that were separated from AMCAE exhibited zero violations, one showed one violation, and three showed more than two violations (**Table 5.5**) (**Figure 5.9**). The phytochemicals from AMCAE that showed more than 2 violations are macabarterin, mucic acid 2-*O*-gallate and corilagin. Although, these compounds are known to have high molecular

weights, which are contributing to violations in Lipinski's rule of 5, further validation is required to exert their drug likeliness.

Table 5.4: SWISS ADME parameters for phytochemicals from HCAE

	MW	Log$P_{o/w}$ (iLOGP)	TPSA (A^o)	TRB	HBA	HBD	Number of violations				
							Lipinski	Ghose	Veber	Egan	Muegge
C1	174	0.4	97	1	5	4	0	2	0	0	1
C2	356	-0.6	198	5	11	6	2	0	1	1	3
C3	170	0.2	97	1	5	4	0	2	0	0	1
C4	126	0.9	50	2	3	1	0	3	0	0	1
C5	154	0.6	77.7	1	4	3	0	3	0	0	1
C6	326	0.2	164	4	9	6	1	1	1	1	2
C7	326	0.2	164	4	9	6	1	1	1	1	2
C8	184	0.9	86	2	5	3	0	0	0	0	1
C9	634	2	310	3	18	11	3	2	1	1	4
C10	636	1.8	310	10	18	11	3	2	1	1	4
C11	954	0.4	447	5	27	13	3	3	1	1	5
C12	956	0.9	447	12	27	13	3	3	2	1	4
C13	302	0.8	141	0	8	4	0	0	1	1	0

MW-Molecular weight, **TRB**-Number of rotatable bonds, **HBA**-Hydrogen bond acceptors, **HBD**-Hydrogen bond donors

Table 5.5: SWISS ADME parameters for phytochemicals from AMCAE

	MW	Log$P_{o/w}$ (iLOGP)	TPSA (A^o)	TRB	HBA	HBD	Number of violations				
							Lipinski	Ghose	Veber	Egan	Muegge
C1	362	-0.03	222.2	8	12	8	2	1	1	1	3
C2	332	1.14	177.1	4	10	7	1	1	1	1	2
C3	170	0.21	97.9	1	5	4	0	2	0	0	1
C4	126	0.91	50.44	2	3	1	0	3	0	0	1
C5	1102	0.69	532.5	3	32	18	3	4	1	1	6
C6	634	2.03	310.6	3	18	11	3	2	1	1	4
C7	302	0.79	141.3	0	8	4	0	0	1	1	0
C8	148	1.55	37.3	2	2	1	0	2	0	0	1

MW-Molecular weight, **TRB**-Number of rotatable bonds, **HBA**-Hydrogen bond acceptors, **HBD**-Hydrogen bond donors

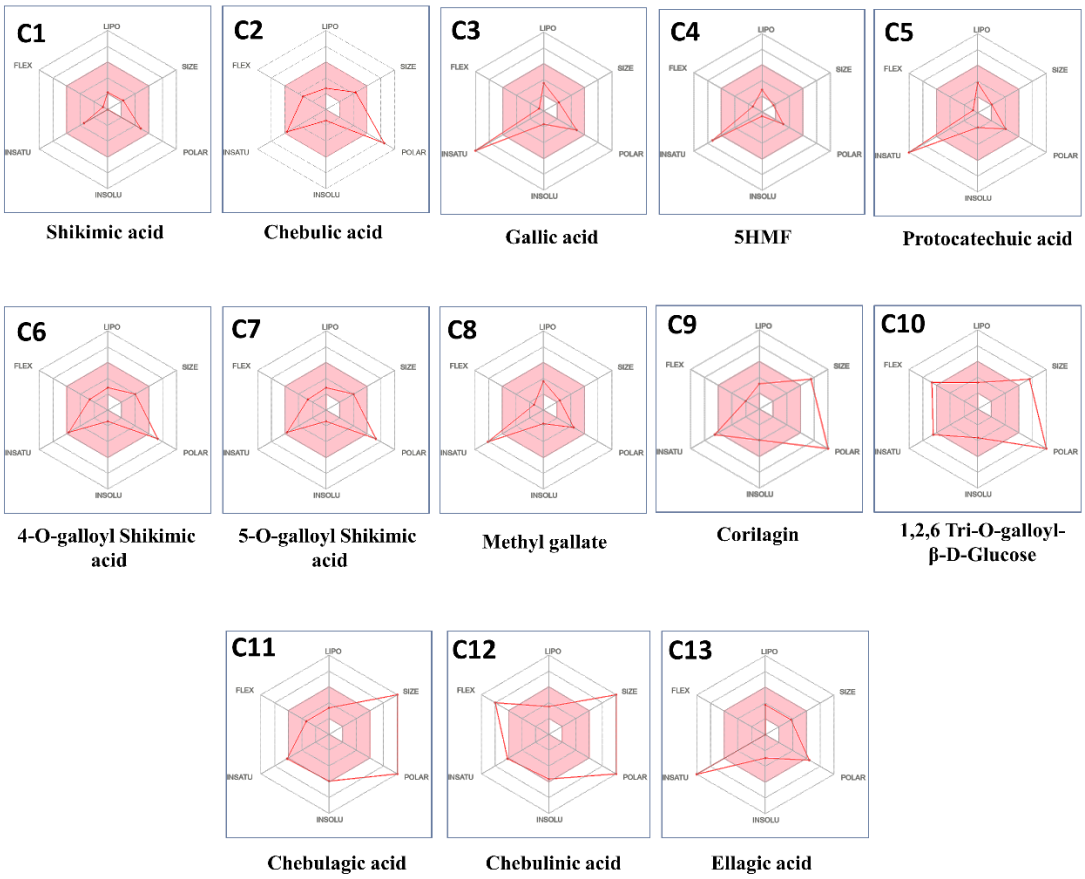

Figure 5.8: ADMET analysis of compounds isolated from HCAE.

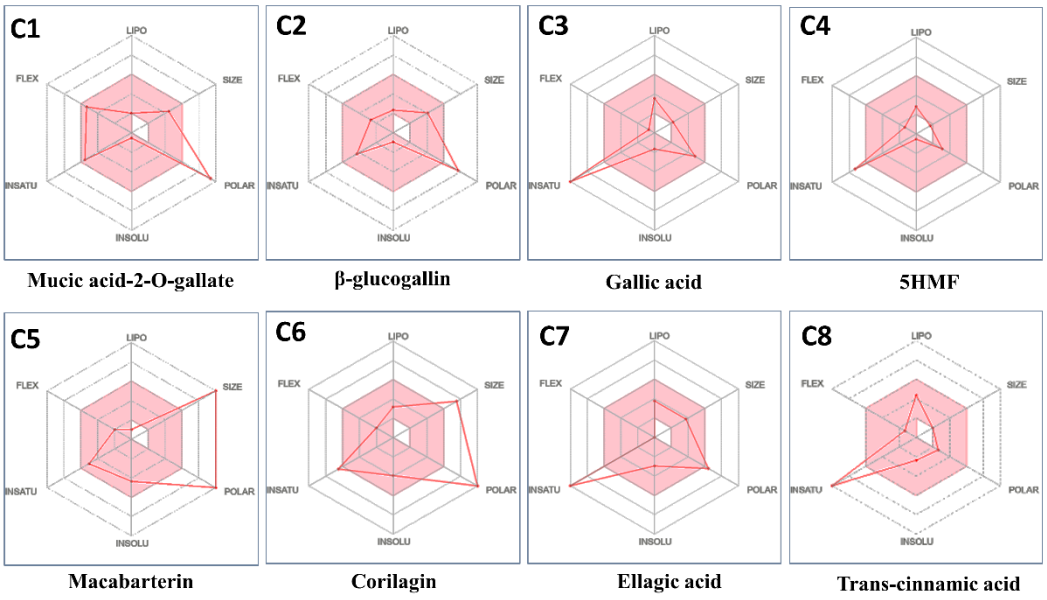

Figure 5.9: ADMET plot of phytochemicals isolated from AMCAE.

5.3.5 Molecular dynamic simulation studies show that protein-phytochemicals complexes are stable: The prospective phytochemical inhibitors' capacity to distinctly inhibit the chosen protein targets is revealed by molecular docking experiments. To further validate our findings, we conducted molecular dynamics (MD) simulations to gain deeper insights into the time-dependent behavioural variations and dynamic transformations of the system. MD simulations investigate the dynamic processes in biological systems, unveiling the fluctuations, conformational changes, and time-dependent behaviour of protein backbones in comparable with protein-ligand interactions. The dynamics of the system were measured using variable parameters such as RMSD (Root mean square deviation), RMSF (Root mean square fluctuation), radius of gyration, number of H bonds and paired distance between ligand and protein for 100 nanoseconds. Comparing the stability of the complexes to their protein backbone counterparts, different characteristics of seven distinct proteins (AR, ESR-α, PIK3R1, EGFR, Akt1, c-Src, and HSP90) and their complexes with specific ligands show that there are negligible impacts on the stability of the complexes (**Table 5.6**). The RMSD difference between the protein and backbone and the ligand complexes were found to be in the range of 0.009 to 0.09 nm which is very negligible. Similarly, the difference in radius of gyration also wavered in the range of 0.001 to 0.09 nm.

Table 5.6: **The mean values of molecular dynamic simulation parameter for proteins and their complexes (Ligands from HCAE).**

		RMSD (nm)	RMSF (nm)	Radius of gyration (nm)	Number of H bonds	Distance (nm)
Androgen receptor	P	0.137	0.111	1.857	-----	-----
	P+L	0.128	0.115	1.847	2.67	0.18
ESRα	P	0.267	0.158	1.868	-----	-----
	P+L	0.176	0.152	1.866	2.79	0.168
EGFR	P	0.266	0.165	2.085	-----	-----
	P+L	0.227	0.141	2.095	4.35	0.169
PI3KR1	P	0.214	0.159	1.333	-----	-----
	P+L	0.169	0.13	1.318	1.19	0.49
Akt1	P	0.474	0.221	2.607	-----	-----
	P+L	0.52	0.218	2.703	5.324	0.166
HSP90	P	0.295	0.179	1.796	-----	-----
	P+L	0.275	0.171	1.778	1.774	0.378
c-Src kinase	P	0.246	0.146	2.477	-----	-----
	P+L	0.279	0.153	2.478	2.71	0.181

(**P**-protein, **P+L**-Protein + ligand). MD simulations of all the proteins and their complexes are run at ambient temperature (300K)

The difference between the RMSD values of c-Src and its complex with chebulinic acid was found to be 0.042 which is very low. Hence there is negligible effect on its stability when chebulinic acid binds c-Src. However, the residues 275-295, which are the protein region containing the binding site, exhibited very little volatility in the RMSF values of c-Src coupled with chebulinic acid. The RMSF analysis was performed in order to assess the binding strength and specificity of chebulinic acid with c-Src. The average RMSF value for c-Src backbone was found to be 0.146 nm which did not differ much with c-Src in complex with chebulinic acid having an average RMSF values of 0.153 when the dynamic system was maintained at 300 K. A similar trend was observed in all the complexes except that of HSP90AA1 and PIK3R1 with their ligand chebulagic acid (**Figure 5.10A-G**). Further, In MD simulation, paired distance gauges the stability of protein-ligand complexes by measuring the distance between chosen atoms/molecules throughout the system. The significant variation observed in the minimum paired distance between chebulagic acid and its protein targets (HSP90AA1 and PIK3R1) suggests that chebulagic acid does not remain consistently bound within the binding pocket throughout the entire duration of the MD simulation, unlike the other complexes which exhibited stable binding interactions (**Figure 5.10F & G**). It is rather well established that donor-acceptor distance in H-bonds (2.2 to 2.4 Å (strong H-bond), 2.5 to 3.2 Å (moderate H-bond) and 3.5 to 4.1 Å (weak H-bond)) tend to vary in protein-ligand interaction6. The phytochemicals from HCAE exhibited paired distance of H-bond below 2Å in all but two complexes (chebulagic acid with HSP90AA1 and PIK3R1). Further, the most important interaction in facilitating the strength of binding of phytochemicals to its protein target are the H-bond interactions between the protein and ligand. Number of H-bonds were extracted from MD trajectory files and the average number of H-bonds were found to be in the range of 1.1 to 4.3 (**Figure 5.10H**). As a result, when their binding postures were retrieved from the MD trajectory file, the stability of all protein-ligand complexes were every 25 nanoseconds. It is evident from the binding poses obtained that the protein ligand complexes c_Src kinase-chebulinic acid, Akt-1, 2, 6 Tri-*O*-galloyl-β-D-glucose, androgen receptor-5-*O*-galloyl shikimic acid, EGFR-chebulagic acid and ESR-α-ellagic acid form stable structures even up to 100 ns simulation run time (**Figure 5.11**). However, chebulagic acid-HSP90AA1 and chebulagic acid-PIK3R1 were the only two complexes that were not stable through the MD simulation run time as it can be seen that the ligands got detached from the backbone.

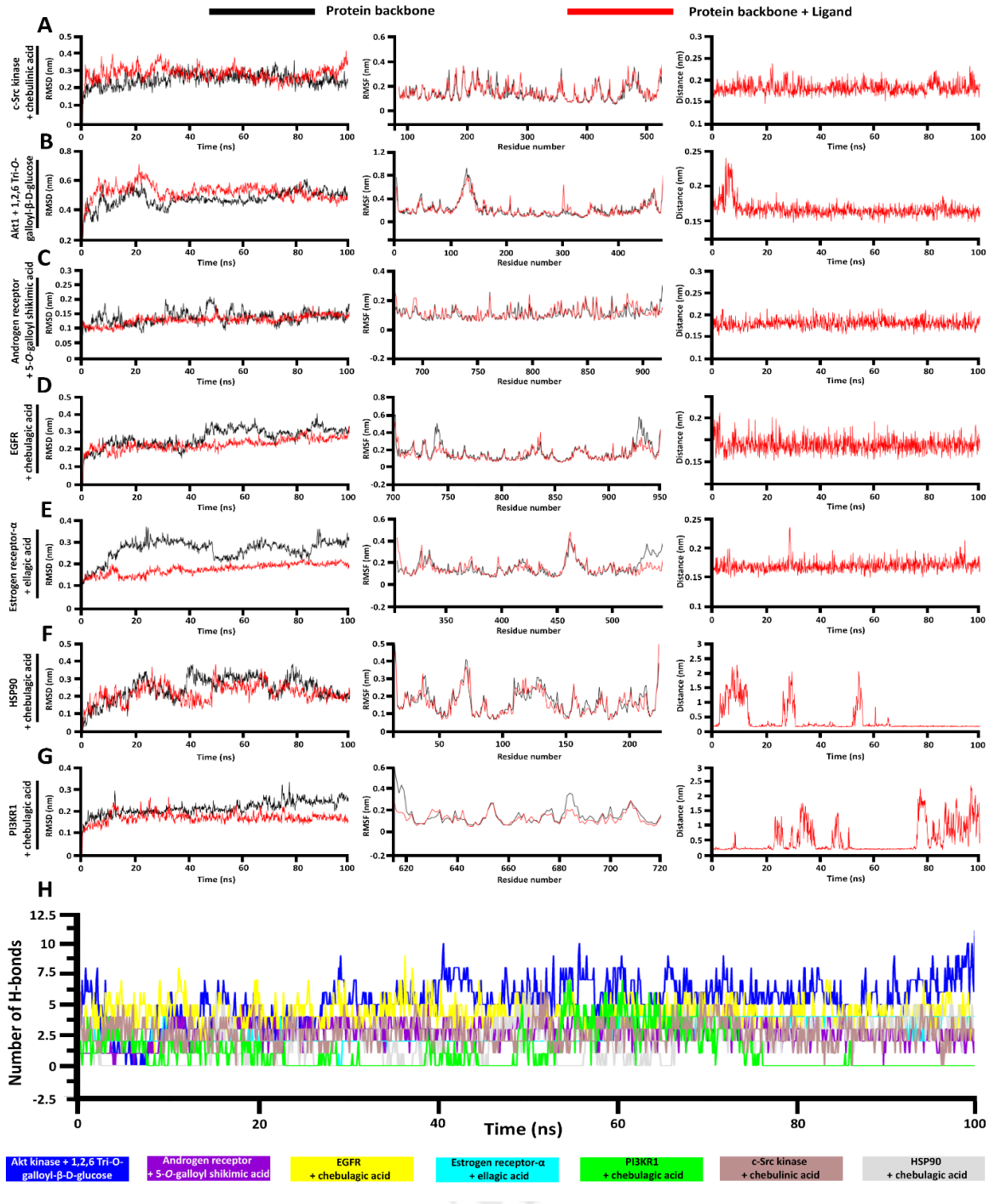

Figure 5.10: Molecular simulation studies demonstrate stable interactions between HCAE phytochemicals and their protein targets. (A) RMSD, RMSF and paired distance plot of c-Src kinase and its complex with chebulinic acid. **(B)** RMSD, RMSF and paired distance plot of Akt1 and its complex with 1, 2, 6 Tri-*O*-galloyl β-D-glucose. **(C)** RMSD, RMSF and paired distance plot of Androgen receptor and its complex with 5-*O*-galloyl Shikimic acid. **(D)** RMSD, RMSF and paired distance plot of EGFR and its complex with chebulagic acid. **(E)** RMSD, RMSF and paired distance plot of ESRα and its complex with ellagic acid. **(F)** RMSD, RMSF and paired distance plot of HSP90AA1 and its complex with chebulagic acid. **(G)** RMSD, RMSF and paired distance plot of PIK3R1 and its complex with chebulagic acid**. (H)** Number of H-bonds for all the protein ligand complexes**.**

MMPBSA (Molecular Mechanics Poisson-Boltzmann Surface Area) is an end-state post-processing method used to calculate free energies of ligand-protein interactions following MD simulations. The binding energies of all seven protein-ligand complexes were obtained from the MD trajectory files using the GROMACS MMPBSA tool.

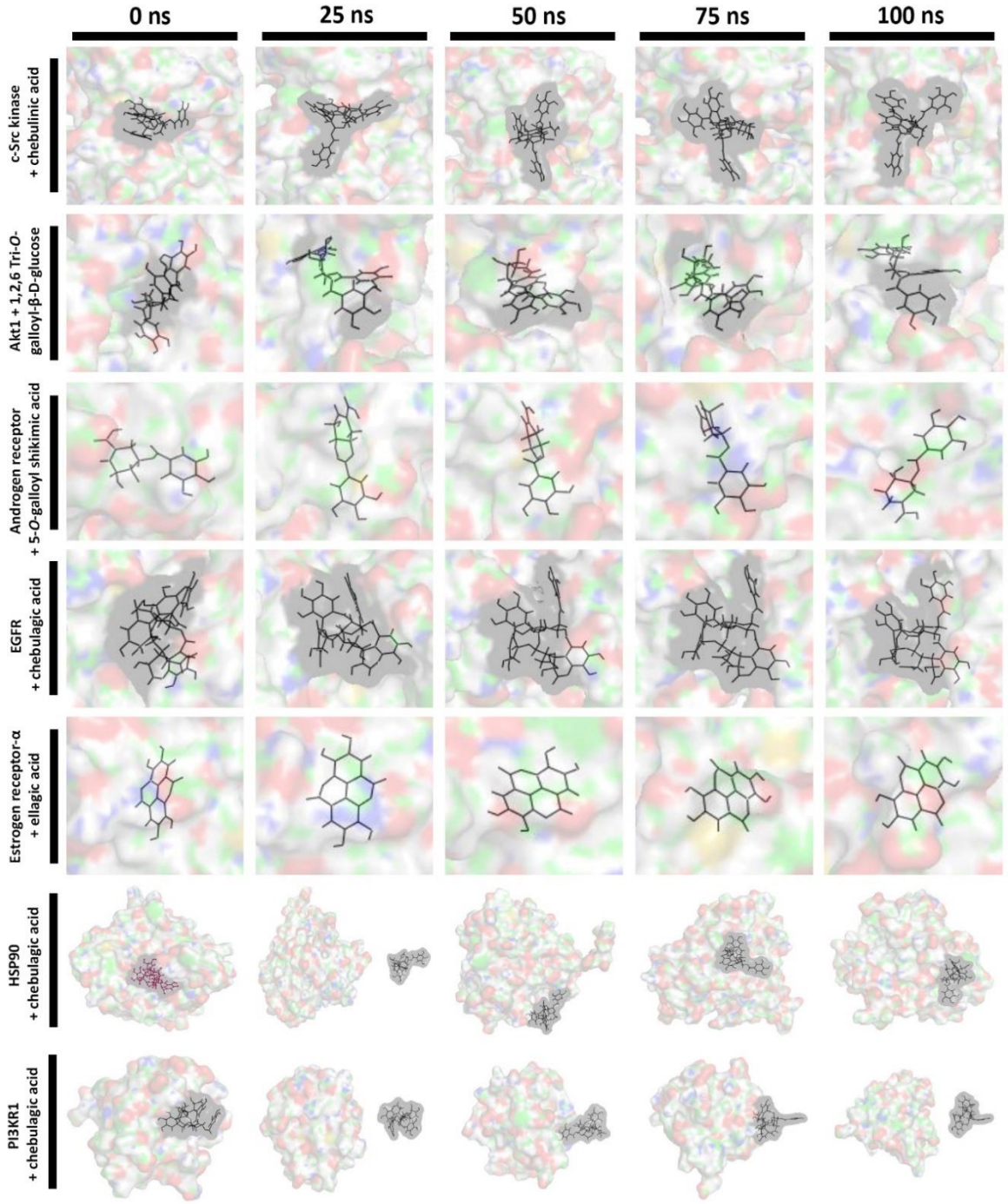

Figure 5.11: Binding poses of phytochemicals (from HCAE) with their respective targets. All the complexes were stable during 100 ns MD simulation run except HSP90AA1-chebulagic acid and PIK3R1-chebulagic acid

The lowest binding energy was found to be for AR and its complex with 5-*O*-galloyl shikimic acid (binding energy = -80.4 kJ/mol) followed by ESR-α in complex with ellagic acid (**Table 5.7**). Based on the structural and functional stability observed in MD-simulation studies, as well as the physiochemical profiling and ADMET analysis, it is apparent that the phytochemicals derived from HCAE exhibit favourable pharmacokinetic and pharmacodynamic parameters. These findings suggest the potential of HCAE phytochemicals as promising drug candidates.

Table 5.7: Binding energies of protein-ligand (from HCAE) complexes using MMPBSA

	Vanderwaal energy (kJ/mol)	Electrostatic energy (kJ/mol)	Polar solvation energy (kJ/mol)	SASA energy (kJ/mol)	Binding energy (kJ/mol)
c-Src_chebulinic acid	-220.6	-54.3	303.2	-25.9	-45.6
EGFR_chebulagic	-207.4	-123.7	342.8	-27.7	-16.04
Esr_ellagic acid	-124.4	-68.5	134.4	-15.6	-74.2
AR_5_O_galloyl shikimic acid	-159.4	-58.6	154.9	-17.1	-80.4
AKT_1,2,6-Tri-*O*-galloyl-β-D-glucose	-266.5	-113.3	394.5	-28.7	-14.1

Similar results were observed in the case of the protein ligand complexes with phytochemicals from AMCAE. Assessment of seven proteins (AR, ESR-α, PIK3R1, EGFR, Akt1, c-Src, and HSP90) and their ligand complexes revealed minimal influence on stability relative to protein backbones (**Table 5.8**). The assessment of structural perturbations in the protein-ligand complexes revealed minimal deviations in both the root mean square deviation (RMSD) values for protein backbones and ligands, as well as the radius of gyration measurements. Particularly noteworthy is the marginal discrepancy observed between the RMSD, root mean square fluctuation (RMSF), and radius of gyration magnitudes of the c-Src protein in isolation and its intricate association with ellagic acid, amounting to 0.01, 0.01, and 0.005 nm, respectively. This negligible impact on stability underscores the subtle influence of ellagic acid binding on c-Src. A parallel trend was observed across the various complexes, except for the PIK3R1 and trans-cinnamic acid pairing (**Figure 5.12A-F**). In-depth exploration through molecular dynamics (MD) simulations further accentuated these observations. Strikingly contrasting the other complexes, the trans-cinnamic acid and PIK3R1 complex exhibited conspicuous fluctuations in their minimum paired distance, indicating the unstable nature of trans-cinnamic

acid's binding within the designated pocket throughout the entire MD simulation duration (**Figure 5.12G**).

Table 5.8: The mean values of molecular dynamic simulation parameter for proteins and their complexes (from AMCAE).

		RMSD (nm)	RMSF (nm)	Radius of gyration (nm)	Number of H bonds	Distance (nm)
c-Src kinase	P	0.23	0.14	2.47	-----	-----
	P+L	0.22	0.15	2.47	1.05	0.21
Akt1	P	0.56	0.22	2.49	-----	-----
	P+L	0.75	0.35	2.5	3.1	0.18
Androgen receptor	P	0.15	0.11	1.85	-----	-----
	P+L	0.17	0.11	1.86	1.56	0.18
EGFR	P	0.29	0.17	2.05	-----	-----
	P+L	0.27	0.15	2.2	3.78	0.198
ESRα	P	0.28	0.17	1.72	-----	-----
	P+L	0.21	0.13	1.96	3.19	0.18
HSP90	P	0.25	0.19	1.76	-----	-----
	P+L	0.25	0.11	1.78	1.34	0.38
PI3KR1	P	0.24	0.19	1.33	-----	-----
	P+L	0.19	0.13	1.38	1.32	0.89

(**P**-protein, **P+L**-Protein + ligand). MD simulations of all the proteins and their complexes are run at ambient temperature (300K)

Enhanced bonding between phytochemicals and their target proteins primarily relies on hydrogen interactions, crucial for bolstering binding strength. Computational scrutiny using molecular dynamics (MD) data unveiled insights, indicating an average of 1.05 to 3.78 hydrogen bonds (**Figure 5.12H**). These bonds were evaluated every 25 nanoseconds, spotlighting stable protein-ligand complexes. Notably, the binding conformations extracted from MD trajectories underscored the robustness of various protein-ligand associations, notably including c_Src kinase with ellagic acid, Akt with corilagin, androgen receptor with ellagic acid, EGFR with ellagic acid, ESR-α with ellagic acid, and HSP90AA1 with corilagin maintained structural resilience over 100 nanoseconds. In contrast, trans-cinnamic acid and PIK3R1 complex exhibited diminished stability in MD, with ligands detaching from the protein (**Figure 5.13**). Using the MMPBSA (g_mmpbsa) tool [15] on gromacs, the binding energies of all seven protein-ligand complexes were retrieved from the MD trajectory data. Androgen receptor coupled with ellagic acid showed least binding energy value of -82.2kJ/mol (**Table 5.9**). Ellagic acid was the most potent of all the phytochemicals from AMCAE since it formed stable complexes with c-Src, AR, ESR-αand EGFR.

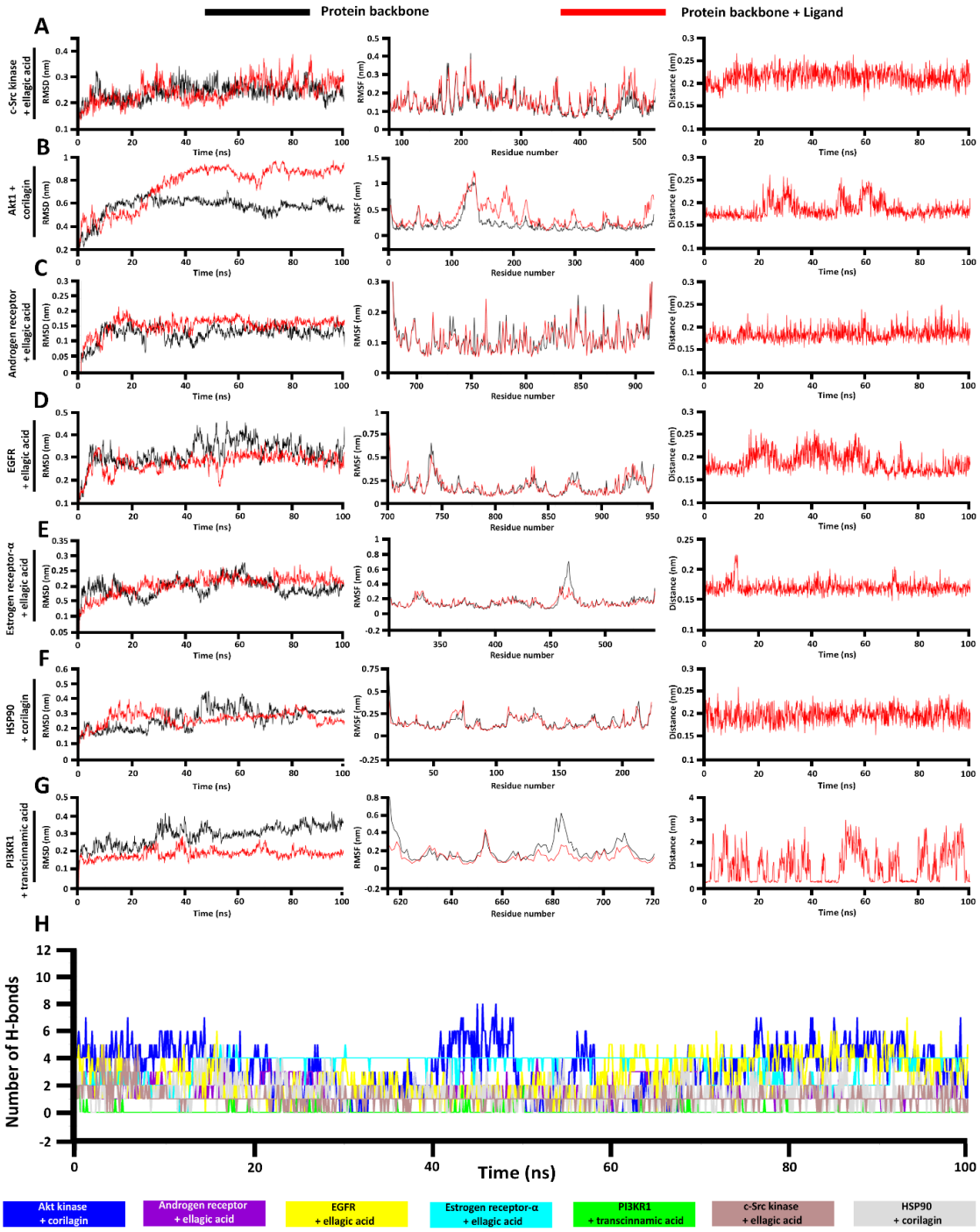

Figure 5.12: Molecular simulation studies demonstrate stable interactions between AMCAE phytochemicals and their protein targets (A) RMSD, RMSF and paired distance plot of c-Src kinase and its complex with ellagic acid. **(B)** RMSD, RMSF and paired distance plot of Akt1 and its complex with corilagin. **(C)** RMSD, RMSF and paired distance plot of Androgen receptor and its complex with ellagic acid. **(D)** RMSD, RMSF and paired distance plot of EGFR and its complex with ellagic acid. **(E)** RMSD, RMSF and paired distance plot of ESRα and its complex with ellagic acid. **(F)** RMSD, RMSF and paired distance plot of HSP90AA1 and its complex with corilagin. **(G)** RMSD, RMSF and paired distance plot of PIK3R1 and its complex with trans-cinnamic acid**. (H)** Number of H-bonds for all the protein ligand complexes.

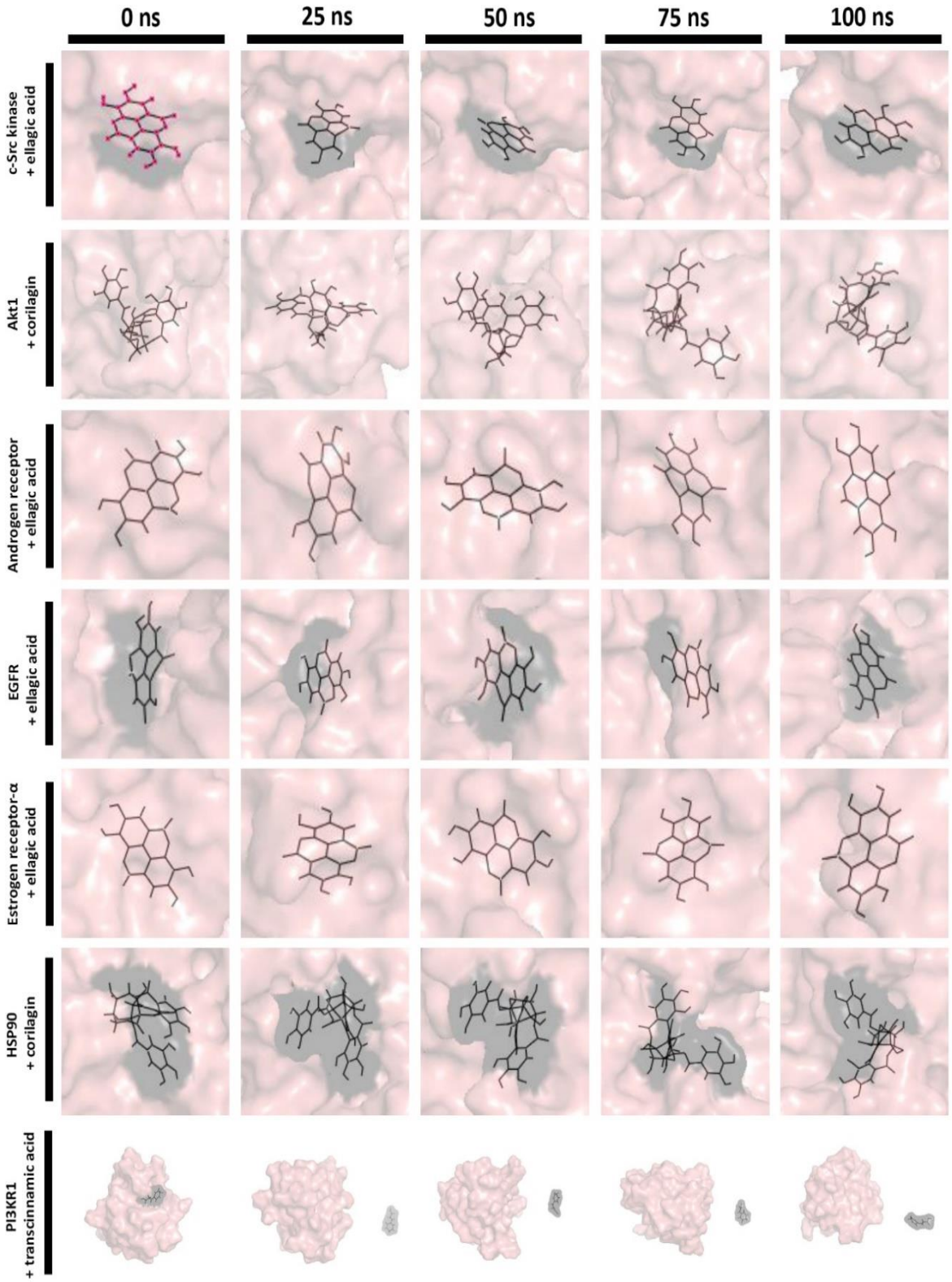

Figure 5.13: Binding poses of phytochemicals (from AMCAE) with their respective targets.

Table 5.9: Binding energies of protein-ligand (From AMCAE) complexes using MMPBSA method.

	Vanderwaal energy (kJ/mol)	Electrostatic energy (kJ/mol)	Polar solvation energy (kJ/mol)	SASA energy (kJ/mol)	Binding energy (kJ/mol)
c-Src_ellagic acid	-122.01	-16.4	91.2	-13.03	-60.2
Androgen receptor_ellagic acid	-167.2	-23.9	123.5	-14.6	-82.2
Estrogen receptor_ellagic acid	-131.6	-67.3	134.5	-15.09	-79.5
EGFR_ellagic acid	-123	-63.5	138	-14.01	-62.6
PI3KR1_transcinnamic acid	-12.3	-18.7	3.6	-2.2	-29.8
Akt1_corilagin	-202.4	-117.2	275.9	-21.6	-65.4
HSP90AA1_corilagin	-153.02	-58.5	249.6	-18.6	19.4

5.3.6 Down regulation of c-Src kinase and its related protein in colorectal cancer cells: Traditionally, Haritaki Churna and Amalaki Churna are well known for treating gastro-intestinal disorders. Since, the Churnas are made with fundamental idea of increasing the absorption of Ayurvedic formulations in gastro-intestinal tracts, we treated colorectal cancer cells HCT-116 and DLD1 with AMCAE and HCAE respectively to observe its effect on loss of cellular viability and cellular signaling using c-Src kinase as a model. HCAE exhibited a potent anticancer effect, resulting in a significant reduction in the viability of cancer cells (HCT-116) with an IC_{50} of 75.2 ± 5.1 µg/ml after 48 hours of treatment. Similarly, AMCAE treatment also led to a notable decrease in cellular viability, albeit slightly higher, with an IC_{50} of 76.2 ± 6.3 µg/ml over the same treatment duration (**Figure 5.14A & B**). In order to validate the in-silico based findings in our study, we chose c-Src as a model. Src family of kinases are undoubtedly related to the pathogenesis of cancer progression in CRC [16]. c-Src itself is a non-receptor protein tyrosine kinase which are involved in a variety of cellular processes such as proliferation, motility, differentiation and migration [17]. c-Src was found to be down-regulated in DLD1 and HCT-116 cells upon treatment with HCAE and AMCAE respectively after 24 and 48 hours of treatment (**Figure 5.14C & D**). c-Src in CRCs is activated by EGFR by forming a Src/EGFR/NADPH complex that activates the overexpression of c-Met [18]. Apart from being regulated by EGFR, c-Src is also regulated by variable proteins such as VEGFR, IL-4, and GPCR [19-23]. The activated EGFR/Src complex helps in the phosphorylation of NF-κB by Akt1 that in turn suppresses the apoptosis mechanism in CRC cells [24].

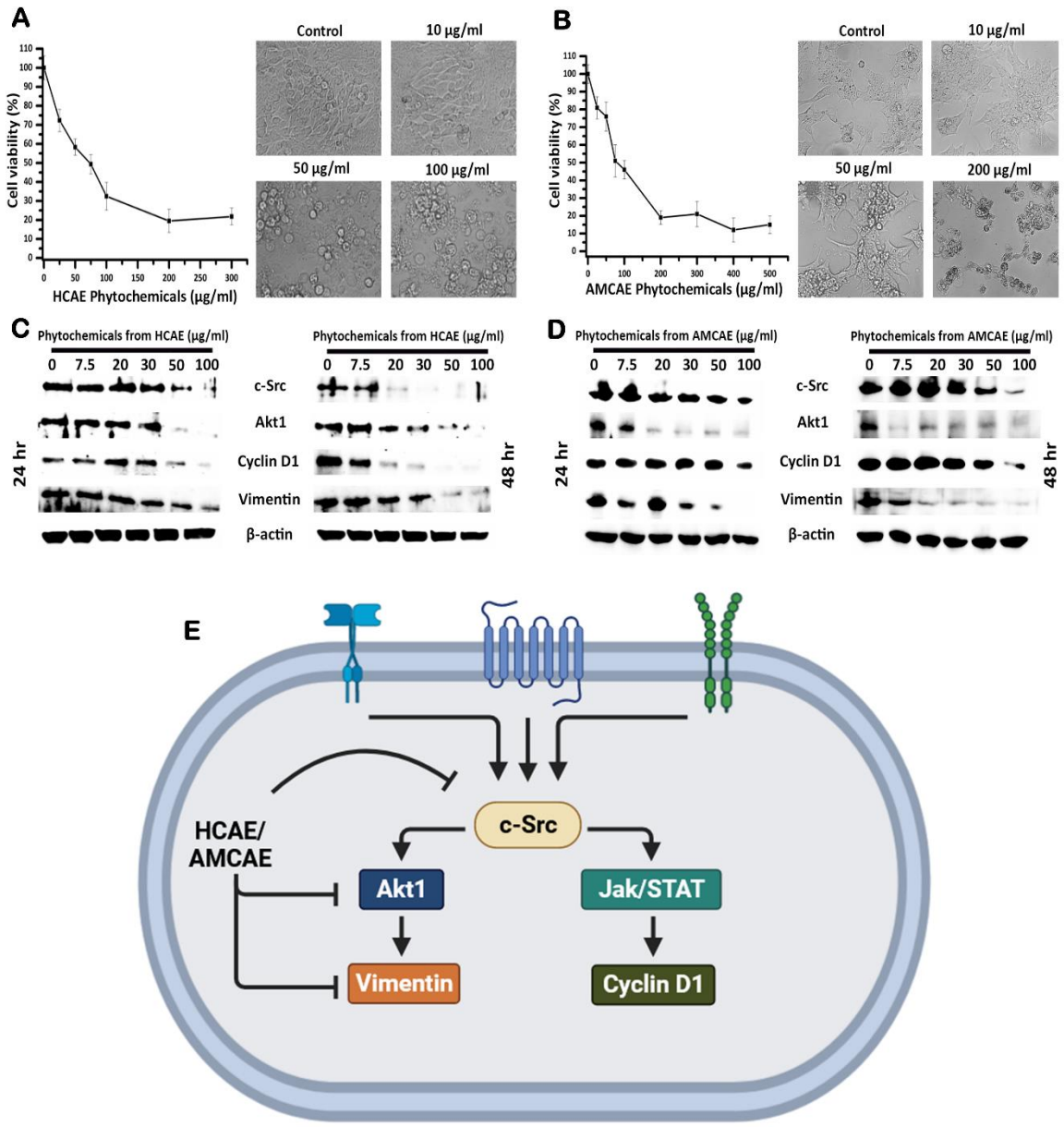

Figure 5.14: Ayurvedic formulations downregulates crucial proteins required for survival (In-vitro validation using c-Src kinase). (A & B) HCAE and AMCAE kills colorectal cancer cells. Colorectal cancer cells were treated with various concentration of HCAE (0-300 µg/ml) and AMCAE (0-500 µg/ml) and the reduction in cell viability was measured using MTT assay. Several images were captured on after observing under microscope using Cytell cell imaging system (GE Healthcare). **(C & D)** Western blot images show reduction in expression of c-Src and its downstream targets Akt1, cyclin D1 and Vimentin after 24 and 48 hours of treatment with HCAE and AMCAE. β-actin was considered as an internal control. **(E)** Mechanism of HCAE/AMCAE induced cell signaling disruption in colorectal cancer cells.

Further, HCAE and AMCAE were also found to down regulate expression of Akt1 protein after 24 and 48 hours of treatment. This might be because of suppression of c-Src which is an upstream regulator of Akt1 in CRCs or by direct phytochemical intervention from

HCAE/AMCAE inhibiting Akt1. Further, HCAE was also found to down regulate cyclin D1 and vimentin after 24 and 48 hours of treatment (**Figure 5.14C & D**). Cyclin D1 and vimentin are known to control cell cycle progression and has a prominent role to play in EMT transition respectively. The down regulation of cyclin D1 could be because of suppression of c-Src or direct inhibition of Cyclin D1 by its inhibitors from HCAE/AMCAE. Furthermore, the activation of c-Src is also closely related with over expression of EMT (Epithelial to mesenchymal transition) markers such as E-cadherin and N-cadherin [25, 26]. c-Src is not known to directly regulate the EMT marker vimentin (**Figure 5.14E**). Although, Akt1 which is a prominent upstream protein of vimentin is known to regulate it by controlling the expression of snail and twist proteins [27].

5.4 References

1. Wishart, D.S., et al., *DrugBank 5.0: a major update to the DrugBank database for 2018.* Nucleic acids research, 2018. **46**(D1): p. D1074-D1082.
2. Gilson, M.K., et al., *BindingDB in 2015: a public database for medicinal chemistry, computational chemistry and systems pharmacology.* Nucleic acids research, 2016. **44**(D1): p. D1045-D1053.
3. Huang, D.W., et al., *DAVID Bioinformatics Resources: expanded annotation database and novel algorithms to better extract biology from large gene lists.* Nucleic acids research, 2007. **35**(suppl_2): p. W169-W175.
4. Szklarczyk, D., et al., *The STRING database in 2017: quality-controlled protein–protein association networks, made broadly accessible.* Nucleic acids research, 2016: p. gkw937.
5. Ashtiani, M., et al., *A systematic survey of centrality measures for protein-protein interaction networks.* BMC systems biology, 2018. **12**(1): p. 1-17.
6. Berman, H., K. Henrick, and H. Nakamura, *Announcing the worldwide protein data bank.* Nature Structural & Molecular Biology, 2003. **10**(12): p. 980-980.
7. Morris, G.M., et al., *AutoDock4 and AutoDockTools4: Automated docking with selective receptor flexibility.* Journal of computational chemistry, 2009. **30**(16): p. 2785-2791.
8. Van Der Spoel, D., et al., *GROMACS: fast, flexible, and free.* Journal of computational chemistry, 2005. **26**(16): p. 1701-1718.

9. Daina, A., O. Michielin, and V. Zoete, *SwissADME: a free web tool to evaluate pharmacokinetics, drug-likeness and medicinal chemistry friendliness of small molecules.* Scientific reports, 2017. **7**(1): p. 1-13.
10. Pandey, K.B. and S.I. Rizvi, *Plant polyphenols as dietary antioxidants in human health and disease.* Oxidative medicine and cellular longevity, 2009. **2**: p. 270-278.
11. Vauzour, D., et al., *Polyphenols and human health: prevention of disease and mechanisms of action.* Nutrients, 2010. **2**(11): p. 1106-1131.
12. Lacroix, S., et al., *A computationally driven analysis of the polyphenol-protein interactome.* Scientific reports, 2018. **8**(1): p. 1-13.
13. Lahti, J.L., et al., *Bioinformatics and variability in drug response: a protein structural perspective.* Journal of The Royal Society Interface, 2012. **9**(72): p. 1409-1437.
14. Safari-Alighiarloo, N., et al., *Protein-protein interaction networks (PPI) and complex diseases.* Gastroenterology and Hepatology from bed to bench, 2014. **7**(1): p. 17.
15. Kumari, R., et al., *g_mmpbsa A GROMACS tool for high-throughput MM-PBSA calculations.* Journal of chemical information and modeling, 2014. **54**(7): p. 1951-1962.
16. Jin, W., *Regulation of Src family kinases during colorectal cancer development and its clinical implications.* Cancers, 2020. **12**(5): p. 1339.
17. Zhang, S. and D. Yu, *Targeting Src family kinases in anti-cancer therapies: turning promise into triumph.* Trends in pharmacological sciences, 2012. **33**(3): p. 122-128.
18. Mao, W., et al., *Activation of c-Src by receptor tyrosine kinases in human colon cancer cells with high metastatic potential.* Oncogene, 1997. **15**(25): p. 3083-3090.
19. Ellis, L.M., et al., *Down-regulation of vascular endothelial growth factor in a human colon carcinoma cell line transfected with an antisense expression vector specific for c-src.* Journal of Biological Chemistry, 1998. **273**(2): p. 1052-1057.
20. Barderas, R., et al., *High Expression of IL-13 Receptor α2 in Colorectal Cancer Is Associated with Invasion, Liver Metastasis, and Poor PrognosisRole of IL-13Rα2 in Colorectal Cancer Metastasis.* Cancer research, 2012. **72**(11): p. 2780-2790.
21. Bartolomé, R.A., et al., *IL13 Receptor α2 Signaling Requires a Scaffold Protein, FAM120A, to Activate the FAK and PI3K Pathways in Colon Cancer MetastasisIL13Rα2 Signaling in Colorectal Cancer Metastasis.* Cancer research, 2015. **75**(12): p. 2434-2444.

22. Pai, R., et al., *Prostaglandin E2 transactivates EGF receptor: a novel mechanism for promoting colon cancer growth and gastrointestinal hypertrophy.* Nature medicine, 2002. **8**(3): p. 289-293.
23. Fukuda, R., B. Kelly, and G.L. Semenza, *Vascular endothelial growth factor gene expression in colon cancer cells exposed to prostaglandin E2 is mediated by hypoxia-inducible factor.* Cancer research, 2003. **63**(9): p. 2330-2334.
24. Lien, G.-S., et al., *Epidermal growth factor stimulates nuclear factor-κB activation and heme oxygenase-1 expression via c-Src, NADPH oxidase, PI3K, and Akt in human colon cancer cells.* PloS one, 2014. **9**(8): p. e104891.
25. Weis, S., et al., *Src blockade stabilizes a Flk/cadherin complex, reducing edema and tissue injury following myocardial infarction.* The Journal of clinical investigation, 2004. **113**(6): p. 885-894.
26. Irby, R.B. and T.J. Yeatman, *Increased Src activity disrupts cadherin/catenin-mediated homotypic adhesion in human colon cancer and transformed rodent cells.* Cancer research, 2002. **62**(9): p. 2669-2674.
27. Xu, W., Z. Yang, and N. Lu, *A new role for the PI3K/Akt signaling pathway in the epithelial-mesenchymal transition.* Cell adhesion & migration, 2015. **9**(4): p. 317-324.

Chapter VI

Phytochemicals from Ayurvedic formulations disrupt multiple cellular pathway in colorectal cancer cells

*The content of this chapter is partly published as **"Khan, M.R.U.Z.,** Yanase, E. and Trivedi, V., 2023**. Extraction, phytochemical characterization and anti-cancer mechanism of Haritaki Churna: An Ayurvedic formulation.** Plos one, 18(5), p.e0286274**."**

6.1 Introduction: In the preceding chapter, an in-depth analysis was conducted to elucidate the intricate interactions between proteins and phytochemicals, revealing pivotal hub proteins as potential targets of Ayurvedic formulations. Notably, the study established that these protein targets predominantly pertain to vital cellular survival pathways crucial for cancer cell viability. This chapter focuses on delineating the anti-cancer mechanisms employed by these Ayurvedic formulations. Furthermore, their safety profile against normal cell lines was assessed, and their bioavailability was rigorously evaluated using biological fluids simulating gastric and intestinal conditions, as depicted in **Figure 6.1**. Employing a deductive approach, specific polyphenols within the Ayurvedic formulations (HCAE/AMCAE) were identified, highlighting their substantial contribution to the overall anti-cancer activity observed in the crude water extract.

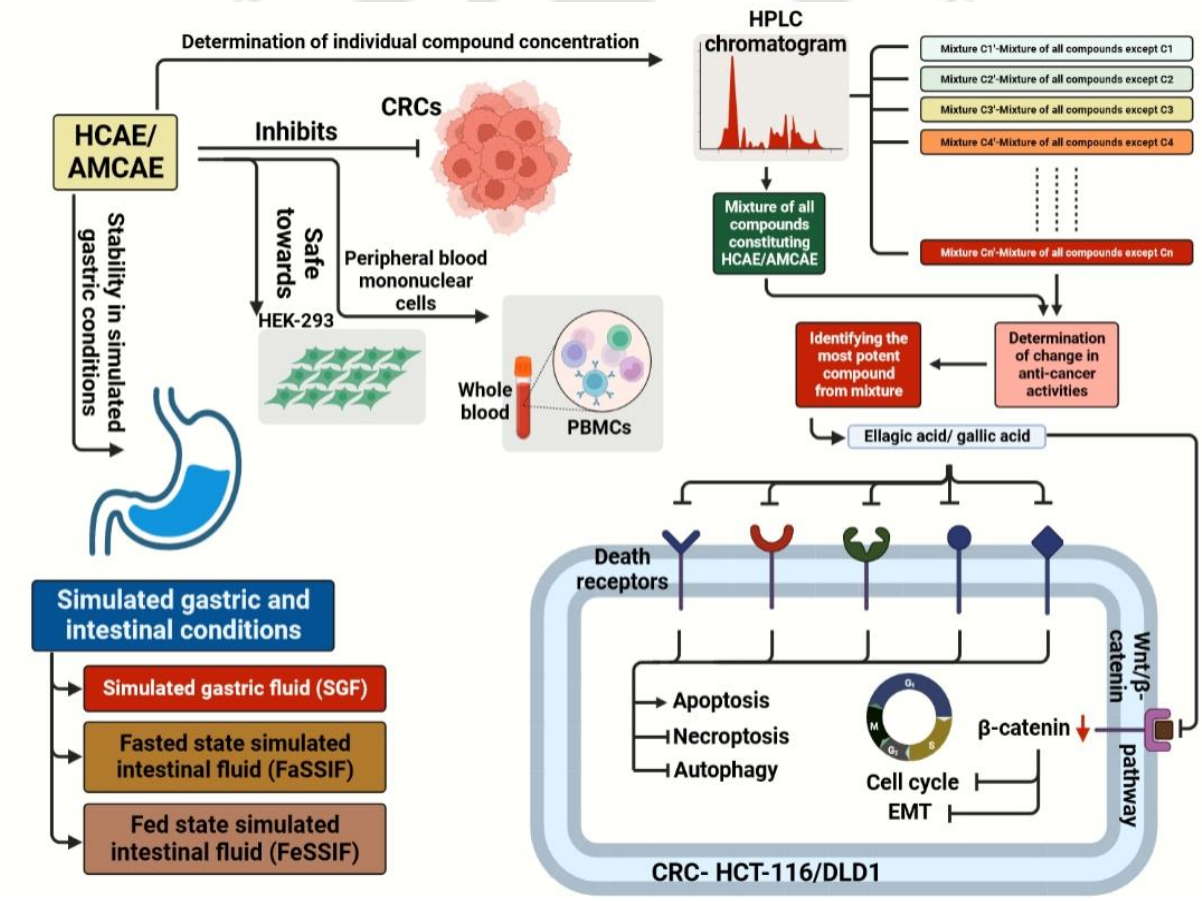

Figure 6.1: Schematic of the experimental approach for anti-cancer mechanism of Haritaki Churna and Amalaki Churna.

6.2 Experimental procedures

6.2.1 Cell Culture: MDAMB-231 cells (Breast cancer cell line), HeLa (Cervical cancer cell line), MG-63 (Osteosarcoma cell line), HEK-293 (Human embryonic kidney) and Colorectal

cancer cell lines DLD1, HT29 and HCT-116 were cultured in DMEM: F12 High glucose media as described in section **3.4**.

6.2.2 MTT cell viability assay: cancer cells were treated with different Ayurvedic formulations at varying concentrations for a period of 48 hours and the loss in cellular viability of CRCs were measured using MTT cell viability assay as described in section **3.5**.

6.2.3 Preparation of peripheral blood mononuclear cells (PBMCs): Blood was taken from a healthy volunteer and PBMCs were isolated using HiSeP from HiMedia^{TM} as per manufacturer's protocol as described in section **3.12**.

6.2.4 Preparation of biological fluids present in digestive system: Simulated gastric fluid, Fasted state Simulated Intestinal Fluid (FaSSIF) and Fed State Simulated Intestinal Fluid (FeSSIF) were prepared as described in section **3.13**.

6.2.5 Identification of the most active ingredient in Ayurvedic formulation (HCAE/AMCAE): The concentrations of each compound identified from HCAE/AMCAE were evaluated by calculating area under the peak from gradient HPLC chromatogram as described in section **3.14.**

6.2.6 Cell cycle analysis: The cells were treated with most potent compound from Ayurvedic formulations at their respective concentrations against HCT-116, DLD1, and HT-29. The cells were treated using serum-free media for 24 and 48 hours, and cell cycle analysis was performed as described in section **3.15**.

6.2.7 Live and apoptotic cell staining by Acridine orange/Propidium iodide method: The cells (HCT-116, DLD1, and HT-29) were treated with most potent compound from Ayurvedic formulation in serum-free media at respective concentrations for 48 hours. The healthy, early apoptotic, late apoptotic, and dead cells were analyzed as described in section **3.16**.

6.2.8 DNA fragmentation assay: The cells (HCT-116, DLD1, and HT-29) were treated most potent compound from Ayurvedic formulations in serum-free media for a period of 48 hours. The fragmented DNA was isolated and analyzed as described in section **3.17**.

6.2.9 Western blotting: HCT-116 cells ($1*10^6$) for gallic acid treatment and DLD1 cells ($1*10^6$) for ellagic acid treatment were seeded in a 6 well plate prior to the day of the experiment. Cells were washed twice with PBS and were treated with ellagic acid (2.5, 5, 10, 15 & 25 µg/ml) and gallic acid (2.5, 5, 10, 20 & 30 µg/ml) for 24 and 48 hours. Cells were

harvested and lysed with RIPA lysis buffer and the protein content was measured using standard protein assays. Proteins were separated on a 10% SDS-polyacrylamide gel and then transferred to nitrocellulose membrane (Bio-Rad cat. # 162-0112) on a Trans-Blot Turbo (Bio-Rad). The membrane was blocked with 5% BSA for 1-2 hours at room temperature. The blots were then incubated with primary antibodies (DR3 (1:2500), DR4 (1:2500), DR5 (1:2500), DR6 (1:2000), TNFR1 (1:2000), TNFR2 (1:2000), Fas (1:2000), RIP (1:2000), MLKL (1:2000) p-RIP (1:1000), p-MLKL (1:1000), Cleaved caspase 3 (1:2000), Cleaved caspase 8 (1:2000), Caspase 3 (1:2000), Caspase 8 (1:2000), Bcl2 (1:2000), Cytochrome-C (1:1000), CyclinA2 (1:4000), Axin-2 (1:5000), GSK-3β (1:5000), LEF-1 (1:5000), β-catenin (1:5000), Cyclin D1 (1:5000), E-cadherin (1:2500), N-cadherin (1:2500), vimentin (1:2500), snail+slug (1:2500), Atg3 (1:2000), Atg5 (1:2000), Atg7 (1:2000), Atg12 (1:2000), Atg16L1 (1:2000), Beclin-1 (1:2000), LC3I/II (1:2000), GAPDH (1:5000) and β-actin (1:5000)) overnight at 4^{o}C followed by incubation with appropriate HRP conjugated secondary antibodies for 1-2 hours at room temperature. Proteins bands were analyzed by using Bio-Rad Clarity^{TM} Western ECL substrate kit and images were developed in Bio-Rad chemiDoc system.

6.2.10 Statistical analysis: Sample values are expressed as mean ± standard deviation (SD), N=3. All the IC_{50} values were calculated using a non-linear curve fit model in ORIGIN 2019 software

6.3 Results

6.3.1 Haritaki Churna and Amalaki Churna aqueous extract has anti-cancer activity: In Ayurveda, it is recommended to soak Churna into cold water overnight and then the water extract can be consumed orally for maximum therapeutic effect. Considering this aspect, we have prepared the aqueous extract of HC and AMC for our studies. The aqueous extract of HC was tested against different cancer cells to evaluate the anti-cancer potential of formulation as described. Cells were treated with different concentrations of aqueous extract of HC for 48 hours and cell viability was measured by MTT assay (**Figure 6.2A**). Cancer cells treated with aqueous extract of HC exhibits dose dependent loss of cellular viability and alternations in cellular morphology (**Figure 6.2B**). The aqueous extract is giving anti-cancer activity against MDAMB-23, HeLa, & MG63 cells with an IC_{50} of 53.1 ± 4.96 µg/ml, 79.35 ± 4.95 µg/ml, & 97.04 ± 4.09 µg/ml respectively. The Haritaki Churna in the Ayurvedic literature is well known for treating GI-track-related disorders. The concentration of bioactive agents present in HC will be very high in GI track and we have asked if the Ayurvedic formulation could have potential to exhibit anti-cancer activity against colorectal cancer.

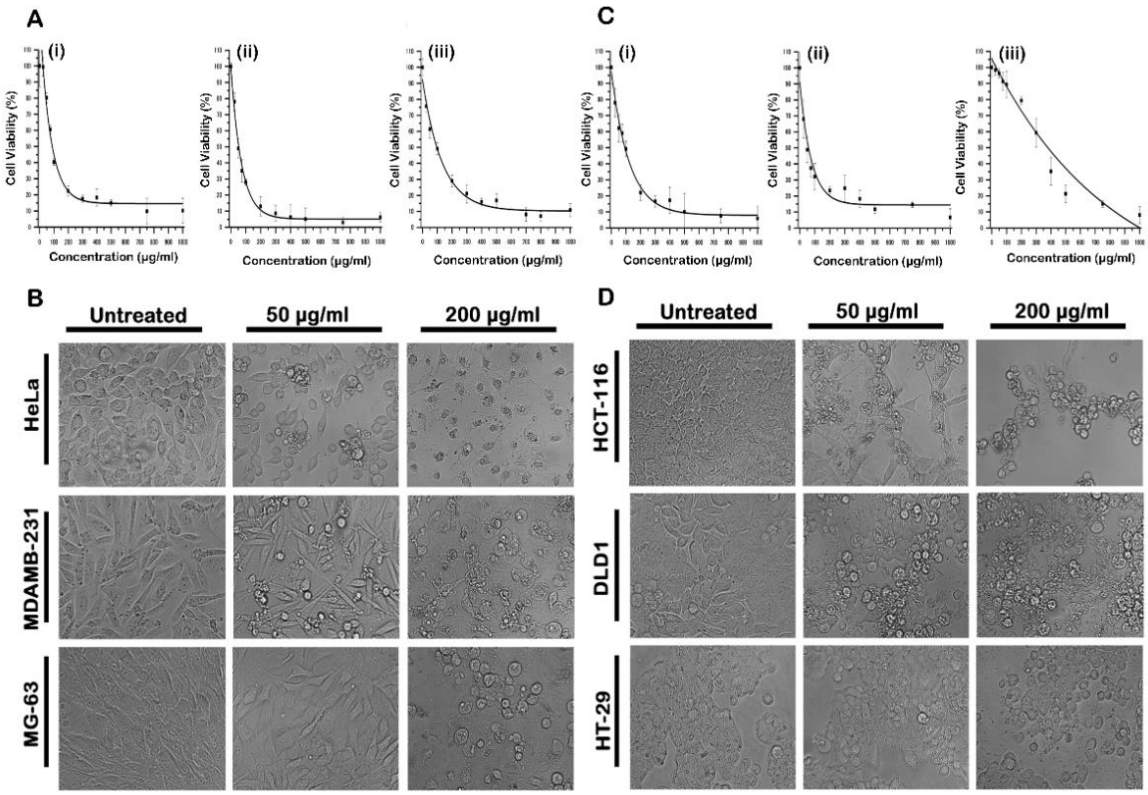

Figure 6.2: Haritaki Churna aqueous extract exhibit anti-cancer activity against different cancers. Cancer cells of different origins were treated with different concentration of Haritaki Churna aqueous extract (0-1000 µg/ml) and the cell viability was measured by MTT assay. The MTT curve presented in **(A(i-iii))** refer to the treatment of HCAE to HeLa, MDAMB-231 and HeLa cells respectively. **(B)** Cells were observed under microscope and different images were acquired from different fields using Cytell cell imaging system (GE Healthcare). Representative images from each treatment are shown. **(C(i-iii))** HCAE kills colorectal cancer cells**.** HCT-116, DLD1 and HT-29 were treated with different concentrations of aqueous extract (0-1000 µg/ml) and cell viability was measured using MTT assay. **(D)** Change in morphology of cells can be observed.

To explore such question, we have treated the colorectal cancer cells HCT-116, DLD-1 and HT29 with aqueous extract of HC and measured the cellular viability by MTT assay. Cancer cells were treated with different concentration of HCAE and it exhibits dose-dependent killing of cancer cells (**Figure 6.2C**). Among the three colorectal cancer cell lines, HCAE showed maximum activity towards DLD1 with an IC_{50} of 70.41 ± 6.35 µg/ml, whereas it showed IC_{50} of 92.69 ± 7.07 µg/ml against HCT-116and 379.93 ± 5.29 µg/ml against HT-29 (**Table 6.1**). In addition, treated cells were exhibiting membrane blebbing and distorted morphology indicating extreme stress inside the cells (**Figure 6.2D**). The data in **Figure 6.2** and **Table 6.1** clearly highlight that the HC has bioactive agents with anti-cancer activity and it can be useful to treat colorectal cancer in patients.

In a similar manner, the aqueous extract of Amalaki Churna (AMCAE) was tested against breast, cervical and bone cancer cells to test the anti-cancer activity of Ayurvedic formulation. Cancer cells treated with AMC aqueous extract demonstrate dose-dependent loss of cellular viability and morphological changes (**Figure 6.3A**). The AMCAE exhibits anti-cancer activity with an IC_{50} of 117.8 ± 7.6 µg/ml, 112.3 ± 7.1 µg/ml, and 165.6 ± 8.02 µg/ml against HeLa, MDAMB-231 and MG-63 respectively. Although, various types of formulations made from Amalaki plant are used for broad spectrum of ailments, they are also used treat gastro-intestinal disorders [1]. The Ayurvedic formulations as well as extracts from *E. Officinalis* (the source for Amalaki and its related formulations) are well known for gastro-intestinal treatments [2-4].

Table 6.1: Anti-cancer activity of HCAE and AMCAE against different cell lines

Cell line	Type	IC_{50} (µg/ml) ± S. D.	
		HCAE	AMCAE
HCT-116	Colorectal cancer	92.69 ± 7.07	74.05 ± 6.5
DLD1	Colorectal cancer	70.41 ± 6.35	95.9 ± 7.3
HT-29	Colorectal cancer	379.93 ± 5.29	269.2 ± 6.2
HeLa	Cervical cancer	79.35 ± 4.95	117.8 ± 7.6
MDAMB-231	Breast cancer	53.1 ± 4.96	112.3 ± 7.1
MG-63	Osteosarcoma	97.04 ± 4.09	165.6 ± 8.02

As the Churna are well known for the better absorption in the gastric tract, and its stability in simulated gastric and intestinal conditions, we further evaluated the anti-cancer potential of aqueous extract of Amalaki Churna against colorectal cancer cells (**Figure 6.3B**). AMCAE showed highest activity against HCT-116 cells with an IC_{50} of 74.05 ± 6.5 µg/ml followed by DLD1 and HT-29 with IC_{50}s of 95.9 ± 7.3 µg/ml and 269.2 ± 6.2 µg/ml respectively (**Table 6.1**). Moreover, the colorectal cells treated with AMCAE evinced blebbing of cell membrane and disfigured morphology which is an indicator of acute stress inside the cells (**Figure 6.3C**).

6.3.2 Haritaki Churna aqueous extract is safe for therapeutic usage: The major drawback of studies with Ayurvedic formulation is systematic exploration of many pharmacological properties such bio-availability, distribution safety and toxicity etc. Before exploring the composition and purification of bioactive anti-cancer agents present in HC aqueous extract, we have performed safety and toxicity analysis. We have used two different models to test the safety and toxicity of HC aqueous extract. In model 1, we have tested the safety of the HC extract using primary cells. The use of peripheral blood mononuclear cells (PBMCs) has been widely accepted as an in-vitro model for testing the safety of anti-cancer drugs [5-8]. PBMCs

were isolated from human blood as described and sub-cultured in DMEM complete medium. PBMCs were treated with different concentration of HC aqueous extract (0-500µg/ml) and cellular viability was measured by MTT assay.

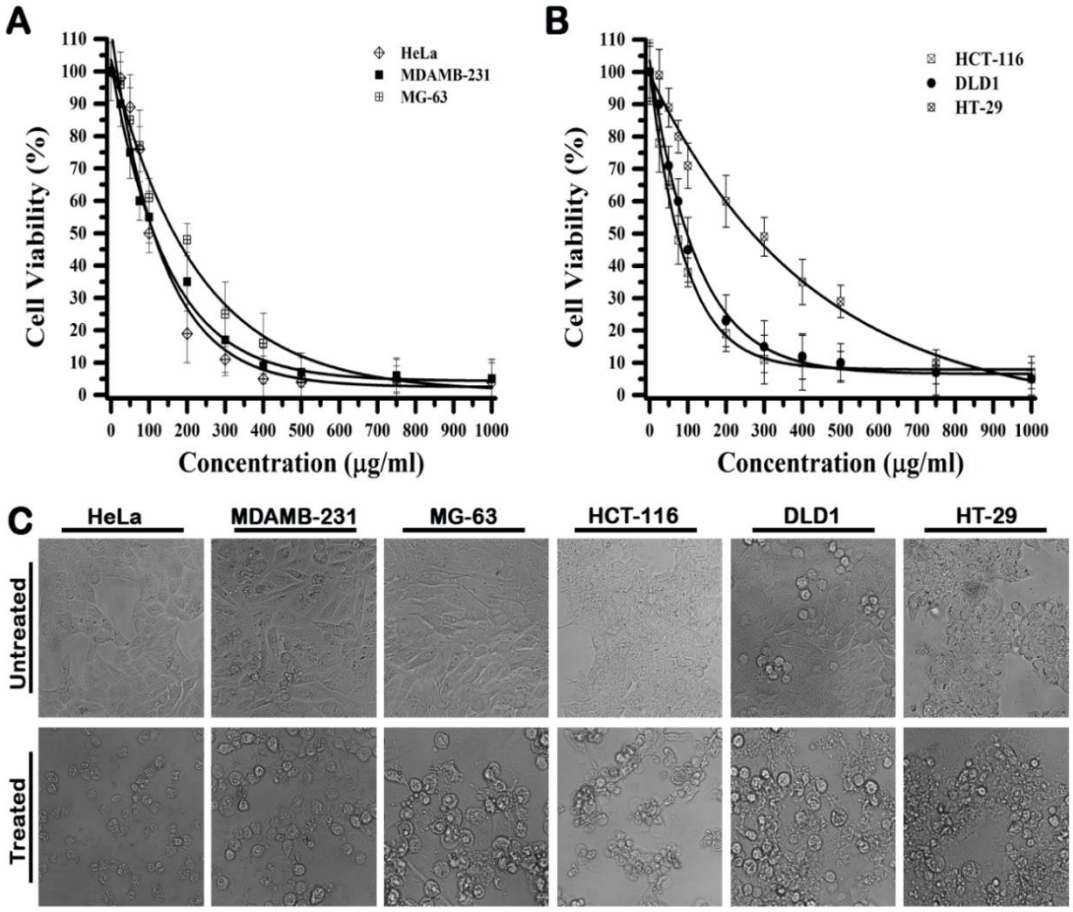

Figure 6.3: Amalaki Churna aqueous extract exhibit anti-proliferative effects towards variable cancer cell lines. Different cancer cells were treated at various concentrations (0-1000 µg/ml) with AMCAE for 48-hours and their cell viability was measured using the MTT assay. **(A)** Cell viability curves of HeLa, MDAMB-231 & MG-63 cells and **(B)** colorectal cancer cells HCT-116, DLD1 & HT-29 are represented. **(C)** Several images of the untreated and treated cells were captured from different fields using Cytell cell imaging system. Only the representative images of the treatment and its control are shown.

We found that HCAE is not affecting cellular viability of PBMCs even at a very high concentration of 500µg/ml (**Figure 6.4A)**. Alteration in cellular morphology is a primary event to monitor the safety of the anti-cancer drug. Observation of HC aqueous extract treated PBMCs indicate no significant alternation in cellular morphology (**Figure 6.4B)**. In model 2, non-cancerous cell line HEK293 was used to test the toxicity of HC aqueous extract. HEK 293 cells were treated with different concentration of HC extract and cellular viability was measured by MTT assay.

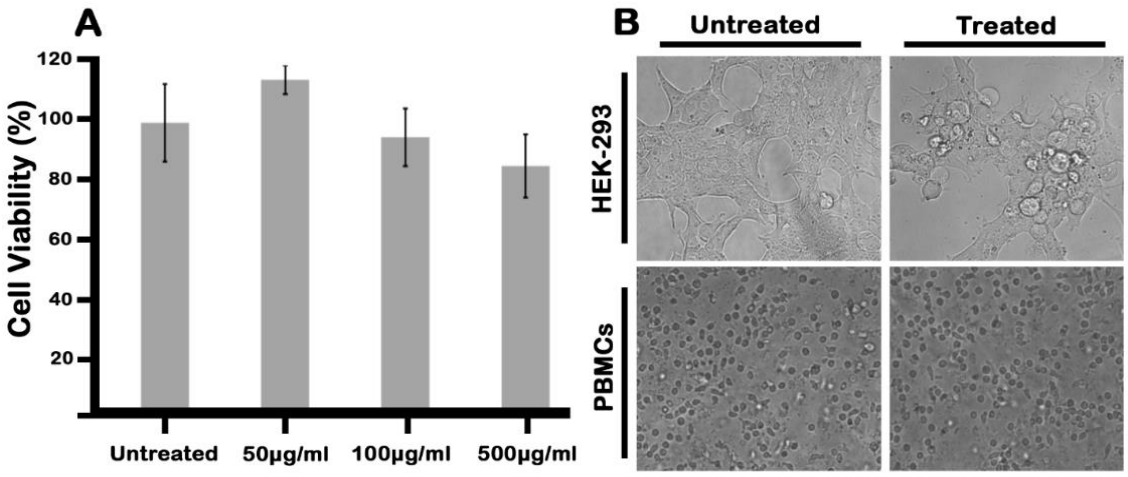

Figure 6.4: Haritaki Churna aqueous extract is safe for Human consumption. (A) The peripheral blood mononuclear cells were isolated from healthy volunteer as described. The cells treated with Haritaki Churna aqueous extract for a period of 48 hours and their cell viability was measured by MTT assay as given in the procedure. **(B)** HEK-293 and PBMC Cells were observed and 5 different random images were taken using Cytell cell imaging system (GE Healthcare). Representative images are shown for untreated and treated cells

HC aqueous extract had not affected the cellular viability of HEK-293 cells up to concentration of 300 µg/ml. Blebbing in HEK-293 cells treated with higher concentration (500µg/ml) of HCAE was observed (**Figure 6.4B**). However, these protrusions have been found in HEK-293 cells at doses greater than those necessary to kill colorectal cancer cells. Our results comply with the study done by suganthy et al, where the activity of methanolic extracts of *Terminalia chebula* fruit (TCF), *Terminalia arjuna* bark (TAB), and 7-methylgallate(7-MG) was checked on PBMCs [9]. They showed that there was no significant decrease in the viability and membrane integrity of PBMCs upon treatment by TCF, TAB & 7MG even at concentrations of 500-2000 µg/ml.

Similarly, the cytotoxicity of AMCAE was checked to assess the safety of herbal extract. HEK-293 cells and PBMCs were taken as two model systems. The isolated PBMCs and HEK-293 cultured in DMEM high glucose media were treated with varying concentrations of AMCAE (0-500µg/ml) for a period of 48-hours in serum free media. AMCAE was found to be safe even up to very high concentration of 300µg/ml for HEK-293. It is even safe up to 300µg/ml for PBMCs (**Figure 6.5A & B**). In addition, there are no alterations in cellular morphology in treated HEK-293 or PBMCs (**Figure 6.5C**). It clearly highlights that cells are healthy and Amalaki Churna is safe to use for human consumption.

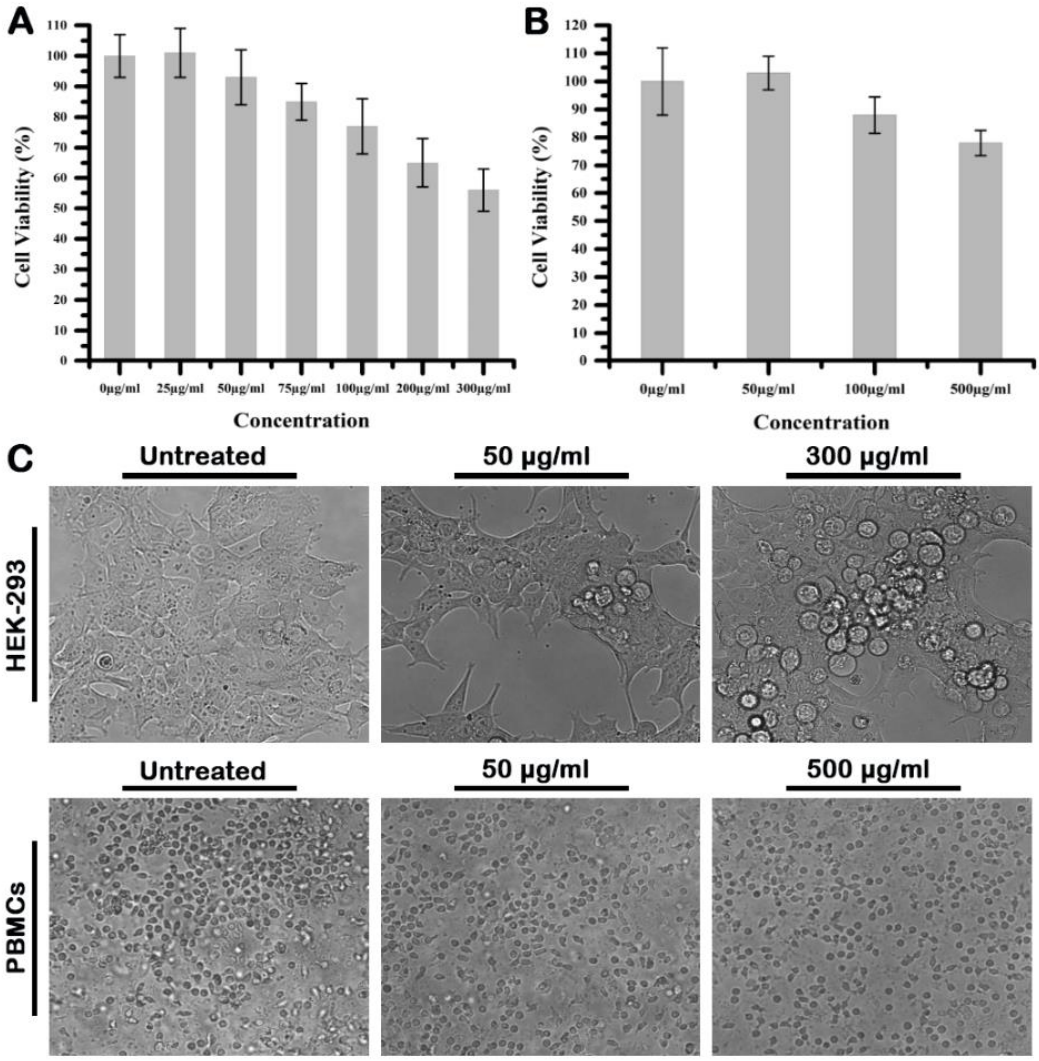

Figure 6.5: AMCAE does not affect cellular viability of normal human cells. (A) HEK-293 cells were treated with AMCAE for a period of 48-hours at different concentrations and its cell viability was developed using MTT assay. **(B)** Peripheral blood mononuclear cells (PBMCs) were isolated from healthy volunteers as per the procedure mentioned in chapter **3.** PBMCs were treated at various concentrations and its cell viability was developed using MTT assay. **(C)** Images from random fields were taken from untreated and treated cells using Cytell cell imaging system and their representative images are shown.

6.3.3 Bioactive agents present in Ayurvedic formulations are stable in physiological gastric condition: The stability of bioactive natural compounds in biological fluid is very crucial for their activity and delivery to the action site. Haritaki Churna is the primarily an Ayurvedic formulation to treat diseases of GI track. The use of dissolution media such as SGF has helped researchers in the approval of effective and stable generic drugs which has been well documented [10]. The Haritaki Churna was incubated in water and stimulated gastric fluid (SGF) and then we assess the stability of bioactive compounds and their anti-cancer activity.

The HPLC chromatograms show that all major peaks were present in both chromatograms no considerable changes in the overall composition of the formulation even after 6 hours of incubation (**Figure 6.6A-D**). In addition, we extracted the Haritaki Churna in SGF to see if differential extraction could result in different proportions of compounds being extracted or whether it alters the yield of extraction. The yield was anyhow similar when extracted in water or SGF. The yield in water was 539.6 ± 14.5 mg whereas it was 541.2 ± 17.3 mg in SGF. However, SGF extract chromatogram shows a decrease in the intensity of compounds 11, 12 & 13 and increase in the intensities of compounds 5, 9 & 10 but there is no change in composition of overall compounds present in both extracts (**Figure 6.6E** & **F**). The IC_{50}s of HCAE incubated in SGF with different time intervals are fundamentally close to the original HCAE IC_{50} value (**Figure 6.6G)**. Further, dissolution media such as FaSSIF and FeSSIF, containing bile salts, pancreatin at relevant pH conditions have been recognised and utilised to mimic the conditions in the stomach before and after meals [11].

Amalaki Churna has diverse applications in the treatment of various ailments, and one of its uses includes the management of gastrointestinal disorders. Since the majority of therapeutic drugs are typically taken orally, their main route of absorption into the human body occurs through the gastrointestinal tract. To understand the effect of gastric fluids on Amalaki Churna, the crude powder of Amalaki Churna was extracted, and its aqueous extract was subjected to incubation in simulated gastric fluid (SGF), to assess their stability under physiological gastric conditions. Given that Amalaki Churna is also consumed in the form of a water extract, we tested its efficacy by incubating the aqueous extract of Amalaki Churna in simulated gastric fluid (SGF) for 6 hours reading at an interval of 2 hours. This allowed us to assess its performance and stability in SGF. It was observed that the aqueous extract of Amalaki Churna remained stable in SGF, as there were no discernible alterations in its compositional makeup even after the 6-hour incubation period. (**Figure 6.7A-D**). Further, when Amalaki Churna was extracted in simulated gastric fluid (SGF), there were no observed alterations in its compositional makeup (**Figure 6.7F**), and the obtained chromatogram was indistinguishable from that of Amalaki Churna extracted in water (**Figure 6.7E**). This immutable condition can be contributed to the low pH of SGF. However, it is rather well-known that bulky polyphenols are unstable at physiological conditions in the pH range of 5-7 [12]. Further, the stability of Amalaki Churna in simulated gastric fluid (SGF) was confirmed through the absence of significant changes in the IC_{50} values of AMCAE (Amalaki Churna aqueous extract) following incubation in SGF for various time intervals. These IC_{50} values closely resembled those of

AMC (Amalaki Churna) extracted in water, indicating that the anti-cancer activity remained unaffected even after subjecting the water extract of Amalaki Churna to harsh pH conditions in the presence of SGF (**Figure 6.7G & H**).

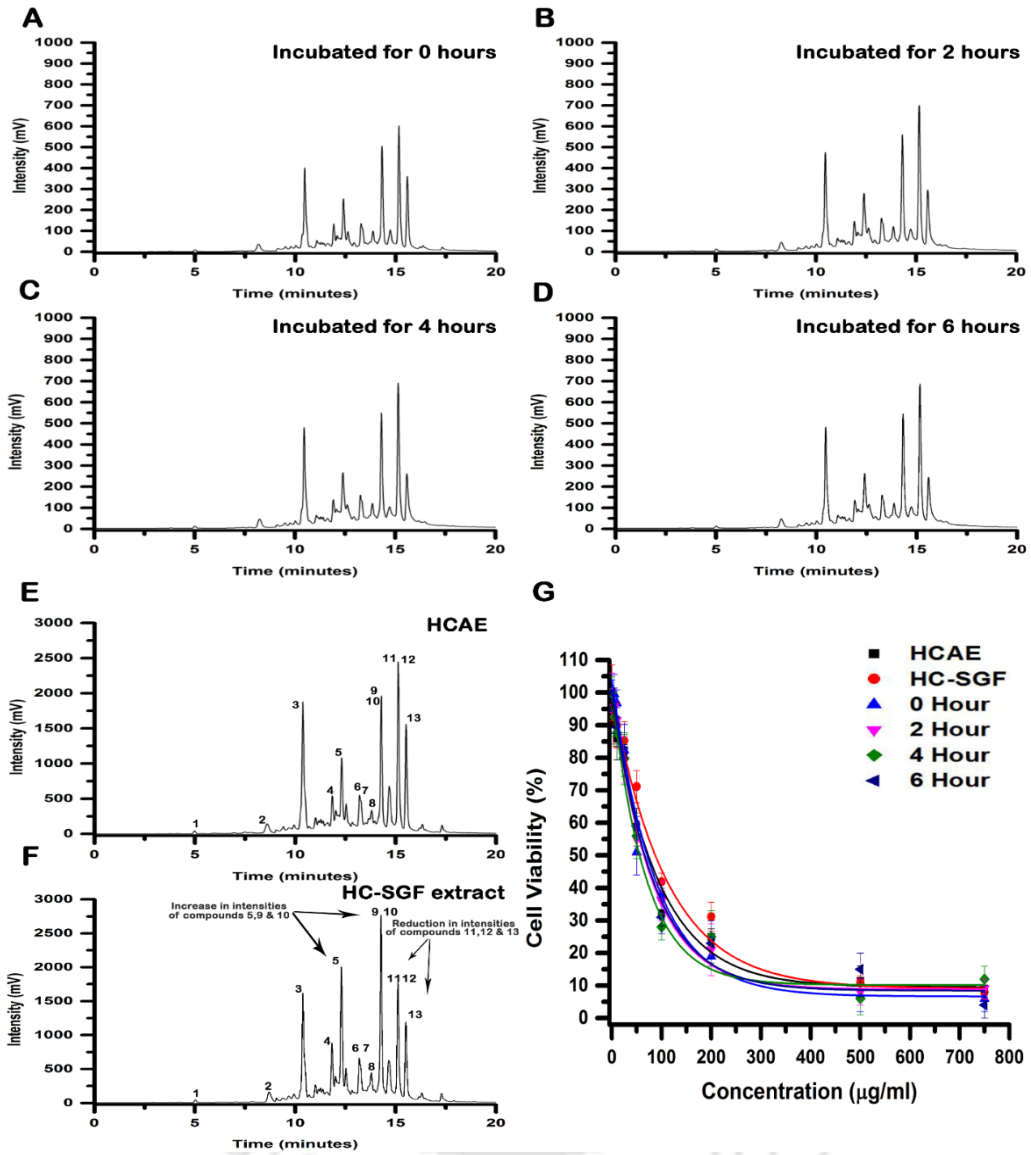

Figure 6.6: Haritaki Churna is stable under simulated gastric environment conditions. Lyophilised HCAE (100mg) was dissolved in 1 ml of SGF and incubated for different time intervals at 37^0C. **(A)** Gradient HPLC chromatogram of HCAE incubated in SGF for 0 Hours. **(B)** Gradient HPLC chromatogram of HCAE incubated in SGF for 2 Hours. **(C)** Gradient HPLC chromatogram of HCAE incubated in SGF for 4 Hours. **(D)** Gradient HPLC chromatogram of HCAE incubated in SGF for 6 Hours. The Haritaki Churna extracted in water and SGF were prepared as mentioned before. **(E)** Gradient HPLC chromatogram of HC extracted in water. **(F)** Gradient HPLC chromatogram of HC extracted in SGF. **(G)** HCAE extract retains the biological activity in SGF. DLD1 cells were treated with different concentration of HCAE and cellular viability was measured. MTT cell viability results seem to be coherent with the chromatogram data. The IC_{50}s of HCAE incubated with 0 Hour, 2 Hour, 4 Hour, and 6 Hour are 67.08± 5.2 µg/ml, 63.9 ± 6.3 µg/ml, 65.76 ± 4.66 µg/ml, and 63.4 ± 5.1 µg/ml respectively.

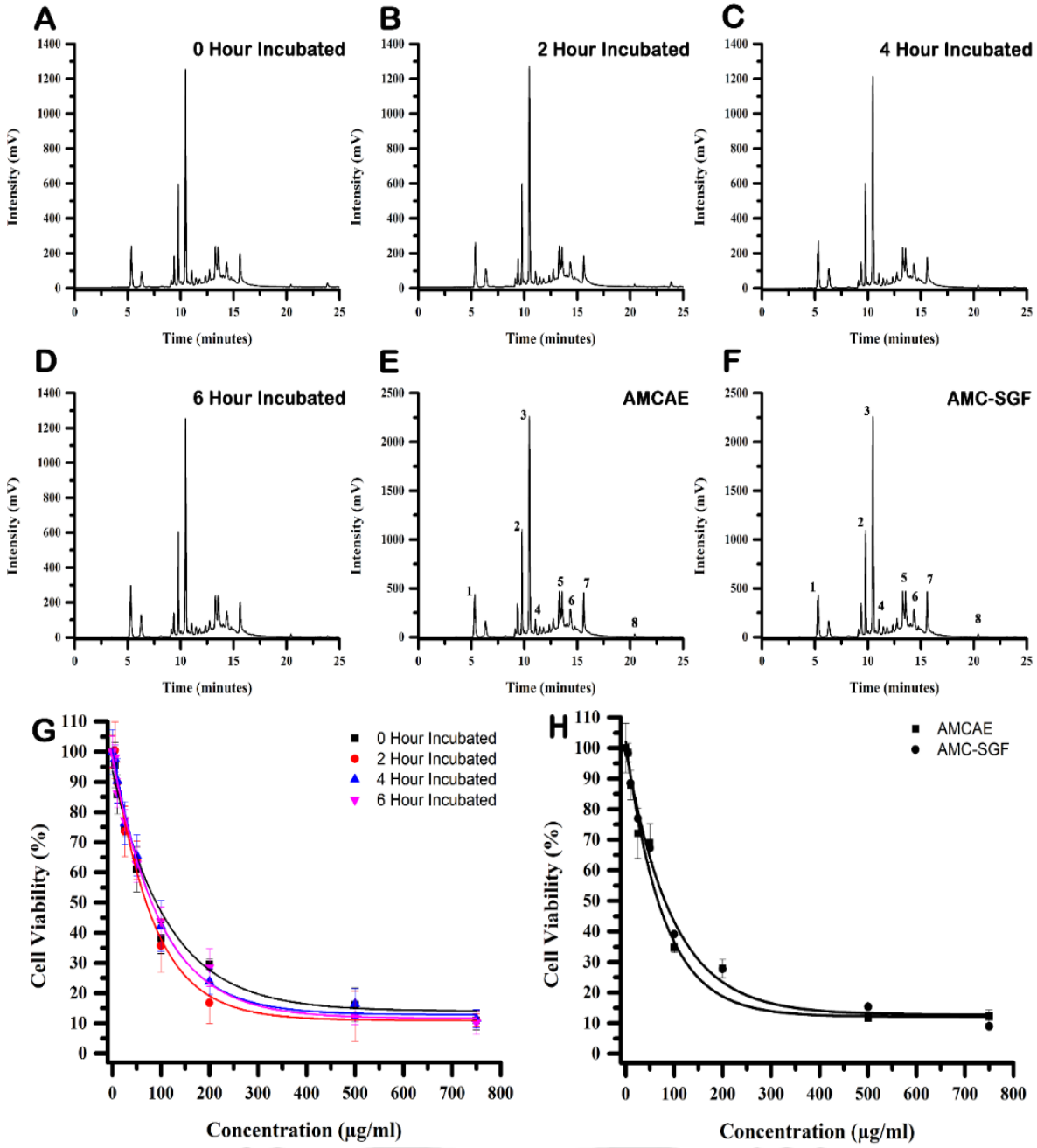

Figure 6.7: Amalaki Churna was found to be stable under simulated gastric conditions. Lyophilised AMCAE (100mg) was dissolved in 1 ml of SGF and incubated for different time intervals of 0 hour, 2 hours, 4 hours and 6 hours at 370C. (A-D) Gradient HPLC chromatograms of AMCAE at different time intervals are represented. (E) Gradient HPLC chromatogram of AMC powder extracted in water. (F) Gradient HPLC chromatogram of AMC powder extracted in SGF. (G) AMCAE retains the biological activity in SGF. HCT-116 cells were treated with different concentration of AMCAE_SGF incubated at different time intervals and cellular viability was measured. MTT cell viability results seem to be coherent with the chromatogram data. The IC_{50}s of AMCAE incubated with 0 Hour, 2 Hour, 4 Hour, and 6 Hour are 81.04± 4.99 µg/ml, 69.5 ± 6.9 µg/ml, 78.7 ± 5.9 µg/ml, and 80.7 ± 4.6 µg/ml respectively. (H) AMC extracted in water and SGF showed no change in activity. The IC_{50}s of AMC extracted in water and SGF are 66.3 ± 4.2 µg/ml and 83.2 ± 6.4 µg/ml respectively.

6.3.3 Bioactive agents present in Ayurvedic formulations are stable in physiological Intestinal condition: Drug dissolution in the proximal part of the small intestine is influenced by whether the drug is taken in a fed or fasted state, with various factors undergoing alterations post-meal, including hydrodynamics, intralumenal volume, pH, buffer capacity, osmolality, and bile output, all of which can impact drug bioavailability. To enhance the simulation of fasting conditions during drug dissolution testing, FaSSIF and FeSSIF were developed as a biorelevant medium designed to mimic the fasting environment present in the upper section of the small intestine. In contrast to HCAE as the control, there were no significant differences in the chromatograms of the formulation incubated with FaSSIF and FeSSIF, indicating that HC was stable in both the fasting and fed phases (**Figure 6.8A-C**). Additionally, the stability of the compounds present in HCAE was tested by incubating it in FaSSIF and FeSSIF at different time intervals. An increase in the intensity of compound 13 **(**ellagic acid**)** and a decrease in the intensity of the compounds 11 & 12 (Chebulagic acid and chebulinic acid) were observed indicating a degradation of those compounds in a time dependent manner (**Figure 6.8D** & **E**). It is well established that bulky polyphenols are known to be unstable at pH in the range of 5-7 [12]. The IC_{50} values of HCAE incubated in FaSSIF and FeSSIF at various time intervals decreased (indicating an increase in anti-cancer activity) because a rise in compound 13's intensity (ellagic acid) was seen in HCAE with their incubations at different time intervals (**Figure 6.8F** & **G**). Given its stability in SGF at low pH circumstances and an increase in anti-cancer activity of HCAE in simulated fasting and fed state intestinal settings, it is reasonable to assume that Haritaki Churna formulation can be employed as an anti-cancer drug due to its high bioavailability.

In a similar manner, AMC extracted in stable FaSSIF (pH 6.5), designed to mimic the fasted state conditions in the small intestine, exhibited stability (**Figure 6.9A**). FaSSIF, composed of bile salts, phospholipids, and buffer components, replicates the composition and pH of the fasted small intestine and is commonly utilized for evaluating drug solubility and absorption in fasting conditions. Moreover, the aqueous extract of AMC demonstrated stability when incubated in FaSSIF for a duration of 6 hours, as evidenced by the absence of any observable changes in the chromatogram, except for an additional peak (Rt=6.4 min), which can be attributed to the components present in FaSSIF (**Figure 6.9C**). FeSSIF simulates the fed state conditions in the small intestine, evaluating drug behaviour in the presence of food and interactions with bile salts, phospholipids, and enzymes. It contains fatty acids to replicate post-meal composition, with a lower pH than FaSSIF. AMC extracted in FeSSIF at pH 5.8

remained stable, with no significant changes observed (**Figure 6.9B**). Additionally, the AMC aqueous extract remained stable in FeSSIF after 6 hours, with no noticeable changes (**Figure 6.9D**). Given its stability at low pH circumstances replicating stomach environment and ideal pH values simulating intestinal conditions, AMC and its aqueous extract can thus be inferred to have excellent bioavailability.

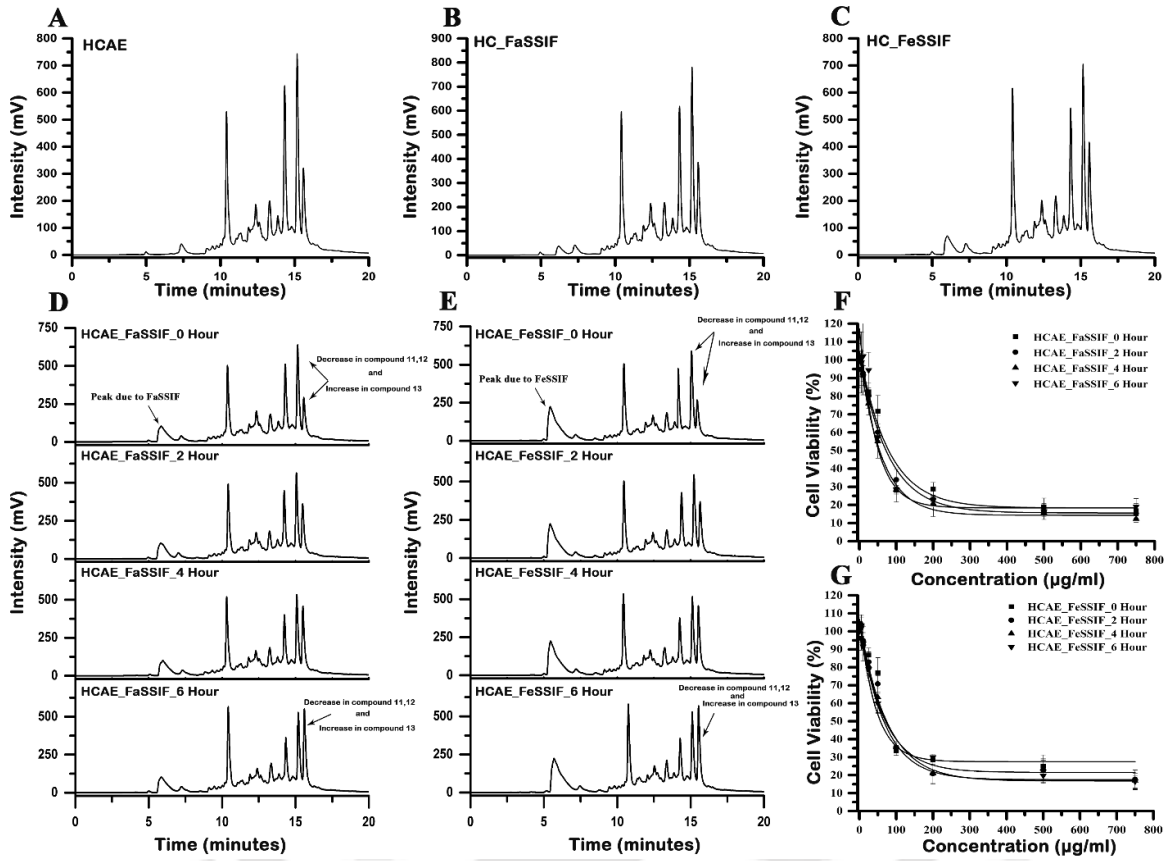

Figure 6.8: Haritaki Churna is stable under simulated Intestinal environment conditions: (A) Gradient HPLC chromatogram of HC incubated in water. **(B)** Gradient HPLC chromatogram of HC incubated in FaSSIF. **(C)** Gradient HPLC chromatogram of HC incubated in FeSSIF. **(D)** Gradient HPLC chromatogram of HCAE incubated in FaSSIF for 0, 2, 4 & 6 Hours. **(E)** Gradient HPLC chromatogram of HCAE incubated in FeSSIF for 0, 2, 4 & 6 Hours. **(F)** DLD1 cells were at different concentrations with HCAE incubated in FaSSIF at different time intervals. The IC_{50} values of HCAE incubated with FaSSIF for 0 Hour, 2 Hour, 4 Hour, and 6 Hour are 77.04 ± 6.4 µg/ml, 72.1 ± 5.4 µg/ml, 66.6 ± 3.7 µg/ml, and 59.6 ± 6.6 µg/ml respectively. **(G)** DLD1 cells were at different concentrations with HCAE incubated in FeSSIF at different time intervals. The IC_{50} values of HCAE incubated with FeSSIF for 0 Hour, 2 Hour, 4 Hour, and 6 Hour are 70.8 ± 4.5 µg/ml, 74.1 ± 4.5 µg/ml, 66.4 ± 6.01 µg/ml, and 57.1 ± 3.7 µg/ml respectively.

Further, the stability of Amalaki Churna in simulated intestinal fluid (SIF), which mimics the composition and pH of the small intestine with bile salts, phospholipids, and buffer components, was confirmed and demonstrated by observing the IC_{50} values of AMCAE

(Amalaki Churna aqueous extract) after incubation in FaSSIF and FeSSIF for different time periods (**Figure 6.9E & F**). The results showed that the IC_{50} values of AMCAE remained largely unchanged during incubation in FaSSIF and FeSSIF. These finding suggests that the active components responsible for the anti-cancer properties of Amalaki Churna are stable and can potentially exert their beneficial effects when passing through the intestinal environment.

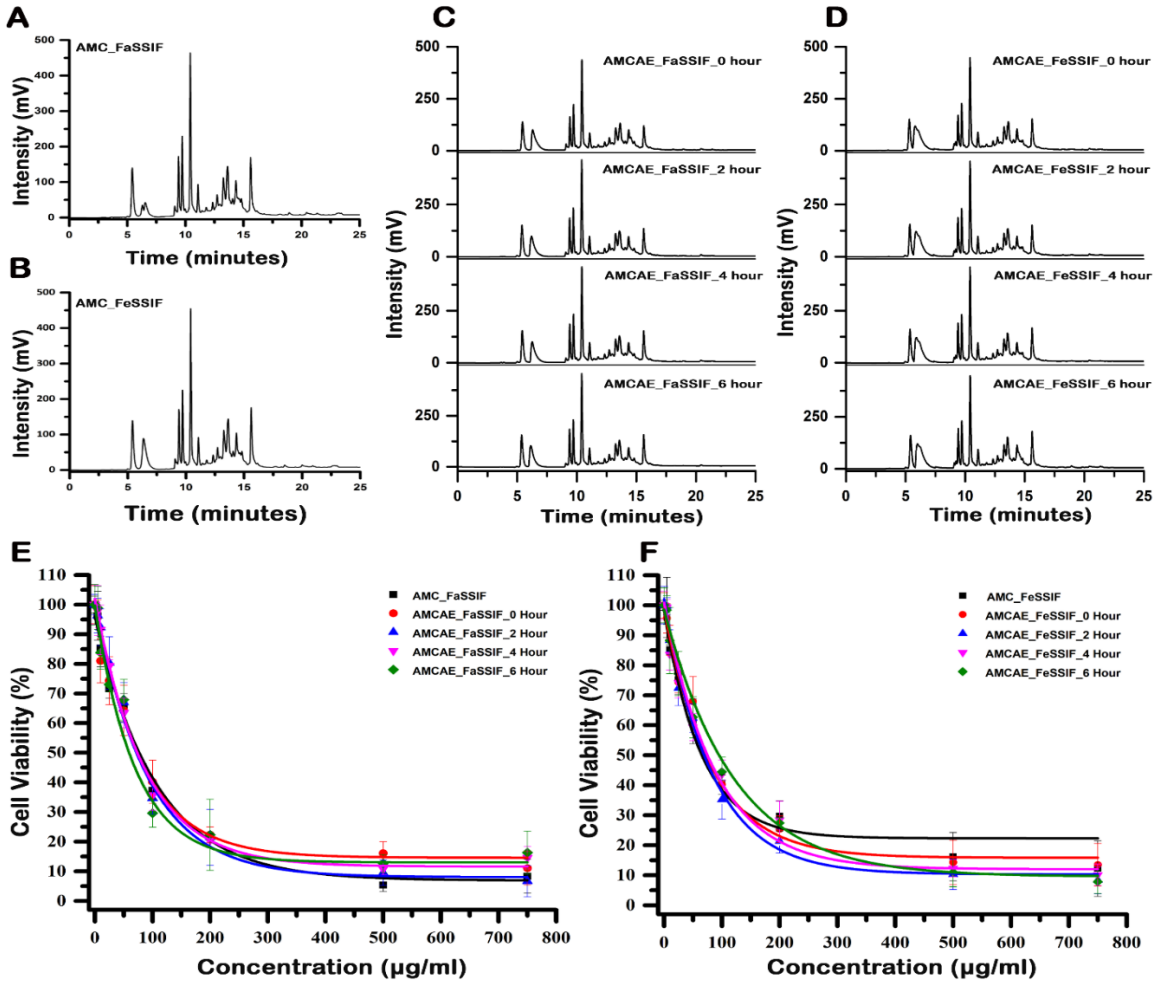

Figure 6.9: **Amalaki Churna was found to be stable under simulated intestinal conditions**. **(A & B)** Gradient HPLC chromatograms of AMC extracted in FaSSIF and FeSSIF. **(C)** Gradient HPLC chromatogram of AMCAE incubated in FaSSIF at 0, 2, 4 and 6 hours. **(D)** Gradient HPLC chromatogram of AMCAE incubated in FeSSIF at 0, 2, 4 and 6 hours. **(E & F)** AMCAE retains the biological activity in presence of FaSSIF and FeSSIF. HCT-116 cells were treated with different concentration of AMC incubated and extracted in FaSSIF and FeSSIF and cellular viability was measured. The IC_{50}s of AMC_FaSSIF, AMCAE_FaSSIF_0 hour, AMCAE_FaSSIF_2 hours, AMCAE_FaSSIF_4 hours and AMCAE_FaSSIF_6 hours were found to be 77.07± 5.88 µg/ml, 74.9 ± 5.9 µg/ml, 71.5 ± 6.1 µg/ml, 67.6 ± 4.6 µg/ml and 65.4 ± 7.2 µg/ml respectively. The IC_{50}s for AMC_FeSSIF, AMCAE_FeSSIF_0 hour, AMCAE_FeSSIF_2 hours, AMCAE_FeSSIF_4 hours and AMCAE_FeSSIF_6 hours were found to be 67.3 ± 5.7 µg/ml, 70.2 ± 5.1 µg/ml, 69.4 ± 4.8 µg/ml, 75.1 ± 4.3 µg/ml and 81.4 ± 5.7 µg/ml respectively.

6.3.4 Ayurvedic formulations have bioactive compounds with anti-cancer activity: Having identified multiple bioactive compounds in the crude extract of Haritaki Churna, we have conducted individual tests on isolated compounds to investigate their specific contributions to the observed anti-cancer activity in the crude extract. As discussed in chapter **3**, the Haritaki Churna aqueous extract (HCAE) was subjected to reverse-phase open column chromatography, resulting in the separation of five major fractions (fractions **1-5**). These fractions were then used to treat cancer cells (HCT-116, DLD1, and HT-29), and the cellular viability was subsequently measured using the MTT assay. Further, there were 13 major compounds identified from the five different fractions. Upon analysing fraction **1**, it was found that both Shikimic acid and Chebulic acid did not exhibit any significant impact on the cellular viability of the cancer cells. In contrast, fraction **2** contained a predominant amount of Gallic acid. When Gallic acid was isolated from fraction **2** and tested, it demonstrated potent anti-cancer activity against various cancer cell lines, with IC_{50} values ranging from 17-37 µg/ml. These experimental findings align well with previously published research, providing further support to the existing body of evidence showcasing Gallic acid's effectiveness in combatting different types of cancer cells [13-17]. Fraction **3** obtained from the reverse-phase open column chromatography of the Haritaki Churna aqueous extract was analyzed, revealing the presence of five major compounds: 5-hydroxymethylfurfural, proto-catechuic acid, methyl-gallate, corilagin, and 1, 2, 6 Tri-*O*-galloyl-β-D-glucose. Our investigation into the effects of 5-Hydroxymethylfurfural and proto-catechuic acid on cancer cell viability revealed that both compounds did not show any significant influence on the growth or survival of the cancer cells. Gallic acid is already known for its potential anti-cancer properties (**Table 6.2**). Interestingly, when Methyl-gallate (structurally similar to gallic acid) was isolated and tested against various cancer cell lines, it demonstrated noteworthy anti-cancer activity. The IC_{50} values ranged from 37-52 µg/ml for different cancer cell lines. Methyl-gallate is a relatively new compound compared with that of gallic acid, but there is still mounting evidence that suggests it exerts anti-cancer activity against a variety of cancer cell lines [18-22]. In addition to gallic acid and methyl-gallate, corilagin displayed significant cytotoxic effects on cancer cells, with IC_{50} values ranging from 23-157 µg/ml across various cancer cell lines. Moreover, Corilagin's anti-cancer potential has been assessed against different cancer types, such as ovarian, nasopharyngeal, osteosarcoma, colorectal, hepatocellular, and lung adenocarcinoma, exhibiting IC_{50} values ranging from 0.25-19 µg/ml. These compelling results highlight corilagin's broad-spectrum anti-cancer activity and its potential as a valuable therapeutic agent for diverse malignancies [23-27]. 1, 2, 6 Tri-*O*-galloyl-β-D-glucose which is structurally

similar to Corilagin also showed loss of cellular viability in cancer cells but at a higher IC_{50} in the range of 100-175 µg/ml. Chebulagic acid and chebulinic acid were the two compounds isolated from fraction **4**.

Table 6.2: Anticancer activity of fractions and compounds isolated from Haritaki Churna aqueous extract.

S. No.	Fraction/ Compound name	IC_{50} (µg/ml ± S.D.)		
		HCT-116	DLD1	HT-29
1	HCAE	92.69 ± 7.07	70.41 ± 6.35	379.93 ± 5.29
2	HC-0 Fraction	> 500	> 500	> 500
3	HC-20 Fraction	33.71 ± 4.24	15.61 ± 4.89	43.57 ± 4.98
4	HC-50 Fraction	155.5 ± 7.59	79.39 ± 4.83	141.43 ± 4.66
5	HC-80 Fraction	71.29 ± 5.4	36.53 ± 3.77	115.7 ± 4.8
6	HC-100 Fraction	14.03 ± 3.46	20.14 ± 3.99	13.32 ± 3.48
7	Shikimic acid	> 500	> 500	> 500
8	Chebulic acid	> 300	> 300	> 300
9	Gallic acid	37.1 ± 4.56	18.1 ± 4.63	35.06 ± 5.31
10	5-Hydroxymethylfurfural	> 500	> 500	> 500
11	Protocatechuic acid	> 300	> 300	> 300
12	4-*O*-galloyl shikimic acid	311.2 ± 6.2	179.6 ± 4.6	161 ± 4.79
13	5-*O*-galloyl shikimic acid	281.5 ± 5.2	136.8 ± 4.8	203.7 ± 5.8
14	Methyl gallate	38.68 ± 4.51	37.8 ± 3.39	30.71 ± 3.76
15	Corilagin	23.91 ± 3.82	63.08 ± 4.21	157.39 ± 4.34
16	1,2,6 Tri-*O*-galloyl β-D glucose	100.11 ± 5.29	157.5 ± 7.64	114.22 ± 4.49
17	Chebulagic acid	> 250	> 250	> 400
18	Chebulinic acid	54.04 ± 5.41	22.63 ± 4.21	122.4 ± 4.02
19	Ellagic acid	10.08± 3.46	17.39± 4.89	13.1± 4.81

Shikimic acid, chebulic acid, gallic acid, 5-hydroxymethylfurfural, protocatechuic acid, 4-*O*-galloyl shikimic acid, 5-*O*-galloyl shikimic acid, methyl gallate, 1, 2, 6, Tri-O-galloyl β-D-glucose, and corilagin, were dissolved in water whereas chebulagic acid, chebulinic acid, and Ellagic acid were dissolved in DMSO (The highest concentration treated contained not more than 0.2% DMSO)

Chebulagic acid did not exert any discernible impact on the cellular viability of cancer cells. However, its structural analogue, chebulinic acid, demonstrated effectiveness against all cancer cell lines tested, with IC_{50} concentrations ranging from 22-122 µg/ml across various cancer types. These findings underscore the significance of subtle structural differences in bioactivity. In recent investigations focusing on chebulinic acid extracted from *Terminalia chebula* Retz., compelling evidence emerged showcasing its anti-cancer potential against HR8348, LoVo, and LS174T colorectal cancer cell lines. The IC_{50} concentrations for these cell lines ranged from

38-40 mg/L, while HOS-1 cells exhibited an IC_{50} of 53.2±0.16 µM. These recent findings underscore the significance of chebulinic acid as a promising candidate for further research and development as an anti-cancer agent [28]. Fraction **5** was found to contain both Chebulinic acid and Ellagic acid, exhibiting IC_{50} concentrations ranging from 10-20 µg/ml against the tested cancer cell lines. Notably, when Ellagic acid was isolated from fraction 5 and assessed separately, it also displayed IC_{50} values falling within the same range (10-20 µg/ml). Remarkably, these experimental IC_{50} values of Ellagic acid align consistently with those reported in the published literature, corroborating its potential as a valuable anti-cancer agent [29, 30] . The corresponding dose-dependent response graphs utilized to determine the anti-cancer activity are displayed (**Appendix I**). Gallic acid, methyl gallate and ellagic acid were found to be the most active polyphenols from HCAE based on their anti-cancer activity.

In similar manner, numerous compounds isolated from Amalaki Churna crude aqueous extract were examined individually to see how they may contribute to the anti-cancer activity shown in the crude extract. The 5 fractions obtained from open column chromatography were subjected to cell viability assay against colorectal cancer cells (HCT-116, DLD1 and HT-29). Fraction **1** and fraction **5**, containing the most hydrophilic & hydrophobic compounds did not show killing of colorectal cancer up to concentrations of 500 µg/ml and 100 µg/ml respectively. Fraction **2**, **3** & **4** which are the intermediary polar fractions were active with fraction **4** being the most cytotoxic to colorectal cancer cells. 8 major compounds were isolated from the crude AMCAE. Mucic acid 2-*O*-gallate & β-glucogallin, the two major compounds present in fraction **1** did not show any killing of cancer cells (**Table 6.3**). Gallic acid the predominant compound present in fraction **2** exerted IC_{50} in the range of 18-37 µg/ml. Gallic acid is a well-known polyphenol that has been widely examined on a variety of cancer cells. Our results are consistent with the literature that has already been published [13-17]. 5-hydroxymethylfurfural, macabarterin and corilagin were the foremost compounds present in fraction **3**. 5-hydroxymethylfurfural did not exhibit killing of cancer cells even at higher concentrations. Macabarterin is a novel compound whose structure has only been reported once before [31]. It exerted anti-cancer activity (IC_{50}) against colorectal cancer cells in a range of 205-250 µg/ml. In addition to macabarterin, corilagin has also shown anti-cancer action (IC_{50}), but at concentrations stretching from 30-163 µg/ml. The resultant IC_{50} graphs are presented in **Appendix-I**. Corilagin is a high molecular weight polyphenol which has been tested against a plethora of cancer cell lines [23-26, 32]. The most effective molecule in the AMCAE was ellagic acid, which was found mostly in fraction **4** and in trace amounts in fraction **3**. Ellagic

acid exerted IC_{50} in the range of 11-16 µg/ml which is also in line with accessible literature [29, 30].

Table 6.3: Anti-cancer activity of fractions and compounds isolated from Amalaki Churna aqueous extract.

S. No	Fraction/ Compound name	IC_{50} (µg/ml ± S.D.)		
		HCT-116	DLD1	HT-29
1	AMCAE	74.05 ± 6.5	95.9 ± 7.3	269.2 ± 6.2
2	Fraction 1	> 500	> 500	> 500
3	Fraction 2	52.2 ± 5.7	81.6 ± 3.5	70.2 ± 5.1
4	Fraction 3	105.1 ± 3.7	99.8 ± 4.5	173.6 ± 4.6
5	Fraction 4	41.33 ± 5.4	35.3 ± 4.2	48.4 ± 4.2
6	Fraction 5	>100	>100	>100
7	Mucic acid 2-*O*-gallate	> 500	> 500	> 500
8	β-glucogallin	> 300	> 300	> 300
9	Gallic acid	29.4 ± 4.7	18.78 ± 5.9	37.13 ± 5.3
10	5-Hydroxymethylfurfural	> 500	> 500	> 500
11	Corilagin	30.35 ± 5.18	56.7 ± 5.2	163.7 ± 5.4
12	Macabarterin	208.5 ± 5.7	205.7 ± 5.6	250.07 ± 6.6
13	Ellagic acid	11.02 ± 5.2	16.6 ± 5.5	11.8 ± 5.4
14	Trans-cinnamic acid	>100	>100	>100

Fractions 1-4, Mucic acid 2-*O*-gallate, β-glucogallin, Gallic acid, 5-hydroxymethylfurfural, corilagin, and macabarterin were dissolved in water whereas ellagic acid & trans-cinnamic acid were dissolved in DMSO (The highest concentration treated contained not more than 0.2% DMSO).

6.3.5 Ellagic acid is the most active ingredient from HCAE: Dietary polyphenols are known to exert their anti-cancer activity by interfering with membrane receptors, disrupting cellular signaling cascades, enzymes in basic metabolic processes, and other targets which basically holds up the cellular machinery [33]. Many crude extracts and their active ingredient have been shown to have anti-cancer action in synergistic and individualistic manner [34]. Often, it is the presence of a particular compound that is responsible for the activity of the crude extract. Thus, a deductive approach was employed to elucidate the polyphenols from HCAE which when removed will have a greater impact on the overall anti-cancer activity of the crude water extract (**Figure 6.10A**). Using the compositional make-up of 13 phytochemicals obtained from gradient HPLC chromatogram, different mixtures of the phytochemicals were made (**Figure 6.10A**). The Complete Mixture (CM: mixture of all 13 identified compounds) did not show much variation in its anti-cancer activity (80.4 ± 5.5 µg/ml) when compared to its crude counterpart HCAE (70.41 ± 6.35 µg/ml). Further, the cellular viabilities (IC_{50} values) of different mixtures (C1′-C13′) against the colorectal cancer cell line DLD1 revealed that subtraction of some polyphenols from the CM were more significant than others in terms of

their anti-cancer activity. For instance, subtractions of individual polyphenols from the complete mixture such as C1′, C5′-C8′, C10′-C12′ observed a decrease in IC_{50} values in the range of 0.99% to 19% that correlates to the gain of anti-cancer activity of HCAE (**Figure 6.10B**).

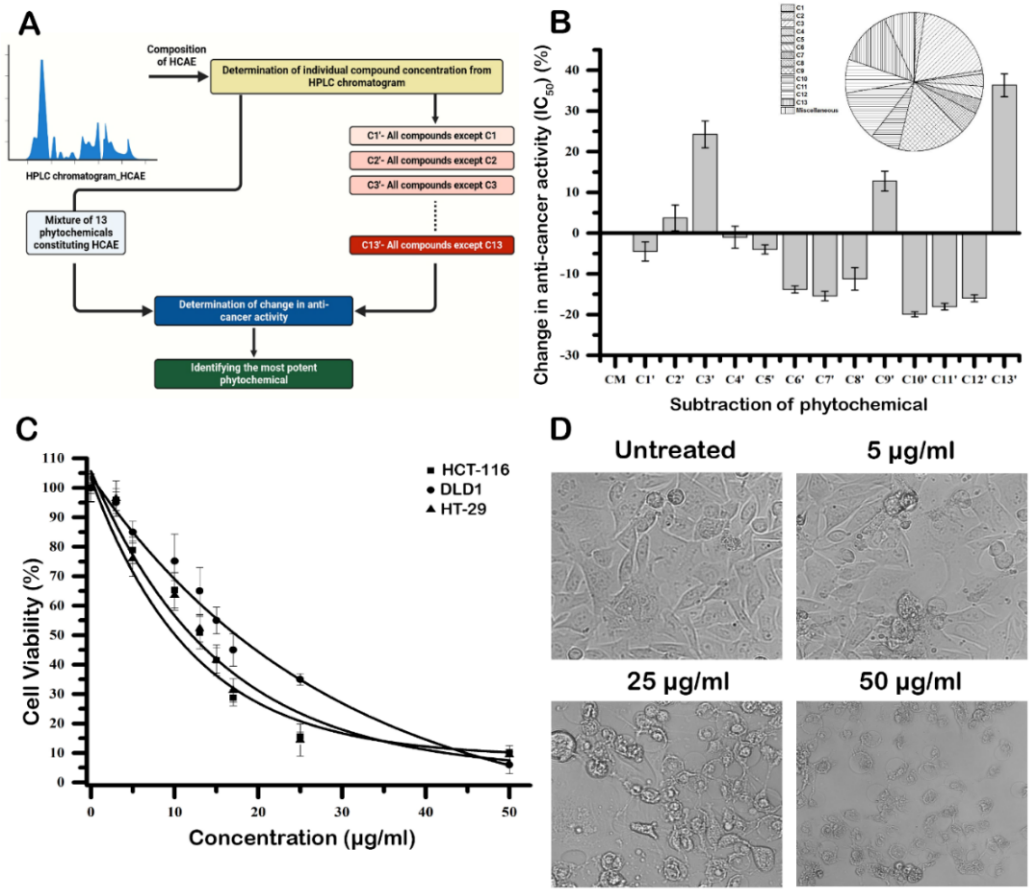

Figure 6.10: Ellagic acid is the active ingredient responsible for anti-cancer activity of HCAE. (A) Schematic of the deductive approach to discover the most active ingredient in HCAE. **(B)** The variation in anti-cancer activity after removal of compounds from HCAE. The term "CM" stands for the complete mixture, which is made up of 13 identified compounds and is created in accordance with the composition of the gradient HPLC chromatogram. **(C)** Colorectal Cancer cells (DLD1) were treated with different concentration of ellagic acid (0-50 µg/ml) and the cell viability was measured by MTT assay. The MTT curve of ellagic acid is presented with an IC_{50} of 17.39± 4.89 µg/ml after treatment of 48 hours. **(D)** DLD1 cells were examined under a microscope, and pictures were captured from various fields using the Cytell cell imaging system (GE Healthcare). Representative images are shown. (**Note**: C1′-Mixture except shikimic acid, C2′-Mixture except chebulic acid, C3′-Mixture-except gallic acid, C4′-Mixture except 5-hydroxymethylfurfural, C5′-Mixture except protocatechuic acid, C6′-Mixture-except 4-*O*-galloyl shikimic acid, C7′-Mixture except 5-*O*-galloyl shikimic acid, C8′-Mixture except methyl gallate, C9′-Mixture-except corilagin, C10′-Mixture except 1,2,6-Tri-*O*-galloyl-β-D glucose, C11′-Mixture except chebulagic acid, C12′-Mixture-except chebulinic acid, C13′-Mixture except ellagic acid).

This increase in anti-cancer activity may be attributed to their antagonistic action. Their antagonistic action may be (a) because of these phytochemicals competing for the same protein which is crucial in pathway of killing cancer cells or (b) may be because of formation of a complex polyphenol mixture which are unable to perform their individual activities [35, 36]. On the other hand, C3′, C9′ and C13′ which corresponds to subtraction of gallic acid, corilagin and ellagic acid respectively, observed an increase in the IC_{50} values that signifies the loss of anti-cancer activity of HCAE. In C3′, C9′ and C13′, an increase in IC_{50} values by 24.2%, 12.7% and 36.3% was observed, thus making ellagic acid as the most crucial polyphenol in the phytochemical makeup of the crude HCAE extract. Cancer cells when treated with ellagic acid exhibited loss of cellular viability and distortions in cellular morphology. Ellagic acid was found to exert anti-cancer activity in a dose dependent manner on colorectal cancer cell lines HCT-116, DLD1 & HT-29 with IC_{50}s of 10.08 ± 3.46 µg/ml, 17.39 ± 4.89 µg/ml, 13.1 ± 4.81 µg/ml respectively (**Figure 6.10C & D**). Ellagic acid is a well-known polyphenol which is known for its various activities that include antioxidant, neuroprotective, hepatoprotective etc., along with anti-cancer potential [30, 37].

6.3.6 Ellagic acid perturbs the cell cycle in cancer cells: Cancer cells treated with ellagic acid is exhibiting cellular stress with the appearance of distortion of cellular morphology. The stress linked signalling is associated with conservation of energy production and adaptation of cell with pro-survival strategies [38]. It in-turn disturbs many basic cellular functions including cell-cycle through reduction in production of various regulatory cyclins. It is well known that a mammalian cell undergoes various stages of cell growth and division [39]. The four phases present during cellular division are G1, S, G2, and M phases. The effect of ellagic acid on cell cycle progression in different colorectal cancer cell lines was assessed by flow cytometry analysis after staining the cells with propidium iodide (**Figure 6.11A**). The 2-D chromatogram was analyzed using FCS Express software. Before treatment, the population of cells in S-phase were 17 ± 3.2%, 18.4 ± 4.1%, and 15.1 ± 6.9% for HCT-116, DLD1, and HT-29 cells respectively. Upon treatment with ellagic acid for 24h, the cell population in S-phase were 40.9 ± 6.1%, 30.8 ± 5.2%, and 31.9 ± 4.9%. The flow cytometry analysis suggests that there is an increase in the population of S-phase cells and cancer cells does not cross S-phase. Further, the protein expression levels of cyclin A2 and cyclin D1 were found to be down-regulated upon treatment with ellagic acid. Although cyclin A2 levels decreased after 24 hours of treatment, there were no significant changes in cyclin D1 expression levels, indicating that cells were arrested primarily in S-phase after 24 hours of treatment. However, after 48 hours of ellagic

acid treatment, both cyclins (A2 and D1) were shown to have reduced expression levels in a dose dependent manner (**Figure 6.11G & H**).

6.3.7 Ellagic acid induces mitochondrial apoptotic pathway in cancer cells: The colorectal cancer cells in stress due to treatment with ellagic acid can induce cell death either by undergoing apoptosis, necrosis, autophagy or necroptosis. As caspase dependent apoptosis is the most common form of programmed cell death (PCD), we first checked DNA fragmentation/laddering which is a hallmark of apoptosis. Treatment of cells with ellagic acid resulted in DNA fragments that was detected by DNA laddering assay (**Figure 6.11B-D**). It was further confirmed by dual staining of treated cells by acridine orange and propidium iodide is done to differentiate the live healthy cells from the apoptotic cells. Untreated cells were shown to have prominently healthy cells ranging from 94-99 % in different cell lines (**Figure 6.11E**). The cells treated with ellagic acid were shown to have changed in the distribution of cells. The early apoptotic was seen in a range of 5-12 % compared to 0-1 % in the untreated cells. There was also an increase in the late apoptotic cells which were seen in a range of 24-32 % compared to 0-1 % in the untreated cells. The FACS analysis was also confirmed by fluorescence imaging of the dually stained cells (**Figure 6.11F**). Further, immunoblotting of caspase 3 and its cleaved form obtained from DLD1 cells treated ellagic acid at 24h and 48 h revealed increased expression of cleaved caspase 3 (17-19 kDa) in a dose dependent manner (**Figure 6.11G & H**). Caspase 3 can be cleaved by two main pathways, the mitochondrial pathway via release of cytochrome-c or death receptor pathway via caspase 8 activation [40]. An increase in cytochrome-c expression was seen after 24 and 48 hours of ellagic acid treatment, indicating that the killing is caused via the mitochondrial apoptosis pathway. The formation of cleaved caspase 3 resulted in the cleavage of PARP-1 (poly (ADP-ribose) polymerase-1) to form cleaved PARP-1, an 89 kDa cleaved fragment indicating onset of apoptosis upon treatment with ellagic acid. The cells undergoing DNA damage/fragmentation or induction of ROS can lead to an over expression of pro-apoptotic proteins and simultaneously decrease anti-apoptotic proteins such as Bcl2 [41]. Hence, treatment with ellagic acid also down-regulated Bcl2. Additionally, the bioactive polyphenol was shown to downregulate caspase 8 and cleaved caspase 8 upon treatment, ruling out the possibility of killing cancer cells via classical death receptor pathway including TNFR1, TNFR2, and Fas receptors. Necroptosis is a type of controlled cell death caused by the activation of death receptors and the downregulation of caspase 8 [42]. The hallmark proteins of necroptosis, RIP (Receptor interacting protein kinase) and MLKL (Mixed lineage kinase domain-like), as well

as their phosphorylated versions, p-RIP and p-MLKL, were shown to be down-regulated by ellagic acid treatment demonstrating no evidence of necroptosis.

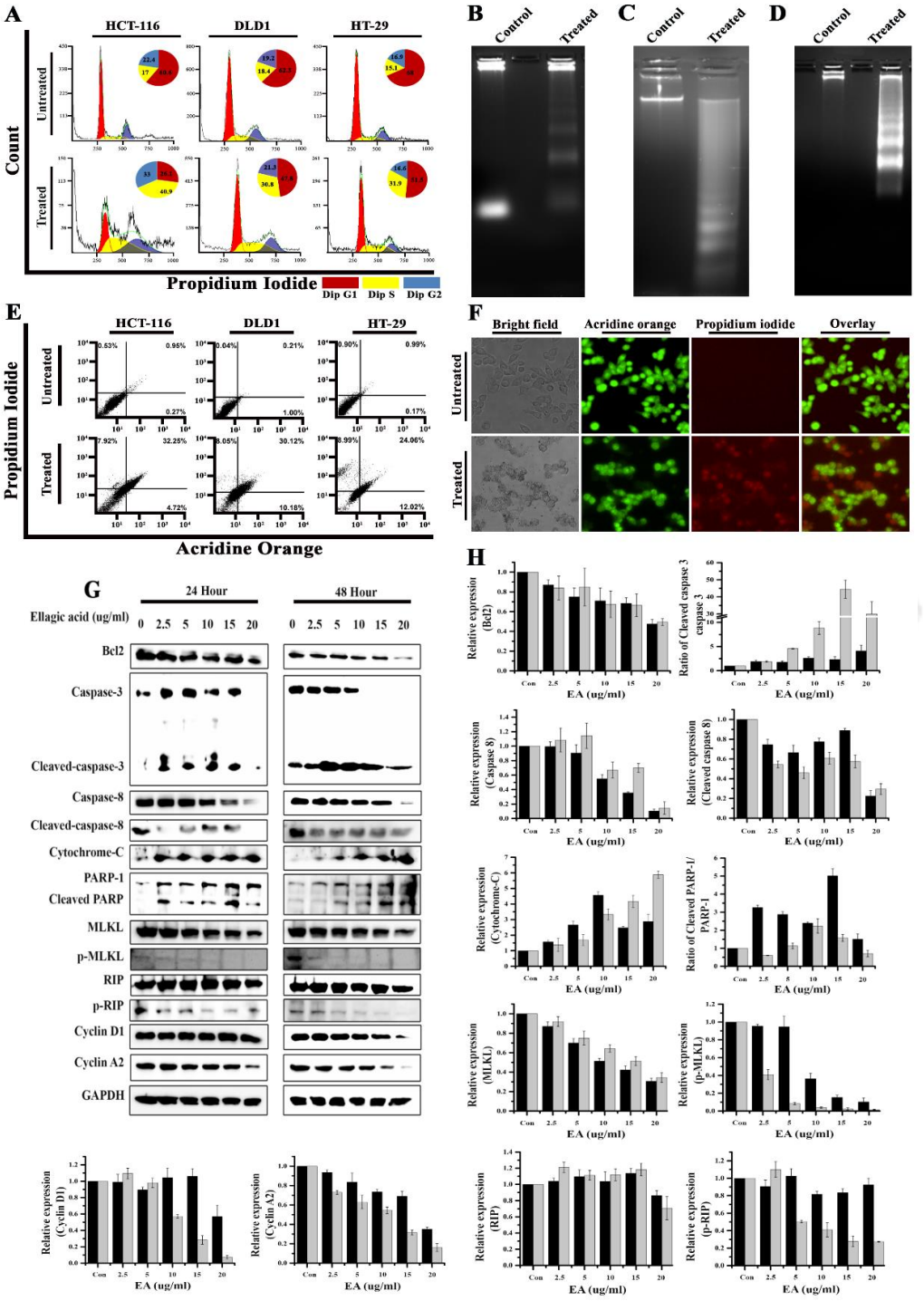

Figure 6.11: Ellagic acid causes cell death in cancer cells by intrinsic apoptosis. (A) Ellagic acid causes perturbations in cell cycle progression in cancer cells. **(B-D)** Ellagic acid caused degradation of genomic DNA in HCT-116 **(B)**, DLD1 **(C)**, and HT29 **(D). (E & F)** Ellagic acid induces apoptosis in cancer cells. **(G & H)** Ellagic acid induced death of colorectal cancer cells (DLD1) was caused by intrinsic pathway of apoptosis.

6.3.8 Ellagic acid down-regulates death receptors in colorectal cancer cells: The death receptor family are a part of the tumour necrosis factor super family [43, 44]. TNFR1, TNFR2, Fas, DR3, DR4, DR5 & DR6 are a part of this death receptor family and are regulated by a variety of ligands. The most important regulator is TNF-α, a cytokine which regulates inflammation, cellular proliferation and even induction of apoptosis and necroptosis. Although, much research suggests that TNF-α acts a tumour suppressor, there is accumulating evidence that it also acts a tumour promoter because of persistent cause of inflammation in pre-neoplastic and malignant diseases [45]. Apart from the ligand itself, over expression of death receptors themselves can be a cause of tumour progression. The default state of TNFR1 signaling results in the activation of NF-kB pathway which is a pro-survival pathway that acts by inducing expression of anti-apoptotic genes such as Bcl-2 [46, 47]. Because of the death receptors being the primary induction molecules of apoptosis, we first checked the expression levels of TNFR1 and TNFR2. A brief schematic of the effect of ellagic acid treatment on DLD1 cells is represented (**Figure 6.12A**). Upon 24h treatment of DLD1 cells with ellagic acid at varying concentrations, we found elevated levels of s-TNFR1 and s-TNFR1 (soluble-TNFR1) in the treated cells but not in untreated cells as shown through western blotting (**Figure 6.12B & C(i-ii)**). TNF-α converting enzyme (TACE) is the proteinase that converts TNFR1 and TNFR2 into s-TNFR1 and s-TNFR2 respectively [48]. s-TNFR1 has a known function of antagonizing and buffering the amount of TNF-α suggesting that s-TNFR1 neutralizes TNF-α to bind to TNFR1, thereby stopping the mechanism of tumour progression. Also, s-TNFR1 is sought induce apoptosis independent of death receptor signaling but dependent on TGF-β signaling [48, 49]. In 48 h treatment, there was no presence of TNFR1 compared to that of the untreated cells, but elevated levels of s-TNFR1 were still present suggesting that ellagic acid might be inducing apoptosis via reverse signaling involving s-TNFR1 and TNF-α.

Further, Fas protein, also known as CD95 or Apo-1, functions as a death receptor that becomes activated upon binding to its ligand, FasL. Accumulating evidence suggests that Fas is involved in non-apoptotic activities that promote tumourigenesis [50, 51]. Specifically, in gastrointestinal cancers, Fas has been found to enhance tumour cell motility through the induction of epithelial-mesenchymal transition, thereby promoting metastasis. This effect is demonstrated by the upregulation of mesenchymal markers and downregulation of epithelial markers upon FasL treatment [52]. Interestingly, the treatment of DLD1 cells with ellagic acid effectively downregulates the expression of Fas in a dose-dependent manner, as confirmed by Western blot analysis in (**Figure 6.12B & C(iii)**). Consequently, ellagic acid treatment appears

to inhibit the non-apoptotic pro-survival Fas-mediated signaling, thereby depriving the cancer cells of their survival advantage.

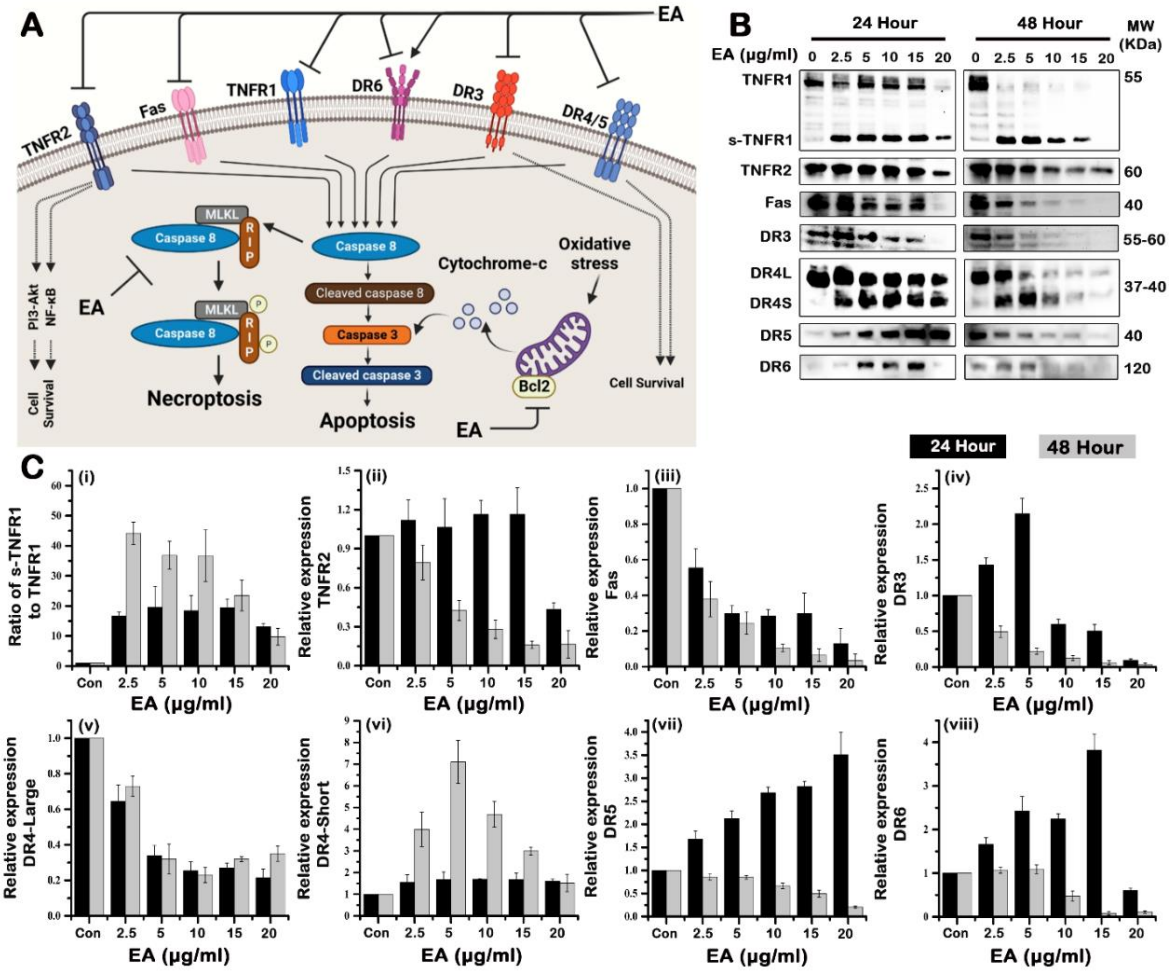

Figure 6.12: Ellagic acid down regulates expression of death receptors in colorectal cancer cells. (A) Schematic of the pathway targeted in DLD1 cells by ellagic acid**. (B)** DLD1 cells were treated with various concentrations (2.5, 5, 10, 15, 20 µg/ml) of ellagic acid for 24 and 48 hours. Western blotting was performed after harvesting the proteins using RIPA lysis buffer. Western blot images of several death receptors are shown. **(C)** Relative expression levels of death receptors are represented.

DR3 is a member of TNFR super family of death receptors. The activation of DR3 is linked with rapid onset of apoptosis which is stimulated by its ligand APO3L/TWEAK. There are several chemotherapeutic drugs available that induces apoptosis through APO3L mediated activation of DR3 such as taxol and vinblastine [53]. Ellagic acid was found to down regulate DR3 expression in 24h and 48h of treatment in a dose dependent manner in DLD1 cells (**Figure 6.12B & C(iv)**). Although primarily DR3 up regulation by conventional drug treatment have been the strategy to halt cancer progression, new evidence suggests that up regulation of DR3 may be linked to cancer metastasis in colon cancer in-vitro tumour models such as HT29 and

LoVo cells [54]. DR3 is a new receptor that have been identified for E-selectin, a protein that is directly involved in epithelial-mesenchymal transition thereby promoting tumour metastasis. Also, silencing of DR3 in hepatocellular carcinomas, have been linked to the inhibition and invasion of cells in-vitro [55]. Treatment of DLD1 cells with ellagic acid suggests that DR3 expression levels are lowered upon treatment (**Figure 6.12B & C(iv)**) and hence could be playing a major role in suppressing tumour metastasis and invasion of colon cells in-vitro.

TRAIL induced apoptosis through DR4 and DR5 death receptors are targets of many new chemotherapeutic drugs [56]. There have been many drugs that activate DR4 and DR5 through TRAIL [57]. Alternatively, rhTRAIL (recombinant human TRAIL) have been extensively employed at preclinical levels for their selective induction of apoptosis. TRAIL induced apoptosis have attracted many science enthusiasts in the field of cancer biology mainly because of their p53 independent status [58]. However, besides its strong pro-apoptotic activities TRAIL also promotes survival, proliferation and migratory signaling in cells. TRAILs activities of promoting pro-survivability in resistant tumour cells have been termed as non-canonical kinase signaling which include RIP1, MAPK, p13/AKT, Src etc, [59]. Although, the TRAIL chemotherapeutics available treat TRAIL sensitive cancers, these therapeutics have little or no effect on intrinsic or acquired TRAIL resistance in many colorectal cancers [60]. Many studies have demonstrated TRAIL receptors such as DR4 and DR5 are expressed in normal and cancerous colorectal adenomas and carcinomas [61, 62]. Also DR4 and DR5 were found to be increased in malignant cells [61]. After 24 hours of treatment, ellagic acid-treated DLD1 cells exhibited both short (DR4S) and long (DR4L) versions of DR4, but no changes in DR5 expression were observed, showing that TRAIL-mediated apoptotic signalling might be occurring (**Figure 6.12B & C(v-vii)**). The expression of different forms of DR4 have already been reported before [63]. DR4L was seen in both untreated and treated, but DR4S was seen only in treated suggesting that DR4S might be involved in death receptor mediated apoptosis signaling. The expression of DR4S also correlates with expression of DR5 since both the receptors are activated by the same ligand. However, we have seen that there is no increase in expression of cleaved caspase-8 upon ellagic acid treatment for 24 hours, there by ruling out the possibility of TRAIL mediated apoptosis. There was a reversal in trend seen in the case of DR4 and DR5 compared to TNFR1, TNFR2 and Fas mediated signaling after 48 hours of treatment with ellagic acid. After 48h of treatment, the expression of DR4 and DR5 were down-regulated. The same trend of treatment was also seen with respect to DR6 expression levels in 24h and 48h of treatment (**Figure 6.12B & C(viii)**).

In conclusion, ellagic acid treatment was found to induce apoptosis in colorectal cancer cells, as evidenced by DNA fragmentation (laddering) and an increase in the expression of cytochrome-c cleaved caspase-3 and cleaved PARP-1, while Bcl2, an anti-apoptotic protein, was down-regulated. Notably, no evidence of necroptosis was observed, as hallmark proteins associated with necroptosis, namely RIP, MLKL, p-RIP, and p-MLKL, were all down-regulated. Additionally, the down-regulation of several death receptors and caspase-8 with its cleaved form (cleaved caspase-8), suggested that the classical death receptor pathway was not involved in the cell death mechanism induced by ellagic acid treatment. Consequently, the results indicate that the extrinsic pathway of apoptosis did not contribute significantly to the observed cell death. Instead, the findings strongly support the involvement of the intrinsic pathway of apoptosis, also known as the mitochondrial pathway of apoptosis.

6.3.9 Ellagic acid inhibits wnt/β-catenin pathway and blocks epithelial to mesenchymal transition (EMT) in colorectal cancer cells: The Wnt/β-catenin signaling pathway plays a pivotal role in coordinating essential cellular processes such as cell polarity, cell differentiation, embryonic development, and tissue homeostasis [64]. Comprising the canonical and non-canonical pathways, its activation relies on the intricate interaction between Wnt ligands and the formidable Fz or LRP4/6 receptors located on the cell membrane [65]. This critical engagement sets off a series of events, ultimately regulating diverse cellular functions, underscoring the pathway's central significance in cellular processes of utmost importance [66, 67]. Canonical wnt pathway is most often discussed because of its direct correlation to cancers particularly colorectal cancers [68]. In the cellular milieu devoid of Wnt stimulation, an intricate assemblage known as the β-catenin destruction box/complex operates, comprising essential proteins such as adenomatosis polyposis coli (APC), casein kinase 1-α (CKI-α), glycogen synthase kinase 3 (GSK-3β), and Axin2 [69]. The primary purpose of this sophisticated machinery is to facilitate the targeted degradation of β-catenin, a pivotal signaling protein endowed with the ability to translocate into the cell nucleus, where it exerts its role as a transcription factor, thereby modulating gene expression and orchestrating critical cellular processes. In the context of Wnt binding to its receptors Fz/LRP5/6, an intricate canonical signaling pathway is triggered, leading to the disruption of the destruction complex responsible for regulating β-catenin. Notably, in colorectal cancer (CRC), an array of proteins, including APC, GSK3-β, and axin2, exhibit elevated expression levels within tumour cells compared to their non-cancerous counterparts [70-74].

Numerous studies have corroborated the presence of mutations in APC, which consequently engender relentless activation of the Wnt/β-catenin pathway [75, 76]. Moreover, within normal cellular contexts, GSK-3β exhibits divergent functions. On one hand, it plays a crucial role in constraining the activity of β-catenin by facilitating its phosphorylation, leading to subsequent degradation. On the other hand, it contributes to cell survival and proliferation by participating in the NF-kβ pathway. Notably, akin to other malfunctioning proteins within the destruction complex, GSK-3β mutations have been identified, resulting in elevated expression levels in numerous colorectal cancers [77-79]. Despite the downregulation of axin2 expression in the cytoplasm through dephosphorylation caused by Wnt stimulation, untreated cells still showed higher levels of axin2 compared to cells treated with ellagic acid (**Figure 6.13A & B**). This discrepancy may be attributed to known mutations present in the axin2 protein [80-82]. Furthermore, ellagic acid treatment consistently resulted in the reduction of axin2 expression at both 24 and 48 hours after treatment. Upon treatment with ellagic acid, there was a down regulation of GSK-3β, and β-catenin after 24 and 48 hours of treatment (**Figure 6.13A & B(ii-iii)**). The application of ellagic acid treatment resulted in a reduction of β-catenin expression levels, which subsequently exerted an influence on its downstream effector, LEF-1. Concomitantly, LEF-1 also underwent downregulation in response to ellagic acid treatment (**Figure 6.13A & B(iv)**). It is noteworthy that the cytosolic accumulation of β-catenin is recognized for its propensity to translocate to the nucleus, where it forms complexes with the LEF-TCF co-transcription factors to regulate gene expression [83]. The transcription factor LEF1 plays a pivotal role in the process of epithelial-mesenchymal transition (EMT) by promoting the transcription of critical EMT effectors, including N-Cadherin, vimentin, and snail+slug [84]. The effectors snail and slug are responsible for suppressing genes that encode proteins like E-cadherin, claudins, and occludin, which are crucial for maintaining the epithelial characteristics of cells [85]. Interestingly, our studies have demonstrated that ellagic acid, exerts a potent inhibitory effect on the Wnt/β-catenin signaling pathway, leading to a reduction in β-catenin expression and its subsequent inability to translocate into the nucleus to facilitate the TCF/LEF complex's action. Remarkably, even at lower concentrations, ellagic acid has been found to down-regulate LEF-1 expression. Consequently, this down-regulation of LEF-1 has been shown to result in a significant decrease in the expression of EMT markers, such as N-cadherin and snail+slug, thereby suggesting the potential of ellagic acid as a promising therapeutic candidate in preventing EMT-associated processes (**Figure 6.13A & B(v-vi)**).

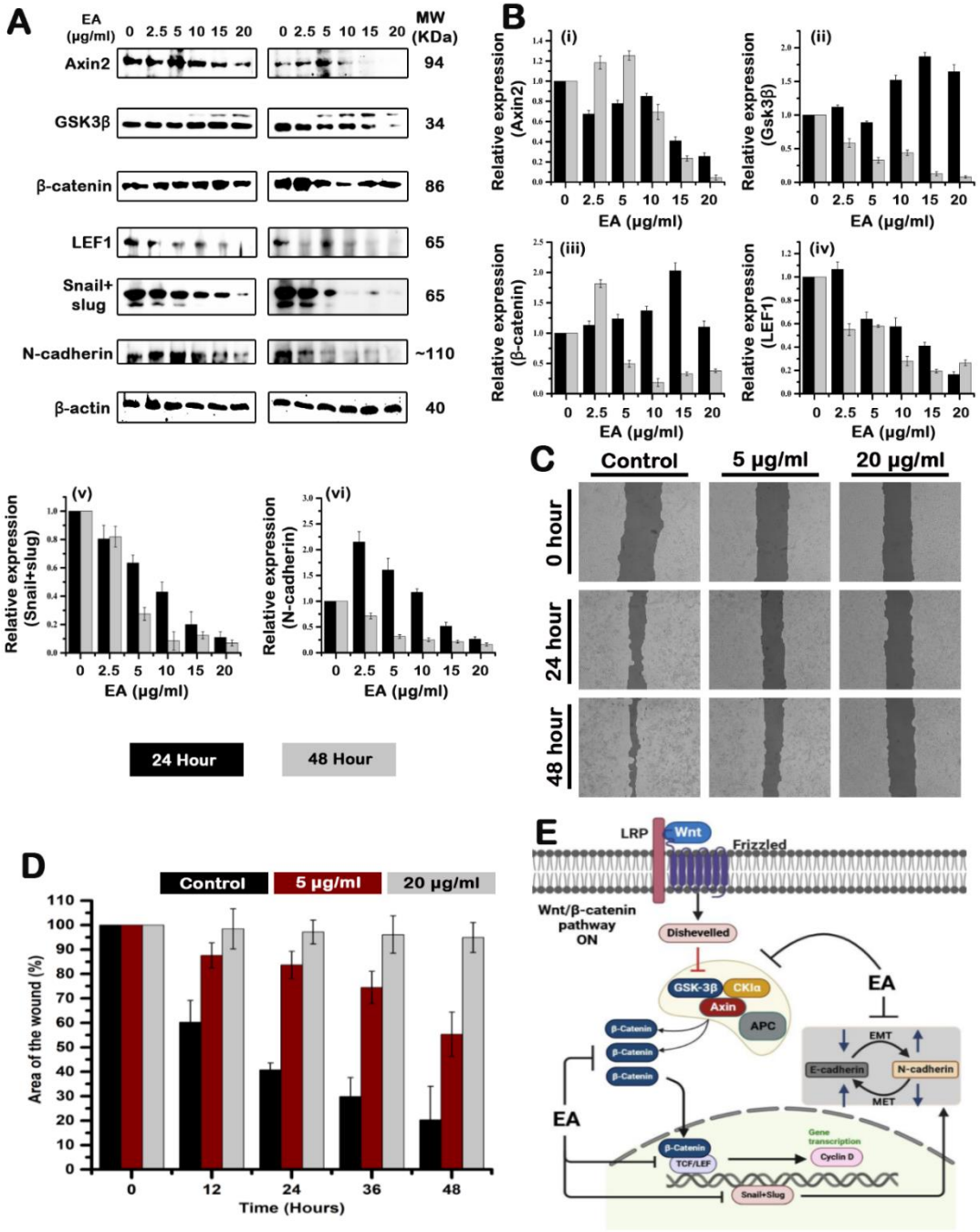

Figure 6.13: Ellagic acid blocks epithelial to mesenchymal transition (EMT) and inhibits wnt/β-catenin pathway in colorectal cancer cells: (A) DLD1 cells were treated with various concentrations (2.5, 5, 10, 15, 20 µg/ml) of ellagic acid for 24 and 48 hours. Western blotting was performed after harvesting the proteins using RIPA lysis buffer. Western blot images of several proteins of wnt/β-catenin pathway and EMT (Epithelial to Mesenchymal Transition) are shown. **(B (i-viii))** Relative expression levels of several proteins of wnt/β-catenin pathway and EMT (Epithelial to Mesenchymal Transition) are shown. **(C)** Ellagic acid halts the migration of DLD1 cells**.** The cells were treated with different concentrations (5, 20 µg/ml) in serum free media and images were taken using the Cytell cell imaging technology at 0, 12, 24, 36 and 48 hours. Representative images of the change in wound area in control and GA treated samples are shown. **(D)** Graph representing the change in area of the wound in control and ellagic acid treated cells is displayed.

Further, the results obtained from western blot analysis pertaining to markers of EMT were confirmed using cell migration assay. The cell migration ability of DLD1 was assessed in the presence of varying concentrations (5 µg/ml and 20 µg/ml) of ellagic acid over a 48-hour period. Regular readings were taken at 12-hour intervals, revealing a decrease in wound area that occurred in a time- and dose-dependent manner (**Figure 6.13C & D**). An abridged synopsis of the impact exerted by ellagic acid on the suppression of the Wnt/β-catenin and epithelial-to-mesenchymal transition (EMT) signaling pathways has been presented (**Figure 6.13E**).

6.3.10 Ellagic acid induces autophagic dysregulation in colorectal cancer cells: Macro autophagy or autophagy is the mechanism by which a cell eats itself in order to degrade and recycle the soluble, aggregated, & damaged proteins, organelles, macromolecular complexes (that are not required by the cell anymore) and foreign bodies. The development of autophagosomes in autophagy, regulated by Atg (autophagy related genes) proteins, aids in the engulfment of cytoplasmic components (damages organelles and proteins) and is then transferred to the lysosome for disintegration after the formation of autophagolysosome. Under normal physiological conditions, autophagy helps the cells to maintain homeostasis and provide an extra source of energy whenever required by the cell [86]. It is well understood that the tumour cells have an increased appetite for the production of energy to meet their demands of uninterrupted proliferation, which is primarily achieved by metabolism. The cells which are in advanced tumour stages tends to undergo autophagy in order to promote tumourigenesis as they are under metabolic stress [87]. Also, the cells can bypass the mechanism of stress developed because of use of chemotherapeutic drugs by up regulation of autophagy [88]. Under non-stress conditions, the level of autophagy is very basal. The autophagy in normal cells mainly starts when the signals of amino acid starvation are rung or when the cells are undergoing stress because of food shortage. The autophagic pathway starts at the birth of the phagophore and ends at death the autophagosomes when it is fused with lysosome. The formation of autophagosomes is overlooked by a group of proteins known as Atg proteins [89]. Some core Atg proteins which helps in the successful formation of autophagosomes includes Atg3, Atg5, Atg7, Atg9 Atg12, and Atg16. Atg9 helps in initiating the phagophore by marking Endoplasmic reticulum for the translocation of the ULK complex at a discrete location. The formation of a phagophore facilitates the recruitment of other Atg related proteins such as E3-complex of Atg5, Atg12 & Atg16L1. The recruitment of E3 complex is done by WIPI2B [90]. Beclin-1 which is a homolog of yeast Atg6 in mammalian cells is the first identified

mammalian autophagy gene and is responsible for the initiation of autophagy. Beclin-1 is also involved with the regulation of apoptosis and is related protein Bcl-2 that acts as a toggling switch between apoptosis and autophagy [91]. The cytosolic LC3 (LC3-I) is conjugated to phosphatidylethanolamine (PE) which requires Atg3 & Atg7 that helps in the membrane elongation and expansion of the forming autophagosomes. The LC3 now bound to PE is known as membrane bound LC3 (LC3-II) [90, 92, 93].

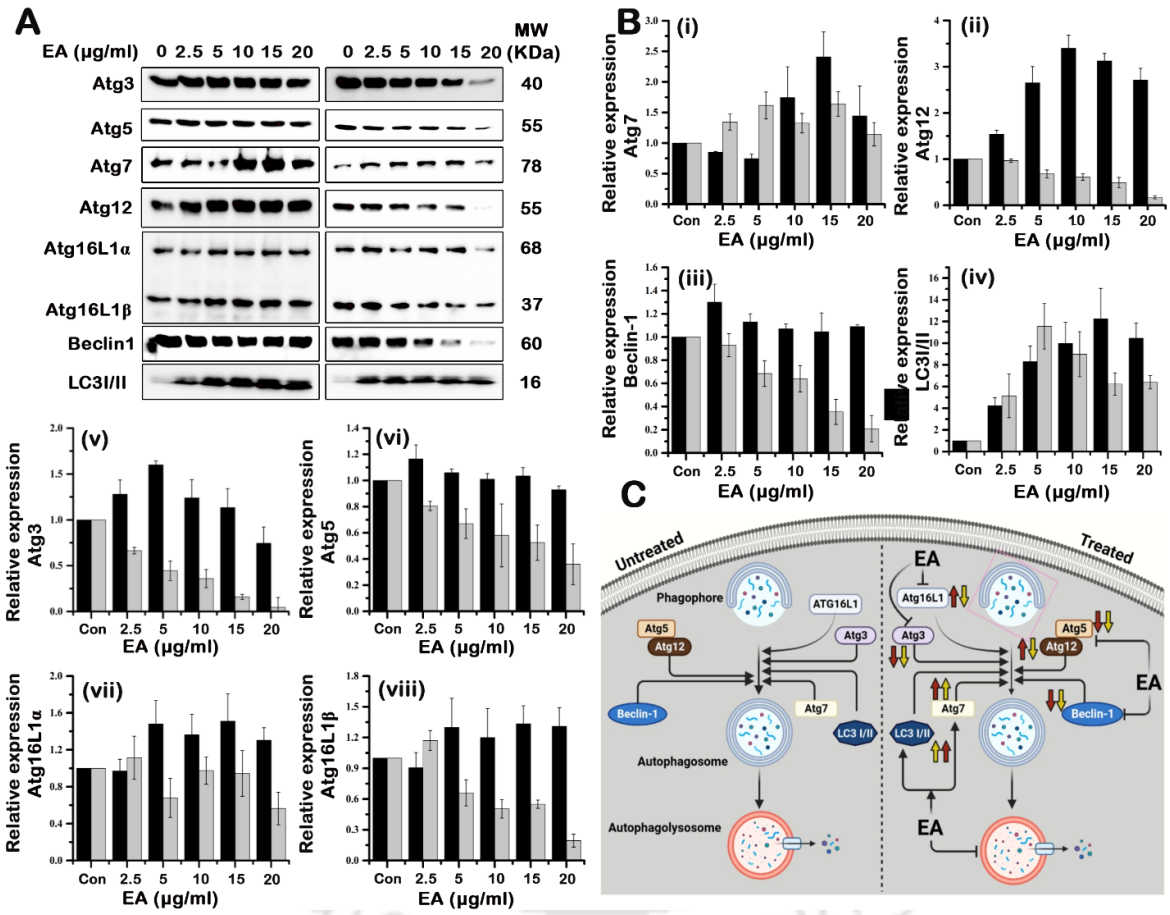

Figure 6.14: Ellagic acid induces autophagic dysregulation in colorectal cancer cells. (A) DLD1 cells were treated with various concentrations (2.5, 5, 10, 15, 20 µg/ml) of ellagic acid for 24 and 48 hours. Western blotting was performed after harvesting the proteins using RIPA lysis buffer. Western blot images of several proteins of autophagy pathway are shown. **(B (i-viii))** Relative expression levels of several proteins' autophagy pathway is shown. (C) Graphical representation of effect of ellagic acid on autophagic dysregulation in CRCs.

Autophagy is context dependent. In malignant cancers, autophagy is active and fulfils the requirement of cells metabolic and energy requirements, while in normal tissues autophagy takes place at a basal level until there is a requirement because of amino acid starvation [94]. Autophagy and its related genes are controversially reported and hence less understood in

CRCs [86, 95, 96]. Regardless, there are numerous studies in which Beclin-1 is overexpressed and helps in tumourigenesis of cancer cells. In our study, DLD1 cells treated with ellagic acid down regulated Beclin-1 at higher concentrations after 48 hours of treatment whereas there were no changes in 24h which was confirmed through western blot analysis (**Figure 6.14A & B**). Along with Beclin-1 we also examined, the autophagy related proteins Atg5, Atg12 and Atg16L1 which forms the E3 complex. There were no significant changes in their expression levels of Atg5 and Atg16L1 but an increase in expression levels of Atg12 after 24 hours of treatment (**Figure 6.14A & B**). Along with Atg12, there was an increase in expression levels of Atg7 and LC3I/II after 24 hours of treatment, indicating an attempt to induce autophagy in response to the stress created by ellagic acid treatment. A brief representation of autophagic dysregulation in CRCs upon ellagic acid treatment is shown (**Figure 6.14C**). All the Atg related proteins were shown to be down-regulated after 48 hours of treatment except LC3I/II. The expression levels of Beclin-1 were analogous with that of E3 complex in both the timelines of treatment at varying concentrations suggesting that the initiation of autophagosomes were inhibited upon treatment with ellagic acid.

6.3.11 Gallic acid is the most effective ingredient from Amalaki Churna: Secondary metabolite bearing a common aromatic ring with one or multiple hydroxyl groups (phenolics) are known to exert anti-cancer activities [97]. The anti-carcinogenic effect of polyphenols is mainly due to its ability to halt cell cycle progression, inhibit crucial pathways that control cell proliferation, metastasis, cell migration, angiogenesis, apoptosis and modulate ROS levels [97, 98]. As demonstrated earlier, Amalaki Churna predominantly contains polyphenols. Many of its crude extracts and their active ingredients have been demonstrated to have anti-cancer effect, both synergistically and individually. More often, it is the presence of a specific bioactive agent that is responsible for the action of the crude extract. With this hindsight, we implemented a deductive approach to elucidate the most important polyphenol which if removed from AMCAE will have a substantial impact on the anti-cancer potential of the crude extract. In order to do so, various phytochemical mixes were created using the compositional make-up of 8 polyphenols derived from the gradient HPLC chromatogram (**Figure 6.15A**). The Complete Mixture (CM: mixture of all 8 identified compounds) did not show much variation in its anti-cancer activity (69.85 ± 6.4 µg/ml) when compared to anti-cancer activity of AMCAE (74.05± 6.5 µg/ml).

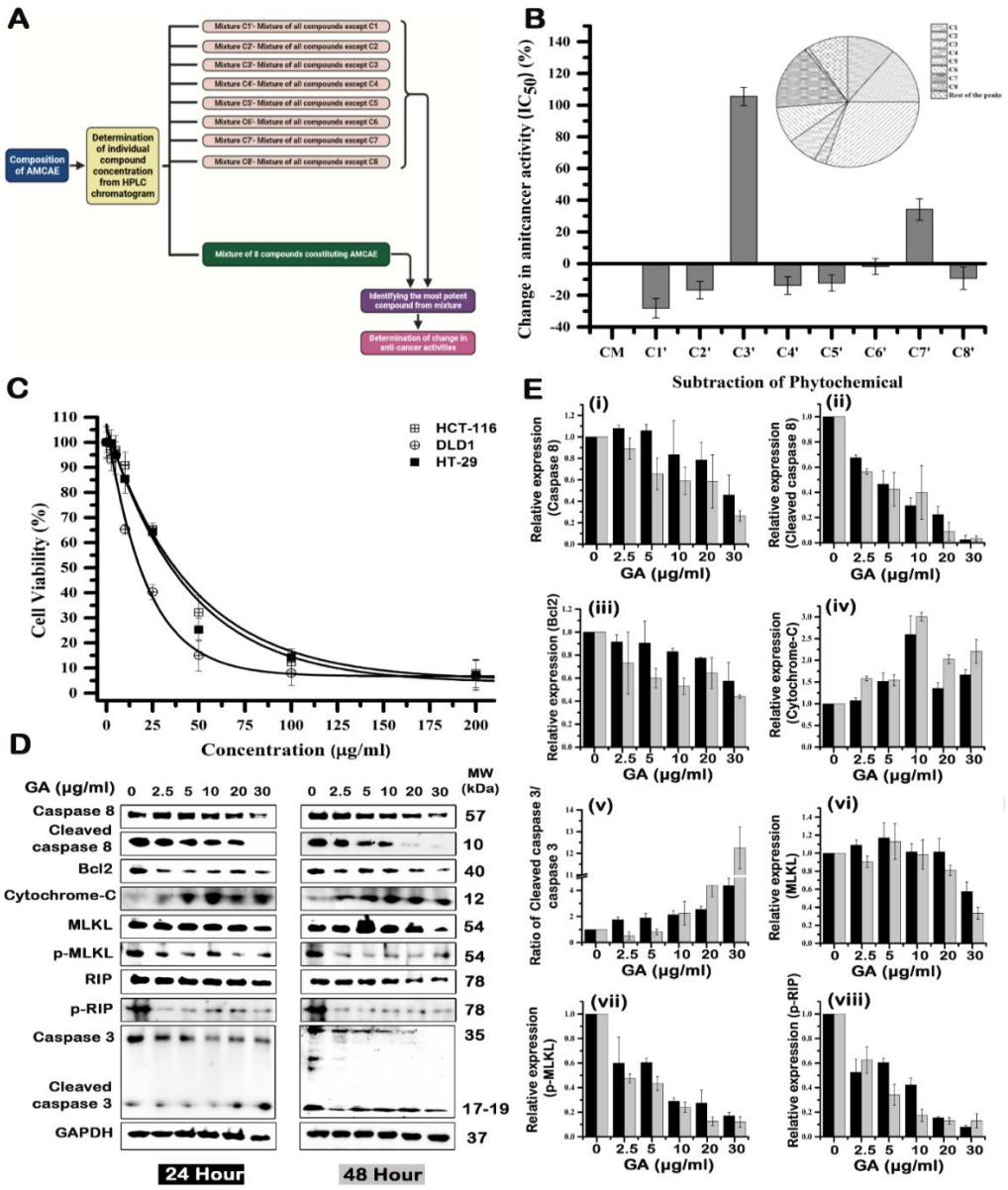

Figure 6.15: Gallic acid is the most active ingredient for anti-cancer activity of AMCAE that induces intrinsic pathway of apoptosis in colorectal cancer cells. (A) Schematic of the procedure followed to find out the most potent compound from AMCAE **(B)** The variation in anti-cancer activity after removal of compounds from AMCAE. The term "CM" stands for the complete mixture, which is made up of 8 identified compounds and is created in accordance with the composition of the gradient HPLC chromatogram. (**Note**: C1′-Mixture except mucic acid 2-*O*-gallate, C2′-Mixture except β-glucogallin, C3′-Mixture-except gallic acid, C4′-Mixture except 5-hydroxymethylfurfural, C5′-Mixture except macabarterin, C6′-Mixture-except corilagin, C7′-Mixture except ellagic acid, C8′-Mixture except transcinnamic acid). **(C)** Colorectal Cancer cells (HCT-116) were treated with different concentration of gallic acid (0-200 µg/ml) and the cell viability was measured by MTT assay. **(D)** HCT-116 cells were treated with various concentrations (2.5, 5, 10, 20, 30 µg/ml) of gallic acid for 24 and 48 hours. Western blotting was performed after harvesting the proteins using RIPA lysis buffer. Western blot images of several proteins related to apoptosis, and necroptosis are shown. **(E (i-viii))** Relative expression levels of proteins related to apoptosis, and necroptosis are represented.

Additionally, the cellular viability (IC_{50} values) of various combinations (C1′-C8′) against the colorectal cancer cell line HCT-116 showed that obliterating specific polyphenols from the CM was more significant than others in terms of their anti-cancer activity. For example, C1', C2', C4', C5' C6' and C8' (which correspond to removal of mucic acid 2-*O*-gallate, β-glucogallin, 5 hydroxymethyfurfural, macabarterin, corilagin and trans-cinnamic acid respectively) observed a decrease in IC_{50} values in the range of 1.7% to 28.1% that correlates to the gain of anti-cancer activity of AMCAE (**Figure 6.15B**). Often times, this decrease in anti-cancer activity may be attributed to their antagonistic action. In contrast, C3′ and C7′, which stand for the removal of gallic acid and ellagic acid respectively, ascertained an increase in the IC_{50} values, indicating a loss of AMCAE's anti-cancer activity. Removal of gallic acid and ellagic acid yielded the IC_{50}s of C3′ and C7′ to be 143 ± 6.8 µg/ml and 93.8 ± 5.5 µg/ml respectively, thus making gallic acid the most crucial polyphenol in the compositional make up of aqueous extract of Amalaki Churna.

6.3.12 Gallic acid induces intrinsic pathway of apoptosis in colorectal cancer cells: Gallic acid was found to exert anti-cancer activity in a dose dependent manner on colorectal cancer cell lines HCT-116, DLD1 & HT-29 with IC_{50}s of 29.4 ± 4.7µg/ml, 18.78 ± 5.9 µg/ml, 37.13 ± 5.3µg/ml respectively (**Figure 6.15C)**. Although, different types of regulated cell death (RCD) are known to exist according to the Nomenclature committee on cell death (NCCD) [99], induction of either extrinsic or intrinsic apoptosis is the primary phenomenon observed when cancer cells are subjected to chemotherapeutic treatments [100]. Apoptotic signaling can induce cell death in cells either by extrinsic or intrinsic pathway. Increased cellular stress, oxidative stress, changes in inner mitochondrial membrane permeability, loss of mitochondrial membrane potential and release of pro-apoptotic proteins such as cytochrome-c, Smac/DIABLO which activate the caspase dependent mitochondrial pathway forming an apoptosome refers to the intrinsic pathway or mitochondrial-mediated pathway [101, 102]. The overexpression of pro-apoptotic proteins and concurrent reduction in anti-apoptotic proteins like Bcl2 can occur in cells that have experienced DNA damage, fragmentation, or ROS induction [41]. Because of the cellular stress caused by GA treatment, the anti-apoptotic protein Bcl2 was shown to be reduced in a dose-dependent way. Further, release of cytochrome-c was observed in cells treated with GA for 24 and 48-hours (**Figure 6.15D & E**). Immunoblotting of caspase 3 and its cleaved form obtained from HCT-116 cells demonstrated enhanced expression of cleaved caspase 3 (17-19 kDa) in a dose dependent manner. Increased

cytochrome-c and cleaved caspase 3 expression in conjunction with non-activated caspase 8 shows that GA causes cancer cell death via the mitochondrial apoptotic pathway.

Furthermore, there was no over-expression of cleaved caspase-8 and caspase-8 hinting towards the possibility that there is no involvement of extrinsic pathway of apoptosis involved hours (**Figure 6.15D & E**). After checking, the expression levels of various apoptotic proteins, we examined the expression levels of necroptotic related proteins such as RIP, p-RIP, MLKL, and p-MLKL. Upon treatment with GA for 24h, we found that GA treatment of HCT-116 cells down-regulated expression levels of RIP, MLKL and their phosphorylated forms suggesting that the cell death is not because of necroptosis (**Figure 6.15D & E**). Apoptosis is activated in order to remove no longer wanted cells or targeted cells. Cellular shrinkage, chromatin condensation, DNA laddering (fragmentation) are some of the hallmarks of apoptosis [103, 104]. Upon treatment with GA for 24-hours, the cells (HCT-116, DLD1 and HT-29) showed DNA laddering, whereas the untreated cells did not show any laddering of the isolated genomic DNA (**Figure 6.16A**). The DNA laddering in treated cells indicate apoptosis taking place in cancer cells. Further, the flow cytometry analysis of GA treated cells have shown an increase in the late apoptotic and necrotic stages as shown in the quadrant analysis (**Figure 6.16B**). The late apoptotic and necrotic cells were found to be in the range of 20-37% and 11-17% in treated cells respectively in contrast to the untreated ones whose late apoptotic and necrotic cells were in minimal populations. In untreated cells, healthy cells were confined to first quadrant indicating only the live cells. Apoptosis was confirmed by dually staining of cells with Acridine orange (AO) and Propidium iodide (PI) (**Figure 6.16C**). The fluorescence imaging of the dually stained cells also confirmed the flow cytometry analysis.

The most frequently used non-invasive therapy, chemotherapy principally targets the cells by setting off apoptosis (either internal or external) [43]. The extrinsic pathway of apoptosis is induced by TNF super family members such as TNFR1, TNFR2, Fas, DR3 (TNFRSF25), DR4 (Apo2/TRAIL-R1), DR5 (TRAIL-R2), and DR6 (TNFRSF21), on the cell surface followed by formation of DISC complex comprising of death domains and caspase 8 [105]. Expression levels of several members TNF superfamily were investigated by immunoblotting after treating HCT-116 cells with GA in a dose dependent manner (**Figure 6.16D**). GA was found to down-regulate TNFR1 and Fas receptors, the two most common receptors which are extensively responsible for inducing extrinsic pathway of apoptosis (**Figure 6.16E(i-ii)**).

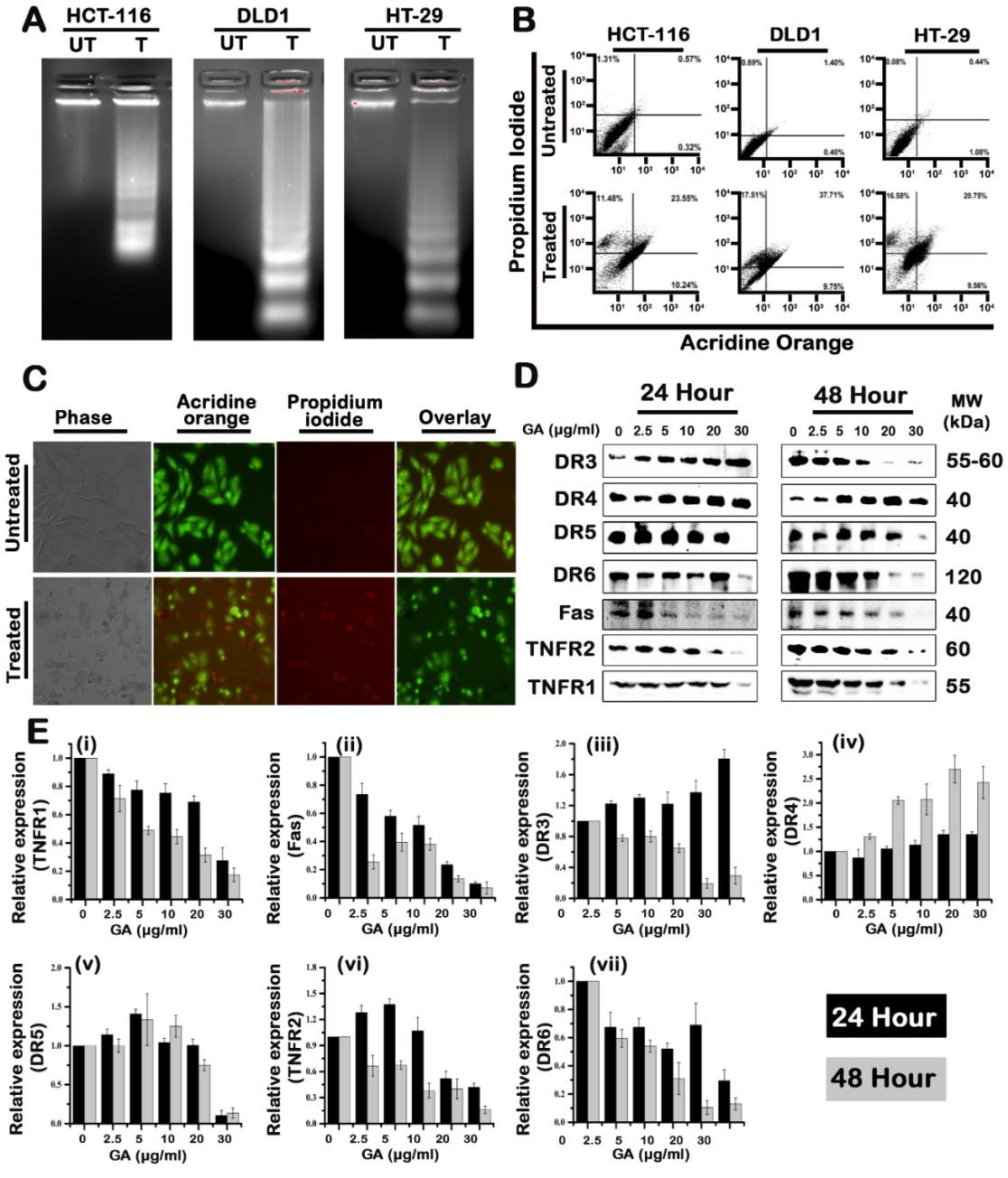

Figure 6.16: Gallic acid from AMCAE triggers intrinsic apoptosis in colorectal cancer cells, not the extrinsic pathway. (A) Gallic fragments DNA in colorectal cancer cells**.** Treatment with gallic acid of HCT-116, DLD1 and HT-29 cells caused DNA to be fragmented, whereas there is no fragmentation of genomic DNA seen in untreated cells. **(B & C)** Induction of apoptosis in colorectal cancer cells by gallic acid. HCT-116, DLD1 and HT-29 cells were dually stained with acridine orange and propidium iodide for evaluating the makeup of healthy, early apoptotic, late apoptotic and necrotic cells after treatment with gallic acid at their respective IC_{50} concentrations for 48 hours. **(D)** Gallic acid downregulates death receptors. HCT-116 cells were treated with various concentrations (2.5, 5, 10, 20, 30 µg/ml) of gallic acid for 24 and 48 hours. Western blotting was performed after harvesting the proteins using RIPA lysis buffer. Western blot images of several proteins related to death receptors are shown. **(E(i-vii))** Relative expression levels of proteins related to death receptors are represented.

Apart from TNFR1 and Fas receptors that trigger extrinsic pathway, other receptors of the TNF super family such as DR3, DR4/5 (Apo2/TRAILR1 and TRAILR2) and DR6 are known to induce apoptosis. The activation of DR3 is linked with rapid onset of apoptosis which is stimulated by its ligand APO3L/TWEAK. There are several chemotherapeutic drugs available that induces apoptosis through APO3L mediated activation of DR3 such as taxol and vinblastine [53]. After 24-hours of GA treatment, there was increase in expression levels of DR3. Although increased expression of death receptors is related with caspase 8 activation, no enhanced expression of caspase 8 and cleaved caspase 8 was detected. Furthermore, there was a reversal in DR3 expression levels after 48-hours of treatment, with DR3 decreasing in a dose dependent manner. TRAIL induced apoptosis through DR4 and DR5 death receptors are targets of many new chemotherapeutic drugs [106]. DR4 was seen to be elevated in both 24 and 48-hours of treatment where as DR5 is mildly up-regulated at lower concentrations.

Because there was no caspase 8 activation after GA treatment, there was no DR4/DR5 mediated apoptosis. All the TNF superfamily members except TNFR2 is associated with death domain. TNFR2 which is overexpressed in several cancers (breast cancer, cervical cancer, renal cancer and colorectal cancer) is mainly involved in activating cell survival pathways such as PI3K-Akt and NF-κB via cIAP1/2 [107]. Similar to TNFR1, TNFR2 was also observed to be down-regulated upon GA treatment. The proteolytic cleavage of caspase-3 from its precursor form, triggered by the up-regulation of cytochrome-c and concurrent down-regulation of cleaved caspase-8 and various death receptors, along with the down-regulation of necroptotic proteins like MLKL and RIP, and their non-phosphorylation following GA treatment, collectively point toward the activation of the intrinsic or mitochondrial pathway of apoptosis

6.3.13 Gallic acid halts the cell cycle machinery in S-phase: Changes in the cell cycle machinery that throw off the balance of populations in distinct cell cycle stages, such as G1, S, and G2/M, are one effect of responding to pro-survival phenomena [39]. After labelling the cells with propidium iodide, the impact of GA on cell cycle progression in colorectal cancer cell lines was evaluated by flow cytometry. Upon treatment of HCT-116 cells with GA for 24-hours, the percentage of population in S-phase changed from 19.02 ± 2.9 % to 33.3 ± 4.2%, whereas it changed from 23.5 ± 3.1% to 38.14 ± 3.5% after 48-hours of treatment. The histograms developed in FCS-5 express software after analysis are demonstrated (**Figure 6.17A**). Cyclin A2 that is responsible for driving the fate of the cell from S-phase to G2 phase was also found to be down-regulated in a dose dependent manner (**Figure 6.17B & C**). Apart from halting cell in S-phase, GA also inhibited the progression of G2 cells to G1 phase.

Treatment with increasing doses of GA resulted in an increase in the number of G2 phased cells after 24 and 48 hours. Upon treatment of HCT-116 cells with GA for 24-hours, the percentage of population in G2-phase changed from 17.9 ± 3.6 % to 33.2 ± 2.2%, whereas it changed from 21 ± 2.1% to 31.7 ± 4.5% after 48-hours of treatment.

6.3.14 Gallic acid down-regulates wnt/β-catenin pathway in colorectal cancer cells: Wnt/β-catenin pathway is one the basic mechanism in cells that can regulate cell polarity, cell differentiation, cell fate during embryonic development, maintaining cellular homeostasis etc. This pathway is activated by binding of wnt to Fz or LRP4/6 receptors present on the cell surface [108]. Aberrant activation of wnt signaling pathway is a characteristic trait of colorectal cancers [109].

In CRC, a number of proteins such as APC, GSK-3β, and axin-2 are found to be in higher levels in tumour cells that in their normal counter parts. Several studies have reported mutations in APC that leads to continuous activation wnt/β-catenin pathway [75, 76]. GSK-3β in normal cells have opposing roles, one is to contain the β-catenin by phosphorylating into destruction and the other is cell survival and proliferation in NF-kβ pathway. GSK-3β is found to be mutated and its elevated levels are found in many colorectal cancers [79].

GSK-3β was found to be lowered in HCT-116 cells upon treatment with GA at higher concentrations but remained steady at lower concentrations (**Figure 6.17B**). Although the wnt stimulation alters down the expression levels of axin-2 in cytoplasm by de-phosphorylating it, we have still seen over expressed axin-2 in the untreated cells. Axin-2, which is intended to function as a negative regulator of canonical wnt signaling, can promote cancer growth as a result of mutations found in the axin-2 protein in HCT-116 cells [80, 82]. Upon treatment with GA, there was a down-regulation of axin-2 and β-catenin in both 24-hour and 48-hour treatment (**Figure 6.17B & C**). Lowered expression levels of β-catenin upon GA treatment, was also found to have an effect on its downstream target LEF-1. LEF-1 was down-regulated as well upon GA treatment. The accumulated β-catenin in the cytosol is known to translocate to the nucleus to bind the LEF-TCF co-transcription factors [108]. Because β-catenin is no longer accessible to attach to the TCF/LEF complex, the expression of its target proteins, such as cyclin-D1 was found to be decreased. After 24 and 48-hour treatments, it was shown that GA treatment reduced cyclin-D1 expression in a dose-dependent way, which is known to be up-regulated in a variety of cancers and occurs in at least one-third of colorectal malignancies [110].

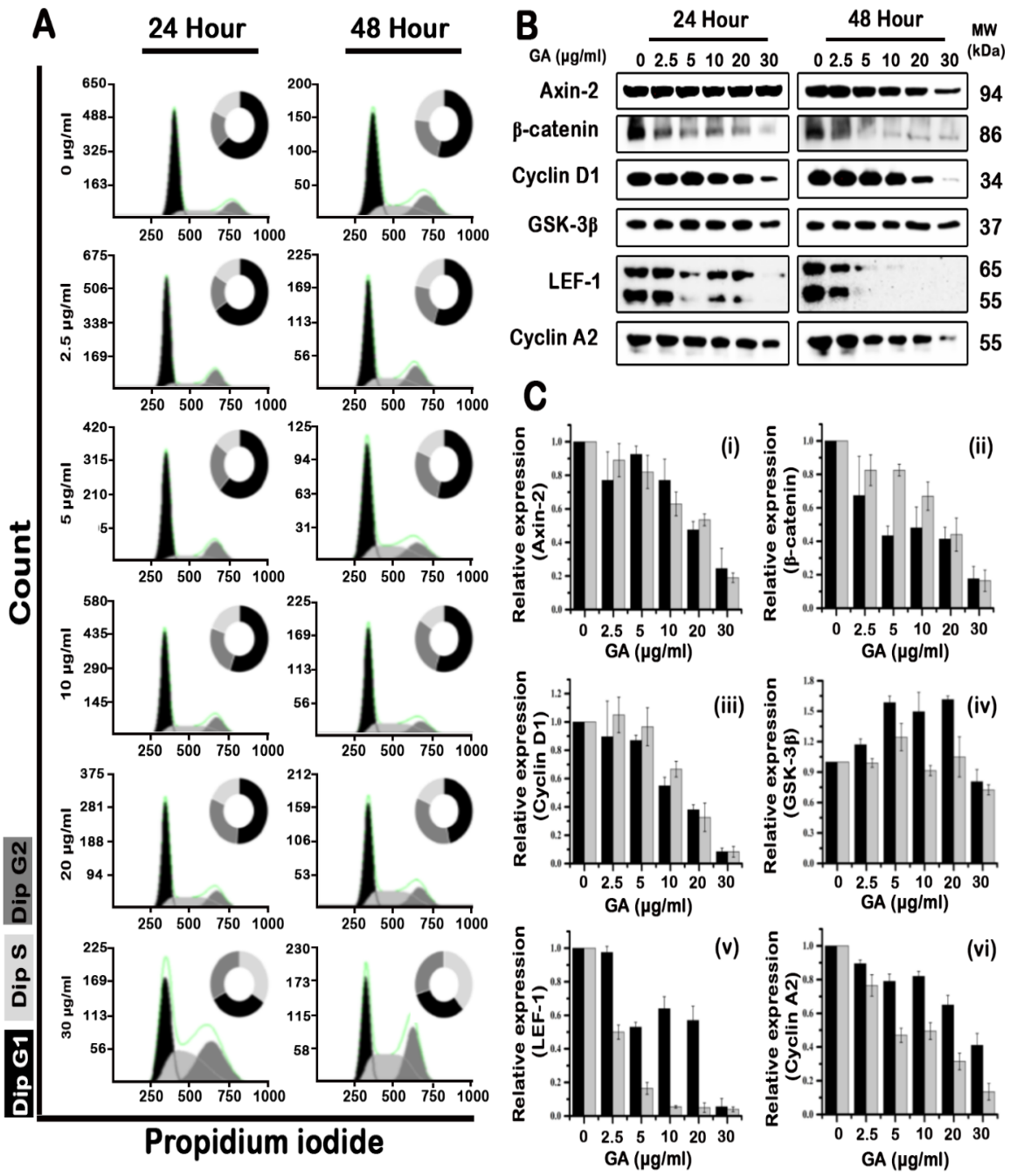

Figure 6.17: Gallic acid isolated from AMCAE arrests cell cycle progression and inhibits wnt/β-catenin pathway: (A) Gallic acid arrests cell cycle progression at S-phase. Gallic acid unsettles cell cycle machinery. HCT-116 was treated at different concentrations (2.5, 5, 10, 20, 30 µg/ml). Cell cycle phases were recorded on BD Biosciences FACS-Calibur to observe changes in the cell cycle phase make up in the untreated and treated cells stained with propidium iodide. The resultant histograms were plotted using FCS-5 express software. **(B)** Gallic acid inhibits wnt/β-catenin pathway**.** HCT-116 cells were treated with various concentrations (2.5, 5, 10, 20, 30 µg/ml) of gallic acid for 24 and 48 hours. Western blotting was performed after harvesting the proteins using RIPA lysis buffer. Western blot images of several proteins related to wnt/β-catenin pathway is shown. **(C(i-vi))** Relative expression levels of proteins related wnt/β-catenin pathway is shown.

6.3.15 Gallic acid suppresses the migration of colorectal cancer cells: Using cell migration assay, the cell migratory ability of HCT-116 cells was put to test against GA at concentrations of 10 µg/ml and 25 µg/ml. The wound area measured at different time intervals (0,12, 24, 36, and 48 hours) shows a reduction in wound area in control cells but not in GA treated cells (**Figure 6.18A**). Although the wound area in control cells was almost closed after 48 hours, the wound area in treated cells showed minimal reduction (**Figure 6.18B**). The results obtained from cell migration assay were further with immunoblotting of several proteins such as cadherins, vimentin and snail/slug. LEF1 plays an important role in epithelial-mesenchymal transition (EMT) by promoting the transcription of key EMT effectors such as N-Cadherin, vimentin, and snail+slug [84]. Snail and slug are the transcription factor that binds to the regulatory regions and repress genes expressing proteins such as E-cadherin, claudins, occluding etc., that maintain the epithelial nature of the cell [85]. As mentioned above, GA successfully inhibits wnt/β-catenin pathway, thereby lowering β-catenin expression and unable to translocate to nucleus to aid TCF/LEF complex. Consequently, GA was also found to down-regulate the LEF-1 expression even at lower concentrations (**Figure 6.17B & C**). The down-regulation of LEF-1 resulted in the decreased expression of EMT markers such as N-cadherin, snail+slug and vimentin. The lack of snail+slug aided in keeping E-cadherin levels stable after 24 hours of treatment, with a modest rise after 48 hours.

6.3.16 Gallic acid induces autophagic dysregulation in colorectal cancer cells: The degradation of the unwanted encapsulated cytoplasmic material via the formation of autophagolysosomal system is often referred as autophagy. Under normal physiological conditions, autophagy helps the cells to maintain homeostasis and provide an extra source of energy whenever required by the cell [111]. Some core Atg (Autophagy related genes) proteins which helps in the successful formation of autophagosomes includes Atg3, Atg5, Atg7, Atg9, Atg12, Atg16, beclin-1 and LC3-I/II. Autophagy is context dependent. While autophagy occurs at a baseline level in healthy tissues until it becomes necessary due to amino acid shortage, it is active and meets the metabolic and energy needs of cells in malignant cancers [112]. Autophagy and its related genes are controversially reported and hence less understood in CRCs [113]. Regardless, there are numerous studies in which Beclin-1 is overexpressed and helps in tumourigenesis of cancer cells [114, 115]. The expression levels of Atg3, Atg5, Atg12, Atg16, beclin-1 and LC3-I/II remain unaltered in HCT-116 cells after 24 hours of GA treatment (**Figure 6.18C & D**).

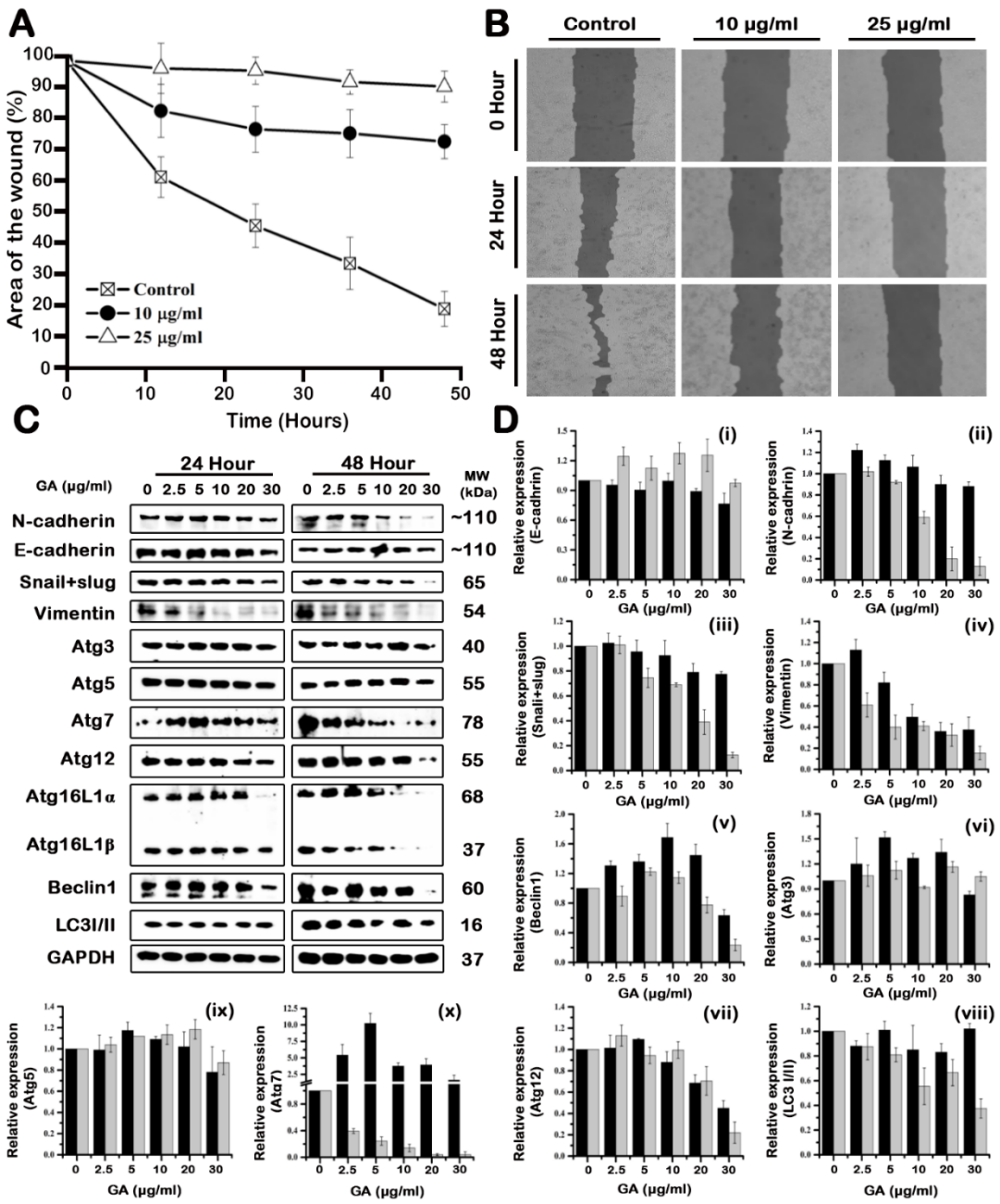

Figure 6.18: Gallic acid isolated from AMCAE blocks epithelial to mesenchymal transition (EMT) and induces autophagic dysregulation in colorectal cancer cells. (A) Gallic acid halts the migration of HCT-116 cells**.** The cells were treated with different concentrations (10, 25 µg/ml) in serum free media and images were taken using the Cytell cell imaging technology at 0, 12, 24, 36 and 48 hours. Graph representing the change in area of the wound in control and GA treated cells is displayed. **(B)** Representative images of the change in wound area in control and GA treated samples are shown. **(C)** Gallic acid block EMT and induces autophagic dysregulation in HCT-116 cells. HCT-116 cells were treated with various concentrations (2.5, 5, 10, 20, 30 µg/ml) of gallic acid for 24 and 48 hours. Western blotting was performed after harvesting the proteins using RIPA lysis buffer. Western blot images of several proteins of EMT (Epithelial to Mesenchymal Transition) and autophagy pathway are shown. **(D(i-x))** Relative expression levels of several proteins of EMT and autophagy pathway are displayed.

Because cells have been shown to circumvent the stress response brought on by the use of chemotherapeutic agents by upregulating autophagy, it is possible that Atg proteins continuously maintain the endolysosomal system even after GA treatment. Additionally, after 24-hour treatment with GA, Atg7 was observed to show a tenfold increase in comparison to untreated cells. This might be due to Atg7's diverse involvement in controlling phagophore production in autophagy, as well as its ability to trigger cell cycle arrest and induce apoptosis via the tumour suppressor gene P53 [116]. Further, following 48 hours of treatment with GA, down-regulation of all Atg-related proteins, beclin-1, and LC3-I/II was seen, demonstrating that GA is suppressing the energy bypass mechanism provided by the autophagic process in HCT-116 cells.

6.4 References

1. Bafna, P. and R. Balaraman, *Anti-ulcer and anti-oxidant activity of pepticare, a herbomineral formulation.* Phytomedicine, 2005. **12**(4): p. 264-270.
2. Bandyopadhyay, S.K., S.C. Pakrashi, and A. Pakrashi, *The role of antioxidant activity of Phyllanthus emblica fruits on prevention from indomethacin induced gastric ulcer.* Journal of Ethnopharmacology, 2000. **70**(2): p. 171-176.
3. Sairam, K., et al., *Antiulcerogenic effect of methanolic extract of Emblica officinalis: an experimental study.* Journal of Ethnopharmacology, 2002. **82**(1): p. 1-9.
4. Khan, K.H., *Roles of Emblica officinalis in medicine-A review.* Bot Res Int, 2009. **2**(4): p. 218-228.
5. Anazetti, M.C., et al., *Comparative cytotoxicity of dimethylamide-crotonin in the promyelocytic leukemia cell line (HL60) and human peripheral blood mononuclear cells.* Toxicology, 2003. **188**(2-3): p. 261-274.
6. Liu, C.-P., et al., *The extracts from Nelumbo nucifera suppress cell cycle progression, cytokine genes expression, and cell proliferation in human peripheral blood mononuclear cells.* Life sciences, 2004. **75**(6): p. 699-716.
7. de Lima, R.M.T., et al., *Antitumoural effects of [6]-gingerol [(S)-5-hydroxy-1-(4-hydroxy-3-methoxyphenyl)-3-decanone] in sarcoma 180 cells through cytogenetic mechanisms.* Biomedicine & Pharmacotherapy, 2020. **126**: p. 110004.
8. Verhoeckx, K., et al., *The impact of food bioactives on health: in vitro and ex vivo models.* 2015.
9. Suganthy, N., S. Muniasamy, and G. Archunan, *Safety assessment of methanolic extract of Terminalia chebula fruit, Terminalia arjuna bark and its bioactive constituent 7-*

methyl gallic acid: In vitro and in vivo studies. Regulatory Toxicology and Pharmacology, 2018. **92**: p. 347-357.

10. Anand, O., et al., *Dissolution testing for generic drugs: an FDA perspective.* The AAPS journal, 2011. **13**(3): p. 328-335.
11. Klein, S., *The use of biorelevant dissolution media to forecast the in vivo performance of a drug.* The AAPS journal, 2010. **12**(3): p. 397-406.
12. Honda, S., et al., *Stability of polyphenols under alkaline conditions and the formation of a xanthine oxidase inhibitor from gallic acid in a solution at pH 7.4.* Food Science and Technology Research, 2019. **25**(1): p. 123-129.
13. You, B.R., et al., *Gallic acid inhibits the growth of HeLa cervical cancer cells via apoptosis and/or necrosis.* Food and Chemical Toxicology, 2010. **48**(5): p. 1334-1340.
14. Bernhaus, A., et al., *Digalloylresveratrol, a new phenolic acid derivative induces apoptosis and cell cycle arrest in human HT-29 colon cancer cells.* Cancer letters, 2009. **274**(2): p. 299-304.
15. Liang, C.-z., et al., *Gallic acid induces the apoptosis of human osteosarcoma cells in vitro and in vivo via the regulation of mitogen-activated protein kinase pathways.* Cancer Biotherapy and Radiopharmaceuticals, 2012. **27**(10): p. 701-710.
16. Shankara, B.R., et al., *Evaluating the anticancer potential of ethanolic gall extract of Terminalia chebula (Gaertn.) Retz.(combretaceae).* Pharmacognosy research, 2016. **8**(3): p. 209.
17. Lee, H.-L., et al., *Gallic acid induces G1 phase arrest and apoptosis of triple-negative breast cancer cell MDA-MB-231 via p38 mitogen-activated protein kinase/p21/p27 axis.* Anti-cancer drugs, 2017. **28**(10): p. 1150-1156.
18. Chaudhuri, D., et al., *Methyl gallate isolated from Spondias pinnata exhibits anticancer activity against human glioblastoma by induction of apoptosis and sustained extracellular signal-regulated kinase 1/2 activation.* Pharmacognosy Magazine, 2015. **11**(42): p. 269.
19. Ahmad, S., et al., *Phytochemicals from Mangifera pajang Kosterm and their biological activities.* BMC complementary and alternative medicine, 2015. **15**(1): p. 1-8.
20. Huang, C.-Y., et al., *Methyl gallate, gallic acid-derived compound, inhibit cell proliferation through increasing ROS production and apoptosis in hepatocellular carcinoma cells.* Plos one, 2021. **16**(3): p. e0248521.
21. Kamatham, S., N. Kumar, and P. Gudipalli, *Isolation and characterization of gallic acid and methyl gallate from the seed coats of Givotia rottleriformis Griff. and their*

anti-proliferative effect on human epidermoid carcinoma A431 cells. Toxicology reports, 2015. **2**: p. 520-529.

22. Afsar, T., et al., *Growth inhibition and apoptosis in cancer cells induced by polyphenolic compounds of Acacia hydaspica: Involvement of multiple signal transduction pathways.* Scientific reports, 2016. **6**(1): p. 1-12.
23. Jia, L., et al., *A potential anti-tumour herbal medicine, Corilagin, inhibits ovarian cancer cell growth through blocking the TGF-β signaling pathways.* BMC complementary and alternative medicine, 2013. **13**(1): p. 1-11.
24. Li, X., et al., *Corilagin, a promising medicinal herbal agent.* Biomedicine & Pharmacotherapy, 2018. **99**: p. 43-50.
25. Deng, Y., et al., *Corilagin induces the apoptosis of hepatocellular carcinoma cells through the mitochondrial apoptotic and death receptor pathways.* Oncology reports, 2018. **39**(6): p. 2545-2552.
26. Zhang, Y.-J., et al., *Antiproliferative activity of the main constituents from Phyllanthus emblica.* Biological and Pharmaceutical Bulletin, 2004. **27**(2): p. 251-255.
27. Liu, Z., et al., *Experiment studies on the pharmacodynamics experiment by corilagin.* Cancer Research On Prevention and Treatment, 2002: p. 05.
28. Saleem, A., et al., *Inhibition of cancer cell growth by crude extract and the phenolics of Terminalia chebula retz. fruit.* Journal of Ethnopharmacology, 2002. **81**(3): p. 327-336.
29. Zhao, J., et al., *Multiple effects of ellagic acid on human colorectal carcinoma cells identified by gene expression profile analysis.* International journal of oncology, 2017. **50**(2): p. 613-621.
30. Ceci, C., et al., *Experimental evidence of the antitumour, antimetastatic and antiangiogenic activity of ellagic acid.* Nutrients, 2018. **10**(11): p. 1756.
31. Ngoumfo, R.M., et al., *Inhibitory effect of macabarterin, a polyoxygenated ellagitannin from Macaranga barteri, on human neutrophil respiratory burst activity.* Journal of natural products, 2008. **71**(11): p. 1906-1910.
32. Liu, Z., et al., *Experiment studies on the pharmacodynamics experiment by corilagin.* Zhongliu Fangzhi Yanjiu, 2002. **29**: p. 356-358.
33. Han, X., T. Shen, and H. Lou, *Dietary polyphenols and their biological significance.* International journal of molecular sciences, 2007. **8**(9): p. 950-988.
34. Greenwell, M. and P. Rahman, *Medicinal plants: their use in anticancer treatment.* International journal of pharmaceutical sciences and research, 2015. **6**(10): p. 4103.

35. Yin, N., et al., *Synergistic and antagonistic drug combinations depend on network topology*. PloS one, 2014. **9**(4): p. e93960.
36. Budman, D.R., A. Calabro, and W. Kreis, *Synergistic and antagonistic combinations of drugs in human prostate cancer cell lines in vitro.* Anti-cancer drugs, 2002. **13**(10): p. 1011-1016.
37. Sharifi-Rad, J., et al., *Ellagic Acid: A Review on Its Natural Sources, Chemical Stability, and Therapeutic Potential.* Oxidative Medicine and Cellular Longevity, 2022. **2022**.
38. Fulda, S., et al., *Cellular stress responses: cell survival and cell death.* International journal of cell biology, 2010. **2010**.
39. Vermeulen, K., D.R. Van Bockstaele, and Z.N. Berneman, *The cell cycle: a review of regulation, deregulation and therapeutic targets in cancer.* Cell proliferation, 2003. **36**(3): p. 131-149.
40. Lossi, L., *The concept of intrinsic versus extrinsic apoptosis.* Biochemical Journal, 2022. **479**(3): p. 357-384.
41. Dhanasekaran, D.N. and E.P. Reddy, *JNK signaling in apoptosis.* Oncogene, 2008. **27**(48): p. 6245-6251.
42. Karlowitz, R. and S.J. van Wijk, *Surviving death: emerging concepts of RIPK3 and MLKL ubiquitination in the regulation of necroptosis.* The FEBS Journal, 2023. **290**(1): p. 37-54.
43. Debatin, K.-M. and P.H. Krammer, *Death receptors in chemotherapy and cancer.* Oncogene, 2004. **23**(16): p. 2950-2966.
44. Lavrik, I., A. Golks, and P.H. Krammer, *Death receptor signaling.* Journal of cell science, 2005. **118**(2): p. 265-267.
45. Szlosarek, P., K.A. Charles, and F.R. Balkwill, *Tumour necrosis factor-α as a tumour promoter.* European journal of cancer, 2006. **42**(6): p. 745-750.
46. Wajant, H. and D. Siegmund, *TNFR1 and TNFR2 in the Control of the Life and Death Balance of Macrophages.* Frontiers in cell and developmental biology, 2019. **7**: p. 91.
47. Luo, J.-L., H. Kamata, and M. Karin, *IKK/NF-κB signaling: balancing life and death–a new approach to cancer therapy.* The Journal of clinical investigation, 2005. **115**(10): p. 2625-2632.
48. Waetzig, G.H., et al., *Soluble tumour necrosis factor (TNF) receptor-1 induces apoptosis via reverse TNF signaling and autocrine transforming growth factor-β1.* The FASEB journal, 2005. **19**(1): p. 91-93.

49. Liu, Z.-w., et al., *Duality of interactions between TGF-β and TNF-α during tumour formation.* Frontiers in Immunology, 2022. **12**: p. 810286.
50. Chen, L., et al., *CD95 promotes tumour growth.* Nature, 2010. **465**(7297): p. 492-496.
51. Peter, M., et al., *The role of CD95 and CD95 ligand in cancer.* Cell death & differentiation, 2015. **22**(4): p. 549-559.
52. Zheng, H., et al., *Fas signaling promotes motility and metastasis through epithelial–mesenchymal transition in gastrointestinal cancer.* Oncogene, 2013. **32**(9): p. 1183-1192.
53. Kashyap, D., V.K. Garg, and N. Goel, *Intrinsic and extrinsic pathways of apoptosis: Role in cancer development and prognosis.* Advances in protein chemistry and structural biology, 2021. **125**: p. 73-120.
54. Gout, S., et al., *Death receptor-3, a new E-Selectin counter-receptor that confers migration and survival advantages to colon carcinoma cells by triggering p38 and ERK MAPK activation.* Cancer research, 2006. **66**(18): p. 9117-9124.
55. Zhang, Y.C., et al., *The role of death receptor 3 in the biological behavior of hepatocellular carcinoma cells.* Molecular medicine reports, 2015. **11**(2): p. 797-804.
56. Yang, A., N.S. Wilson, and A. Ashkenazi, *Proapoptotic DR4 and DR5 signaling in cancer cells: toward clinical translation.* Current opinion in cell biology, 2010. **22**(6): p. 837-844.
57. Ralff, M.D. and W.S. El-Deiry, *TRAIL pathway targeting therapeutics.* Expert review of precision medicine and drug development, 2018. **3**(3): p. 197-204.
58. Dubuisson, A. and O. Micheau, *Antibodies and derivatives targeting DR4 and DR5 for cancer therapy.* Antibodies, 2017. **6**(4): p. 16.
59. Azijli, K., et al., *Non-canonical kinase signaling by the death ligand TRAIL in cancer cells: discord in the death receptor family.* Cell Death & Differentiation, 2013. **20**(7): p. 858-868.
60. Van Geelen, C.M., E.G. de Vries, and S. de Jong, *Lessons from TRAIL-resistance mechanisms in colorectal cancer cells: paving the road to patient-tailored therapy.* Drug resistance updates, 2004. **7**(6): p. 345-358.
61. Koornstra, J.J., et al., *Expression of TRAIL (TNF-related apoptosis-inducing ligand) and its receptors in normal colonic mucosa, adenomas, and carcinomas.* The Journal of Pathology: A Journal of the Pathological Society of Great Britain and Ireland, 2003. **200**(3): p. 327-335.

62. Sträter, J.r., et al., *Expression of TRAIL and TRAIL receptors in colon carcinoma: TRAIL-R1 is an independent prognostic parameter.* Clinical cancer research, 2002. **8**(12): p. 3734-3740.
63. Yoshida, T., et al., *Glycosylation modulates TRAIL-R1/death receptor 4 protein: different regulations of two pro-apoptotic receptors for TRAIL by tunicamycin.* Oncology reports, 2007. **18**(5): p. 1239-1242.
64. Liu, J., et al., *Wnt/β-catenin signalling: function, biological mechanisms, and therapeutic opportunities.* Signal transduction and targeted therapy, 2022. **7**(1): p. 3.
65. Mehta, S., S. Hingole, and V. Chaudhary, *The emerging mechanisms of Wnt secretion and signaling in development.* Frontiers in Cell and Developmental Biology, 2021. **9**: p. 714746.
66. MacDonald, B.T., K. Tamai, and X. He, *Wnt/β-catenin signaling: components, mechanisms, and diseases.* Developmental cell, 2009. **17**(1): p. 9-26.
67. Komiya, Y. and R. Habas, *Wnt signal transduction pathways.* Organogenesis, 2008. **4**(2): p. 68-75.
68. Yoshida, N., et al., *Analysis of Wnt and β-catenin expression in advanced colorectal cancer.* Anticancer research, 2015. **35**(8): p. 4403-4410.
69. Stamos, J.L. and W.I. Weis, *The β-catenin destruction complex.* Cold Spring Harbor perspectives in biology, 2013. **5**(1): p. a007898.
70. Sparks, A.B., et al., *Mutational analysis of the APC/β-catenin/Tcf pathway in colorectal cancer.* Cancer research, 1998. **58**(6): p. 1130-1134.
71. Koveitypour, Z., et al., *Signaling pathways involved in colorectal cancer progression.* Cell & bioscience, 2019. **9**: p. 1-14.
72. Mori, Y., et al., *Somatic mutations of the APC gene in colorectal tumours: mutation cluster region in the APC gene.* Human molecular genetics, 1992. **1**(4): p. 229-233.
73. Zhong, Z.A., et al., *Regulation of Wnt receptor activity: Implications for therapeutic development in colon cancer.* Journal of Biological Chemistry, 2021. **296**.
74. Segditsas, S. and I. Tomlinson, *Colorectal cancer and genetic alterations in the Wnt pathway.* Oncogene, 2006. **25**(57): p. 7531-7537.
75. Aghabozorgi, A.S., et al., *Role of adenomatous polyposis coli (APC) gene mutations in the pathogenesis of colorectal cancer; current status and perspectives.* Biochimie, 2019. **157**: p. 64-71.
76. Talseth-Palmer, B.A., *The genetic basis of colonic adenomatous polyposis syndromes.* Hereditary cancer in clinical practice, 2017. **15**(1): p. 1-7.

77. Luo, J., *Glycogen synthase kinase 3β (GSK3β) in tumourigenesis and cancer chemotherapy.* Cancer letters, 2009. **273**(2): p. 194-200.
78. Shakoori, A., et al., *Deregulated GSK3β activity in colorectal cancer: its association with tumour cell survival and proliferation.* Biochemical and biophysical research communications, 2005. **334**(4): p. 1365-1373.
79. Vidri, R.J. and T.L. Fitzgerald, *GSK-3: An important kinase in colon and pancreatic cancers.* Biochimica et Biophysica Acta (BBA)-Molecular Cell Research, 2020. **1867**(4): p. 118626.
80. Mazzoni, S.M. and E.R. Fearon, *AXIN1 and AXIN2 variants in gastrointestinal cancers.* Cancer letters, 2014. **355**(1): p. 1-8.
81. Salahshor, S. and J. Woodgett, *The links between axin and carcinogenesis.* Journal of clinical pathology, 2005. **58**(3): p. 225-236.
82. Wu, Z.-Q., et al., *Canonical Wnt suppressor, Axin2, promotes colon carcinoma oncogenic activity.* Proceedings of the National Academy of Sciences, 2012. **109**(28): p. 11312-11317.
83. Koelman, E.M., A. Yeste-Vázquez, and T.N. Grossmann, *Targeting the interaction of β-catenin and TCF/LEF transcription factors to inhibit oncogenic Wnt signaling.* Bioorganic & Medicinal Chemistry, 2022: p. 116920.
84. Santiago, L., et al., *Wnt signaling pathway protein LEF1 in cancer, as a biomarker for prognosis and a target for treatment.* American journal of cancer research, 2017. **7**(6): p. 1389.
85. Huang, Z., et al., *Epithelial–mesenchymal transition: The history, regulatory mechanism, and cancer therapeutic opportunities.* MedComm, 2022. **3**(2): p. e144.
86. Mathew, R. and E. White, *Autophagy in tumourigenesis and energy metabolism: friend by day, foe by night.* Current opinion in genetics & development, 2011. **21**(1): p. 113-119.
87. Mokarram, P., et al., *New frontiers in the treatment of colorectal cancer: Autophagy and the unfolded protein response as promising targets.* Autophagy, 2017. **13**(5): p. 781-819.
88. Schneider, J.L. and A.M. Cuervo, *Autophagy and human disease: emerging themes.* Current opinion in genetics & development, 2014. **26**: p. 16-23.
89. Burada, F., et al., *Autophagy in colorectal cancer: An important switch from physiology to pathology.* World journal of gastrointestinal oncology, 2015. **7**(11): p. 271.

90. Yu, L., Y. Chen, and S.A. Tooze, *Autophagy pathway: cellular and molecular mechanisms.* Autophagy, 2018. **14**(2): p. 207-215.
91. Marquez, R.T. and L. Xu, *Bcl-2: Beclin 1 complex: multiple, mechanisms regulating autophagy/apoptosis toggle switch.* American journal of cancer research, 2012. **2**(2): p. 214.
92. He, C. and D.J. Klionsky, *Regulation mechanisms and signaling pathways of autophagy.* Annual review of genetics, 2009. **43**: p. 67-93.
93. Kang, R., et al., *The Beclin 1 network regulates autophagy and apoptosis.* Cell Death & Differentiation, 2011. **18**(4): p. 571-580.
94. Yun, C.W. and S.H. Lee, *The roles of autophagy in cancer.* International journal of molecular sciences, 2018. **19**(11): p. 3466.
95. Lim, S.M., E.A. Mohamad Hanif, and S.-F. Chin, *Is targeting autophagy mechanism in cancer a good approach? The possible double-edge sword effect.* Cell & bioscience, 2021. **11**(1): p. 1-13.
96. Li, X., S. He, and B. Ma, *Autophagy and autophagy-related proteins in cancer.* Molecular cancer, 2020. **19**(1): p. 1-16.
97. Briguglio, G., et al., *Polyphenols in cancer prevention: New insights.* International Journal of Functional Nutrition, 2020. **1**(2): p. 1-1.
98. Kampa, M., et al., *Polyphenols and cancer cell growth.* Reviews of physiology, biochemistry and pharmacology, 2007: p. 79-113.
99. Galluzzi, L., et al., *Molecular mechanisms of cell death: recommendations of the Nomenclature Committee on Cell Death 2018.* Cell Death & Differentiation, 2018. **25**(3): p. 486-541.
100. Kaufmann, S.H. and W.C. Earnshaw, *Induction of apoptosis by cancer chemotherapy.* Experimental cell research, 2000. **256**(1): p. 42-49.
101. Singh, V., et al., *Apoptosis and pharmacological therapies for targeting thereof for cancer therapeutics.* Sci, 2022. **4**(2): p. 15.
102. Arfin, S., et al., *Oxidative stress in cancer cell metabolism.* Antioxidants, 2021. **10**(5): p. 642.
103. Kerr, J.F., A.H. Wyllie, and A.R. Currie, *Apoptosis: a basic biological phenomenon with wideranging implications in tissue kinetics.* British journal of cancer, 1972. **26**(4): p. 239-257.
104. Zhang, J.H. and M. Xu, *DNA fragmentation in apoptosis.* Cell research, 2000. **10**(3): p. 205-211.

105. Diaz Arguello, O.A. and H.J. Haisma, *Apoptosis-inducing TNF superfamily ligands for cancer therapy.* Cancers, 2021. **13**(7): p. 1543.
106. Snajdauf, M., et al., *The TRAIL in the treatment of human cancer: an update on clinical trials.* Frontiers in Molecular Biosciences, 2021. **8**: p. 628332.
107. Sheng, Y., F. Li, and Z. Qin, *TNF receptor 2 makes tumour necrosis factor a friend of tumours.* Frontiers in immunology, 2018. **9**: p. 1170.
108. Zhang, Y. and X. Wang, *Targeting the Wnt/β-catenin signaling pathway in cancer.* Journal of hematology & oncology, 2020. **13**: p. 1-16.
109. Zhao, H., et al., *Wnt signaling in colorectal cancer: Pathogenic role and therapeutic target.* Molecular Cancer, 2022. **21**(1): p. 144.
110. Li, Y., et al., *Prognostic significance of cyclin D1 expression in colorectal cancer: a meta-analysis of observational studies.* PloS one, 2014. **9**(4): p. e94508.
111. Rangel, M., et al., *Autophagy and tumourigenesis.* The FEBS Journal, 2022. **289**(22): p. 7177-7198.
112. Huang, T., et al., *Autophagy and hallmarks of cancer.* Critical Reviews™ in Oncogenesis, 2018. **23**(5-6).
113. Mahgoub, E., et al., *The role of autophagy in colorectal cancer: Impact on pathogenesis and implications in therapy.* Frontiers in Medicine, 2022. **9**.
114. Koukourakis, M., et al., *Beclin 1 over-and underexpression in colorectal cancer: distinct patterns relate to prognosis and tumour hypoxia.* British journal of cancer, 2010. **103**(8): p. 1209-1214.
115. Bednarczyk, M., et al., *Transcription of Autophagy Associated Gene Expression as Possible Predictors of a Colorectal Cancer Prognosis.* Biomedicines, 2023. **11**(2): p. 418.
116. Collier, J.J., et al., *Emerging roles of ATG7 in human health and disease.* EMBO molecular medicine, 2021. **13**(12): p. e14824.

6.5 Appendix-I: Individual Cellular viability assays for fractions and compounds isolated from aqueous extracts of Haritaki Churna and Amalaki Churna

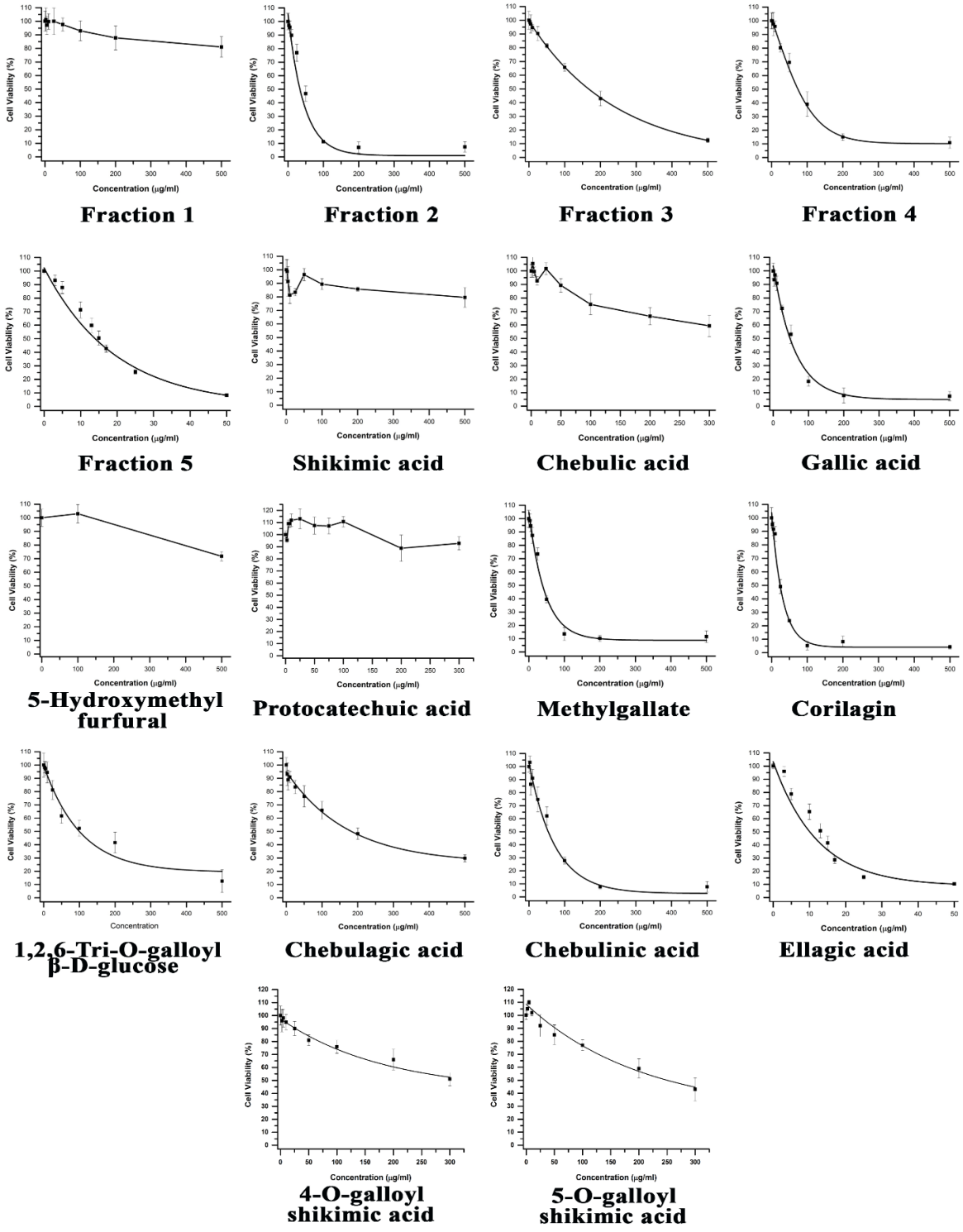

Figure 6.19: **Cell Viability graphs for HCAE fractions and compounds against HCT-116 cell line after 48 hours of treatment**

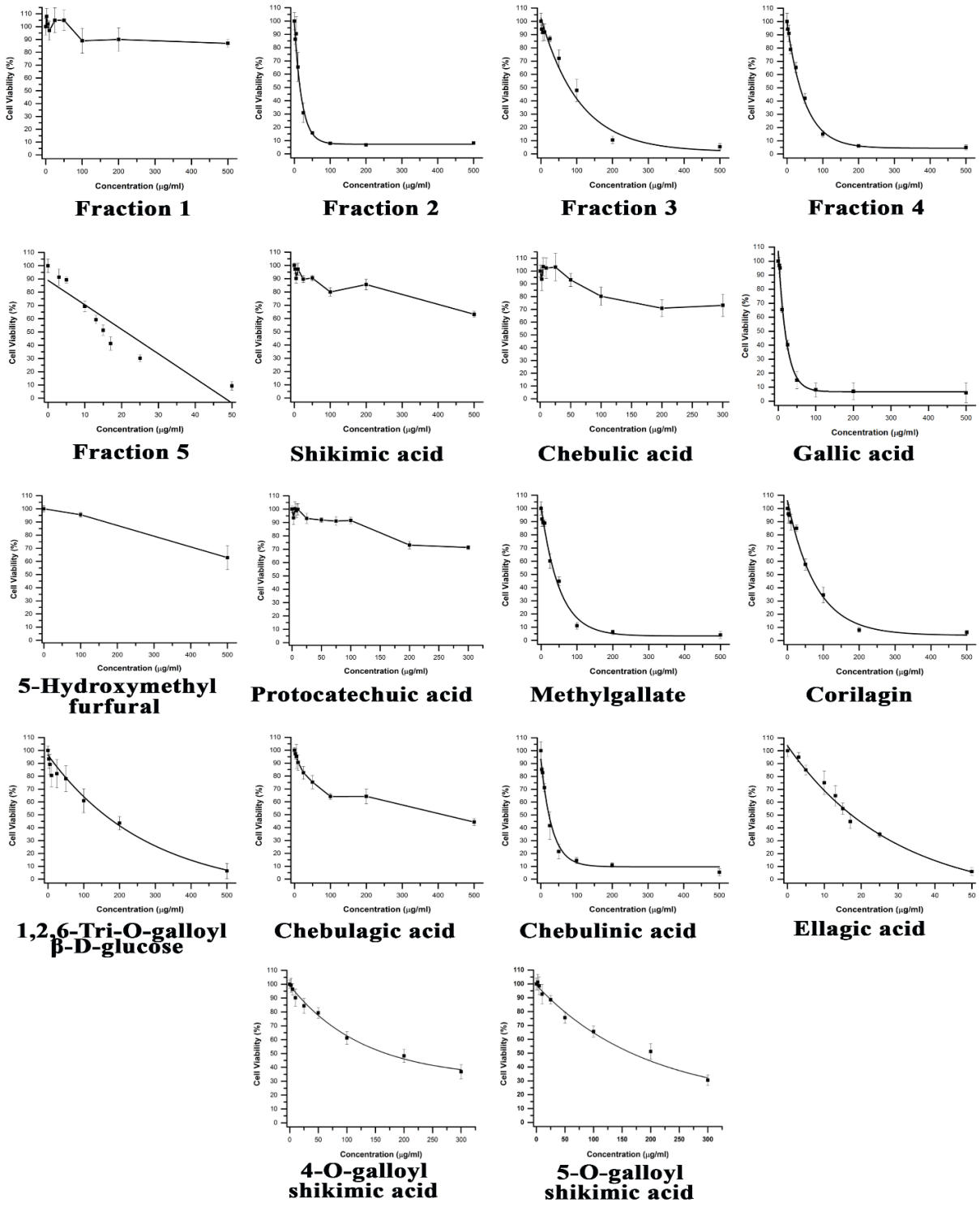

Figure 6.20: **Cell Viability graphs for HCAE fractions and compounds against DLD1 cell line after 48 hours of treatment**

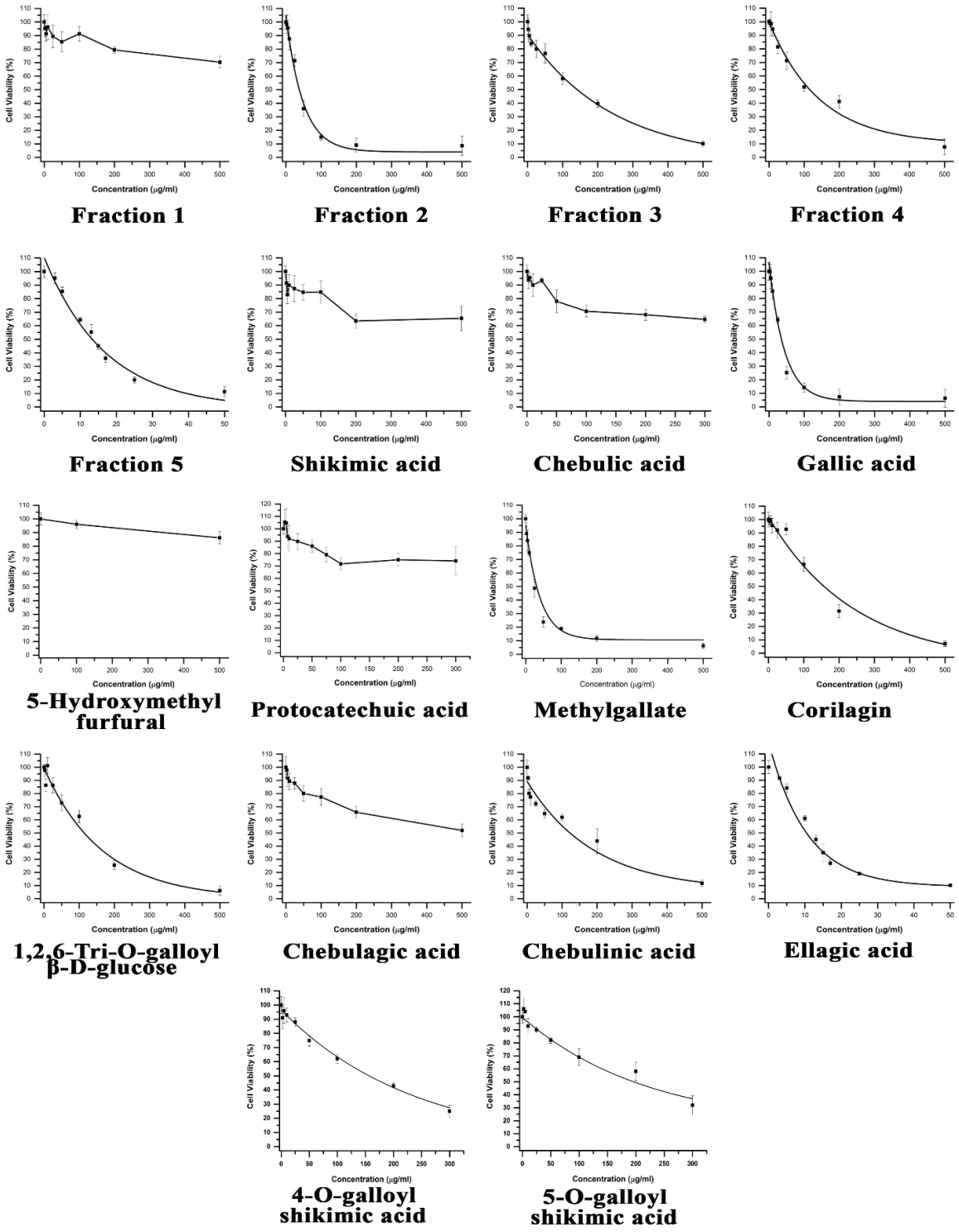

Figure 6.21: **Cell Viability graphs for HCAE fractions and compounds against HT-29 cell line after 48 hours of treatment**

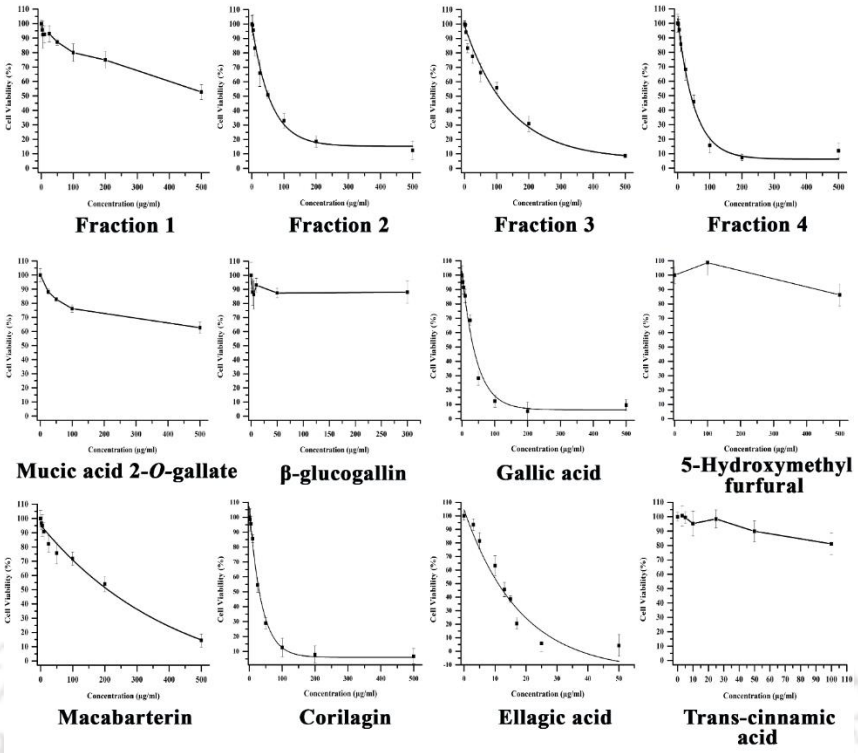

Figure 6.22: **Cell Viability graphs for AMCAE fractions and isolated compounds against colorectal (HCT-116) after 48 hours of treatment.**

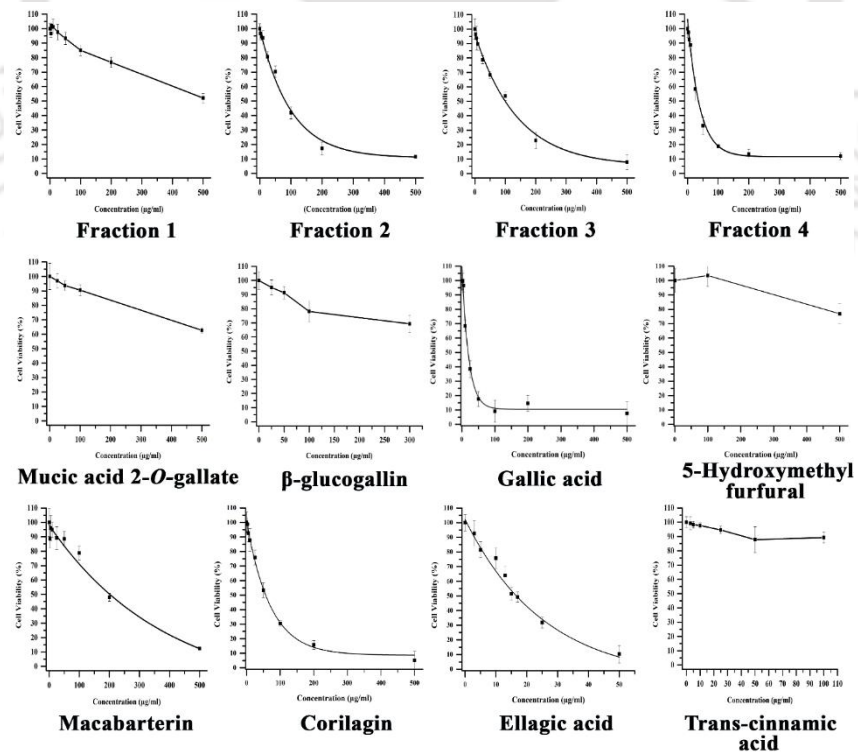

Figure 6.23: **Cell Viability graphs for AMCAE fractions and isolated compounds against colorectal (DLD1) after 48 hours of treatment.**

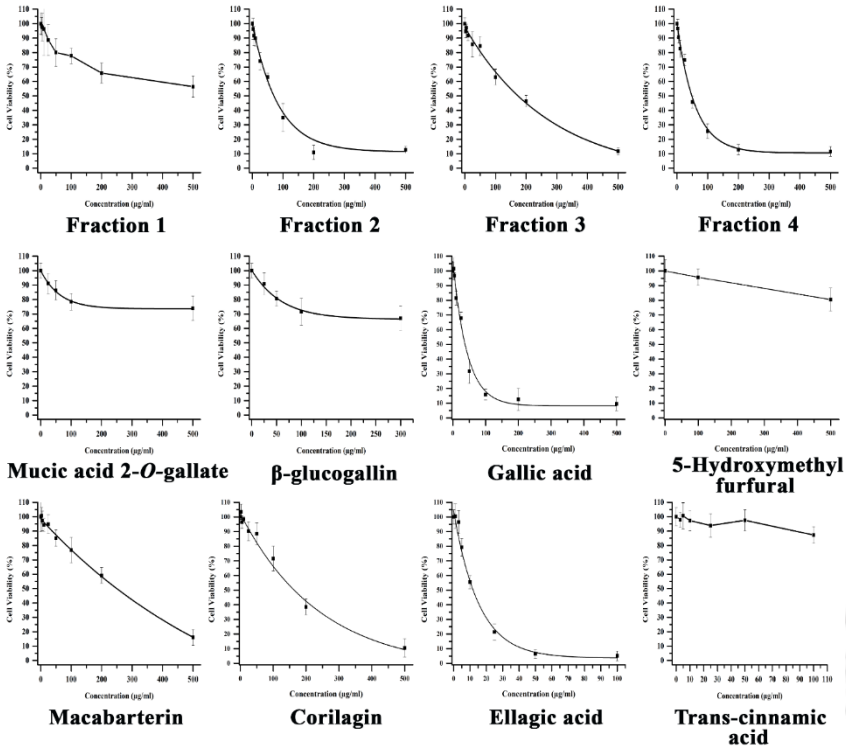

Figure 6.24: **Cell Viability graphs for AMCAE fractions and isolated compounds against colorectal (HT-29) after 48 hours of treatment**

Chapter VII

Summary and conclusions

7.1 Summary: The field of modern medicine has witnessed substantial progress driven by systematic research and the integration of evidence-based methodologies. Scientific advancements have led to the rigorous evaluation of therapeutic modalities through the analysis of data from multiple independent studies, culminating in the emergence of systematic reviews as invaluable tools. These systematic reviews empower clinicians and researchers, forming the foundation of evidence-based medicine (EBM), which seeks to align clinical practice with robust scientific evidence. However, prior to the inception of EBM, societies relied on diverse therapeutic approaches, exemplified by traditional medical systems in India, China, and Iran. Challenges such as ineffective remedies for chronic illnesses, financial barriers to treating complex conditions like cancer, and adverse effects of conventional treatments have spurred renewed interest in ancient healing methods. This trend reflects a quest for alternative solutions rooted in historical wisdom, emphasizing the integration of traditional and contemporary medical advancements. Ayurveda, a holistic system originating in the Indian subcontinent, offers personalized herbal remedies, lifestyle adjustments, and dietary interventions, emphasizing the synergy of mind, body, and spirit. The wealth of knowledge from traditional medicine, combined with the extensive experience of Ayurvedic practices, holds great potential for drug discovery. The exploration of Ayurvedic formulations entails looking into existing remedies to address new health applications, grounded in the belief that the constituent herbs and botanical combinations exhibit a wide range of therapeutic properties. Scientific validation, including the study of active constituents, mechanisms of action, and contemporary uses, is imperative to integrate Ayurvedic remedies effectively into conventional healthcare. This integration necessitates rigorous research to harness the potential of complex herbal, mineral, and natural components for specific and efficacious outcomes.

In this study, a comprehensive evaluation of 28 distinct Ayurvedic formulations was conducted, each specifically designed to address various historical therapeutic requirements associated with a range of disorders and ailments. The primary objective of this study was to investigate the potential ability of these formulations for the treatment of various cancer types, with a particular emphasis on colorectal cancer. After a rigorous analysis of the 28 Ayurvedic formulations, two notable compositions, Haritaki Churna and Amalaki Churna, both derived from *Terminalia chebula* and *Emblica officinalis* fruits, respectively, were identified. Leveraging ethnopharmacological knowledge, this study harnessed the rich repository of phytochemicals present in Ayurvedic plants and herbal sources as a promising avenue for novel therapeutic development. Biochemical methodologies unveiled crucial constituents including

alkaloids, terpenoids, flavonoids, proteins, and polyphenols within the aqueous extracts of these formulations, denoted as HCAE (Haritaki Churna aqueous extract) and AMCAE (Amalaki Churna aqueous extract). Remarkably, polyphenols emerged as the predominant fraction, constituting approximately 92% of HCAE and 85% of AMCAE. Advanced spectroscopic techniques, encompassing ^{1}H and ^{13}C NMR, UPLC-MS, and HPLC, were employed for the characterization of 13 distinct polyphenols from HCAE (*Shikimic acid, Chebulic acid, gallic acid, 5-hydroxymethylfurfural, Protocatechuic acid, 4-O-galloyl-shikimic Acid, 5-O-galloyl-shikimic Acid, Methyl gallate, corilagin, 1, 2, 6, Tri-O-galloyl β-D-glucose, chebulagic acid, chebulinic acid,* and *Ellagic acid*) and 8 polyphenols from AMCAE (*Mucic acid-2-O-gallate, β-glucogallin, gallic acid, 5-hydroxymethylfurfural, macabarterin, corilagin, ellagic acid* and *trans-cinnamic acid*).

The development of promising drug candidates from Ayurvedic extracts faces challenges due to intricate phytochemical interactions, making it difficult to identify suitable protein targets and mechanisms of action. To comprehensively understand the individual and synergistic effects of phytochemicals in Ayurvedic formulations and predict potential therapeutic protein targets, we utilized a network-based pharmacological approach for polyphenols derived from both HCAE and AMCAE. Using structure-based similarity, we identified 469 protein targets for 13 HCAE polyphenols and 387 protein targets for 8 AMCAE polyphenols from Drug Bank and Binding DB. Pathway enrichment analysis revealed that HCAE predominantly affects metabolic pathways crucial for energy production, nutrient utilization, and cellular homeostasis. Furthermore, it influences cancer-related pathways involving cell proliferation, apoptosis, angiogenesis, and metastasis. Similarly, AMCAE targets kinases within plasma membrane and cytoplasm, modulating intricate signal transduction pathways like MAP-K signaling, calcium signaling, and PI3K-AKT signaling. This underscores the diverse impact of HCAE and AMCAE on metabolic, cancer-related, and signal transduction pathways. Further, a comprehensive protein-protein interaction (PPI) analysis, several key proteins were identified, including HSP90AA1, Src kinase, NCOA1, PIK3R1, AKT1, ESR-α, EGFR, and AR. These proteins played pivotal roles in governing the bioactivity of both HCAE and AMCAE extracts, as they shared common compounds like gallic acid, ellagic acid, corilagin, and 5-hydroxymethylfurfural. ESR-α also emerged as a significant target due to its numerous shared phytochemical neighbors. Notably, c-Src kinase, Akt1, PIK3R1, and EGFR were associated with vital cellular processes, while HSP90AA1, androgen receptor, and ESR-α contributed to structural maintenance, signal regulation and gene

expression. These findings underscored the importance of these polyphenolic constituents and proteins in driving the observed bioactivities within the aqueous extracts. Additionally, our molecular docking and molecular dynamics simulation studies have yielded valuable insights into the stability and binding strength of protein-ligand complexes. Among the ligands sourced from HCAE, the majority of complexes demonstrated remarkable stability, as evidenced by minimal fluctuations in key parameters such as RMSD, RMSF, the number of hydrogen bonds, and radius of gyrations. These findings suggest that the selected phytochemicals hold promise as potential drug candidates. The MMPBSA binding energy calculations corroborated the stability of all complexes. Furthermore, a significant proportion of the 13 phytochemicals from HCAE adhered to Lipinski's rule, suggesting the drug-like candidacy of HCAE as a whole. Similarly, most complexes involving ligands from AMCAE exhibited minimal perturbations in critical parameters, highlighting their potential as promising therapeutic candidates. Within the subset of eight compounds from AMCAE, six compounds demonstrated adherence to Lipinski's rule, with only minor deviations, reinforcing the drug-like attributes inherent to the compounds within AMCAE as a collective entity.

Furthermore, we conducted investigations into the application of AMCAE and HCAE on colorectal cancer cell lines, specifically HCT-116 and DLD1, aiming to assess their impact on cellular viability and intracellular signaling. We employed c-Src kinase as a representative model to validate our in-silico findings. Treatment with HCAE/AMCAE demonstrated a notable capacity to modulate the cellular landscape of DLD1/HCT-116 cells. This modulation was characterized by substantial downregulation of key protein entities, including c-Src, Akt1, cyclin D1, and Vimentin. Notably, the discernible impact of HCAE/AMCAE treatment was observed in the time-dependent reduction of Akt1 levels after 24/48-hour exposure in both colorectal cell lines. This outcome may be attributed to c-Src inhibition or direct intervention mechanisms. The intricate network of protein downregulation highlighted here underscores the profound interconnectedness inherent in phytochemical interactions, as previously elucidated.

Additionally, we investigated the therapeutic potential of two prominent Ayurvedic formulations, Haritaki Churna (HC) and Amalaki Churna (AMC), which have long been recognized in Ayurvedic literature for their efficacy in addressing various ailments and gastrointestinal issues. Our research focused on assessing their anti-colorectal cancer properties through a comprehensive examination of their behaviour within simulated gastric and intestinal environments. Both HC and AMC demonstrated significant cytotoxic effects on cancer cells in the range of 50-300 µg/ml across various cancer cell lines, with particular efficacy against

colorectal cancer cells, as evidenced by lower IC_{50} values on HCT-116 and DLD1 cells. Importantly, both the raw Ayurvedic preparations and their aqueous extracts exhibited remarkable stability under simulated gastric conditions as well as fasted and fed state intestinal conditions, highlighting their suitability for oral administration and potential therapeutic applications. To further elucidate the safety profiles of HC and AMC, we conducted in-depth investigations using two distinct cell models, Human Embryonic Kidney 293 (HEK-293) and Peripheral Blood Mononuclear Cells (PBMCs), which are representative models for safety and toxicity assessments.

The anti-cancer activity of HCAE investigated in this study is primarily ascribed to the presence of polyphenols, with ellagic acid emerging as the most potent constituent. Cell viability assays conducted on colorectal cancer cells unequivocally demonstrate that ellagic acid exerts a dual effect by inhibiting cell growth at lower concentrations and inducing cell death at higher concentrations. Mechanistic investigations reveal that ellagic acid triggers DNA fragmentation, a hallmark of apoptosis, and induces the release of cytochrome-c from mitochondria. Moreover, it upregulates cleaved caspase 3 while downregulating caspase 8 and Bcl2 expression, implicating the activation of the mitochondrial pathway of apoptosis. Conversely, the extrinsic pathway of apoptosis is ruled out as ellagic acid downregulates death receptors, including TNFR1, TNFR2, Fas, DR3, DR4, DR5, and DR6, and does not activate caspase 8. Additionally, ellagic acid induces cell cycle arrest in the S-phase, associated with reduced expression levels of cyclin A2 and cyclin D1. Furthermore, in colorectal cancer cells, ellagic acid treatment significantly downregulates canonical Wnt pathway proteins, including GSK-3β, axin-2, β-catenin, LEF-1, and cyclin-D1, thereby implicating its role in inhibiting the Wnt/β-catenin pathway. Notably, ellagic acid also modulates epithelial-mesenchymal transition (EMT)-related gene expression by downregulating snail, slug, LEF-1, and N-cadherin. Moreover, it exerts influence over autophagic processes by downregulating Beclin-1 at higher concentrations after 48 hours of treatment, while showing no significant changes at 24 hours. Interestingly, there is an increase in expression levels of Atg12, Atg7, and LC3I/II after 24 hours of treatment, suggesting an attempt to induce autophagy in response to ellagic acid-induced stress (**Figure 7.1**). However, the downregulation of various Atg-related proteins after 48 hours of treatment, except for LC3I/II, indicates an inhibition of autophagosome initiation. Collectively, EA's multifaceted molecular interventions demonstrate its potential to impede Wnt-driven carcinogenesis, suppress EMT-related transitions, and hinder migration and invasion in various cancer types. This preliminary study sheds light on the ability of ellagic

acid on interrupting basic cell machinery such as apoptosis regulation, necroptosis, cell cycle regulation, wnt/β-catenin pathway, epithelial to mesenchymal transition and autophagic dysregulation.

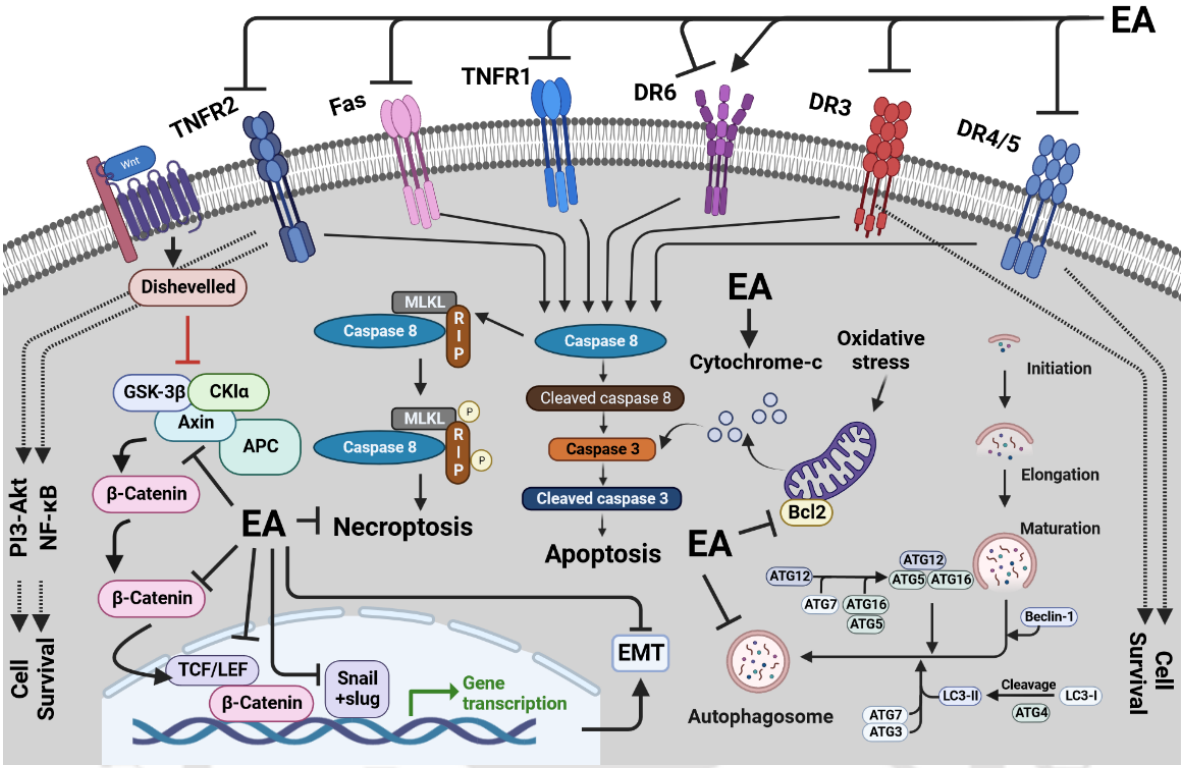

Figure 7.1: Ellagic acid perturbs multiple cellular pathway in colorectal cancer cells.

The potent anti-cancer attributes of Amalaki Churna can be attributed to its rich polyphenolic composition, particularly encompassing gallic acid, corilagin, and ellagic acid. Among these constituents, the well-established anti-cancer effects of gallic acid, corilagin, and ellagic acid not only corroborate but also augment the reliability of our empirical findings. These compounds derived from Amalaki Churna exhibit the potential for personalized bioactivity while concurrently presenting the prospect of orchestrated synergistic actions. In our efforts to elucidate the distinct roles of these constituents in Amalaki Churna's anti-cancer efficacy, we conducted a deductive analysis, which yielded gallic acid as the most crucial component in AMCAE. Exclusion of gallic acid was found to significantly diminish the inherent anti-cancer properties of Amalaki Churna. Gallic acid (GA) demonstrated the capacity to induce apoptosis in colorectal cancer cells within a concentration range of 17-35 µg/ml, as evidenced by DNA fragmentation. Mechanistic investigations revealed that GA-induced apoptosis did not follow the extrinsic pathway, as multiple death receptors, including DR3, DR5, DR6, TNFR1, TNFR2, and Fas, were down-regulated, without a concurrent increase in caspase 8 expression or its cleaved form (**Figure 7.2**). Instead, GA-induced cell death was

mediated through the mitochondrial pathway of apoptosis, as indicated by elevated levels of cytochrome-c and cleaved caspase-3, coupled with reduced caspase 8 expression and decreased expression of the anti-apoptotic protein Bcl2.

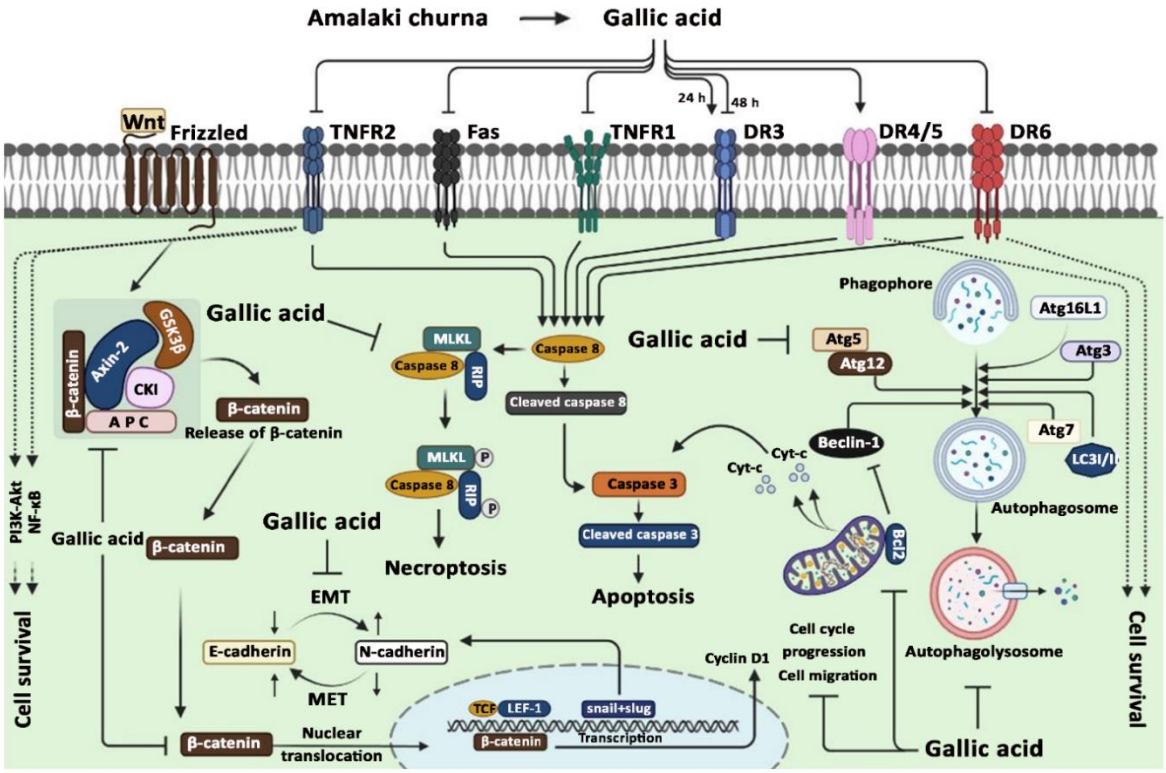

Figure 7.2: Gallic acid disrupts multiple cellular processes in colorectal cancer cells.

These observed cellular alterations can be attributed to the induction of oxidative stress through the generation of reactive oxygen species (ROS), resulting in a significant reduction in mitochondrial membrane potential. Furthermore, the administration of gallic acid (GA) elicited a distinctive response in colorectal cancer cells (HCT-116) by instigating a robust S-phase cell cycle arrest. This effect was accompanied by a substantial down-regulation of key cell cycle regulators, specifically cyclin A2 and cyclin D1. Notably, cyclin D1 serves as a pivotal component within the Wnt/β-catenin signaling pathway, and GA treatment exerted a concurrent inhibitory influence on this crucial pathway. Beyond cell cycle modulation, GA treatment also exerted a discernible impact on cellular autophagy processes. It markedly down-regulated key proteins integral to the autophagic pathway, most notably beclin-1. This substantial down-regulation of beclin-1 suggests a profound interference with the autophagic machinery, thereby impeding the cell's capacity to employ autophagy as a secondary survival mechanism.

7.2 Conclusions: This comprehensive investigation seamlessly integrates traditional Ayurvedic medicine with rigorous scientific methodologies to elucidate the potential of Haritaki Churna (HC) and Amalaki Churna (AMC) as formidable contenders in the battle against colorectal cancer (CRC). Thorough examinations have confirmed the stability of these Ayurvedic formulations under simulated gastric and intestinal conditions, mirroring the gastrointestinal milieu, while their benignity for therapeutic applications has been established through testing on normal cell lines. Leveraging extensive phytochemical analysis, network pharmacology, molecular docking, and dynamic simulations, we have successfully forged connections between isolated compounds and specific protein targets. This exhaustive network-centric pharmacological exploration has unveiled intricate interplays between polyphenols and their respective targets, unraveling both individual and synergistic impacts intrinsic to these formulations. These revelations have shed light on their profound modulatory effects on diverse cancer-related pathways within the intricate network. Noteworthy highlights of our investigation encompass the robust anti-cancer attributes attributed to polyphenols, with particular emphasis on the remarkable efficacy of ellagic acid and gallic acid. These compounds exhibit adept targeting of pivotal proteins that govern the proliferation, viability, and metastasis of cancer cells. Particularly remarkable is our pioneering revelation of their capacity to induce autophagic dysregulation in CRCs, a phenomenon hitherto unreported in the existing scientific literature.

The extensive examination conducted on Haritaki Churna (HC) and Amalaki Churna (AMC) within the framework of colorectal cancer (CRC) yields promising prospects for subsequent research endeavours and potential clinical implementations. The investigation encompasses multifaceted aspects, including pharmacokinetics and pharmacodynamics assessment, formulation optimization, mechanistic elucidation, comprehensive evaluation of long-term safety and side effects, and comprehensive animal studies. These findings collectively contribute to an enriched understanding of the potential applications and implications of HC and AMC in the context of CRC, fostering the development of novel therapeutic approaches and avenues for further scientific inquiry.

List of Publications

1. **Khan MR**, Yanase E, Trivedi V. Extraction, phytochemical characterization and anti-cancer mechanism of Haritaki Churna: An Ayurvedic formulation. Plos one. 2023 May 31;18(5):e0286274. **(https://doi.org/10.1371/journal.pone.0286274).**
2. **Khan MR** and Trivedi V. Molecular modelling, docking and network analysis of phytochemicals from Haritaki Churna: role of protein cross-talks for their action. Journal of Biomolecular Structure and Dynamics. 2023 May 30:1-6. **(https://doi.org/10.1080/07391102.2023.2220036).**
3. **Khan MR** and Trivedi V. Phytochemical Cross-talk in Indian Gooseberry Preparation to Explain Therapeutic Potentials of Dietary Supplements. Pharmacognosy Research (2023-In Print).
4. **Khan MR**, Yanase E, Trivedi V. Gallic acid is the most potent polyphenol from Amalaki Churna responsible for its anti-cancer activity. (In Communication).
5. **Khan MR** and Trivedi V. Repurposing of Ayurvedic formulations to overcome disease burden- Review paper (In Communication).
6. Katari JK, **Khan MR**, Trivedi V, Das D. Extraction, purification, characterization and bioactivity evaluation of high purity C-phycocyanin from Spirulina sp. NCIM 5143. Process Biochemistry. 2023 Jul 1;130:322-33. **https://doi.org/10.1016/j.procbio.2023.04.022).**
7. Mostakim SK, **Khan MR**, Das A, Nandi S, Trivedi V, Biswas S. A phthalimide-functionalized UiO-66 metal–organic framework for the fluorogenic detection of hydrazine in live cells. Dalton Transactions. 2019;48(33):12615-21. **(https://doi.org/10.1039/C9DT02459J).**